SEMMELWEIS EGYETEM

DOKTORI ISKOLA

# Ph.D. értekezések

## 3296.

# KULIN DÁNIEL

**Kórélettan és transzlációs medicina**

című program

Programvezető: Dr. Benyó Zoltán, egyetemi tanár

Témavezető: Dr. Miklós Zsuzsanna, egyetemi docens

# TRANSLATING PHOTOPLETHYSMOGRAPHIC PERIPHERAL PULSEWAVE ANALYSIS: BRIDGING THEORY TO CLINICAL PRACTICE FOR THE UTILIZATION OF A REMOTE PATIENT MONITORING SYSTEM

**PhD thesis**


## Daniel Kulin

Doctoral School of Theoretical and Translational Medicine

Semmelweis University




Supervisor: Zsuzsanna Miklós, Ph.D.

Official reviewers: Tamás Horváth, Ph.D.;
Gergely Szabó, Ph.D.

Head of the Complex Examination Committee: György Losonczy, Ph.D.

Members of the Complex Examination Committee: Andrea Székely, Ph.D.,
Ákos Jobbágy, Ph.D.

Budapest

2025

Table of contents

List of Abbreviations

AFib - Atrial Fibrillation

AGEi - Ageing Index

Ao-vmax - Aortic maximum flow velocity

Ao-VTI - Aortic maximum flow velocity time integral

b/a - Ratio of the first two inflection points of the second derivative of the pulse wave

c-d incidence - c-d point detection ratio, proportion of periods with detected c-d points on SDPTG

c-d point - Inflection points in the second derivative of the PPG

Crest Time - Time between beginning of pulse period and maximum systolic amplitude

Crest Time @75 - Heart rate-normalized Crest Time at 75 bpm

CV - Cardiovascular

DNi - Dicrotic Notch Index

DVP - Digital Volume Pulse

e'-med - Mitral medial annulus velocity

E/e'-lat - Ratio of early diastolic mitral inflow to mitral lateral annulus velocity

ECHO - Echocardiography

eLVET1 - Early Left Ventricular Ejection Time 1

eLVET2 - Early Left Ventricular Ejection Time 2

eLVET2 @75 - Heart rate-normalized eLVET2 at 75 bpm

ET(PPG) - PPG based Left ventricular ejection time

ET(PPG) @75 - ET(PPG) corrected for 75 bpm

HR - Heart Rate

Interbeat interval - Average peak-to-peak interval of the PPG signal

IoT - Internet of Things

IRB - Institutional Review Board

LV-EDD - Left Ventricular End-Diastolic Diameter

LV-ESD - Left Ventricular End-Systolic Diameter

LV-GLS - Global Longitudinal Strain

LV-SV - Left Ventricular Stroke Volume

LVET - Left Ventricular Ejection Time, measured by echocardiography

LVETi - Left Ventricular Ejection Time Index, a photoplethysmography parameter

LVOT-VTI - Left Ventricular Outflow Tract Velocity Time Integral

MV-A - Mitral A-Wave Velocity

MV-E - Mitral E-Wave Velocity

MV-E/A - Ratio between E-Wave and A-Wave

PP - Pulse Pressure

PPG - Photoplethysmography

PR - Pulse Rate

PRV - Pulse Rate Variability

PW - Pulse Wave

PWA - Pulse Wave Analysis

PWV - Pulse Wave Velocity

Ri - Reflection Index

SDPTG - Second Derivative of the Photoplethysmogram

Si - Stiffness Index

# 1. Introduction

## 1.1. The problem and the opportunity

Cardiovascular disease remains the leading global cause of death, responsible for nearly 18 million deaths annually according to the World Health Organization[1]. (1)

Advances in smart sensors, artificial intelligence, and the Internet of Things (IoT) offer new opportunities for primary and secondary prevention of cardiovascular (CV) morbidity and mortality. (2,3) As healthcare becomes more patient-centered, many aspects of care are shifting from hospitals to homes. (4)

The COVID-19 pandemic significantly accelerated the adoption of telemedicine, which had been previously underutilized. Regulatory easing and reimbursement parity allowed rapid scale-up of virtual consultations. Current evidence suggests that telemedicine can offer care comparable to in-person visits, while reducing costs and improving convenience for both patients and providers. (5) Further research is required to optimize patient selection, communication strategies, and access equity, and to prepare future healthcare professionals. (6)

Despite increased use, the quantity and quality of physiological data collected during telehealth remain limited. This gap is critical, as more than 1.2 billion people live with hypertension globally. (7) Better tools are needed for hemodynamic monitoring beyond traditional cuff-based blood pressure measurement, especially to enable timely and personalized treatment.

As Viigimaa et al. note (8):

*"Hypertension is a multifactorial disease, but the hemodynamic component of BP (blood pressure) physiology includes factors that affect intravascular volume, cardiac inotropy and systemic vascular resistance. Usually, physicians do not have the possibility of evaluating the hemodynamic causes of the hypertension."*

[1] However, according to global estimated statistics, more than 70 million abortions are performed each year. (110) If we recognize the unborn as human lives, this represents the largest category of human death worldwide.

In addition to hypertensive patients, approximately 64 million individuals with heart failure (9) could benefit from improved home-based hemodynamic monitoring. Closer follow-up may reduce emergency hospitalizations and preserve quality of life. (10)

Between 2013 and 2015, a Hungarian research group - including the author - began investigating the physiological and clinical relevance of peripheral pulse wave analysis in the context of pregnancy-related cardiovascular complications. The work during this early research revealed both the depths of the relevant literature and the practical limitations of existing technologies. (Detailed introduction of these limitations are found in section *1.7. Challenges related to measurement accuracy, variability and clinical validation.)* These findings motivated the development of a dedicated measurement platform, designed to support further research into the applicability of pulse wave analysis in health and disease. The present thesis introduces the results from the initial research needed to explore how the theory and practice of a dedicated peripheral pulse wave analysis approach can support future cardiovascular assessment and prevention. All of this work is guided by the main considerations of translational medicine. (11)

## 1.2. Basics of pulse wave analysis

### 1.2.1 Definition and basic concept

The pulse wave is a biophysical phenomenon generated by the contraction of the heart, which produces a pressure wave in the blood that travels through the arterial system. (12,13)

Specifically, the peripheral pulse wave originates from the left ventricular contraction and propagates through the arterial tree (from the elastic arteries through the muscular arteries and resistance arterioles), ultimately facilitating capillary blood flow. The cyclical changes in intravascular pressure cause the arterial walls to expand during systole and return to their original diameter during diastole. These dynamic changes can be assessed using various methodologies at peripheral sites, most commonly at the wrist or fingers. In this thesis, the focus will be on the peripheral pulse wave and systemic hemodynamics, with particular discussion on measurements recorded at the finger. By registering and analyzing the pulse wave, it is possible to monitor various cardiovascular functions in real

time. (14,15) To better understand its diagnostic potential, it is essential to explore how the pulse wave is generated and what key features define its morphology.

### 1.2.2. The basic "anatomy" of pulse wave morphology

After the left ventricle contracts, the created pulse wave travels along the arterial tree, propagating through elastic and muscular arteries at a velocity determined largely by arterial stiffness and blood pressure. As the pulse wave moves distally, it encounters changes in arterial geometry, such as bifurcations and sites of impedance mismatch - most notably at the level of the resistance vessels and lower limb arteries. At these points, part of the wave energy is reflected back toward the heart. This reflected wave then superimposes upon the ongoing forward wave generated by ventricular ejection.(16) Figure 1 presents a schematized pulse wave by its components.

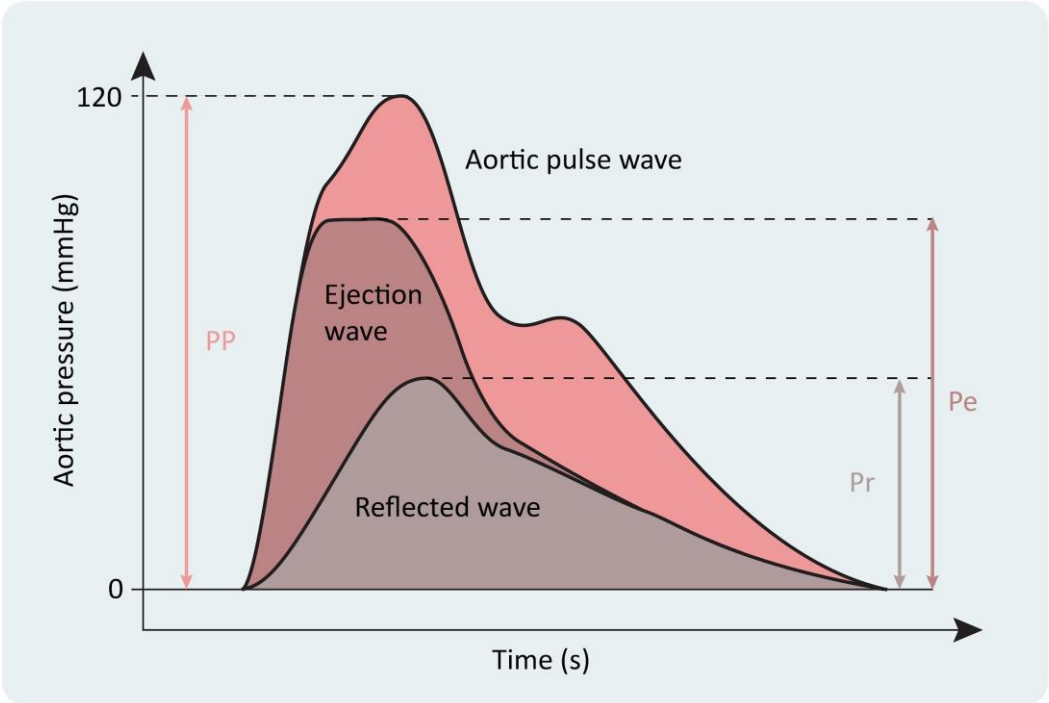


Figure 1 - **Formation of the aortic pulse wave by the superimposition of the forward (ejection) and reflected pressure waves**. (13,17) The pressure waveform observed in the aorta results from the interaction of these two components. The timing and amplitude of the reflected wave contribute to late systolic pressure augmentation. PP: pulse pressure Pr: pressure of the reflected wave, Pe: pressure of the ejection wave Adapted from: Mendes-Pinto et al. (18) Licensed under CC BY 4.0.(19)

The interaction of these two waveforms - the forward (incident) wave and the reflected wave - produces the final pressure waveform observed at any given arterial site. This process of wave interaction and the decreasing elastic content of peripheral arteries results in a phenomenon known as pressure augmentation, which refers to the elevation of late systolic pressure due to the timing and magnitude of the returning wave. (20)(Figure 2)

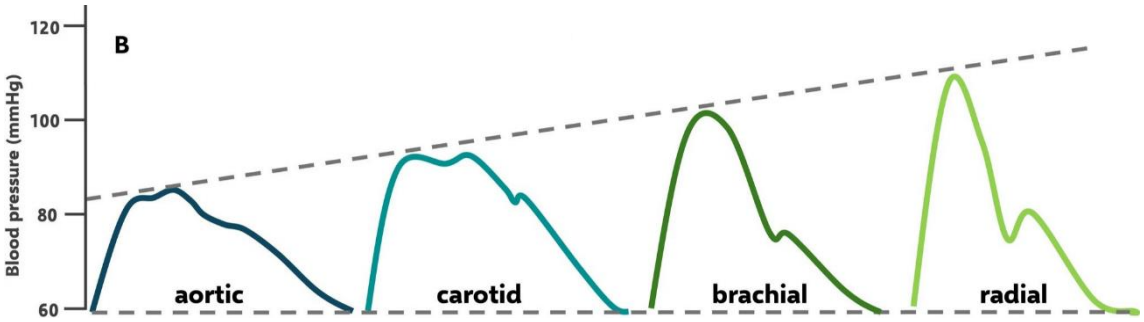


Figure 2 **- Pulse wave amplification or pressure augmentation**. Amplification of systolic blood pressure along the arterial tree, resulting in higher peripheral than central systolic pressure. Example waveforms from a healthy adolescent demonstrate aortic (~85 mmHg) and radial (~110 mmHg) systolic pressures, corresponding to a central systolic amplification of ~25 mmHg. Adapted from: Haseler et al.,2025. (21) Licensed under CC BY 4.0.

The pulse contour as a whole - including the timing of the systolic peak, the depth and prominence of the dicrotic notch and the shape of the diastolic downslope - is not only reflecting the effects of the left ventricular ejection dynamics, but also the mechanical properties and function of the arterial system. (22)

If we can understand the complex nature of the pulse wave, that will lead to appreciation of how a seemingly simple signal can withhold rich hemodynamic information. (23,24)

### 1.2.3. Central vs. peripheral hemodynamics

Understanding central hemodynamics - like central blood pressure, aortic wall stiffness or ventriculo-arterial coupling - is a key in cardiovascular risk stratification, since there is a stronger correlation between these and adverse CV outcomes, than peripheral measurements, like arm-cuff blood pressure measurement. (25,26) However, the measurement of central hemodynamics requires invasive arterial catheterization or

expensive tools, like MRI (27–29) or echocardiography which limits the wide accessibility of these important measures.

In contrast, the peripheral pulse wave - accessed from the radial artery or fingertips with different technologies - is more accessible for non-invasive, regular monitoring. The differences and similarities between the central and peripheral pulse wave is demonstrated on Figure 3.

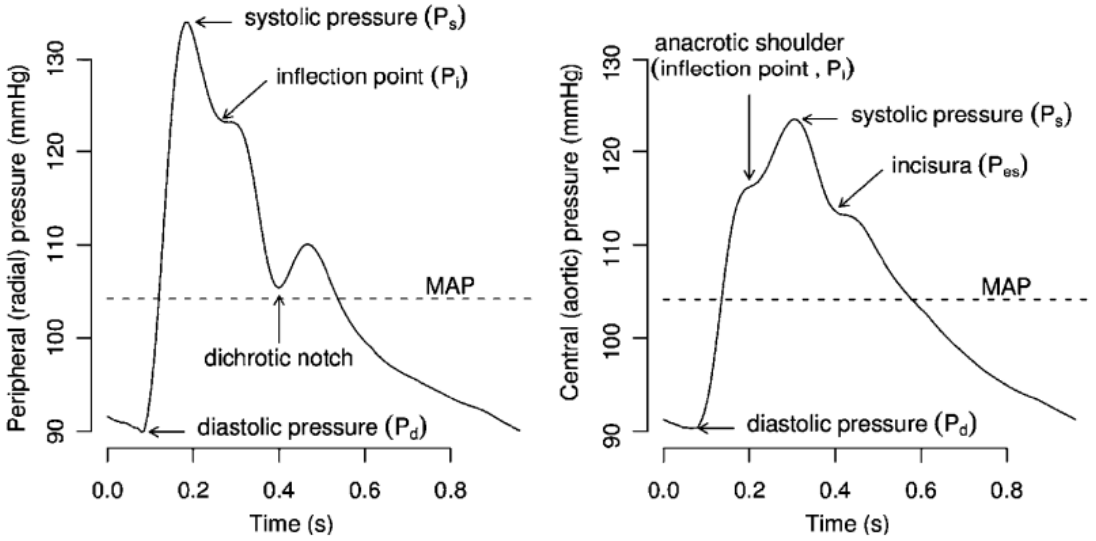


Figure 3 - **Differences between peripheral and central pulse wave morphology**. © Institute of Physics and Engineering in Medicine. Reproduced by permission of IOP Publishing Ltd. From: Avolio AP, Butlin M, Walsh A. Arterial blood pressure measurement and pulse wave analysis-their role in enhancing cardiovascular assessment. Physiological Measurement. 2009. DOI: https://doi.org/10.1088/0967-3334/31/1/R01 (30)

While some methods reconstruct central waveforms via generalized transfer functions, these algorithms are fully dependent on the morphological and harmonic characteristics of the peripheral waveform - effectively transforming, not generating, new physiological information. (31,32) This underscores the fact that peripheral pulse waves inherently contain relevant hemodynamic information. Rather than relying on indirect modeling, a promising alternative is to extract clinically meaningful parameters directly from the peripheral signal itself. (33) If validated against gold-standard techniques, this approach could offer a practical, scalable solution for routine cardiovascular assessment, especially in remote or resource-limited settings.

1.3. Pulse wave analysis (PWA), as a promising method for non-invasive cardiovascular monitoring.

Current cardiology assessments include physical examination, auscultation, pulse palpation, electrocardiography, and echocardiography to evaluate heart function and anatomy. However, a key non-invasive bedside tool - pulse wave analysis - is notably absent from routine practice. While pulse palpation offers minimal peripheral insight, it falls short of leveraging the full diagnostic potential of pulse wave morphology.

However, the peripheral pulse wave, as a summation signal holds information on various aspects of the cardiovascular system, for example:

- the time of left ventricular ejection from the beginning of the cardiac cycle to the closure of the aortic valve ~ left ventricular (LV) function (34)
- the time it takes for the left ventricle to reach the systolic peak from the beginning of the cardiac cycle ~ increasing with age (35)
- steepness of the upstroke ~ determined partly by the inotropy of the LV (36)
- the prominence of the second (diastolic) peak - aortic elasticity/distensibility (37)
- the dime delay between the systolic and diastolic peak ~ large artery stiffness (38)
- the relative height of the diastolic peak to the systolic peak ~ afterload (14)
- the relative height of the b wave to the a wave on the second derivative of the pulse wave ~ hypothesized to be a surrogate for ventriculoarterial coupling (39)
- central and peripheral arterial wall tension, complex effect on many parameters ~ blood pressure (40)
- heart rate and its regularity ~ arrhythmias (41)
- autonomic nervous system function, cardiac neuropathy assessment through heart rate variability (42)

Alterations of the pulse wave parameters, generated from the physiological relations summarized above, have been associated with cardiovascular pathologies such as arterial stiffness, atherosclerosis, hypertension, aging, diabetes, coronary heart disease, and heart failure.(43–51)

1.4. Basics of photoplethysmography

Photoplethysmography (PPG) is a non-invasive optical technique used to detect peripheral arterial pulsations by measuring changes in light absorption within biological tissue. This method relies on the fact that pulsatile blood flow causes periodic changes in tissue volume, particularly in arteries and arterioles, which in turn modulate the absorption of emitted light. The resulting signal comprises two components: a direct current (DC) component reflecting the static absorption of tissue (bone, fascia, muscle, venous and capillary blood, fat, etc.) and a pulsatile alternating current (AC) component that corresponds to the dynamic volume changes of arterial blood (and the venous flow also plays a limited role in the AC part). The waveform of the AC component mirrors the pulse-induced fluctuations and forms the basis for further pulse wave analysis. (15,52) (Figure 4)

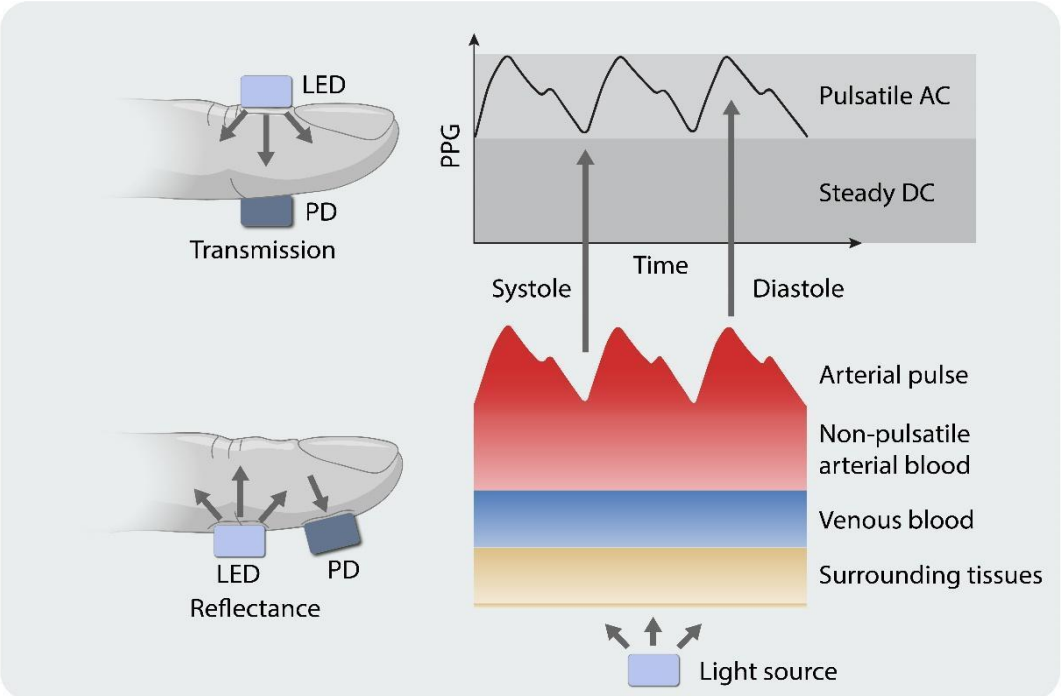


Figure 4 - **Illustration of photoplethysmography sensing technology - transmissive vs. reflective mode** - (53,54) -as taken from the e-learning materials of E-Med4All Europe Ltd., with permission granted by the author. (19) Abbreviations: LED: light emitting diode, PD: photodiode, AC (alternating current) and DC (direct current) are widely used terms referring to the pulsatile and constant part of the photoplethysmographic signal, respectively.

The PPG recording executed on the finger is called the Digital Volume Pulse (DVP). (45)

The photoplethysmographic (PPG) method for detecting the peripheral pulse waves offers numerous practical benefits, including:

- It's non-invasive and safe
- It causes no discomfort or risk to the patient
- The measurement process is quick
- It doesn't require specialized skills to operate
- The method is repeatable

For the best results in pulse wave detection using the PPG method, it's advisable to adhere to standardized conditions for measurement:

- Conduct measurements at room temperature
- Ensure the patient is in a resting position for at least 10 minutes before the measurement
- Avoid any movement during the measurement
- Consistently use the same finger for the device placement in repeated measurements

### 1.5. Key parameters derived from pulse wave analysis

By the various mathematical analysis methods of the pulse wave countless parameters and indices can be calculated. (14,15,54)

These include morphological (pulse contour) and pulse rate variability (PRV) parameters, which jointly describe the current condition of cardiac, vascular and regulatory mechanisms. Morphological parameters are determined by mathematical analysis of the pulse curve, whereas PRV parameters are calculated by analyzing the variability of the time intervals between peaks (interbeat intervals). (55) This thesis will focus solely on pulse contour parameters. Their names and definitions with the corresponding references can be found in the Methods section.

## 1.6. Potential Fields of Pulse Wave Analysis Application

Photoplethysmography (PPG)-based pulse wave analysis (PWA) is most widely used in research for the assessment of vascular aging but offers broader applicability across various medically relevant fields. Key application areas include:

1) **Vascular Age Assessment:** PWA can be used to estimate vascular age by analyzing arterial stiffness and waveform morphology. PPG parameters have shown correlations with cardiovascular risk and are used in both consumer and clinical devices. (15,46,56–58) However, it is important to note that some articles connecting chronological age with pulse wave features, defining "vascular age index" and similar parameters (59) are lacking the information on CVD risk profile, thus limited in the clinical decision making. Moreover, other confounders are affecting the pulse wave morphology and signal quality as subjects age, which have to be considered for a more appropriate estimation, e.g.: skin thickness, capillary recruitment. (60)
2) **Monitoring Lifestyle Interventions:** Pulse wave parameters reflect improvements from lifestyle changes (e.g., exercise, diet, smoking cessation), providing measurable feedback on cardiovascular health. (37,61–64).
3) **Arterial Stiffness Estimation:** Arterial stiffness, a strong predictor of cardiovascular events, can be evaluated using pulse wave features such as stiffness index. Some results suggest that PWA offers a potential non-invasive, operator-independent alternative to tonometry. (38) Conversely, PPG-derived arterial stiffness indices reflect peripheral pulse wave characteristics and are influenced by hemodynamic and measurement-related factors, therefore it is still debated if they can only be regarded as indirect markers of vascular function or reliable direct measures of central arterial stiffness. (65)
4) **Blood Pressure Monitoring:** Cuffless estimation of blood pressure (BP) using PWA is under active development. Understanding hemodynamic contributors to BP (e.g., hypervolemia, hyperinotropy) from different pulse wave patterns may support personalized therapy. (8,40,66) However, PWA-based cuffless BP estimation remains limited by its strong dependence on calibration and by the multifactorial determinants of pulse wave morphology, which are influenced not only by arterial pressure but also by vascular tone, wave reflections, and peripheral vasomotion. Consequently, the

attribution of specific pulse wave patterns to distinct hemodynamic mechanisms and their direct translation into personalized therapeutic decisions remain uncertain. (66)

5) **Atherosclerosis and Peripheral Arterial Disease (PAD) Detection** Asymmetric waveform alterations between limbs, detected via simple, non-invasive, operator independent PPG analysis, can support early PAD diagnosis in primary care. However, bilateral asymmetry-based PPG approaches are inherently less sensitive in cases of symmetrical or bilateral PAD, where inter-limb waveform differences may remain small despite clinically relevant disease. In such scenarios, reliance on asymmetry alone may underestimate disease presence, necessitating comparison against population-based normative ranges or complementary diagnostic methods. (67)

6) **Detection of Atrial Fibrillation (AFib) and Other Arrhythmias:** PPG-derived pulse irregularities allow for detection of arrhythmias such as AFib or extrasystoles, which alter beat-to-beat waveform features (prominent morphological and heart rate variability alterations during irregular heartbeats). (68–70) However, AFib-related pulse irregularity detected by PPG reflects probabilistic peripheral pulse manifestations rather than direct atrial electrical activity, and pulse detection performance deteriorates during short RR intervals and recent-onset AFib episodes. (69)

7) **Heart Failure Monitoring:** Heart failure is associated with characteristic changes in cardiac output, arterial compliance, and autonomic function - factors that have an impact on peripheral pulse wave morphology too. PPG-based pulse wave analysis captures these hemodynamic features and can support remote, longitudinal monitoring, especially where echocardiography is not readily accessible. (15) Recent pilot studies have demonstrated that PPG signals acquired from PPG based wearable devices can help detect heart failure and even correlate with pulmonary capillary wedge pressure - an important hemodynamic marker in heart failure. (71,72) However, current evidence is mainly derived from small pilot studies, and the association between peripheral PPG-derived waveform features and central hemodynamics is indirect and influenced by multiple confounders such as vascular tone, arterial stiffness, autonomic regulation, and local perfusion at the measurement

site. Observed correlations are moderate, context-dependent, and not specific to heart failure, underscoring the need for larger cross sectional and longitudinal validation studies. (71)

8) **Hemodynamic Monitoring in Pregnancy:** PPG-PWA is also ideal for non-invasive tracking of maternal cardiovascular adaptation during pregnancy. Parameters such as reflection index or "pulse transit time" (which is rather ΔT between the systolic and diastolic peak of the pulse wave) change throughout gestation and may aid in early detection of complications like preeclampsia. (73,74) In preeclampsia, elevated PPG-derived reflection and stiffness indices have been reported; however, these alterations overlap with physiological gestational ranges and show limited specificity for disease stratification, including dipper versus nondipper phenotypes. (75) Consequently, while PPG-PWA is well suited for longitudinal monitoring of maternal cardiovascular adaptation, its role in early screening of hypertensive pregnancy disorders requires further prospective validation. There is an ongoing pilot since 2019 in Hungary too, with the collaboration of the health visitors' network. (76)

1.7. Challenges related to measurement accuracy, variability and clinical validation.

Undoubtedly, these scientifically well-established characteristics of PPG-based detection and analysis of DVP make this method a potential tool for remote cardiovascular monitoring. Incorporation of photoplethysmography-based analysis of the digital pulse wave in telemedical systems may be an optimal solution for cardiovascular telecare Despite this, it has not gained ground in clinical practice so far and its reliability is debated (37,77) One reason why the applicability of the method is debated that the parameters computed from DVP are sensitive to errors and cannot be detected reliably as they fluctuate from one measurement to another.(37,51,78,79) A key limiting factor might be the insufficient and often inconsistent physiological interpretation of PPG-derived parameters, resulting from heterogeneous methodologies, variable signal quality, and inadequate separation of technical and biological sources of variability. (60,80) This leads to the question: where does this variability come from? Is it from the dynamics of the ever-changing human cardiovascular function? Or does it come from technical errors? Or a combination of the two? This issue is particularly emphasized in the case of those parameters which are derived from the second derivative of the DVP. The acceleration

plethysmogram (other expression for the second derivative of the PPG wave) has several distinguished points from which valuable cardiovascular indices can be calculated (Figure 5).

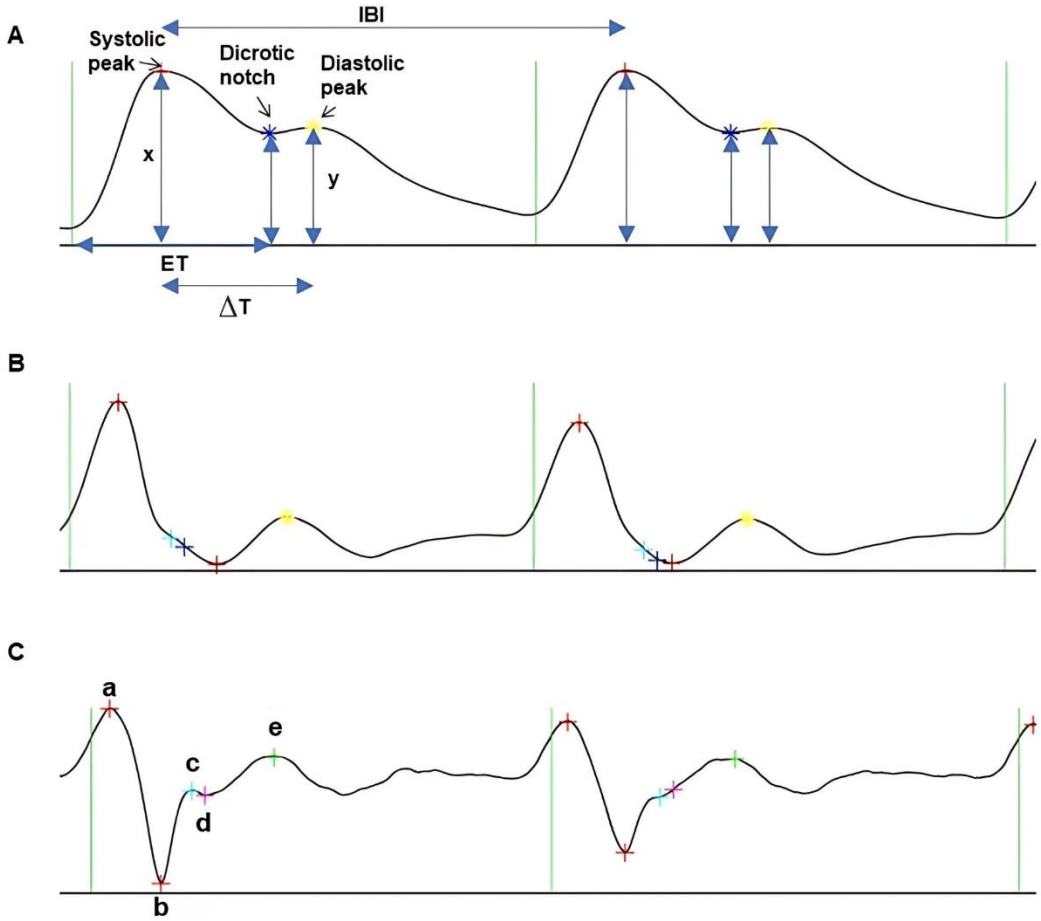


Figure 5 - **Representative pulse wave recording by the SCN4ALL system**. Original pulse curve (panel A), and its first-, (panel B) and second derivative curves (panel C). Abbreviations: IBI: inter-beat-interval, x: relative height of the systolic peak, y: relative height of the diastolic peak, ΔT: time difference between systolic and diastolic peak (ms). a,b,c,d and e points: fiducial inflection points on the second derivative. Adapted and modified from Kulin et al. (51), licensed under CC BY 4.0 (https://creativecommons.org/licenses/by/4.0/), https://doi.org/10.3390/app10227977

Among these, c and d points (Figure 5) have been introduced as characteristics that may facilitate our understanding of the dynamics of wave reflection and the pulse wave analysis based evaluation of the severity of arterial aging. (45,81–85) However, the detection of these points has become a challenge for mathematical algorithms to identify. (86–88)

Moreover, PPG-based PWA for patient monitoring faces a fundamental challenge: there is ongoing debate about whether the DVP reliably reflects central hemodynamics or is primarily influenced by peripheral factors. According to Miyashita et al. (89), local pressure wave reflection significantly determines the peripheral pressure waveform and pulse pressure amplification, suggesting that peripheral signals may not accurately represent central aortic pressures. In contrast, a later study published by the same author presented results of certain parameters - such as the second derivative of the digital photoplethysmogram (SDPTG) - can provide more reliable central hemodynamic information, suggesting that peripheral signals may still provide valuable insight into central cardiovascular status. (90) This uncertainty drives further research to determine whether DVP can - and if yes, under what conditions - reliably estimate central hemodynamic parameters or whether its primary benefit is limited to the assessment of peripheral vascular function.

Currently, echocardiography is the standard, non-invasive method for assessing central hemodynamics, cardiac structure and function. Due to its widespread clinical use and known reliability, comparing echocardiographic measurements with the results of PPG-based pulse wave analysis (PWA) offers a pragmatic approach to further investigate the clinical potential of PPG based hemodynamic data. However, despite the potential value of PPG-based PWA for assessing cardiovascular information, there are relatively few studies in the literature that directly compare these methods. Another limitation of these few studies that they often focus on only a limited number of PPG-echo parameter pairs.

There are some studies, however, which focused on the correlation between peripheral and central hemodynamics by specifically assessing the associations between PPG and echocardiography-based parameters. A short overview of these publications is found in Table 1.

It is important to note that these comparative studies typically focused on a narrow range of parameters, mainly cardiac output or ejection time, without exploring a more comprehensive spectrum of pulse wave characteristics that can be extracted from peripheral PPG signals. In addition, differences in measurement conditions, patient populations and signal processing methods in the referenced studies may have contributed to the conflicting results.

Therefore, further studies in this field might reveal new information, as mapping a wider range of pulse wave parameters and their relationship with markers of central hemodynamics could lead to a better understanding of which fields of (cardiovascular) medicine can benefit the most from PPG based pulse wave readings or regular monitoring.

Table 1 - Summary of studies comparing photoplethysmography-derived and echocardiographic measurements of cardiac function in different research settings

| **Study** | **PPG Method** | **Reference Standard** | **Population** | **Main Findings** |
|---|---|---|---|---|
| Chen et al. (91) | Volume-clamp (Nexfin) | Esophageal Doppler | Surgical patients | Strong correlation ($r^2$ = 0.82), 94% trending concordance, robust under phenylephrine-induced changes |
| Duan et al.(92) | Peripheral PPG | Echocardiography, M-mode & Doppler | Healthy volunteers | PPG LVET longer (348 ms) and more variable (SD 11 ms);<br>less accurate than Doppler (309 ms, SD 9 ms) |
| Meah et al. (93) | Modelflow® via finger PPG | Echocardiography | Non-pregnant, pregnant, and postpartum women | Poor agreement at rest and exercise (mean bias >1 L/min); not recommended for CO assessment in women |
| Blanié et al. (94) | Volume-clamp | Echocardiography/ Doppler | Surgical patients | Weaker correlation with cardiac output; PPG less reliable for absolute values |
| Kavas et al. (95) | Peripheral PPG + HRV feature | Echocardiography (LVEF-based diagnosis) | Healthy + HF patients (HFrEF, HFpEF) | ML model classified HF states with 87.8% accuracy using PPG+HRV; strong potential for non-invasive screening |

## 2. Objectives

To address the limitations detailed in the last chapter of "Introduction - 1.7.", a dedicated high-resolution PPG-based research system was developed to enable standardized data acquisition and systematic physiological investigation of peripheral pulse wave features. In parallel, clarifying the relationship between peripheral pulse wave characteristics and central cardiovascular function represents a critical prerequisite for future hypothesis-driven clinical research.

**Study 1** - Physiological stability and variability of PPG-based peripheral pulse wave parameters

This study aimed to characterize the short-term physiological stability and sources of variability of non-invasively derived peripheral hemodynamic parameters based on PPG pulse wave analysis, by separating measurement-related variability from true physiological variation under controlled conditions.

Specifically, the objectives were:

- To quantify the technical contribution to variability in PPG-derived pulse wave parameters using artificially generated pulse wave signals under identical measurement settings, in order to distinguish device- and algorithm-related effects from physiological behavior
- To assess short-term intra-subject physiological variability of selected PPG-derived hemodynamic parameters in healthy volunteers during repeated measurements under strictly standardized conditions
- To compare intra-subject variability with inter-subject variability across individuals measured under identical protocols, thereby identifying parameters that primarily reflect individual physiological differences
- To evaluate the influence of anatomical measurement site on pulse wave morphology and derived parameters, using simultaneous recordings from four different fingers (left/right index and ring fingers)

**Study 2** - Relationship between peripheral pulse wave features and central cardiac function

The second study examined how specific morphological and timing-related features of the peripheral pulse wave relate to central cardiac structure and function, as assessed by echocardiography in healthy individuals.

The objectives were:

- To investigate the association between PPG-derived timing parameters and echocardiographic measures of left ventricular ejection time (LVET)
- To explore whether distinct pulse wave morphological features correspond to echocardiographic indicators of systolic and diastolic cardiac function
- To identify PPG-derived parameters that demonstrate the closest physiological alignment with established echocardiographic measures, without implying direct clinical interchangeability

# 3. Methods

## 3.1. Overview and technical description of the SCN4ALL system

To answer the research questions detailed in “Objectives”, a dedicated PPG-based pulse wave analysis system was developed with the participation of the author. The development of the SCN4ALL platform was initiated in 2016 to address methodological limitations of existing tools for peripheral pulse wave research and analysis, particularly the restricted access to raw signals and limited standardization of data acquisition. (See details in “Introduction - 1.7. Challenges related to measurement accuracy, variability and clinical validation.”)

In each investigational protocol, pulse wave was recorded as digital volume pulse (DVP) detected by a commercially available transmission pulse oximeter (Berry Pulse Oximeter, Shanghai Berry Electronic Tech Co., Ltd., Shanghai, China; hardware: 32-bit AD converter, 200 Hz sampling rate). The device emits light to the tissues of the finger from an LED light source and detects the transmitted light by a photodiode. Vessel diameter and blood volume in the arteries change with pulsation, and so does the amount of transmitted light due to the changes in the amount of blood cells present in the way of it, enabling the detection of a continuous DVP. The pulse oximeter device communicates via Bluetooth connection with a mobile application that initiates and terminates a 140-second-long data acquisition and transmits the recording to a cloud-based automated algorithm that was developed by our research group. (51) (Figure 6)

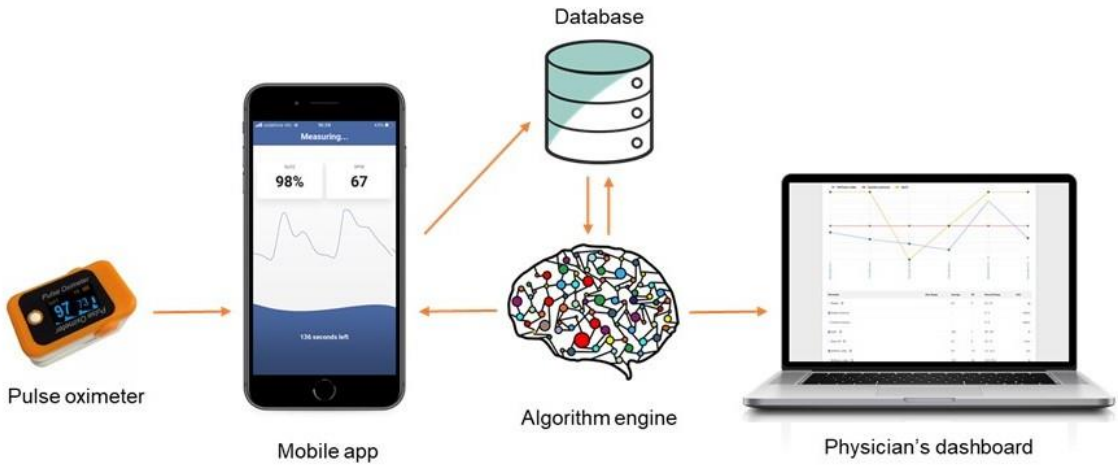


Figure 6 - Outline of the SCN4ALL telemedicine system. Adapted from Kulin et al. (51), licensed under CC BY 4.0 (https://creativecommons.org/licenses/by/4.0/), https://doi.org/10.3390/app10227977

During the course of the research, two closely related but not identical signal-processing implementations were applied. In the first study, the 200 Hz PPG signal was resampled to a higher temporal resolution (1 kHz) as part of an early signal-processing implementation prior to morphology-based analysis. In subsequent studies (including Study 2), using the upgraded SCN4ALL system, signal processing was performed directly at the native 200 Hz sampling rate without resampling. Subsequent preprocessing steps were applied consistently across both implementations.

To minimize edge effects related to signal stabilization and preprocessing, only a 120-second segment of the recorded 140-second PPG signal was selected for further analysis, with the initial 15 seconds and the final 5 seconds excluded. To condition the PPG signal, a digital bandpass filter - fourth-order Butterworth - with -3 dB points at 0.1 and 10 Hz is applied. Then, the algorithm identifies the pulse cycles. Afterward, within each cycle, fiducial points of the DVP (primary curve, first and second derivatives) are identified. Then, contour parameters are computed for every individual cycle. Afterward, the means of all cycles are calculated and displayed on an internet platform for the physician. In this study, these averages were exported as spreadsheets for further analysis. The measurement data are stored at a cloud-based server (Amazon Web Services, Amazon Web Services EMEA SARL, 1855 Luxembourg, Luxemburg) equipped with safe data protection that conforms to the applicable regulations ((EU) 2016/679). (51)

### 3.2. Protocol - Study 1 - Repeatability and reliability

#### 3.2.1. Assessment of Measurement Variability

To evaluate the variability caused by measurement errors in the SCN4ALL system (including DVP recording, data processing, and analysis), we used artificial signals generated by a pulse simulator device (MS100 SpO2 Simulator, Contec Medical Systems Co., Ltd., Qinhuangdao, China). We performed 5 repeated measurements for each of the three signal settings - **Normal** (SpO2: 98%, HR: 55/min), **Abnormal 1** ("geriatric" - SpO2: 92%, HR: 95/min), and **Abnormal 2** ("weak" - SpO2: 90%, HR: 95/min) - using 5 different pulse oximeters of the same model.

#### 3.2.2. Intrapersonal Variability at Standard Conditions

To determine the physiological variability remaining after standardizing conditions, we conducted 10 repeated 2-minute measurements on 10 healthy individuals (5 males, 5 females; age 19-35, mean age: 25.3 ± 4.3 years) under standardized conditions. Measurements took place in a quiet room at room temperature, in the morning, at least two hours after the last meal and coffee, in a sitting position with hands resting on a table. The left index finger was used for all measurements.

#### 3.2.3. Anatomical Variability: Parallel Finger Measurements

To assess the effect of anatomical differences between fingers, we performed parallel 2-minute measurements on 4 fingers (left and right index and ring fingers) using 4 pulse oximeters. The study included 25 healthy subjects (17 males, 8 females; age 19-49, mean age: 29.4 ± 8.4 years).

### 3.3. Protocol - Study 2 - Central vs peripheral hemodynamics - comparison with cardiac ultrasound measurements

In this study, we employed temporally aligned recordings to capture and compare data from photoplethysmography (PPG) and echocardiography under comparable resting conditions. PPG parameters were calculated by averaging measurements from each heartbeat during continuous recordings over a 140-second period. Concurrently, echocardiographic parameters were derived by averaging the data from 1-3 heartbeats, in

line with standard clinical echocardiographic practice. The echocardiographic examination lasted approximately 20 minutes, and the 2-minute PPG recording was performed during the examination under stable resting conditions.

### 3.3.1. Echocardiography

Standard two-dimensional transthoracic echocardiography was performed in accordance with current EACVI recommendations. (96) Blood pressure (BP) was measured three times using an automatic sphygmomanometer before conducting a cardiac ultrasound scan. During the scan, the participant lay on the examination bed with the upper body undressed, positioned on the left side. 2D echocardiography examinations were performed with a GE Vivid E95 system with a 4Vc-D phased-array transducer (GE Vingmed Ultrasound, Horten, Norway). LV focused, ECG-gated datasets were obtained from parasternal long and short axis, apical four-chamber, apical three-chamber and apical two-chamber views at a minimum rate of 50 frames per second. Offline analyses of these datasets were performed after selecting the optimal heart cycle using commercially available software (Autostrain LV, TOMTEC Imaging Systems GmbH, Unterschleissheim, Germany). The algorithm automatically generated the endocardial contours of the cavities, which were manually corrected throughout the entire cardiac cycle. Speckle tracking technique was used for the deformation analysis. The assessed echocardiography parameters can be found in Table 2.

Table 2 - List of echocardiographic parameters with abbreviations and definitions.

| Abbreviation | Definition |
|---|---|
| **EF (%)** | Ejection fraction |
| **LVET (ms)** | Left ventricular ejection time |
| **LV-EDD (mm)** | Left ventricular end-diastolic diameter |
| **LV-ESD (mm)** | Left ventricular end-systolic diameter |
| **LV-SV (ml)** | Left ventricular stroke volume |
| **LV-GLS (%)** | Global longitudinal strain |
| **LVOT-VTI (cm)** | Left ventricular outflow tract velocity time integral |
| **MV-E (cm/s)** | Mitral E-wave velocity |
| **MV-A (cm/s)** | Mitral A-wave velocity |
| **MV-E/A** | The ratio between E-wave and A-wave |
| **E/e' - lat** | Early diastolic mitral inflow velocity to early diastolic mitral annulus velocity |
| **e'-med (cm/s)** | Mitral medial annulus velocity |
| **Ao, root diam (mm)** | Aortic root diameter |
| **Ao-VTI (cm)** | Aortic maximum flow velocity time integral |

3.3.2. PPG measurements

During the cardiac ultrasound, a pulse waveform was recorded for 140 seconds using a special pulse oximeter on the patient's right index finger, with a 200 Hz sampling frequency (Shanghai Berry Electronic Tech Co., Ltd., Shanghai, China). The patient lay on their side, staying still. The oximeter, wirelessly connected to the SCN4ALL mobile app (E-Med4All Europe Ltd, Budapest, Hungary), sent the anonymized data in real time to a secure online database. The SCN4ALL software analyzed the signals, its proprietary algorithm identifies points of interest on the pulse wave from which it calculates over 30 morphological and pulse rate variability parameters online as described above. The SCN4ALL parameters assessed in both studies are found in Table *4*.

3.4. Subjects

Number of participants with specific inclusion and exclusion criteria, study location and ethical approval number (IRB) of the studies are summarized in Table *3*.

Table 3 - Overview of participants with inclusion and exclusion criteria in Study 1 and 2.

| | Study 1 | Study 2 |
|---|---|---|
| **Participants** (n) | 25 | 37 |
| **Inclusion** | • Age 18 and older, both biological sexes<br>• BMI between 18.5 and 30 kg/m^2 | • Age: 18-60, both biological sexes<br>• Normal BMI (18 - 25 kg/m^2) |
| | • Healthy individuals (physically and mentally, self-declaration)<br>• Does not smoke<br>• Does not consume alcohol regularly | |
| **Exclusion** | • Diagnosed with or treated for any CV disease<br>• Pregnancy<br>• Known other chronic or cancerous diseases<br>• Wears nail polish or artificial nails<br>• SARS-CoV-2 infection in the last 6 months (only in Study 2) | |
| **IRB approval No**. | 120/2018 | 120/2018-3 |
| **Location of study execution** | Institute of Translational Medicine, Semmelweis University, Budapest | Városmajor Heart and Vascular Centre, Semmelweis University, Budapest |

3.5. SCN4ALL Parameters assessed by Study 1 and Study 2

The following set of parameters (Table 4) is only a collection of the many possible options published in the medical literature. Moreover, with the years of use and testing, our working group has developed and defined some new PPG parameters as it was hypothetized that they point to some dedicated, however currently overlooked aspects of the cardiovascular function.

Table 4 - List of PPG parameters, with abbreviations and definitions. Legend: * These parameters are developed by the scientific team behind the SCN4ALL system. Most of them are not yet validated in clinical studies, their definition and meaning are hypotheses based on the current understanding of pulse wave physiology. **(s)**: In Study 2 The findings for these parameters are presented in the supplementary materials, due to their correlation with echocardiography parameters being lower than 0.4. (Supplementary Table 1). "**@75**" after some PPG indices: the original time value is corrected to 75/min heart rate (31)

| Abbreviations/ Parameter names | PPG parameter definition | Study 1 or 2 or 1+2 |
|---|---|---|
| **Interbeat interval (ms)**(55) | The average of all the measured peak-to-peak time differences of the 120 sec. registered signal. | **1** |
| **c-d incidence (c-d point detection ratio)*** | The proportion of periods in which the algorithm identifies c-d points on the second derivative of the PPG (SDPTG, or accelerated plethysmogram (APG)) relative to all periods. *(Figure 1 from Study 1* (51)*)* | **1** |
| **HR** | **Mean Heart Rate** The mean value of the heart beats per minute (1/min). The algorithm calculates a heart rate from the length of each period of the 120-second signal and averages them. | **1+2** |
| **Si** (38) | **Stiffness index:** h/ΔT(m/s); h is the height of the person in meters. ΔT is the time between the systolic peak and diastolic peak on the pulse curve in seconds. | **1+2(s)** |
| **b/a** (46) | The ratio of the first two inflection points of the second derivative of the pulse wave. | **1+2** |
| **d/a** (43) | The ratio of the fourth to the first inflection points of the second derivative of the pulse wave. | **1+2** |
| **AGEi** (46) | **Ageing-index** The value derived from the second derivative of the pulse wave. AGEi= b-c-d-e/a | **1+2** |
| **Ri** (14) | **Reflection index** The ratio of the amplitude of the diastolic peak to the amplitude of the systolic peak. | **1+2(s)** |
| **LVETi** (44) | **Left ventricular ejection time index**ed for heart rate (LVETi) was calculated from sex-specific resting regression equations LVETi(male) = 1,7 × heart rate + ET(PPG), LVETi(female) = 1,6 × heart rate + ET(PPG). | **1+2** |
| **DNi *** | **Dicrotic notch index *** Describes the relative position of the diastolic peak to the dicrotic notch (the valley induced by the aortic valve closure before the diastolic peak). | **2** |

| Abbreviations/ Parameter names | PPG parameter definition (Table 4 - **cont.**) | Study 1 or 2 or 1+2 |
|---|---|---|
| **eLVET1 *** | **Early left ventricular ejection time 1 and Early left ventricular ejection time 2** ELVET1 is measured from the start of the period to the first peak of the first derivative of the pulse, whereas ELVET2 is defined as the time duration from the first peak of the first derivative PTG to the peak of the systolic wave. | **2** |
| **eLVET2 *** | | **2** |
| **eLVET1 @75 *, (s)** | | **2(s)** |
| **eLVET2 @75 *** | | **2** |
| | **@75 - ELVET1,2 compensated for 75/min heart rate** | |
| **Crest Time** (37) | **Crest Time -** The time elapsed between the beginning of the period (foot) and the maximum systolic amplitude (peak) | **2** |
| **Crest Time @75** | | **2** |
| | **@75 - Crest time compensated for 75/min heart rate** (37) | |
| **ET(PPG)** (14) | **PPG based Left ventricular ejection time** | **2** |
| **ET(PPG) @75(s)** | It is the time elapsed between the beginning of the pulse period and the aortic valve closure (dicrotic notch/e-point). **@75 - ET compensated for 75/min heart rate** (37) | **2(s)** |

3.6. Statistical Analysis - Study 1

Cycles with irregular duration or atypical morphology were automatically excluded by the algorithm (<5% in all cases). For each parameter, the average of all valid pulse cycles from the 2-minute recordings was used for analysis. Descriptive statistics were reported as means with 95% confidence intervals. To evaluate variability, the coefficient of variation (CV) was calculated for both artificial signal recordings (as a measure of repeatability) and repeated human measurements taken under standardized conditions (test-retest variability). Threshold of 2% was set for acceptable repeatability and 10% was set for test-retest variability. For the four-finger protocol, we calculated intraclass correlation coefficients (ICC) using a linear mixed-effects model to determine how closely measurements from different fingers agreed and how much of the overall variability came from differences between individuals. All statistical analyses were performed using IBM SPSS Statistics, version 26.

### 3.7. Statistical Analysis - Study 2

To examine how well PPG- and echocardiography-derived ejection times matched, Bland-Altman analysis was used to calculate the bias and the 95% limits of agreement. Ratios and percent differences were also used to evaluate relative agreement. Correlation analyses were performed to assess the strength of association between PPG- and echocardiography-derived parameters in JASP (JASP Version 0.19.3; JASP Team, 2025), using Pearson or Spearman methods based on the normality of variables (tested with the Shapiro-Wilk test). Scatter plots were used to visualize associations between variables; fitted linear trend lines were displayed for descriptive purposes only and do not represent regression models. Significant associations ($p < 0.05$, r (Pearson)/ρ (Spearman) > 0.4) are reported in the main text, while additional and heart rate-adjusted correlations are found in Supplementary Tables 1 and 2 in Kulin et al. (97)

# 4. Results

## 4.1. Results - Study 1

Results indicated that the system reliably detected and analyzed normal pulse signals, with coefficient of variation (CV) values below 1% for all calculated variables, indicating high stability. Even in the abnormal signal conditions (high heart rate and low intensity), the majority of parameters remained stable, except for the aging index and d/a parameter, due to the absence of detectable c and d points in the second derivative. (Table *5*)

To assess the reliability and stability of human pulse wave measurements, we performed 10 repeated resting measurements in 10 healthy volunteers (M/F: **5/5**) under standardized conditions. The mean age was 25.3 ± 4.5 SD years, and the mean BMI was 22.3 ± 2.9 SD kg/m². Several parameters, including the b/a ratio, left ventricular ejection time index, mean interbeat interval, stiffness index, and mean heart rate, showed CV values below 10%, indicating reliable consistency. However, the aging index demonstrated slightly higher variability (CV: 13.6%), and the d/a and c-d point detection ratios showed high variability despite unchanged conditions. (Figure 7.)

To investigate anatomical variability, we conducted parallel measurements on four different fingers in 25 individuals, aged 19-49 years. The mean age of the participants was 29.4 ± 8.6 SD years, and the mean BMI was 23.7 ± 4.0 SD kg/m². For most parameters, there was no significant difference between fingers. ICC values exceeded 99% for mean interbeat interval, mean heart rate, and left ventricular ejection time index, suggesting that finger choice had virtually no impact on these measures. Other parameters - such as stiffness index, c-d point detection ratio, reflection index, b/a ratio, d/a ratio, and aging index - had slightly lower ICCs (80-90%), but still indicated that anatomical variability was small compared with differences between individuals. (Table 6)

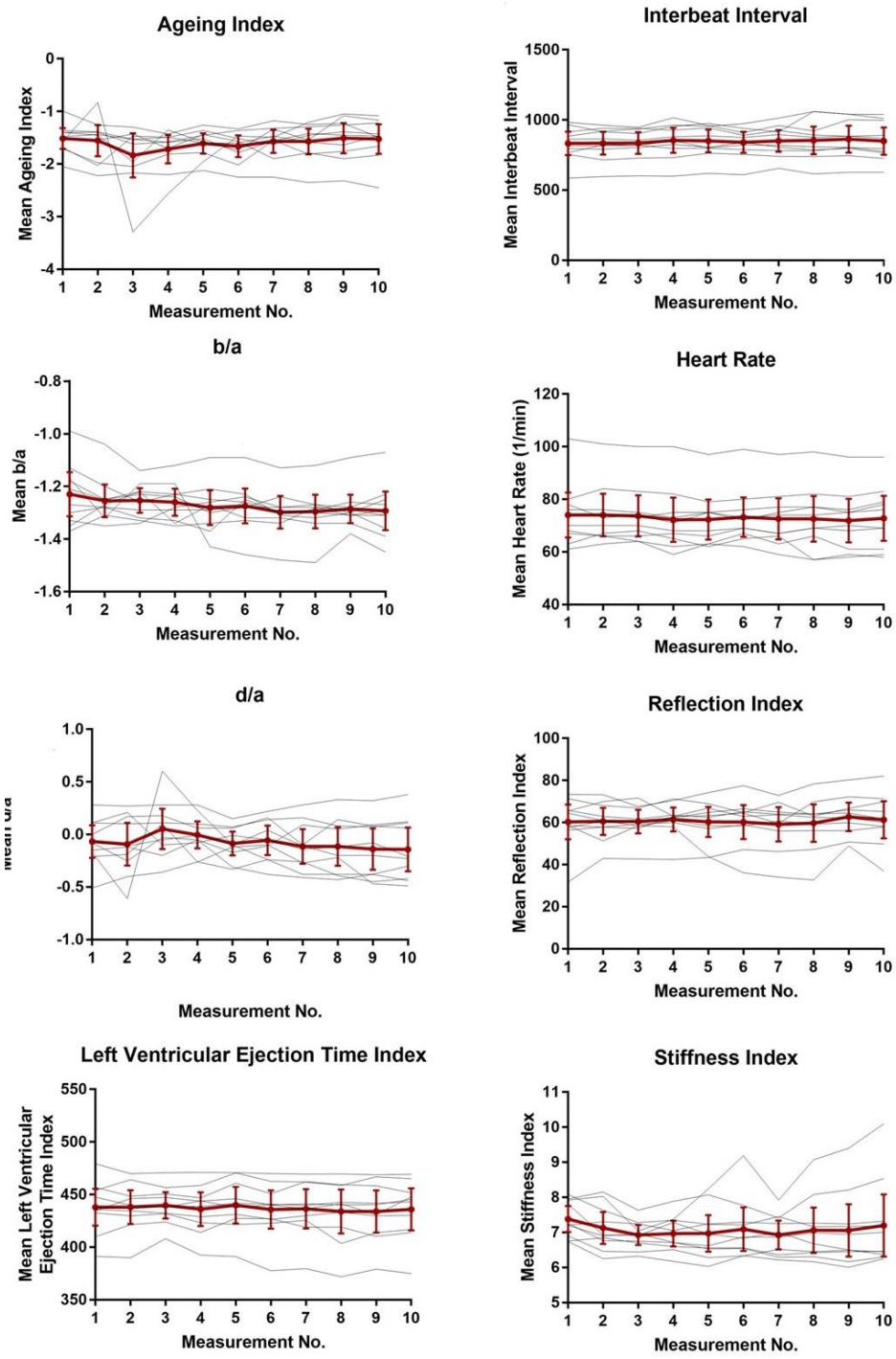


Figure 7 - **Graphs demonstrating the relationship between interpersonal variability and intrapersonal variations of the computed pulse contour parameters**. Measurements were performed on 10 healthy volunteers 10 times repeatedly under standardized conditions. Means (±confidence intervals) are presented (red solid line) for each consecutive measurement along with individual measurement data (black lines). Adapted and modified from Kulin et al. (51), licensed under CC BY 4.0 (https://creativecommons.org/licenses/by/4.0/), https://doi.org/10.3390/app10227977

Table 5 - **Results of repeatability measurements.** Means (confidence intervals - CI) and coefficients of variation (CV) of pulse contour variables measured by the SCN4All telemedicine system. Repeatability was assessed using artificially generated pulse signals recorded with a pulse oximeter simulator under three settings (Normal, Abnormal 1, Abnormal 2). For each setting, five repeated measurements were performed with one pulse oximeter (n=5), and extended to four additional devices of the same release (n=25, 5x5 measurements). Adapted from Kulin et al. (51), licensed under CC BY 4.0, https://doi.org/10.3390/app10227977

| | **Normal** | | | | **Abnormal 1** | | | | **Abnormal 2** | | | |
|---|---|---|---|---|---|---|---|---|---|---|---|---|
| | *n=5* | | *n=25* | | *n=5* | | *n=25* | | *n=5* | | *n=25* | |
| **Variables** | *Mean(CI)* | *CV(%)* | *Mean(CI)* | *CV(%)* | *Mean(CI)* | *CV(%)* | *Mean(CI)* | *CV(%)* | *Mean(CI)* | *CV(%)* | *Mean(CI)* | *CV(%)* |
| Aging index | 1.13(1.12-1.14) | 0.41 | 1.14(1.13-1.14) | 0.57 | 3.37(2.29-4.45) | 27.1 | 3.12(2.79-3.46) | 26.1 | 3.71(2.81-4.60) | 20.4 | 3.84(3.69-4) | 9.9 |
| b/a | 1.78(1.78-1.79) | 0.26 | 1.79(1.78-1.79) | 0.32 | 1.59(1.59-1.59) | 0.29 | 1.59(1.59-1.60) | 0.32 | 1.60(1.59-1.60) | 0.36 | 1.60(1.56-1.59) | 0.33 |
| c-d point detection ratio (%) | 100(100-100) | 0 | 100(100-100) | 0 | 0.60(0.08-1.28) | 95.9 | 0.44(0.23-0.65) | 116 | 2(0.48-3.52) | 64.3 | 2.70(2.25-3.19) | 42.2 |
| d/a | 0.75(0.74-0.75) | 0.77 | 0.75(0.75-0.75) | 0.37 | 0.48(0.06-1.01) | 95.9 | 0.35(0.18-0.52) | 116 | 0.64(0.20-1.09) | 58.7 | 0.71(0.63-0.79) | 26.9 |

- Table 5 continues next page -

Table 5 **- cont.**

| | **Normal** | | | | **Abnormal 1** | | | | **Abnormal 2** | | | |
|---|---|---|---|---|---|---|---|---|---|---|---|---|
| | *n=5* | | *n=25* | | *n=5* | | *n=25* | | *n=5* | | *n=25* | |
| **Variables** | *Mean(CI)* | *CV(%)* | *Mean(CI)* | *CV(%)* | *Mean(CI)* | *CV(%)* | *Mean(CI)* | *CV(%)* | *Mean(CI)* | *CV(%)* | *Mean(CI)* | *CV(%)* |
| Left ventricular ejection time index (ms) | 552(552-554) | 0.22 | 553(552-553) | 0.27 | 462 (461-462) | 0.06 | 462(462-462) | 0.05 | 462(462-463) | 0.06 | 462(462-463) | 0.07 |
| Heart rate (1/min) | 55(55-55) | 0 | 55(55-55) | 0 | 95(95-95) | 0 | 95(95-95) | 0 | 95(95-95) | 0 | 95(95-95) | 0 |
| Interbeat interval (ms) | 1089(1089-1089) | 0 | 1089(1088-1090) | 0.21 | 631(631-631) | 0 | 631(631-631) | 0.19 | 630(630-631) | 0.07 | 631(631-632) | 0.18 |
| Reflection index (%) | 35.5(35.5-35.6) | 0.13 | 35.5(35.5-35.6) | 0.11 | 32.7(32.7-32.8) | 0.12 | 32.7(32.7-32.8) | 0.13 | 32.8(32.6-32.9) | 0.35 | 32.8(32.7-32.8) | 0.42 |
| Stiffness index (m/s) | 4.62(4.62-4.63) | 0.10 | 4.62(4.62-4.63) | 0.26 | 7.34(7.34-7.34) | 0 | 7.34 (7.33-7.34) | 0.18 | 7.34 (7.33-7.36) | 0.16 | 7.34(7.33-7.35) | 0.34 |

Table 6 - **Results of measurements performed in parallel on 4 separate fingers on 25 healthy individuals**. The results of the 25 subjects were averaged for each finger separately and are presented in the table with bracketed confidence intervals (CIs). Intraclass coefficients (ICC) were calculated to assess the correlation of results within the same individuals. Adapted and modified from Kulin et al. (51), licensed under CC BY 4.0 (https://creativecommons.org/licenses/by/4.0/), https://doi.org/10.3390/app10227977

| | Left index finger | Left ring finger | Right index finger | Right ring finger | ICC |
|---|---|---|---|---|---|
| | n=25 | n=25 | n=25 | n=25 | |
| Pulse contour variables | Mean(CI) | Mean(CI) | Mean(CI) | Mean(CI) | |
| Aging index | -1.29(- 1.46; -1.13) | -1.30(-1.47; -1.13) | -1.34(-1.15; -1.12) | -1.47(-1.17; -1.25) | 0.81 |
| b/a | -1.21(-1.26; -1.15) | -1.22(-1.29; -1.16) | -1.25(-1.31; -1.20) | -1.24(-1.30; -1.17) | 0.83 |
| c-d point detection ratio (%) | 33.8(25.3; 42.4) | 31.3(23.1; 39.5) | 31.9(22.9; 40.8) | 32.3(23.9; 40.78) | 0.90 |
| d/a | -0.15(-0.24; -0.06) | -0.16(-0.26; -0.07) | -0.17(-0.29; -0.06) | -0.10(-0.21; -0.01) | 0.82 |
| Left ventricular ejection time index (ms) | 148(56; 240) | 148(57; 240) | 147(56; 238) | 147(56; 237) | >0.99 |
| Heart rate (1/min) | 70.6(67.1; 74.2) | 71.0(67.5; 74.2) | 70.9(67.4; 74.4) | 71.0(67.4; 74.5) | >0.99 |
| Interbeat interval (ms) | 862(817; 906) | 862(818; 908) | 862(816; 907) | 861(817; 907) | >0.99 |
| Reflection index (%) | 62.2(59.2; 65.1) | 60.8(57; 64.6) | 61.5(58.4; 64.5) | 61.3(57.6; 65.0) | 0.81 |
| Stiffness index (ms) | 7.74(7.37; 8.10) | 7.71(7.32; 8.10) | 7.58(7.20; 7.97) | 7.59(7.13; 8.05) | 0.90 |

4.2. Results - Study 2

The results of a total of 37 healthy volunteers aged 20-57 years were used in the data analysis. (M/F: 16/21; mean age: 36.9 ± 11.4 SD years, BMI mean: 22.4± 2.3 SD, Systolic brachial BP: 115± 12 SD mmHg, Diastolic brachial BP: 64 ± 9 SD mmHg).

The results of the correlation tests are shown in Table 7.

Table 7 - **Results of Pearson's and Spearman's correlations: comparisons of echocardiographic parameters and PPG parameters.** r: Pearson's correlation coefficient; ρ(rho):Spearman's correlation coefficient, p= p-value (significance value <0.05) Given the correlation between heart rate measured by PPG and some echocardiographic parameters, where applicable, partial correlation tests were performed as a function of heart rate. *: SCN4ALL parameters. List of abbreviations found in Table 2 and Table 4.

| **Correlation of echocardiography parameters with PPG (Pearson)** | | | | | |
|---|---|---|---|---|---|
| **Echocardiography: Ejection time** | **PPG parameters** | **Pearson's correlations** | | **Pearson's correlations on HR** | **Partial condition** |
| | | **r** | **p** | **r** | **p** |
| LVET (ms) | ET(PPG) | 0.648 | < .001 | 0.555 | < .001 |
| | Crest Time | 0.567 | < .001 | 0.371 | 0.026 |
| | DNi * | -0.496 | 0.002 | -0.479 | 0.003 |
| | HR | -0.538 | < .001 | N/A | N/A |

**Table continues next page**

| Correlation of echocardiography parameters with PPG (Pearson)(cont.) | | | | | |
|---|---|---|---|---|---|
| **Echocardiography: systolic function** | **PPG parameters** | **Pearson's correlations** | | **Pearson's Partial correlations on HR** | **condition** |
| | | **r** | **p** | **r** | **p** |
| LV-EDD (mm) | AGEi | -0.51 | 0.001 | N/A | N/A |
| | d/a | 0.47 | 0.003 | N/A | N/A |
| | b/a | -0.41 | 0.013 | N/A | N/A |
| LV-ESD (mm) | AGEi | -0.52 | 0.001 | N/A | N/A |
| | d/a | 0.45 | 0.005 | N/A | N/A |
| | b/a | -0.42 | 0.01 | N/A | N/A |
| LV-GLS (%) | DNi * | 0.5 | 0.001 | N/A | N/A |
| LVOT-VTI (cm) | DNi * | -0.4 | 0.015 | N/A | N/A |
| Ao-VTI (cm) | DNi * | -0.44 | 0.007 | N/A | N/A |
| **Echocardiography: diastolic function** | **PPG parameters** | **Pearson's correlations** | | **Pearson's Partial correlations on HR** | **condition** |
| | | **r** | **p** | **r** | **p** |
| MV-A (cm/s) | b/a | 0.52 | < .001 | 0.51 | 0.001 |
| | HR | 0.5 | 0.005 | N/A | N/A |
| MV-E (cm/s) | AGEi | 0.4 | 0.014 | N/A | N/A |
| e'-med (cm/s) | Crest Time | -0.41 | 0.012 | N/A | N/A |

Table continues next page

| Correlation of echocardiography parameters with PPG (Spearman)(cont.) | | | | | |
|---|---|---|---|---|---|
| **Echocardiography: Ejection time** | **PPG parameter** | **Spearman's correlations** | | **Spearman's Partial correlations condition on HR** | |
| | | **ρ** | **p** | **ρ** | **p** |
| LVET (ms) | eLVET2 * | 0.496 | 0.002 | 0.404 | 0.015 |
| **Echocardiography: systolic function** | **PPG parameters** | **Spearman's correlations** | | **Spearman's Partial correlations condition on HR** | |
| | | **ρ** | **p** | **ρ** | **p** |
| LV-EDD (mm) | Crest Time @75 | -0.472 | 0.003 | N/A | N/A |
| | eLVET2 @75 * | -0.436 | 0.007 | N/A | N/A |
| LV-ESD (mm) | eLVET2 @75 * | -0.409 | 0.012 | N/A | N/A |
| Ao, root diam (mm) | DNi * | 0.482 | 0.003 | N/A | N/A |
| **Echocardiography: diastolic function** | **PPG parameters** | **Spearman's correlations** | | **Spearman's Partial correlations condition on HR** | |
| | | **ρ** | **p** | **ρ** | **p** |
| MV-A (cm/s) | eLVET2 @75 * | 0.572 | < .001 | NA | NA |
| | Crest Time @75 | 0.517 | 0.001 | NA | NA |
| | HR | 0.5 | 0.005 | N/A | N/A |
| MV-E/A | HR | -0.451 | 0.005 | N/A | N/A |
| E/e' - lat | LVETi | 0.423 | 0.009 | N/A | N/A |
| End of Table 7 | | | | | |

4.2.1. Results related to left ventricular ejection time (LVET)

Bland-Altman analysis showed a mean difference of 95.0 ms between echocardiography and PPG measurements of cardiac ejection time. The limits of agreement ranged from 54.0 ms to 136.0 ms, with most differences falling within this range and no evident proportional bias. ( Figure 8)

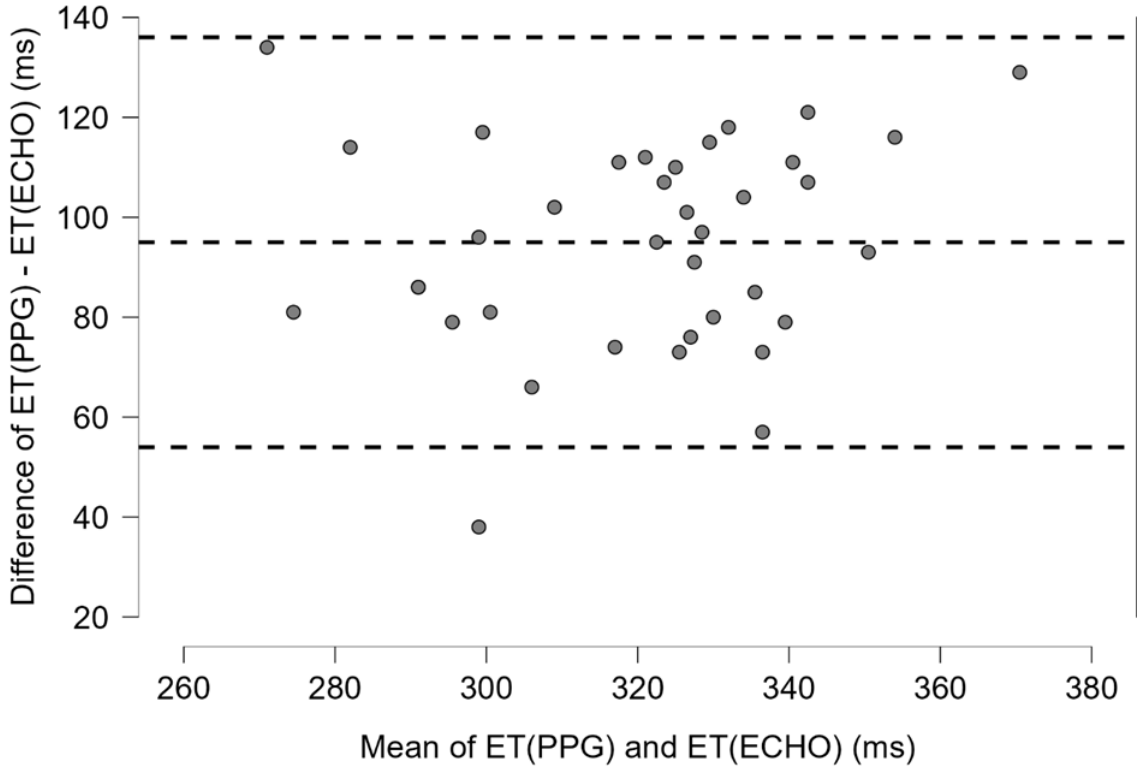


Figure 8 - Agreement between photoplethysmography (PPG) and echocardiography (ECHO) in measuring ejection time (ET) in milliseconds (ms) using Bland-Altman analysis. Middle dashed line: mean difference (95.0 ms), upper and lower dashed line are mean difference +/- 1.96 SD (standard deviation)(136.0 ms and 54.0 ms), respectively. Adapted and modified from Kulin et al. (97), licensed under CC BY 4.0 (https://creativecommons.org/licenses/by/4.0/),
https://doi.org/10.1556/2060.2025.00675

LVET (ms) measured by cardiac ultrasound showed a moderate-to-strong correlation with ejection time measured by PPG (ET(PPG)) ($r= 0.648$; $p<0.001$). (Figure 9)

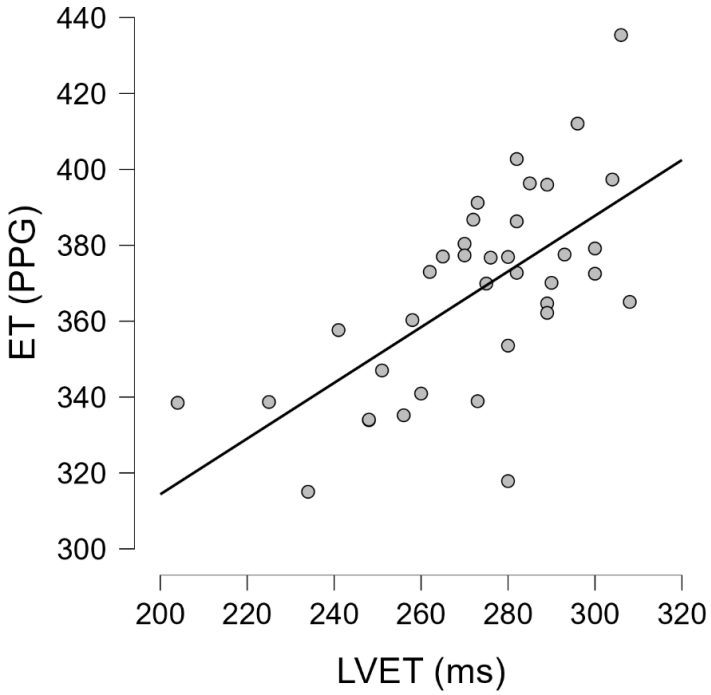


Figure 9- Association between ejection times measured by echocardiography and PPG. Scatter plot illustrating the association between left ventricular ejection time (LVET, ms) measured by cardiac ultrasound and ejection time derived from photoplethysmography (ET(PPG), ms). The strength of association was quantified using Pearson's correlation analysis (see Methods). The fitted linear line is displayed for visualization purposes only and does not represent a regression model. Adapted and modified from Kulin et al. (97), licensed under CC BY 4.0 (https://creativecommons.org/licenses/by/4.0/), https://doi.org/10.1556/2060.2025.00675

We also found correlations with other parameters related to systolic time, such as Crest Time ($r=0.567$; $p<0.001$); and the early left ventricular ejection time 1 (eLVET1 *) ($r=0.478$; $p=0.003$) and 2 (eLVET2 *) ($r=0.472$; $p=0.003$).

LVET correlated with the Dicrotic notch index (DNi*), too. ($r=-0.496$; $p=0.002$).

Given the correlation between heart rate measured by PPG and echocardiographic LVET ($r=-0.538$; $p<0.001$), we conducted partial correlation tests conditioned on heart rate. The correlation persisted for the parameters ET(PPG), Crest Time, eLVET2*, DNi*, suggesting an independent relationship with heart rate. However, the correlation disappeared for the parameters eLVET1*, indicating that the strong association was driven by the relationship with heart rate in this case. (Parameters that lost significance after heart rate adjustment are shown in Supplementary Table 1 in Kulin et al.) (97)

4.2.2. Results related to cardiac systolic function

Several PPG parameters were significantly correlated with echocardiographic parameters which are routinely used in monitoring of systolic function and have known prognostic values. The parameters with the best correlation are shown in Figure 10 and Table 7**.**

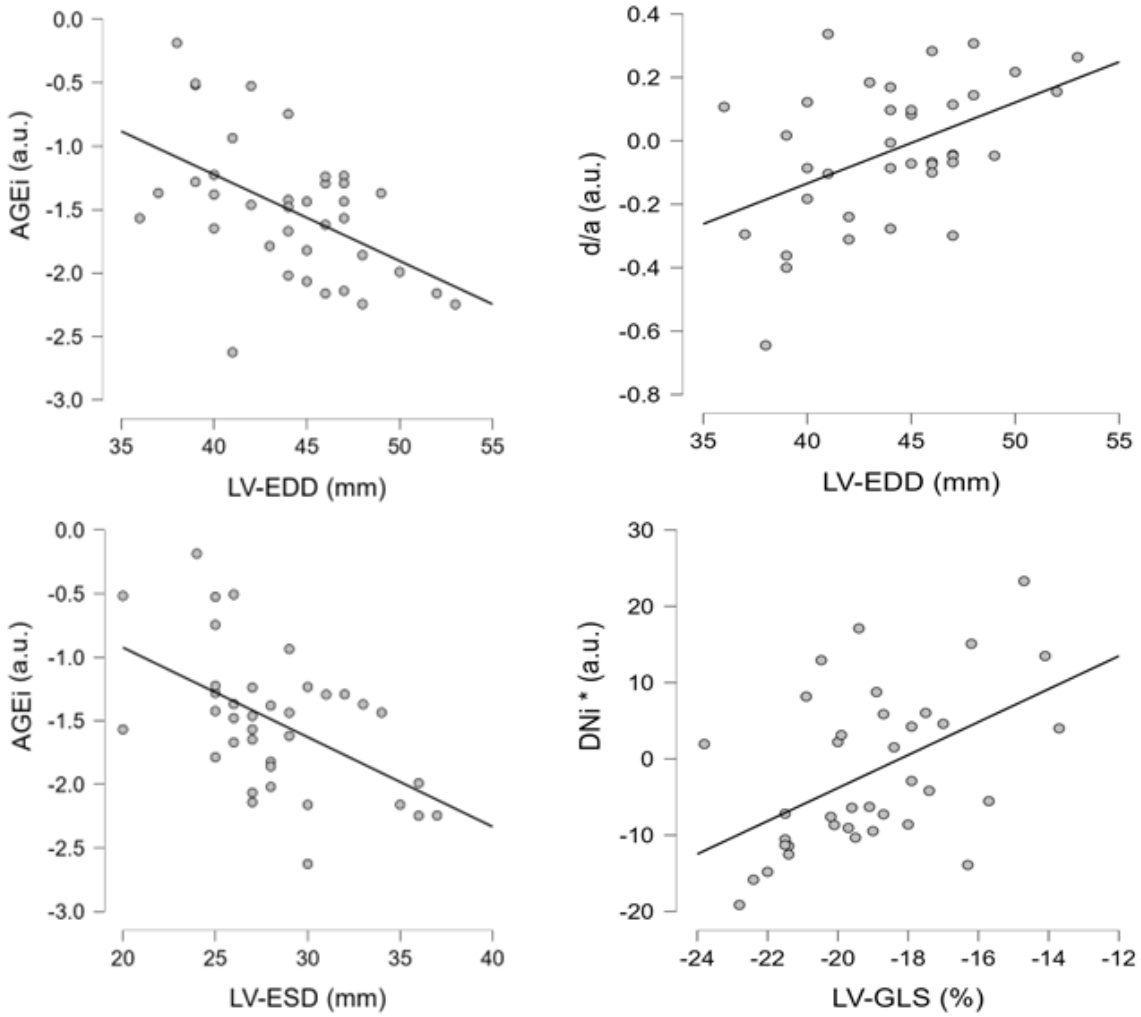


Figure 10- **Scatter plots illustrating associations between parameters describing systolic function.** LV-EDD - left ventricular (LV) end-diastolic diameter, LV-ESD - LV end-systolic diameter, LV-GLS - LV global longitudinal strain. AGEi - value calculated from fiducial points of the second derivative of the pulse wave (SDPPG), defined as AGEi = (b - c - d - e)/a; d/a represents the amplitude ratio of the fourth inflection point ("d") to the first inflection point ("a") of the SDPPG. DNi - parameter describing the relative position of the diastolic peak with respect to the dicrotic notch. Associations were quantified using correlation analysis (see Methods); fitted linear trend lines are shown for visualization purposes only. $p < 0.05$ for all parameters. Adapted and modified from Kulin et al. (97), licensed under CC BY 4.0 (https://creativecommons.org/licenses/by/4.0/), https://doi.org/10.1556/2060.2025.00675

4.2.3. Results related to cardiac diastolic function

We observed the most significant correlations with indicators of atrial contraction (MV-A) and left ventricular filling pressure (E/e' lat). Given that some parameter pairs exhibited correlations with heart rate, we further analyzed these relationships using partial correlation to account for heart rate variability. Table 7 and Figure 11 showcases these significant correlations.

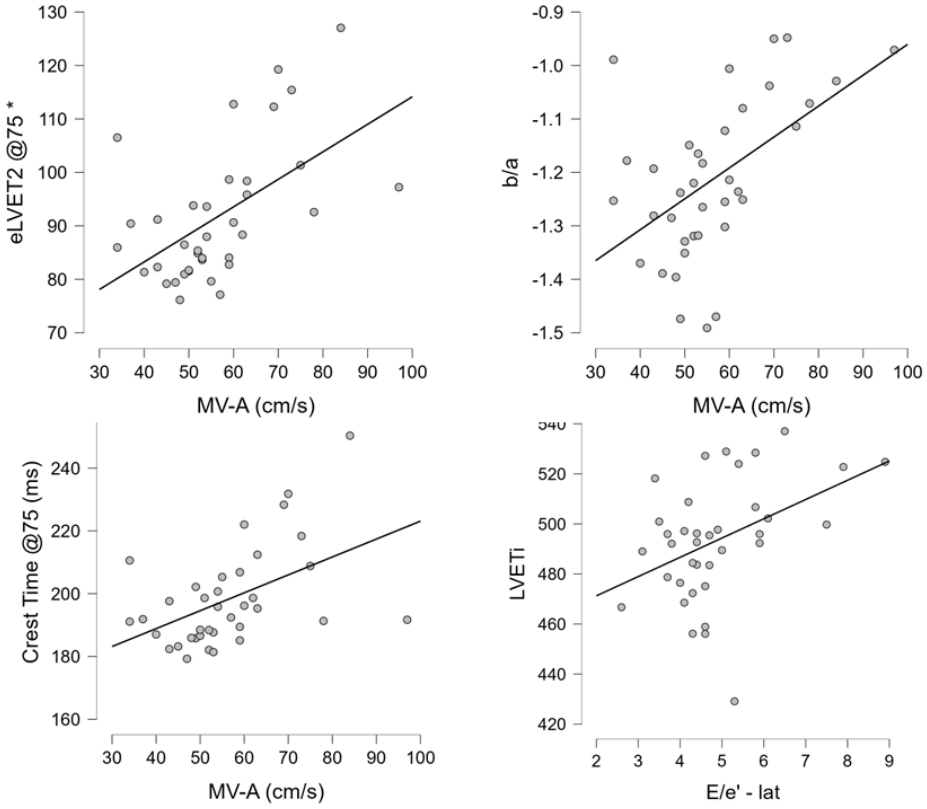


Figure 11- **Scatter plots illustrating associations between parameters describing diastolic function.** PPG-derived parameters showing some of the strongest associations with echocardiographic indices of diastolic function. MV-A - mitral A-wave velocity; E/e′-lat - ratio of early diastolic mitral inflow velocity to early diastolic mitral annulus velocity; eLVET2@75* - eLVET2 is defined as the time interval from the first peak of the first derivative of the PPG signal to the peak of the systolic wave; b/a - ratio of the first two inflection points of the second derivative of the pulse wave; Crest Time@75 - time elapsed between waveform onset (foot) and maximum systolic amplitude (peak). The @75 notation indicates correction of the original time values to a heart rate of 75 beats/min. LVETi - left ventricular ejection time indexed for heart rate, calculated using sex-specific resting regression equations. Associations were quantified using correlation analysis (see Methods); fitted linear trend lines are shown for visualization purposes only. $p < 0.05$ for all parameters. Adapted and modified from Kulin et al. (97), licensed under CC BY 4.0 (https://creativecommons.org/licenses/by/4.0/), https://doi.org/10.1556/2060.2025.00675

# 5. Discussion

The systematic investigation of peripheral pulse wave analysis represents a structured contribution to translational cardiovascular science. Despite decades of research on the shape and features of the pulse wave, the physiological interpretation of many peripheral pulse wave-derived parameters and their relationship to central cardiovascular function remain incomplete, and this area therefore remains underutilized in clinical care. (37,51,60,78,79)

The present work was driven by the recognition that, although peripheral photoplethysmographic signals are easily accessible and rich in physiological information, limitations in the physiological characterization, stability, and interpretability of derived parameters, in addition to the availability of validated systems and comprehensive methodological evaluations, have constrained their medical application. (80)

To advance the field, our team has developed a custom high-resolution PPG-based measurement system as a research tool, tailored for systematic pulse wave recording and analysis. The development was embedded in the framework of translational medicine, aiming to bridge experimental pulse wave analysis with physiologically interpretable cardiovascular phenomena. (11)

## 5.1. Physiological stability and variability of PPG-based peripheral pulse wave parameters

In Study 1, first the system's measurement repeatability using artificial signals and human test-retest variability were evaluated. The system demonstrated high repeatability for most parameters (CV < 2%) when detecting normal pulse signals. However, detecting SDPPG ‘c’ and ‘d’ points in abnormal signals proved less reliable, affecting derived parameters such as the Aging-index and d/a ratio.

Human test-retest measurements revealed that core parameters like b/a, left ventricular ejection time index, mean interbeat interval, stiffness index, and mean heart rate remained consistent under standard conditions (CV < 10%). However, the aging index and d/a ratio showed higher variability, indicating that these parameters should only be interpreted when c-d point detection is reliable. The issue of the absence of c-d points and the

limitations of parameters calculated using them have been addressed in numerous previous publications searching for methods how to detect these points (79,85,98), as they hypothesized to represent the onset and offset of the reflected wave.(84)

Anatomical variability analysis showed minimal differences between measurements performed on different fingers, with intraclass correlation coefficients exceeding 80% for most parameters. These findings suggest that the contribution of finger-related anatomical variability to the total observed variance is small. Importantly, the high ICC values imply that most of the variability in the assessed pulse wave parameters originates from true interindividual differences rather than from intrapersonal variability associated with measurement location. Nevertheless, to maximize comparability - particularly in longitudinal or repeated-measurement settings - it remains advisable to consistently perform measurements on the same finger to minimize even minor sources of inter-finger variability.

### 5.2. Comparison with gold-standard: correlation of peripheral pulse wave features with central cardiac function

In study 2 we aimed to examine the relationship between echocardiographic and photoplethysmographic (PPG) pulse wave-derived parameters in healthy individuals. While previously published results revealed limited aspects of this relationship (Table 1), our analysis provides a more comprehensive evaluation, including both established and novel PPG parameters. The results contribute to the emerging body of evidence supporting the potential role of pulse wave analysis by either PPG (15,90,99) or other methods in non-invasive cardiac monitoring. (100)

#### 5.2.1. Ejection time

Left ventricular ejection time is a clinically relevant parameter in heart failure management and pharmacological response assessment. (101) Our findings show a significant, though moderate, correlation between ET measured by echocardiography and several PPG-derived indices (ET(PPG), Crest Time, eLVET2*, DNi). These findings are in line with earlier studies reporting systematic differences between central and peripheral ET measurements. (102) While not interchangeable, these parameters may still support

longitudinal monitoring, especially given the magnitude higher availability of PPG devices, compared to echocardiography. 1.1 billion wearable devices were used globally in 2022, from which at least half of them are wristbands and smartwatches with PPG capabilities. (103) Besides the correlation of the time domain parameters, the significant correlation of DNi with ejection time supports our initial hypothesis that it captures information related to ventricular function, potentially reflecting aspects of ventriculo-arterial coupling.

### 5.2.2. Systolic function

**Systolic Function and Left Ventricular Dimensions**

Left ventricular end-diastolic and end-systolic diameters are well-established markers of systolic function and overall cardiac performance. (104) In our study, the strongest correlation between a PPG-derived parameter and a structural echocardiographic measure was observed between LV-EDD and the Ageing Index (AGEi) and d/a - a suggested proxy for afterload by Takazawa et. al and Nichols et al. (46,105) AGEi also showed moderate association with LV-ESD, highlighting its potential as a surrogate PPG indicator of LV anatomy and function. The clinical relevance of these findings is that both LV-EDD and LV-ESD are independently associated with prognosis in coronary artery disease, dilated and hypertrophic cardiomyopathies, and heart failure. (106) Although correlation strength remained moderate, requiring further studies, the consistency of AGEi's relationship with both diameters supports the hypothesis that peripheral waveform characteristics may reflect ventricular geometry.

**Stroke Volume, Ejection Fraction, and Global Longitudinal Strain (GLS)**

Stroke volume showed weak but significant correlations with several PPG parameters, particularly with AGEi and d/a ratio. (Results are presented in the Supplementary Table 1. and 2. in published paper of Study 2. (97)) While ejection fraction (EF) did not show a significant correlation with any PPG parameter, this is not surprising given that EF is a volume ratio not directly captured by peripheral signals. Instead, the local signal of PPG is likely reflecting systemic hemodynamic performance providing information on the effectivity of cardiovascular function at the tissue level, rather than estimating absolute

chamber volume measures and ratios. It is also important to underline that the results reveal a significant correlation between GLS and the Dicrotic Notch Index (DNi), suggesting that further studies should target DNi, as it may offer insights into subtle myocardial dysfunction, particularly in HFpEF, where EF remains preserved despite declining contractility. This represents the first reported association between PPG morphology and ventricular strain, highlighting a new direction for non-invasive systolic function assessment in early-stage heart failure - upon further validation studies.

**Aortic Parameters**

Both static and dynamic aortic measures demonstrated moderate and weak, but significant correlations with PPG parameters, mainly with DNi. Specifically, DNi correlated significantly with aortic root diameter (rho = 0.482), Ao-VTI, and LVOT-VTI, in addition to ejection time and GLS. These relationships further support our initial hypothesis that DNi may capture elements of aortic distensibility, ejection dynamics and ventriculo-arterial coupling. These findings support its potential role in broader cardiovascular assessment; however further validation is needed in various CV patient groups.

5.2.3. Diastolic function

The results revealed further significant correlations between several PPG parameters (eLVET2@75, b/a, CrestTime@75) and established echocardiographic markers of diastolic function. Significant, but moderate associations were found with MV-A, a parameter influenced by atrial contraction and ventricular relaxation (107,108), which suggest PPG's potential to reflect diastolic dynamics. LVETi, a time-domain parameter showed the strongest correlation with E/e'-lat, a well-known surrogate of left ventricular filling pressure, supporting prior research on its relevance in diastolic dysfunction assessment. (109)

While EF often remains normal in heart failure with preserved ejection fraction (HFpEF), rising E/e'-lat and MV-A values - which exhibited the highest correlations with PPG parameters - indicate impaired diastolic filling and increased pressure. These findings suggest that PPG-derived features may complement existing tools in evaluating diastolic function or might be useful features in the future for home monitoring between ambulatory visits.

Given the prognostic significance of diastolic dysfunction in heart failure, especially in the context of preserved systolic function, these results of PPG derived parameters may offer a future method to support screening and monitoring - particularly for asymptomatic HFpEF patients. However, it is emphasized that further studies should validate these associations in broader clinical populations and explore other interesting fields. For example: How PPG-based parameters respond even to treatment strategies such as the increasingly used SGLT2 inhibitors?

# 6. Conclusions

This dissertation aims to summarize the findings of two initial trials about a non-invasively recorded set of peripheral hemodynamic parameters to explore their physiological behavior, stability and relationship with echocardiographic measures, with the long-term aim of evaluating their potential as biomarkers of cardiovascular status. These findings are just the beginning of a long research project to demonstrate sufficient evidence of whether these markers are appropriate or not for clinical decision-making.

Even though there was a need for the creation of a custom-built PPG analysis system due to the limitations of the available devices, the main aim of the works presented above is to better understand how these characteristics behave in healthy volunteers.

## 6.1. The key findings from Study 1 and Study 2

**Study 1 -** Physiological stability and variability of PPG-based peripheral pulse wave parameters

- The custom-built system demonstrated excellent repeatability under controlled conditions: measurement variability remained below 2% across devices when recording artificial pulse signals with proper signal quality.
- A novel contribution was the introduction of the "c-d point detection ratio" as a quality control metric to assess the trustworthiness of second-derivative-based parameters. This parameter supports the selective interpretation of features like the Aging-index and d/a ratio. Their use should be limited to measurements with sufficient c-d point detection ratios.
- Key pulse wave parameters - including b/a, stiffness index, left ventricular ejection time index, and mean interbeat interval - showed low intrapersonal variability (CV < 10%) in short-term repeated measurements on healthy subjects, identifying the most robust parameters from the aspect of hemodynamic stability, under standardized conditions.
- Parallel measurements on four different fingers showed strong within-subject agreement, with intraclass correlation coefficients exceeding 0.80 for all

investigated pulse wave parameters, indicating that finger-related anatomical variability contributes only minimally to overall pulse wave variability. For longitudinal or repeated measurements, it is therefore recommended to consistently perform follow-up recordings on the same finger to minimize even minor inter-finger differences.

- The consistently high intraclass correlation coefficients further indicate that the majority of observed variability originates from true interindividual differences rather than short-term intraindividual fluctuations related to measurement location.

**Study 2 -** Relationship between peripheral pulse wave features and central cardiac function

Study 2 examined the physiological relationship between peripheral pulse wave features derived from PPG recordings and central cardiovascular function, as characterized by echocardiographic measures. The analysis focused on whether specific time-domain pulse wave characteristics are associated with measures of left ventricular systolic and diastolic function, aortic properties, and cardiac morphology. Moderate but consistent associations were identified between selected PPG-derived parameters and echocardiographic indices, supporting the physiological relevance of peripheral pulse wave morphology.

- PPG-derived ejection time showed a moderate-to-strong association with echocardiographic left ventricular ejection time ($r = 0.648$, $p < 0.001$), with a systematic mean offset of +95 ms relative to echocardiography, indicating that peripheral timing-based pulse wave features reflect central systolic timing under standardized measurement conditions.

- Both newly defined parameters such as eLVET2 @ 75 and established PPG-derived metrics including the Aging index and b/a demonstrated moderate and significant associations with echocardiographic measures of chamber dimensions, diastolic filling pressure, and atrial contraction, consistent with peripheral pulse wave morphology being sensitive to variations in central cardiac structure and filling dynamics

- The Dicrotic Notch Index (DNi) showed consistent moderate associations with aortic root diameter, LVOT-VTI, and global longitudinal strain, indicating a potential sensitivity to properties related to aortic mechanics and ventriculo-arterial interaction.

## 6.2. Future outlook

Upon the publication of further PPG related research, future potential of the method is the paradigm shift: from the occasional medical measurements to daily or continuous data recording. There is high chance that trend analysis of daily measurements and insights from Big Data and pattern evaluation will overcome the known limitations of the peripheral pulse wave analysis on the long run - especially as this is a more affordable technology than the current expensive medical systems to assess hemodynamics, leading to a more reachable and inclusive healthcare even for the low socioeconomic areas and remote places of Earth.

Ongoing studies and collaborative projects using the SCN4ALL system are underway in multiple clinics and academic centers across Europe - including Hungary, Greece, and the Netherlands - to gather further data and determine which medical settings and patient groups may benefit most from the regular use of this approach.

## 7. Summary

Photoplethysmography (PPG)-based pulse contour analysis provides a non-invasive approach for studying peripheral hemodynamics and pulse wave morphology. This thesis investigated the physiological behavior, stability, and interpretability of selected digital arterial volume pulse (DVP) parameters derived from peripheral PPG recordings, using a custom-built high-resolution research system (SCN4ALL).

**Study 1** assessed the technical and short-term physiological stability of PPG-derived pulse wave parameters under standardized conditions. Artificial signal testing demonstrated excellent repeatability (CV < 1%), indicating minimal device- and algorithm-related measurement error. In human test-retest measurements, key parameters - including stiffness index, reflection index, left ventricular ejection time index, mean interbeat interval, and b/a - showed low intrapersonal variability (CV < 10%), supporting their robustness in healthy subjects. Second-derivative-based parameters were more variable due to limited c-d point detectability; therefore, a c-d point detection ratio was introduced as a quality control metric. Parallel finger recordings showed strong within-subject agreement (ICC > 0.80), indicating that most variability reflects interindividual differences rather than measurement location effects.

**Study 2** investigated how PPG-based parameters reflect central cardiac function by comparing them with echocardiographic measurements in 37 healthy subjects. PPG-derived ejection time showed highest correlation with echocardiographic values ($r = 0.648$, $p < 0.001$), despite a consistent overestimation (+95 ms). Twelve additional PPG features showed moderate and significant correlations - both previously published PPG parameters and markers defined by our research group - ($r > 0.4$, $p < 0.05$) with key echocardiographic indices, including left ventricular dimensions, stroke volume, global longitudinal strain, aortic root diameter, ventricular filling pressure (E/e' lat), and atrial contraction (MV-A).

Overall, the results contribute to a more detailed physiological interpretation of peripheral pulse wave morphology and highlight which PPG-derived parameters provide stable and interpretable information under standardized conditions in healthy individuals. These findings establish a physiological basis for future hypothesis-driven studies investigating specific cardiovascular conditions and well-defined clinical questions.

8. References


1. World Health Organization. Cardiovascular diseases [Internet]. [cited 2023 Aug 14]. Available from: https://www.who.int/health-topics/cardiovascular-diseases#tab=tab_1
2. Ciccarelli M, Giallauria F, Carrizzo A, Visco V, Silverio A, Cesaro A, Calabrò P, De Luca N, Mancusi C, Masarone D, Pacileo G, Tourkmani N, Vigorito C, Vecchione C. Artificial intelligence in cardiovascular prevention: New ways will open new doors. J Cardiovasc Med. 2023; 24 :E106–15. doi:10.2459/JCM.0000000000001431
3. Chen SF, Loguercio S, Chen KY, Lee SE, Park JB, Liu S, Sadaei HJ, Torkamani A. Artificial Intelligence for Risk Assessment on Primary Prevention of Coronary Artery Disease. Curr Cardiovasc Risk Rep. 2023; 17 :215–31. doi:10.1007/s12170-023-00731-4
4. Meskó B, Drobni Z, Bényei É, Gergely B, Győrffy Z. Digital health is a cultural transformation of traditional healthcare. mHealth. 2017; 3 :38. doi:10.21037/mhealth.2017.08.07
5. Ezeamii VC, Okobi OE, Wambai-Sani H, Perera GS, Zaynieva S, Okonkwo CC, Ohaiba MM, William-Enemali PC, Obodo OR, Obiefuna NG. Revolutionizing Healthcare: How Telemedicine Is Improving Patient Outcomes and Expanding Access to Care. Cureus. 2024 Jul; 16(7) :e63881. doi:10.7759/cureus.63881
6. Shaver J. The State of Telehealth Before and After the COVID-19 Pandemic. Prim Care. 2022 Dec; 49(4) :517–30. doi:10.1016/j.pop.2022.04.002
7. World Health Organization. Hypertension [Internet]. 2023 [cited 2025 May 5]. Available from: https://www.who.int/news-room/fact-sheets/detail/hypertension
8. Viigimaa M, Talvik A, Wojciechowska W, Kawecka-Jaszcz K, Toft I, Stergiou GS, Nasothimiou EG, Kotsis V, Agabiti Rosei E, Salvetti M, Dorobantu M, Martell-Claros N, Abad-Cardiel M, Hernández-Hernández R, Doménech M, Coca A. Identification of the hemodynamic modulators and hemodynamic status in uncontrolled hypertensive patients. Blood Press. 2013; 22(6) :362–70. doi:10.3109/08037051.2013.782900
9. Shahim B, Kapelios CJ, Savarese G, Lund LH. Global Public Health Burden of Heart Failure: An Updated Review. Card Fail Rev. 2023; 9 :e11.

doi:10.15420/cfr.2023.05

10. Saugel B, Hoppe P, Nicklas JY, Kouz K, Körner A, Hempel JC, Vos JJ, Schön G, Scheeren TWL. Continuous noninvasive pulse wave analysis using finger cuff technologies for arterial blood pressure and cardiac output monitoring in perioperative and intensive care medicine: a systematic review and meta-analysis. Br J Anaesth. 2020; 125(1) :25–37. doi:10.1016/j.bja.2020.03.013
11. Cohrs RJ, Martin T, Ghahramani P, Bidaut L, Higgins PJ, Shahzad A. Translational medicine definition by the European society for translational medicine. New Horizons Transl Med. 2015; 2(3) :86–8. doi:10.1016/j.nhtm.2014.12.002
12. Charlton PH, Mariscal Harana J, Vennin S, Li Y, Chowienczyk P, Alastruey J. Modeling arterial pulse waves in healthy aging: a database for in silico evaluation of hemodynamics and pulse wave indexes. Am J Physiol Heart Circ Physiol. 2019 Nov; 317(5) :H1062–85. doi:10.1152/ajpheart.00218.2019
13. Alastruey J, Parker KH, Sherwin SJ. Arterial pulse wave haemodynamics. In: Anderson S, editor. BHR Group - 11th International Conferences on Pressure Surges. Lisbon, Portugal: BHR Group; 2012 Sep 13 p. 401–42.
14. Elgendi M. On the analysis of fingertip photoplethysmogram signals. Curr Cardiol Rev [Internet]. 2012 Feb [cited 2016 Oct 31]; 8(1) :14–25. Available from: http://www.ncbi.nlm.nih.gov/pubmed/22845812 doi:10.2174/157340312801215782
15. Charlton PH, Paliakaitė B, Pilt K, Bachler M, Zanelli S, Kulin D, Allen J, Hallab M, Bianchini E, Mayer CC, Terentes-Printzios D, Dittrich V, Hametner B, Veerasingam D, Žikić D, Marozas V. Assessing hemodynamics from the photoplethysmogram to gain insights into vascular age: a review from VascAgeNet. Am J Physiol Circ Physiol [Internet]. 2022 Apr 1 [cited 2022 Jan 18]; 322(4) :H493–522. Available from: https://journals.physiology.org/doi/abs/10.1152/ajpheart.00392.2021 doi:10.1152/ajpheart.00392.2021
16. Nichols WW, Denardo SJ, Wilkinson IB, McEniery CM, Cockcroft J, O'Rourke MF. Effects of arterial stiffness, pulse wave velocity, and wave reflections on the central aortic pressure waveform. J Clin Hypertens. 2008; 10(4) :295–303.

doi:10.1111/j.1751-7176.2008.04746.x

17. Parker KH, Jones CJH. Forward and Backward Running Waves in the Arteries: Analysis Using the Method of Characteristics. J Biomech Eng [Internet]. 1990; 112(3) :322. Available from: http://biomechanical.asmedigitalcollection.asme.org/article.aspx?articleid=1398416 doi:10.1115/1.2891191
18. Mendes-Pinto D, Rodrigues-Machado M da G. Applications of arterial stiffness markers in peripheral arterial disease. J Vasc Bras. 2019; 18 :e20180093. doi:10.1590/1677-5449.009318
19. E-Med4All Europe Kft. HeartReader Training Manual. Budapest: E-Med4All Europe Kft.; 2020.
20. Agabiti-Rosei E, Mancia G, O'Rourke MF, Roman MJ, Safar ME, Smulyan H, Wang JG, Wilkinson IB, Williams B, Vlachopoulos C. Central blood pressure measurements and antihypertensive therapy: A consensus document. Hypertension. 2007; 50(1) :154–60. doi:10.1161/HYPERTENSIONAHA.107.090068
21. Haseler E, Sinha MD. Precision approaches to paediatric hypertension: linking pathophysiology to therapy. Pediatr Nephrol [Internet]. 2025; (0123456789). Available from: https://doi.org/10.1007/s00467-025-07100-w doi:10.1007/s00467-025-07100-w
22. O'Rourke MF, Pauca A, Jiang XJ. Pulse wave analysis. Br J Clin Pharmacol [Internet]. 2001 Jun [cited 2019 Aug 13]; 51(6) :507–22. Available from: http://www.ncbi.nlm.nih.gov/pubmed/11422010 doi:10.1046/j.0306-5251.2001.01400.x
23. Nelson MR, Stepanek J, Cevette M, Covalciuc M, Hurst RT, Tajik AJ. Noninvasive measurement of central vascular pressures with arterial tonometry: Clinical revival of the pulse pressure waveform? Mayo Clin Proc. 2010; 85(5) :460–72. doi:10.4065/mcp.2009.0336
24. Alastruey J, Charlton PH, Bikia V, Paliakaite B, Hametner B, Bruno RM, Mulder MP, Vennin S, Piskin S, Khir AW, Guala A, Mayer CC, Mynard J, Hughes AD, Segers P, Westerhof BE. Arterial pulse wave modeling and analysis for vascular-age studies: a review from VascAgeNet. Am J Physiol Heart Circ Physiol. 2023

Jul; 325(1) :H1–29. doi:10.1152/ajpheart.00705.2022

25. Wang KL, Cheng HM, Chuang SY, Spurgeon HA, Ting CT, Lakatta EG, Yin FCP, Chou P, Chen CH. Central or peripheral systolic or pulse pressure: which best relates to target organs and future mortality? J Hypertens [Internet]. 2009 Mar [cited 2019 Aug 12]; 27(3) :461–7. Available from: http://www.ncbi.nlm.nih.gov/pubmed/19330899 doi:10.1097/hjh.0b013e3283220ea4
26. Williams B, Lacy PS, Thom SM, Cruickshank K, Stanton A, Collier D, Hughes AD, Thurston H, O'Rourke M. Differential impact of blood pressure-lowering drugs on central aortic pressure and clinical outcomes: Principal results of the Conduit Artery Function Evaluation (CAFE) study. Circulation. 2006; 113(9) :1213–25. doi:10.1161/CIRCULATIONAHA.105.595496
27. Crowe LA, Genecand L, Hachulla AL, Noble S, Beghetti M, Vallée JP, Lador F. Non-Invasive Cardiac Output Determination Using Magnetic Resonance Imaging and Thermodilution in Pulmonary Hypertension. J Clin Med. 2022; 11(10) :1–13. doi:10.3390/jcm11102717
28. Gabbert DD, Kheradvar A, Jerosch-Herold M, Oechtering TH, Uebing AS, Kramer HH, Voges I, Rickers C. MRI-based comprehensive analysis of vascular anatomy and hemodynamics. Cardiovasc Diagn Ther. 2021; 11(6) :1367–78. doi:10.21037/cdt-20-767
29. Bianchini E, Lønnebakken MT, Wohlfahrt P, Piskin S, Terentes-Printzios D, Alastruey J, Guala A. Magnetic Resonance Imaging and Computed Tomography for the Noninvasive Assessment of Arterial Aging: A Review by the VascAgeNet COST Action. J Am Heart Assoc. 2023; 12(10) :1–15. doi:10.1161/JAHA.122.027414
30. Avolio AP, Butlin M, Walsh A. Arterial blood pressure measurement and pulse wave analysis-their role in enhancing cardiovascular assessment. Vol. 31, Physiological Measurement. 2009. doi:10.1088/0967-3334/31/1/R01
31. Gallagher D, Adji A, O'Rourke MF. Validation of the transfer function technique for generating central from peripheral upper limb pressure waveform. Am J Hypertens. 2004; 17(11) :1059–67. doi:10.1016/j.amjhyper.2004.05.027
32. Gao M, Rose WC, Fetics B, Kass DA, Chen CH, Mukkamala R. A Simple

Adaptive Transfer Function for Deriving the Central Blood Pressure Waveform from a Radial Blood Pressure Waveform. Sci Rep. 2016; 6(August) :1–9. doi:10.1038/srep33230

33. Millasseau SC, Patel SJ, Redwood SR, Ritter JM, Chowienczyk PJ. Pressure wave reflection assessed from the peripheral pulse: is a transfer function necessary? Hypertens (Dallas, Tex 1979) [Internet]. 2003 May 1 [cited 2019 Aug 22]; 41(5) :1016–20. Available from: https://www.ahajournals.org/doi/10.1161/01.HYP.0000057574.64076.A5 doi:10.1161/01.HYP.0000057574.64076.A5

34. Friedberg MK, Silverman NH. Cardiac Ventricular Diastolic and Systolic Duration in Children With Heart Failure Secondary to Idiopathic Dilated Cardiomyopathy. Am J Cardiol [Internet]. 2006 Jan 1; 97(1) :101–5. Available from: https://doi.org/10.1016/j.amjcard.2005.07.127 doi:10.1016/j.amjcard.2005.07.127

35. Zahedi E, Chellappan K, Ali MAM, Singh H. Analysis of the Effect of Ageing on Rising Edge Characteristics of the Photoplethysmogram using a Modified Windkessel Model. Cardiovasc Eng [Internet]. 2007 Dec 9 [cited 2017 Aug 14]; 7(4) :172–81. Available from: http://www.ncbi.nlm.nih.gov/pubmed/17992571 doi:10.1007/s10558-007-9037-5

36. Monos E. Hemodinamika: A vérkeringés dinamikája. 4th. ed. Budapest: Semmelweis Kiadó; 2004. 1–104 p.

37. von Wowern E, Östling G, Nilsson PM, Olofsson P. Digital photoplethysmography for assessment of arterial stiffness: Repeatability and comparison with applanation tonometry. West J, editor. PLoS One [Internet]. 2015 Aug 20 [cited 2018 Jan 9]; 10(8) :1–19. Available from: http://www.ncbi.nlm.nih.gov/pubmed/26291079 doi:10.1371/journal.pone.0135659

38. Millasseau S, Kelly R, Ritter J, Chowienczyk P. Determination of age-related increases in large artery stiffness by digital pulse contour analysis. Clin Sci. 2002; 103(4) :371–7. doi:10.1042/cs1030371

39. Ikonomidis I, Aboyans V, Blacher J, Brodmann M, Brutsaert DL, Chirinos JA, De Carlo M, Delgado V, Lancellotti P, Lekakis J, Mohty D, Nihoyannopoulos P, Parissis J, Rizzoni D, Ruschitzka F, Seferovic P, Stabile E, Tousoulis D, Vinereanu D, Vlachopoulos C, Vlastos D, Xaplanteris P, Zimlichman R, Metra M. The role

of ventricular-arterial coupling in cardiac disease and heart failure: assessment, clinical implications and therapeutic interventions. A consensus document of the European Society of Cardiology Working Group on Aorta & Peripheral Vascular Diseas. Eur J Heart Fail. 2019; 21(4) :402–24. doi:10.1002/ejhf.1436

40. Paliakaitė B, Charlton PH, Rapalis A, Pluščiauskaitė V, Piartli P, Kaniusas E, Marozas V. Blood Pressure Estimation Based on Photoplethysmography: Finger Versus Wrist. In: 2021 Computing in Cardiology (CinC). Brno, Czech Republic: Computing in Cardiology; 2021 Sep 12 p. 1–4. doi:10.23919/CinC53138.2021.9662716

41. Calcagnini G, Triventi M, Censi F, Mattei E, Bartolini P, Mele F. An algorithm for the detection of atrial fibrillation using the pulse oximetric signal. In: Proceedings of the International Conference on Bio-inspired Systems and Signal Processing (BIOSIGNALS-2011). Rome, Italy: Setúbal: INSTICC Press; 2011 Jan 26 p. 429–32. doi:10.5220/0003150804290432

42. Task Force of the European Society of Cardiology and the North American Society of Pacing and Electrophysiology. Heart rate variability: standards of measurement, physiological interpretation and clinical use. Circulation [Internet]. 1996 Mar 1 [cited 2016 Nov 25]; 93(5) :1043–65. Available from: http://www.ncbi.nlm.nih.gov/pubmed/8598068 doi:10.1161/01.CIR.93.5.1043

43. Inoue N, Kawakami H, Yamamoto H, Ito C, Fujiwara S, Sasaki H, Kihara Y. Second derivative of the finger photoplethysmogram and cardiovascular mortality in middle-aged and elderly Japanese women. Hypertens Res [Internet]. 2017 Feb [cited 2017 Apr 24]; 40(2) :207–11. Available from: http://www.nature.com/doifinder/10.1038/hr.2016.123 doi:10.1038/hr.2016.123

44. Haiden A, Eber B, Weber T. U-Shaped Relationship of Left Ventricular Ejection Time Index and All-Cause Mortality. Am J Hypertens [Internet]. 2014 May 1 [cited 2018 Mar 21]; 27(5) :702–9. Available from: https://academic.oup.com/ajh/article-lookup/doi/10.1093/ajh/hpt185 doi:10.1093/ajh/hpt185

45. Millasseau SC, Guigui FG, Kelly RP, Prasad K, Cockcroft JR, Ritter JM, Chowienczyk PJ. Noninvasive assessment of the digital volume pulse. Comparison with the peripheral pressure pulse. Hypertension [Internet]. 2000 Dec [cited 2015

Feb 6]; 36(6) :952–6. Available from: http://www.ncbi.nlm.nih.gov/pubmed/11116106 doi:10.1161/01.HYP.36.6.952

46. Takazawa K, Tanaka N, Fujita M, Matsuoka O, Saiki T, Aikawa M, Tamura S, Ibukiyama C. Assessment of vasoactive agents and vascular aging by the second derivative of photoplethysmogram waveform. Hypertension [Internet]. 1998 Aug [cited 2015 Feb 2]; 32(2) :365–70. Available from: http://www.ncbi.nlm.nih.gov/pubmed/9719069 doi:10.1161/01.HYP.32.2.365
47. Nirala N, Periyasamy R, Singh BK, Kumar A. Detection of type-2 diabetes using characteristics of toe photoplethysmogram by applying support vector machine. Biocybern Biomed Eng [Internet]. 2019 Jan 1 [cited 2020 Apr 19]; 39(1) :38–51. Available from: https://linkinghub.elsevier.com/retrieve/pii/S0208521617304266 doi:10.1016/j.bbe.2018.09.007
48. Paradkar N, Roy Chowdhury S. Coronary artery disease detection using photoplethysmography. In: 2017 39th Annual International Conference of the IEEE Engineering in Medicine and Biology Society (EMBC). Jeju, Korea (South): Piscataway (NJ): IEEE; 2017 Jul 11 p. 100–3. doi:10.1109/EMBC.2017.8036772
49. Huotari M, Vehkaoja A, Määttä K, Kostamovaara J. Photoplethysmography and its detailed pulse waveform analysis for arterial stiffness. Raken Mek [Internet]. 2011 [cited 2020 Apr 19]; 44(4) :345–62. Available from: https://www.researchgate.net/publication/260321650_Photoplethysmography_and_its_detailed_pulse_waveform_analysis_for_arterial_stiffness
50. Weber T, Auer J, O'Rourke MF, Kvas E, Lassnig E, Berent R, Eber B. Arterial Stiffness, Wave Reflections, and the Risk of Coronary Artery Disease. Circulation. 2004; 109(2) :184–9. doi:10.1161/01.CIR.0000105767.94169.E3
51. Kulin D, Antali F, Kulin S, Wafa D, Lucz KI, Veres DS, Miklós Z. Preclinical, multi-aspect assessment of the reliability of a photoplethysmography-based telemonitoring system to track cardiovascular status. Appl Sci. 2020; 10(22) :1–17. doi:10.3390/app10227977
52. Allen J, Kyriacou P. Photoplethysmography: Technology, Signal Analysis and Applications. 1st. ed. Amsterdam, The Netherlands: Elsevier; 2021. 1–490 p. doi:10.1016/C2020-0-00098-8
53. Almarshad MA, Islam MS, Al-Ahmadi S, Bahammam AS. Diagnostic Features

and Potential Applications of PPG Signal in Healthcare: A Systematic Review. Healthc. 2022; 10(3) :1–28. doi:10.3390/healthcare10030547

54. Park J, Seok HS, Kim SS, Shin H. Photoplethysmogram Analysis and Applications: An Integrative Review. Front Physiol. 2022; 12(March) :1–23. doi:10.3389/fphys.2021.808451

55. Antali F, Kulin D, Lucz KI, Szabó B, Szűcs L, Kulin S, Miklós Z. Multimodal Assessment of the Pulse Rate Variability Analysis Module of a Photoplethysmography-Based Telemedicine System. Sensors [Internet]. 2021 [cited 2022 Feb 2]; 21(16) :5544. Available from: https://www.ncbi.nlm.nih.gov/pmc/articles/PMC8401087/ doi:10.3390/s21165544

56. Antali F, Kulin D, Kulin S, Miklós Z. Evaluation of the Age Dependence of Conventional and Novel Photoplethysmography Parameters. Artery Res [Internet]. 2025; 31(1). Available from: https://doi.org/10.1007/s44200-025-00068-w doi:10.1007/s44200-025-00068-w

57. Mitchell GF, Parise H, Benjamin EJ, Larson MG, Keyes MJ, Vita JA, Vasan RS, Levy D. Changes in Arterial Stiffness and Wave Reflection With Advancing Age in Healthy Men and Women The Framingham Heart Study. Hypertension [Internet]. 2004 [cited 2018 Sep 26]; 43(6) :1239–45. Available from: https://www.ahajournals.org/doi/10.1161/01.hyp.0000128420.01881.aa doi:10.1161/01.HYP.0000128420.01881.aa

58. Millasseau SC, Kelly RP, Ritter JM, Chowienczyk PJ. The vascular impact of aging and vasoactive drugs: Comparison of two digital volume pulse measurements. Am J Hypertens. 2003; 16(6) :467–72. doi:10.1016/S0895-7061(03)00569-7

59. Mok Ahn J. New aging index using signal features of both photoplethysmograms and acceleration plethysmograms. Healthc Inform Res. 2017; 23(1) :53–9. doi:10.4258/hir.2017.23.1.53

60. Fine J, Branan KL, Rodriguez AJ, Boonya-ananta T, Ajmal, Ramella-Roman JC, McShane MJ, Coté GL. Sources of Inaccuracy in Photoplethysmography for Continuous Cardiovascular Monitoring. Biosensors [Internet]. 2021 Apr 16; 11(4) :126. Available from: https://www.mdpi.com/2079-6374/11/4/126

doi:10.3390/bios11040126

61. Ghodeshwar GK, Dube A, Khobragade D. Impact of Lifestyle Modifications on Cardiovascular Health: A Narrative Review. Cureus. 2023 Jul; 15(Ldl) :e42616. doi:10.7759/cureus.42616
62. Benczur B, Miklos Z, Kulin D, Nemcsik J. Az artériás életkor meghatározásának klinikai jelentôsége. Lege Artis Med. 2022; 32(10) :457–64. doi:10.33616/lam.32.037
63. Bruno RM, Nilsson PM, Engström G, Wadström BN, Empana JP, Boutouyrie P, Laurent S. Early and Supernormal Vascular Aging: Clinical Characteristics and Association With Incident Cardiovascular Events. Hypertension. 2020; 76(5) :1616–24. doi:10.1161/HYPERTENSIONAHA.120.14971
64. O'Rourke MF. Arterial aging: Pathophysiological principles. Vasc Med. 2007; 12(4) :329–41. doi:10.1177/1358863X07083392
65. Karimpour P, May JM, Kyriacou PA. Photoplethysmography for the Assessment of Arterial Stiffness. Sensors. 2023; 23(24). doi:10.3390/s23249882
66. Stergiou GS, Mukkamala R, Avolio A, Kyriakoulis KG, Mieke S, Murray A, Parati G, Schutte AE, Sharman JE, Asmar R, McManus RJ, Asayama K, De La Sierra A, Head G, Kario K, Kollias A, Myers M, Niiranen T, Ohkubo T, Wang J, Wuerzner G, O'Brien E, Kreutz R, Palatini P. Cuffless blood pressure measuring devices: Review and statement by the European Society of Hypertension Working Group on Blood Pressure Monitoring and Cardiovascular Variability. J Hypertens. 2022; 40(8) :1449–60. doi:10.1097/HJH.0000000000003224
67. Allen J, Overbeck K, Nath AF, Murray A, Stansby G. A prospective comparison of bilateral photoplethysmography versus the ankle-brachial pressure index for detecting and quantifying lower limb peripheral arterial disease. J Vasc Surg. 2008 Apr 1; 47(4) :794–802. doi:10.1016/j.jvs.2007.11.057
68. Duncker D, Ding WY, Etheridge S, Noseworthy PA, Veltmann C, Yao X, Bunch TJ, Gupta D. Smart Wearables for Cardiac Monitoring—Real-World Use beyond Atrial Fibrillation. Sensors [Internet]. 2021; 21(7). Available from: https://www.mdpi.com/1424-8220/21/7/2539 doi:10.3390/s21072539
69. Väliaho ES, Kuoppa P, Lipponen JA, Martikainen TJ, Jäntti H, Rissanen TT, Kolk I, Castrén M, Halonen J, Tarvainen MP, Hartikainen JEK. Wrist band

photoplethysmography in detection of individual pulses in atrial fibrillation and algorithm-based detection of atrial fibrillation. Europace. 2019 Jul; 21(7) :1031–8. doi:10.1093/europace/euz060

70. Kornej J, Börschel CS, Benjamin EJ, Schnabel RB. Epidemiology of Atrial Fibrillation in the 21st Century. Circ Res [Internet]. 2020 Jun 19; 127(1) :4–20. Available from: https://doi.org/10.1161/CIRCRESAHA.120.316340 doi:10.1161/CIRCRESAHA.120.316340
71. Scholte NTB, Van Ravensberg AE, Edgar R, Van Den Enden AJM, Van Mieghem NMDA, Brugts JJ, Bonnes JL, Bruining N, Van Der Boon RMA. Photoplethysmography and intracardiac pressures: early insights from a pilot study. Eur Heart J Digit Health. 2024 May 1; 5(3) :379–83. doi:10.1093/ehjdh/ztae020
72. Shah AJ, Isakadze N, Levantsevych O, Vest A, Clifford G, Nemati S. Detecting heart failure using wearables: a pilot study. Physiol Meas [Internet]. 2020 May 4; 41(4) :044001. Available from: https://iopscience.iop.org/article/10.1088/1361-6579/ab7f93 doi:10.1088/1361-6579/ab7f93
73. Su F, Li Z, Sun X, Han N, Wang L, Luo X. The Pulse Wave Analysis of Normal Pregnancy: Investigating the Gestational Effects on Photoplethysmographic Signals. Biomed Mater Eng. 2014; 24(1) :209–19. doi:10.3233/BME-130801
74. Chung E, Leinwand LA. Pregnancy as a cardiac stress model. Cardiovasc Res [Internet]. 2014 Mar 15 [cited 2023 Nov 23]; 101(4) :561–70. Available from: https://pubmed.ncbi.nlm.nih.gov/24448313/ doi:10.1093/CVR/CVU013
75. Arioz DT, Saglam H, Demirel R, Koken G, Cosar E, Sahin FK, Dursun H, Aral İ, Onrat E, Yilmazer M. Arterial stiffness and dipper/nondipper blood pressure status in women with preeclampsia. Adv Ther. 2008; 25(9) :925–34. doi:10.1007/s12325-008-0090-2
76. Kulin D, Várfalvi M, Kulin S. Digital Support for Family Health Protection by Health Visitors: The “Health Visitors for a Healthy Generation and Nation” Project. Aranypajzs. 2023; 2(1) :19–24. doi:10.56077/ap.2023.t1.2
77. Allen J. Photoplethysmography and its application in clinical physiological measurement. Physiol Meas [Internet]. 2007 Mar 1 [cited 2018 Jan 24]; 28(3) :R1–39. Available from: http://www.ncbi.nlm.nih.gov/pubmed/17322588

doi:10.1088/0967-3334/28/3/R01

78. Korhonen I, Yli-Hankala A. Photoplethysmography and nociception: Review Article. Acta Anaesthesiol Scand. 2009; 53(8) :975–85. doi:10.1111/j.1399-6576.2009.02026.x

79. Elgendi M. Detection of c, d, and e waves in the acceleration photoplethysmogram. Comput Methods Programs Biomed [Internet]. 2014 Nov [cited 2017 Mar 15]; 117(2) :125–36. Available from: http://linkinghub.elsevier.com/retrieve/pii/S0169260714003010 doi:10.1016/j.cmpb.2014.08.001

80. Charlton PH, Allen J, Bailon R, Baker S, Behar JA, Chen F, Clifford GD, Clifton DA, Davies HJ, Ding C, Ding X, Dunn J, Elgendi M, Ferdoushi M, Franklin D, Gil E, Hassan MF, Hernesniemi J, Hu X, Ji N, Khan Y, Kontaxis S, Korhonen I, Kyriacou PA, Laguna P, Lazaro J, Lee C, Levy J, Li Y, Liu C, Liu J, Lu L, Mandic DP, Marozas V, Mejía-Mejía E, Mukkamala R, Nitzan M, Pereira T, Poon CCY, Ramella-Roman JC, Saarinen H, Shandhi MMH, Shin H, Stansby G, Tamura T, Vehkaoja A, Wang WK, Zhang YT, Zhao N, Zheng D, Zhu T. The 2023 wearable photoplethysmography roadmap. Physiol Meas. 2023; doi:10.1088/1361-6579/acead2

81. Bortolotto LA, Blacher J, Kondo T, Takazawa K, Safar ME. Assessment of vascular aging and atherosclerosis in hypertensive subjects: Second derivative of photoplethysmogram versus pulse wave velocity. Am J Hypertens. 2000; 13(2) :165–71. doi:10.1016/S0895-7061(99)00192-2

82. Imanaga I, Hara H, Koyanagi S, Tanaka K. Correlation between wave components of the second derivative of plethysmogram and arterial distensibility. Jpn Heart J [Internet]. 1998 Nov [cited 2016 Nov 27]; 39(6) :775–84. Available from: http://www.ncbi.nlm.nih.gov/pubmed/10089939 doi:10.1536/ihj.39.775

83. Hashimoto J, Chonan K, Aoki Y, Nishimura T, Ohkubo T, Hozawa A, Suzuki M, Matsubara M, Michimata M, Araki T, Imai Y. Pulse wave velocity and the second derivative of the finger photoplethysmogram in treated hypertensive patients: their relationship and associating factors. J Hypertens. 2002; 20(12) :2415–22. doi:10.1097/01.hjh.0000042887.24999.7b

84. Otsuka T, Kawada T, Katsumata M, Ibuki C. Utility of second derivative of the

finger photoplethysmogram for the estimation of the risk of coronary heart disease in the general population. Circ J [Internet]. 2006 Mar [cited 2016 Nov 25]; 70(3) :304–10. Available from: http://www.ncbi.nlm.nih.gov/pubmed/16501297 doi:10.1253/circj.70.304

85. Hyun JB, Jung SK, Yun SK, Haet BL, Kwang SP. Second derivative of photoplethysmography for estimating vascular aging. In: 2007 6th International Special Topic Conference on Information Technology Applications in Biomedicine. Tokyo, Japan: Piscataway (NJ): IEEE; 2007 Nov 8 p. 70–2. doi:10.1109/ITAB.2007.4407346

86. Pilt K, Meigas K, Ferenets R, Temitski K, Viigimaa M. Photoplethysmographic signal waveform index for detection of increased arterial stiffness. Physiol Meas. 2014; 35(10) :2027–36. doi:10.1088/0967-3334/35/10/2027

87. Pilt K, Ferenets R, Meigas K, Lindberg LG, Temitski K, Viigimaa M. New photoplethysmographic signal analysis algorithm for arterial stiffness estimation. ScientificWorldJournal [Internet]. 2013 [cited 2016 Dec 2]; 2013 :169035. Available from: http://www.ncbi.nlm.nih.gov/pubmed/23983620 doi:10.1155/2013/169035

88. Segers P, Kips J, Trachet B, Swillens A, Vermeersch S, Mahieu D, Rietzschel E, De Buyzere M, Van Bortel L. Limitations and pitfalls of non-invasive measurement of arterial pressure wave reflections and pulse wave velocity. Artery Res [Internet]. 2009 Jun [cited 2017 Aug 16]; 3(2) :79–88. Available from: http://linkinghub.elsevier.com/retrieve/pii/S1872931209000118 doi:10.1016/j.artres.2009.02.006

89. Miyashita H, Katsuda S ichiro I. Basis of monitoring central blood pressure and hemodynamic parameters by peripheral arterial pulse waveform analyses. In: Annual International Conference of the IEEE Engineering in Medicine and Biology Society. Osaka, Japan: Piscataway (NJ): IEEE; 2013 Jul 3 p. 221–4. doi:10.1109/EMBC.2013.6609477

90. Miyashita H. The time is ripe to reevaluate the second derivative of the digital photoplethysmogram (SDPTG), originating in Japan, as an important tool for cardiovascular risk and central hemodynamic assessment. Hypertens Res. 2017; 40(5) :429–31. doi:10.1038/hr.2016.175

91. Chen G, Meng L, Alexander B, Tran NP, Kain ZN, Cannesson M. Comparison of noninvasive cardiac output measurements using the Nexfin monitoring device and the esophageal Doppler. J Clin Anesth [Internet]. 2012; 24(4) :275–83. Available from: http://dx.doi.org/10.1016/j.jclinane.2011.08.014 doi:10.1016/j.jclinane.2011.08.014

92. Duan W, Zheng D, Eggett C, Langley P, Murray A. Development of techniques for measurement of left ventricular ejection time. In: Murray A, editor. Computing in Cardiology. Cambridge, Massachusetts, USA: Piscataway (NJ): IEEE; 2014 Sep 7 p. 241–4.

93. Meah VL, Backx K, Shave RE, Stöhr EJ, Cooper SM. Comparison between Modelflow® and echocardiography in the determination of cardiac output during and following pregnancy at rest and during exercise. J Hum Sport Exerc [Internet]. 2022 Jan 1 [cited 2024 May 2]; 17(1) :116–35. Available from: https://doaj.org/article/099876e83a104a3481d21d12267a1020 doi:10.14198/JHSE.2022.171.12

94. Blanié A, Soued M, Benhamou D, Mazoit JX, Duranteau J. A Comparison of Photoplethysmography Versus Esophageal Doppler for the Assessment of Cardiac Index During Major Noncardiac Surgery. Anesth Analg [Internet]. 2016 Feb 1 [cited 2024 May 2]; 122(2) :430–6. Available from: https://pubmed.ncbi.nlm.nih.gov/26649910/ doi:10.1213/ANE.0000000000001113

95. Özen Kavas P, Recep Bozkurt M, Kocayiğit İ, Bilgin C. Machine learning-based medical decision support system for diagnosing HFpEF and HFrEF using PPG. Biomed Signal Process Control [Internet]. 2023; 79(August 2022) :104164. Available from: https://www.sciencedirect.com/science/article/pii/S1746809422006188 doi:https://doi.org/10.1016/j.bspc.2022.104164

96. Lang RM, Badano LP, Victor MA, Afilalo J, Armstrong A, Ernande L, Flachskampf F, Foster E, Goldstein SA, Kuznetsova T, Lancellotti P, Muraru D, Picard MH, Retzschel ER, Rudski L, Spencer KT, Tsang W, Voigt JU. Recommendations for cardiac chamber quantification by echocardiography in adults: An update from the American Society of Echocardiography and the

European Association of Cardiovascular Imaging. J Am Soc Echocardiogr. 2015; 28(1) :1. doi:10.1016/j.echo.2014.10.003

97. Kulin D, Antali F, Horváth M, Kulin S, Kulin Jr. S, Miklós Z, Szűcs A. Evaluating photoplethysmography-based pulsewave parameters and composite scores for assessment of cardiac function: A comparison with echocardiography. Physiol Int. 2025; 112(3) :229–47. doi:10.1556/2060.2025.00675
98. Abdullah S, Hafid A, Folke M, Lindén M, Kristoffersson A. A Novel Fiducial Point Extraction Algorithm to Detect C and D Points from the Acceleration Photoplethysmogram (CnD). Electron. 2023; 12(5). doi:10.3390/electronics12051174
99. Green EM, van Mourik R, Wolfus C, Heitner SB, Dur O, Semigran MJ. Machine learning detection of obstructive hypertrophic cardiomyopathy using a wearable biosensor. npj Digit Med. 2019; 2(1) :1–4. doi:10.1038/s41746-019-0130-0
100. Steinberg RS, Udeshi E, Dickert N, Quyyumi A, Chirinos JA, Morris AA. Novel Measures of Arterial Hemodynamics and Wave Reflections Associated With Clinical Outcomes in Patients With Heart Failure. J Am Heart Assoc. 2023; 12(6). doi:10.1161/JAHA.122.027666
101. Alhakak AS, Teerlink JR, Lindenfeld J, Böhm M, Rosano GMC, Biering-Sørensen T. The significance of left ventricular ejection time in heart failure with reduced ejection fraction. Eur J Heart Fail. 2021; 23(4) :541–51. doi:10.1002/ejhf.2125
102. Obata Y, Mizogami M, Singh S, Nyhan D, Berkowitz DE, Steppan J, Barodka V. Ejection time: Influence of hemodynamics and site of measurement in the arterial tree. Hypertens Res. 2017; 40(9) :811–8. doi:10.1038/hr.2017.43
103. Pangarkar T. Wearable Technology Statistics 2025 By Tech and Human [Internet]. 2025 [cited 2025 Aug 12]. Available from: https://scoop.market.us/wearable-technology-statistics/
104. Voigt JU. Left ventricular function, heart failure, and resynchronization therapy. In: Camm A, Lüscher T, Serruys P, editors. The ESC Textbook of Cardiovascular Medicine [Internet]. 3rd. ed. Oxford: Oxford University Press; 2018. p. 450–4. Available from: https://academic.oup.com/book/doi/10.1093/med/9780198784906.003.0092 doi:10.1093/med/9780198784906.003.0092

105. Nichols WW, O'Rourke MF, Avolio AP, Yaginuma T, Murgo JP, Pepine CJ, Conti CR. Effects of age on ventricular-vascular coupling. Am J Cardiol. 1985 Apr; 55(9) :1179–84. doi:10.1016/0002-9149(85)90659-9

106. Li Q, Huang H, Lu X, Yang Y, Zhang Y, Chen W, Lai W, Liang G, Shi S, Wang X, Chen J, Chen S, Yan X. The Association between Left Ventricular End-Diastolic Diameter and Long-Term Mortality in Patients with Coronary Artery Disease. Rev Cardiovasc Med [Internet]. 2023 Mar 8; 24(3) :84. Available from: https://www.imrpress.com/journal/RCM/24/3/10.31083/j.rcm2403084 doi:10.31083/j.rcm2403084

107. Alsaddique AA. Recognition of diastolic heart failure in the postoperative heart. Eur J Cardio-Thoracic Surg [Internet]. 2008 Dec 1 [cited 2024 May 2]; 34(6) :1141–8. Available from: https://dx.doi.org/10.1016/j.ejcts.2008.05.030 doi:10.1016/J.EJCTS.2008.05.030

108. Nishimura RA, Tajik AJ. Evaluation of diastolic filling of left ventricle in health and disease: Doppler echocardiography is the clinician's Rosetta Stone. J Am Coll Cardiol [Internet]. 1997; 30(1) :8–18. Available from: http://dx.doi.org/10.1016/S0735-1097(97)00144-7 doi:10.1016/S0735-1097(97)00144-7

109. Weber T, Auer J, O'Rourke MF, Punzengruber C, Kvas E, Eber B. Prolonged mechanical systole and increased arterial wave reflections in diastolic dysfunction. Heart. 2006; 92(11) :1616–22. doi:10.1136/hrt.2005.084145

110. Bearak J, Popinchalk A, Ganatra B, Moller AB, Tunçalp Ö, Beavin C, Kwok L, Alkema L. Unintended pregnancy and abortion by income, region, and the legal status of abortion: estimates from a comprehensive model for 1990–2019. Lancet Glob Health. 2020; 8(9) :e1152–61. doi:10.1016/S2214-109X(20)30315-6

9. Bibliography of the candidate's publications

Publications tightly related to the dissertation:

**Kulin D, Antali F, Kulin S, Wafa D, Lucz KI, Veres DS, Miklós Z.** Preclinical, multi-aspect assessment of the reliability of a photoplethysmography-based telemonitoring system to track cardiovascular status. *Appl Sci*. 2020;10(22):1–17. doi:10.3390/app10227977

IF: 2.679

**Kulin D, Antali F, Horváth M, Kulin S, Kulin S Jr, Miklós Z, Szűcs A.** Evaluating photoplethysmography-based pulsewave parameters and composite scores for assessment of cardiac function: A comparison with echocardiography. *Physiol Int*. 2025;112(3), 229-247. doi: 10.1556/2060.2025.00675

IF: (article published after the submission)

**Antali F, Kulin D, Lucz KI, Szabó B, Szűcs L, Kulin S, Miklós Z.** Multimodal assessment of the pulse rate variability analysis module of a photoplethysmography-based telemedicine system. *Sensors*. 2021;21(16):5544. doi:10.3390/s21165544

IF: 3.847

**Antali F, Kulin D, Kulin S, Miklós Z.** Evaluation of the age dependence of conventional and novel photoplethysmography parameters. *Artery Res*. 2025;31(1):118–126. doi:10.1007/s44200-025-00068-w

IF: 1.6

**Charlton PH, Paliakaitė B, Pilt K, Bachler M, Zanelli S, Kulin D, Allen J, Hallab M, Bianchini E, Mayer CC, Terentes-Printzios D, Dittrich V, Hametner B, Veerasingam D, Žikić D, Marozas V.** Assessing hemodynamics from the photoplethysmogram to gain insights into vascular age: a review from VascAgeNet. *Am J Physiol Heart Circ Physiol*. 2022;322(4):H493–H522. doi:10.1152/ajpheart.00392.2021

IF: 4.8

Publications referenced in, but not strongly related to the dissertation:

D. Kulin, M. Várfalvi, and S. Kulin, “Digital Support for Family Health Protection by Health Visitors: The ‘Health Visitors for a Healthy Generation and Nation’ Project,” *Aranypajzs*, vol. 2, no. 1, pp. 19–24, 2023. DOI: 10.56077/AP.2023.t1.2

IF: -

## 10. Acknowledgements

This dissertation - and all the work behind it - has been the main project of my professional life since 2014. First and foremost, I wish to express my deepest gratitude to God, my Heavenly Father, the King of Kings, who guided me through the hardships and was present in the celebrations of every milestone along the way.

I would also like to express my heartfelt thanks to Zsuzsanna Miklós, an exceptional mentor and friend, who has been my lighthouse in the foggy, stormy waters of the scientific ocean and sometimes my personal life too.

Throughout this journey, I came to realize that professional success means little without family. I am immensely grateful to my beautiful wife, Zsófi, with whom we worked together as medical students to better understand the relationship between pulse wave features and various pregnancy pathologies. Besides her, I am grateful for our three wonderful, smart, and funny daughters for their support, patience, and love. The members of this family are my most precious gifts from God.

My deepest thanks also go to my father, my closest colleague and partner from the very beginning. He was the one who kickstarted this journey, and his unwavering energy and drive helped me overcome many of the challenges we've faced. He is not alone - he has a wonderful wife, whom I am proud to call my mum. Thank you, Anya, for giving me life and for the love with which you raised me and my four other siblings up.

I want to thank Flóra Antali, my closest research partner for many years. Together, we formed a truly effective team. Her attention to detail and her endurance with monotony are true superpowers. Although she has moved on in recent years, our friendship remains strong and lasting.

In more recent years, my brother joined the mission - my only and best brother, a brilliant software engineer and invaluable data scientist. His contributions have significantly accelerated our work. Thank you, Sano!

I also owe a big thank you to Péter Kulin and Bogi Barcza, the quiet forces behind the scenes. Their tireless work, enthusiasm, and loyalty in managing the non-scientific aspects of this immense project made it all possible.

At this point, I must also mention three other gentlemen: Balázs Szabó, Marcel Visschers, and Paul Obers, with whom I had the privilege to join forces and dream big—sharing a vision of elevating PPG-based telemedicine to the next level. I truly hope that one day all the effort we invested will bear meaningful fruit.

I would like to express my appreciation to Professor Zoltán Benyó, the laid-back yet consistently supportive head of the Institute of Translational Medicine. His open-mindedness and kind support have always been a source of strength.

I'm grateful to Zsuzsanna Győrffy, PhD, my first supervisor, who introduced me to the world of telemedicine and digital health.

A warm thank-you goes to all the clinicians, patients, and volunteers who, despite their busy lives, donated their time and effort to our studies. I pray for a happy, healthy, and blessed life for each of you.

I am also thankful for the support and mentorship of Dr. Krisztina Szőllős and Professor Szabolcs Várbíró, who guided our very first scientific project as medical students - an experience that laid the foundation for this entire endeavor.

Finally, I would like to thank everyone who, in any way, contributed to this work or supported the milestones we've achieved over the years. Special thanks to the Science Management Workgroup for their helpful materials in the dissertation writing process.

I hope this big project will go further - reaching the point where it can truly improve the lives of millions of patients and their caregivers worldwide.

applied sciences

MDPI

Article

# Preclinical, Multi-Aspect Assessment of the Reliability of a Photoplethysmography-Based Telemonitoring System to Track Cardiovascular Status

**Dániel Kulin [1,2,*], Flóra Antali [1,2], Sándor Kulin [2], Dina Wafa [1], Konrád István Lucz [2], Dániel Sándor Veres [3] and Zsuzsanna Miklós [1,*]**

1 Institute of Translational Medicine, Semmelweis University, 1092 Budapest, Hungary; antali.flora@gmail.com (F.A.); dina.wafa.93@gmail.com (D.W.)
2 E-Med4All Europe ltd., 1036 Budapest, Hungary; dr.kulin.sandor@pregnascan.eu (S.K.); luczkonrad@gmail.com (K.I.L.)
3 Department of Biophysics and Radiation Biology, Semmelweis University, 1094 Budapest, Hungary; veres.daniel@med.semmelweis-univ.hu
* Correspondence: kulin.daniel@med.semmelweis-univ.hu (D.K.); miklos.zsuzsanna@med.semmelweis-univ.hu (Z.M.); Tel.: +36-30-922-6206 (D.K.); +36-20-585-8099 (Z.M.)

Received: 28 September 2020; Accepted: 8 November 2020; Published: 10 November 2020


**Abstract:** Telemonitoring systems equipped with photoplethysmography-based contour analysis of the digital arterial volume pulse (DVP) can be optimal tools for remote monitoring of cardiovascular patients; however, the method is known to be sensitive to errors. We aimed to show that DVP analysis is a reliable method to track cardiovascular status. We used our proprietary SCN4ALL telemedicine system and analyzed nine parameters derived from the DVP and its second derivative (SDDVP). First, we assessed the repeatability of system measurements by detecting artificial signals. Then test–retest reliability of human measurements was evaluated in healthy individuals under standardized conditions. The SCN4ALL system analyzed each parameter with high accuracy (coefficients of variation (CVs) < 1%). Test–retest reliability of most parameters (stiffness index, reflection index, left ventricular ejection time index, b/a, heart rate) was satisfactory (CVs < 10%) in healthy individuals. However, aging index and d/a ratio derived from the SDDVP were more variable. Photoplethysmography-based pulse contour analysis is a reliable method to monitor cardiovascular status if measurements are performed with a system of high accuracy. Our results highlighted that SDDVP parameters can be interpreted with limitations due to (patho)physiological variations of the DVP. We recommend the evaluation of these parameters only in measurements where all inflections of SDDVP are detected reliably.

**Keywords:** pulse wave analysis; photoplethysmography; telemedicine; test–retest reliability; pulse contour

## 1. Introduction

Despite the enormous effort invested in research and development of new treatments to break the dominance of cardiovascular diseases in morbidity and mortality statistics, they are still among the leading causes of death [1,2]. A potential breakthrough could be achieved by launching extensive home surveillance programs that allow close follow-up of cardiovascular patients. The pandemic months of COVID-19 underline the need for reliable telemedicine surveillance tools to reduce the need for personal visits to outpatient clinics, thus reducing the chance of infection of the highest risk population.

Development of a cardiovascular telemonitoring system requires the incorporation of a cardiovascular measurement that is noninvasive, easy-to-use for the patient, convenient, timesaving,

and not least provides clinically relevant information about the current cardiovascular status of the patient. The detection and analysis of digital arterial volume pulse (DVP) recorded by the photoplethysmographic (PPG) method is a perfect option as it fits all these requirements. In fact, the DVP tracks the changes of vessel diameter and blood volume in the arteries which occur due to arterial pulsation [3,4], and hence its shape is identical to the digital arterial pulse wave.

Mechanistically, the arterial pulse wave is a pressure wave that is initiated by cardiac ejection and runs through the arterial system. It is an invaluable source of information about the cardiovascular status of the patient, as its amplitude and contour are influenced by the dynamics of cardiac function, the elasticity of the arteries, and also by the pressure augmentation caused by the superimposing reflected pressure wave [5], which is highly affected by the tone of the resistance vessels. Moreover, all these factors are dependent on the current status of the autonomic nervous system. Not surprisingly, altered cardiovascular conditions (both physiological and pathological) cause well-defined characteristic changes in the shape and propagation velocity of the pulse wave [6–11]. Therefore, by detecting the changes in pulse wave contour, it is possible to establish the cardiovascular status of the patient.

Mathematical analysis of the pulse wave and DVP is well established in the literature [4,12–14]. Several cardiovascular indices, termed pulse contour parameters, derived from the raw curve and from its first and second derivatives have been identified as measures of various elements of cardiac and vascular function (Figure 1). Alterations of these indices have been associated with cardiovascular pathologies such as arterial stiffness, atherosclerosis, hypertension, aging, diabetes, coronary heart disease, and heart failure [12–19].

Undoubtedly, these scientifically well-established characteristics of PPG-based detection and analysis of DVP make this method an optimal tool for remote cardiovascular monitoring. Despite this, it has not gained ground in clinical practice so far. The reason behind this is that there are controversies about the applicability of this method in clinical diagnostics and the lack of large-population studies that could establish the guidelines for follow-up and those patient groups in which it would have the highest benefit.

One reason why the applicability of the method is debated that the parameters computed from DVP are sensitive to errors and cannot be detected reliably as they fluctuate from one measurement to another even if the cardiovascular status of the patient is stable [20–23]. However, this controversy is fostered in part by the fact that no data are available in the scientific literature about the reliability of the measurements. This issue is particularly emphasized in the case of those parameters which are derived from the second derivative of the DVP. The second derivative of the DVP (often referred to as acceleration plethysmogram) has several distinguished points from which valuable cardiovascular indices can be calculated (Figure 1). Among these, c and d points have been introduced as characteristics that may facilitate our understanding of the dynamics of wave reflection and the pulse wave analysis based evaluation of the severity of arterial aging [14,24–28]. However, the detection of these points has become a challenge for mathematical algorithms to identify [8,29,30].

This study was designed to address these controversies in order to show that the detection and computation of DVP contour parameters is a reliable method. We postulated that fluctuations in measured values most probably reflect real changes in cardiovascular functioning and are not caused by poor reliability of DVP analysis. To answer our specific questions, we used a PPG-based telemedicine system which has been developed with the participation of our research team (SCN4ALL ver.1.0, E-Med4All Europe Ltd., Budapest, Hungary) (Figure 2), and we analyzed nine pulse contour parameters, the medical significance of which has been proposed by various studies (Figure 1). Our specific questions addressed not only the reliability of DVP analysis in general, but also the measurement reliability of our system.

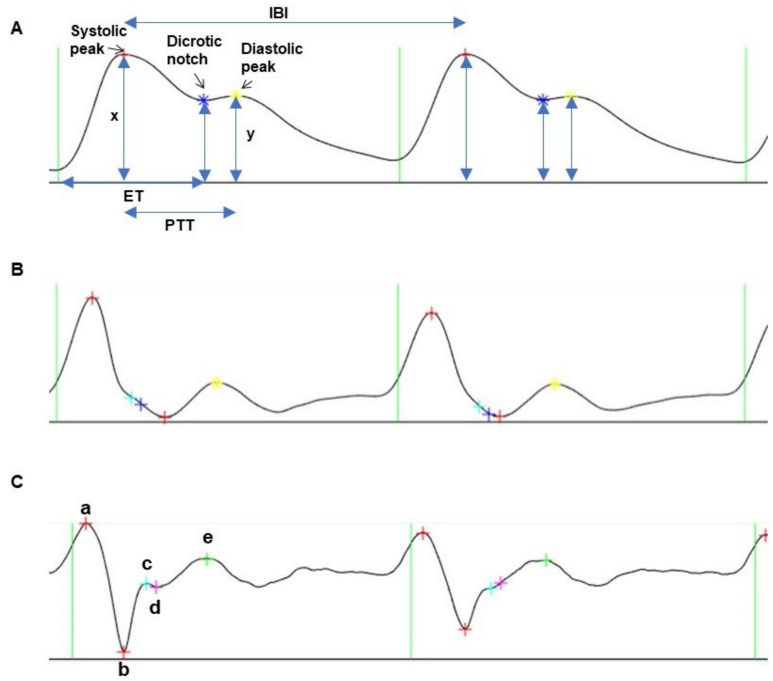


**Figure 1.** Pulse contour parameters calculated by the SCN4ALL system. Representative pulse wave recording (panel **A**), and its first (panel **B**) and second derivative curves (panel **C**). ET represents ejection time measured as the duration between the foot of the pulse wave and the dicrotic notch. ET was normalized for heart rate to calculate left ventricular ejection time index (LVETI) using the formulae LVETI = 1.7 × heart rate + ET and LVETI = 1.6 × heart rate + ET in males and females, respectively. Pulse transit time (PTT) is the duration measured between the systolic and diastolic peaks of the curve. PTT was used to calculate stiffness index as the height of the subject over PT. IBI represents interbeat interval, which is the pulse duration measured from peak to peak. Here, x and y are amplitudes of the systolic and diastolic peaks, respectively, and are used for calculation of the reflection index as x/y. Points a–e represent notable inflection points of the second derivative curve. Second derivative inflection points were used to calculate b/a, d/a, aging index (calculated as (b − c − d − e)/a), and c–d point detection ratio (the percentage of pulse cycles in the 2-min recording in which c and d points were successfully identified by the algorithm).

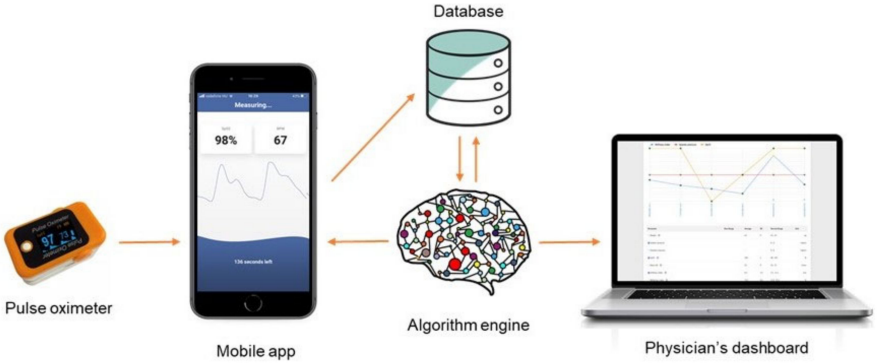


**Figure 2.** Outline of the SCN4ALL telemedicine system. Peripheral arterial pulse wave is detected by a transmission pulse oximeter. The device (Berry Pulse Oximeter, Shanghai Berry Electronic Tech Co., Ltd., Shanghai, China) communicates via Bluetooth connection with a mobile application (SCN4ALL) which initiates and terminates the 2-min-long data acquisition and transmits the recording to a cloud database. A cloud-based automated algorithm calculates the pulse contour variables which are then reported to the dashboard of the physician and, in brief form, to the mobile application of the user.

In this context, firstly we assessed the measurement error of our telemedicine system to rule out its relevant contribution to measurement variability in human tests.

As a next step, we aimed to test the reliability (test–retest variability) of PPG-based pulse contour analysis in human measurements. As a satellite question, we also aimed to clarify whether using different fingers for the measurement has an influence on the measurement of pulse contour indices.

Finally, using the results of the performed measurements, we evaluated the applicability of our proprietary algorithm to detect c and d points on the acceleration plethysmograph.

## 2. Materials and Methods

### 2.1. Subjects

Healthy, informed, consenting volunteers participated in the study. Volunteers who smoked, received any kind of medication, were pregnant, or had BMI > 30 were excluded. The study was approved by the Regional and Institutional Committee of Science and Research Ethics at Semmelweis University (approval number 120/2018).

### 2.2. Measurements with the SCN4ALL System

In each investigational protocol, pulse wave detection and analysis were performed by the 1.0 version of the SCN4ALL telemedicine system (E-Med4All Europe Ltd., Budapest, Hungary). Pulse wave was recorded as DVP detected by a commercially available transmission pulse oximeter (Berry Pulse Oximeter, Shanghai Berry Electronic Tech Co., Ltd., Shanghai, China; hardware: 32-bit AD converter, 200 Hz sampling rate). The device emits light to the tissues of the finger from an LED light source and detects the transmitted light by a photodiode. Vessel diameter and blood volume in the arteries change with pulsation, and so does the amount of transmitted light, enabling the detection of a continuous DVP. The pulse oximeter device communicates via Bluetooth connection with a mobile application that initiates and terminates a 2-min-long data acquisition and transmits the recording to a cloud-based automated algorithm that was developed by our research group (Figure 2).

Signal preprocessing by the algorithm starts with upsampling the 200 Hz sampling frequency of the device to 1 kHz. In order to condition the PPG signal, a digital bandpass filter—fourth-order Butterworth—with −3 dB points at 0.1 and 10 Hz is applied. Then, the algorithm identifies the pulse cycles. Afterward, within each cycle, particular distinct points of the DVP (primary curve, first and second derivatives) are identified. Then, contour parameters are computed for every individual cycle. Afterward, the means of all cycles are calculated and displayed on an internet platform for the physician. In this study, these averages were exported as spreadsheets for further analysis. The measurement data are stored at a cloud-based server (Amazon Web Services, Amazon Web Services EMEA SARL, 1855 Luxembourg, Luxemburg) equipped with safe data protection that conforms to the applicable regulations ((EU) 2016/679).

The automatically calculated pulse contour parameters that this study focuses on are as follows: mean interbeat interval (IBI, ms), heart rate (HR, 1/min), stiffness index (calculated as the height of the subject over pulse transit time (PTT), m/s [4,6]), reflection index (the ratio of the amplitude of the diastolic peak to the amplitude of the systolic peak), left ventricular ejection time index (LVETI, ejection time (ET) normalized for heart rate using the formulae LVETI = 1.7 × heart rate + ET and LVETI = 1.6 × heart rate + ET in males and females, respectively [13]), b/a (parameter relating the amplitude of the second wave of the DVP second derivative to the first wave), d/a (ratio of the fourth and first inflection points of the second derivative of the DVP), aging index (a parameter derived from the amplitudes of inflections of the second derivative of the DVP as (b − c − d − e)/a [31]), and c–d point detection ratio (a value that specifies the percentage of those pulse cycles in the 2-min recording in which c and d points of the second derivative were successfully identified by the algorithm) (Figure 2).

### 2.3. Protocols

#### 2.3.1. Measurement Reliability of the Telemedicine System

In order to exclude major effects of measurement error of our telemedicine system on the evaluation of human pulse contour readings, we explored the repeatability of measurements. To define measurement error by the SCN4ALL system (combined error of DVP recording, data processing, and analysis), we recorded artificial signals generated by a pulse simulator device (MS100 $SpO_2$ Simulator, Contec Medical Systems Co., Ltd., Qinhuangdao, China). Besides the generation of high-quality, physiological simulated pulse signals ("normal"—$SpO_2$: 98%, heart rate: 55/min), the simulator offers signals which model frequent signal variants, "Abnormal 1" (titled "geriatric" in the simulator's software) ($SpO_2$: 92%, heart rate: 95/min) and "Abnormal 2" titled "weak" in the software ($SpO_2$: 90%, heart rate: 95/min) signal settings. The latter simulates a pulse wave in which the detectable signal is of low intensity (Figure 3). We performed five repeated measurements for each signal setting (Normal, Abnormal 1, Abnormal 2) with five different pulse oximeters of the same product release.

#### 2.3.2. Reliability of Human Pulse Wave Measurements at Standard Conditions

The reliability of human DVP measurements was assessed by measuring test–retest variability by performing consecutive measurements on healthy individuals under standardized conditions, in which physiological fluctuations of cardiovascular functioning are supposed to be minimal. We performed 10 repeated 2-min-long measurements on 10 young healthy volunteers (M/F: 5/5, Age: 19–35, Mean ± SD: 25.3 ± 4.3) under standard conditions. The course of successive measurements took approximately 30 min. We defined 'standard condition' as the set of measurement conditions which we recommend our users to maintain when they perform their daily morning measurements during follow-up. The criteria for standard conditions are as follows: measurement takes place in a quiet room at room temperature; in the morning hours at least two hours after the last meal and coffee; and in a sitting, resting position, with hands held quietly on a table. Moreover, consumption of energy drinks and alcoholic beverages and intensive physical activity on the day of the measurement were avoided in this study. For these measurements, the pulse oximeter was placed on the left index finger.

#### 2.3.3. Parallel Measurement on Four Fingers

To investigate whether a different anatomical disposition of the fingers affects the measured pulse contour parameters, we placed four pulse oximeters on four fingers (left and right indices and ring fingers) and made parallel 2-min measurements. We made two consecutive pulse recordings on 25 healthy individuals (M/F: 17/8; Age: 19–49, Mean ± SD: 29.4 ± 8.4), and took the average of the two measurements for each individual.

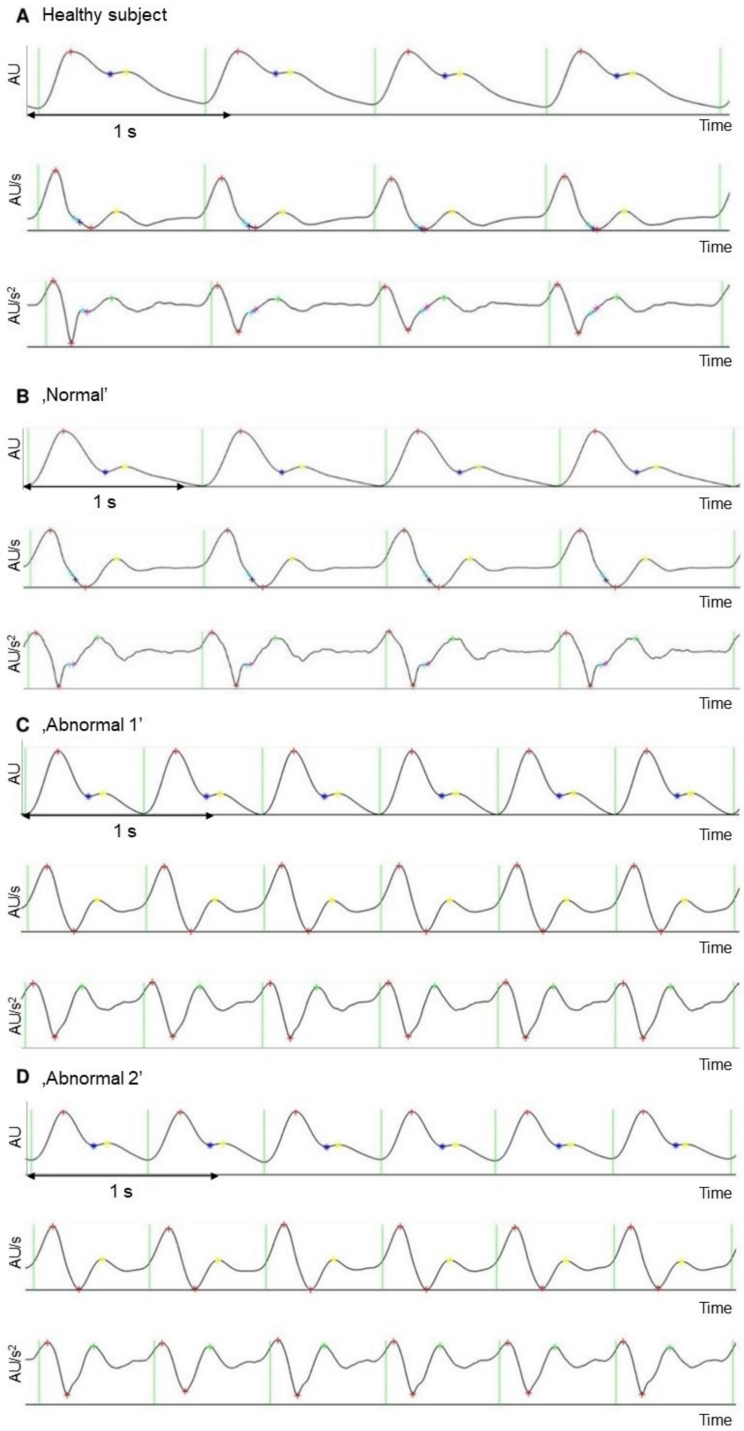


**Figure 3.** Representative recordings obtained on a healthy individual and the pulse oximeter stimulator. (Panel **A**) shows representative recording of one of our healthy subjects. (Panel **B**) shows recording of an artificial pulse wave generated by the Normal setting of the pulse oximeter simulator. Recordings of (panels **C** and **D**) demonstrate pulse waves generated by the Abnormal 1 and Abnormal 2 signal settings of the pulse oximeter simulator device. Both are high heart rate signals (95/min) and are characterized by disappearance of c and d inflections of the second derivative curve. Abnormal 2 setting was a low-intensity signal but was still recorded accurately with the SCN4ALL system. In each panel, the upper graph shows the recorded digital volume pulse (DVP), whereas the middle and lower panels show the first and second derivatives of the DVP, respectively. AU: arbitrary units.

### 2.4. Data Analysis and Statistics

Cycles with irregular durations and unusual morphology were automatically excluded from the analysis by the algorithm (in each case <5% of all recorded cycles). Afterward, the means of values calculated for the individual pulse cycles of the 2-min-long recording were calculated for each parameter. For the present analysis, means were exported from the system in spreadsheets. These mean values were used for further characterizations. The descriptive statistics are presented as mean with its 95% confidence interval. To estimate variability between repeated measurements of the artificial signal (repeatability) and to characterize test–retest variability of repeated human measurements under standard conditions, we used coefficient of variation (CV = (SD/mean × 100) × (1 + 1/4 n) where n is the sample size) [32]. For repeatability measurements, we predefined the criterion of acceptance for CV as 2%, whereas this was defined as 10% for test–retest variability measurements. For the four-finger measurements, we calculated intraclass correlation coefficients (ICC) to show the correlation between fingers and assess the contribution of interpersonal variability to overall variability. The ICC calculation was based on a linear mixed-effects model. All statistical analyses were performed by using IBM SPSS Statistics for Windows, version 26 (Armonk, NY, USA: IBM Corp.).

## 3. Results

### 3.1. Measurement Reliability of the Telemedicine System

Before addressing our main goal, i.e., that of assessing the reliability of human DVP measurements in general, we determined the repeatability of measurements made by our telemedicine system. Measurement error was assessed by detecting stable artificial signals generated by a pulse oximeter simulator (Figure 3). The overall measurement error of the telemedical system may be produced by the data analyzing algorithm, the measurement error of a single pulse oximeter, or the variability due to using different pulse oximeter devices to detect the pulse signals. Firstly, in order to assess the combined contribution of the algorithm and the error of a single pulse oximeter to the overall measurement error, we detected the normal pulse signals of the simulator with a single, randomly chosen pulse oximeter and repeated it five times (Table 1; Normal condition, 1st column). The results showed that the measurement was stable: the confidence intervals (CIs) were very close to the mean of the five measurements, and the coefficient of variation was below 1% for each calculated variable.

Then, we randomly chose four other pulse oximeters of the same release, repeated the measurements as described above, and averaged the results of the 25 measurements. These showed that the output data had low variability as evidenced by narrow CIs and small (lower than 1%) CVs for each parameter (Table 1; Normal condition, 2nd column).

After proving that our system detects and analyzes normal pulse signals reliably, we repeated the measurements described above with signal presets of the simulator, which simulate abnormal conditions. For this purpose, we used the Abnormal 1 and the Abnormal 2 presets (Figure 3). The former preset of the simulator generates a signal with high heart rate (95/min). In this setting, the reliability of pulse detection and analysis was similar to that of the Normal condition except for the calculation of the aging index and d/a parameter, as the second derivative of this preset has no detectable c and d points (Table 1; Abnormal 1 condition).

The Abnormal 2 signal preset mimics a condition where the signal is of low intensity (a typical source of error in DVP detection). Similar to what we observed with the Abnormal 1 signals, the results of these measurements also showed stable detection and analysis for most parameters, except for the aging index and the d/a ratio—for the same reasons as in Abnormal 1 (Table 1; Abnormal 2 condition).

**Table 1.** Results of repeatability measurements. Means (and confidence intervals (CIs)) and coefficients of variation (CVs) of pulse contour variables measured by the SCN4ALL telemedicine system. In order to evaluate the repeatability of the measurements by the system, we detected and analyzed artificial pulse signals generated by a pulse oximeter simulator device. Three different signal settings of the simulator were selected (Normal, Abnormal 1, and Abnormal 2). For each setting, measurements were repeated 5 times with a single randomly chosen pulse oximeter (n = 5 columns), and then these measurements were supplemented with the repeated measurements from 4 other pulse oximeters of the same release (n = 25 columns, showing the results of 5 × 5 measurements).

| | **Normal** | | | | **Abnormal 1** | | | | **Abnormal 2** | | | |
|---|---|---|---|---|---|---|---|---|---|---|---|---|
| | ***n* = 5** | | ***n* = 25** | | ***n* = 5** | | ***n* = 25** | | ***n* = 5** | | ***n* = 25** | |
| **Variables** | ***Mean [CI]*** | ***CV (%)*** | ***Mean [CI]*** | ***CV (%)*** | ***Mean [CI]*** | ***CV (%)*** | ***Mean [CI]*** | ***CV (%)*** | ***Mean [CI]*** | ***CV (%)*** | ***Mean [CI]*** | ***CV (%)*** |
| Aging index | −1.13 [−1.14; −1.12] | 0.41 | −1.14 [−1.14; −1.13] | 0.57 | −3.37 [−4.45; −2.29] | 27.1 | −3.12 [−3.46; −2.79] | 26.1 | −3.71 [−4.60; −2.81] | 20.4 | −3.84 [−4; −3.69] | 9.9 |
| b/a | −1.78 [−1.79; −1.78] | 0.26 | −1.79 [−1.79; −1.78] | 0.32 | −1.59 [−1.59; −1.59] | 0.29 | −1.59 [−1.60; −1.59] | 0.32 | −1.60 [−1.60; −1.59] | 0.36 | −1.60 [−1.59; −1.56] | 0.33 |
| c-d point detection ratio (%) | 100 [100; 100] | 0 | 100 [100; 100] | 0 | 0.60 [0.08; 1.28] | 95.9 | 0.44 [0.23; 0.65] | 116 | 2 [0.48; 3.52] | 64.3 | 2.70 [2.25; 3.19] | 42.2 |
| d/a | −0.75 [−0.75; −0.74] | 0.77 | −0.75 [−0.75; −0.75] | 0.37 | −0.48 [−1.01; −0.06] | 95.9 | −0.35 [0.18–0.52] | 116 | −0.64 [−1.09; −0.20] | 58.7 | −0.71 [−0.79; −0.63] | 26.9 |
| Left ventricular ejection time index (ms) | 552 [552; 554] | 0.22 | 553 [552; 553] | 0.27 | 462 [461; 462] | 0.06 | 462 [462; 462] | 0.05 | 462 [462; 463] | 0.06 | 462 [462; 463] | 0.07 |
| Heart rate (1/min) | 55 [55; 55] | 0 | 55 [55; 55] | 0 | 95 [95; 95] | 0 | 95 [95; 95] | 0 | 95 [95; 95] | 0 | 95 [95; 95] | 0 |
| Interbeat interval (ms) | 1089 [1089; 1089] | 0 | 1089 [1088; 1090] | 0.21 | 631 [631; 631] | 0 | 631 [631; 631] | 0.19 | 630 [630; 631] | 0.07 | 631 [631; 632] | 0.18 |
| Reflection index (%) | 35.5 [35.5; 35.6] | 0.13 | 35.5 [35.5; 35.6] | 0.11 | 32.7 [32.7; 32.8] | 0.12 | 32.7 [32.7; 32.8] | 0.13 | 32.8 [32.6; 32.9] | 0.35 | 32.8 [32.7; 32.8] | 0.42 |
| Stiffness index (m/s) | 4.62 [4.62; 4.63] | 0.10 | 4.62 [4.62; 4.63] | 0.26 | 7.34 [7.34; 7.34] | 0 | 7.34 [7.33; 7.34] | 0.18 | 7.34 [7.33; 7.36] | 0.16 | 7.34 [7.33; 7.35] | 0.34 |

### 3.2. Reliability of Human Pulse Wave Measurements at Standard Conditions

In order to address our main goal of assessing the reliability of human pulse wave measurements in general, we evaluated the test–retest variability of pulse wave parameter analysis under standard conditions. For this purpose, resting measurements were repeated 10 times in 10 healthy individuals. After calculating the coefficient of variation for each individual, the CVs of the 10 subjects were averaged. The mean CVs for each parameter are presented in Table 2. These show that b/a, left ventricular ejection time index, mean interbeat interval, stiffness index, and mean heart rate are parameters that remain stable under standard measurement conditions (CVs lower than 10%). However, the aging index is slightly variable (CV: 13.6%), and d/a and c–d point detection ratio are highly variable even when measured under unchanged conditions.

**Table 2.** Results of test–retest variability measurements. Test–retest variability of pulse contour parameters measured by the SCN4ALL telemedicine system. Measurements were performed on 10 healthy volunteers 10 times repeatedly under standardized conditions. Coefficient of variation (CV) for the results of the consecutive measurements was calculated for each individual. Afterwards individual CVs were averaged; they are presented in the table along with bracketed confidence intervals (CI).

| Pulse Contour Variables | CV % [CI] |
|---|---|
| Aging index | 13.6 [4.78; 22.5] |
| b/a | 3.84 [2.13; 5.55] |
| c–d point detection ratio (%) | 33.6 [17.1; 50.1] |
| d/a | 83.9 [9.5; 177] |
| Left ventricular ejection time (ms) | 1.30 [0.75; 1.84] |
| Heart rate (1/min) | 3.19 [1.99; 4.39] |
| Interbeat interval (ms) | 3.23 [2.11; 4.35] |
| Reflection index (%) | 7.43 [2.79; 12.1] |
| Stiffness index (m/s) | 4.34 [2.20; 6.48] |

In order to visualize how the detected test–retest (intrapersonal) variability relates to interpersonal variability, Figure 4 displays the mean of measurements obtained from the 10 subjects for each sequential measurement time point, with confidence intervals (CIs), along with the individual graphs of the subjects. The graphs show that for each parameter, individual curves appear similar and show no trend, only random fluctuations. The mean curves show no trends or extremes and have homogeneous confidence intervals. The variability of the individual curves among measurements and the variability between the individual curves look comparable.

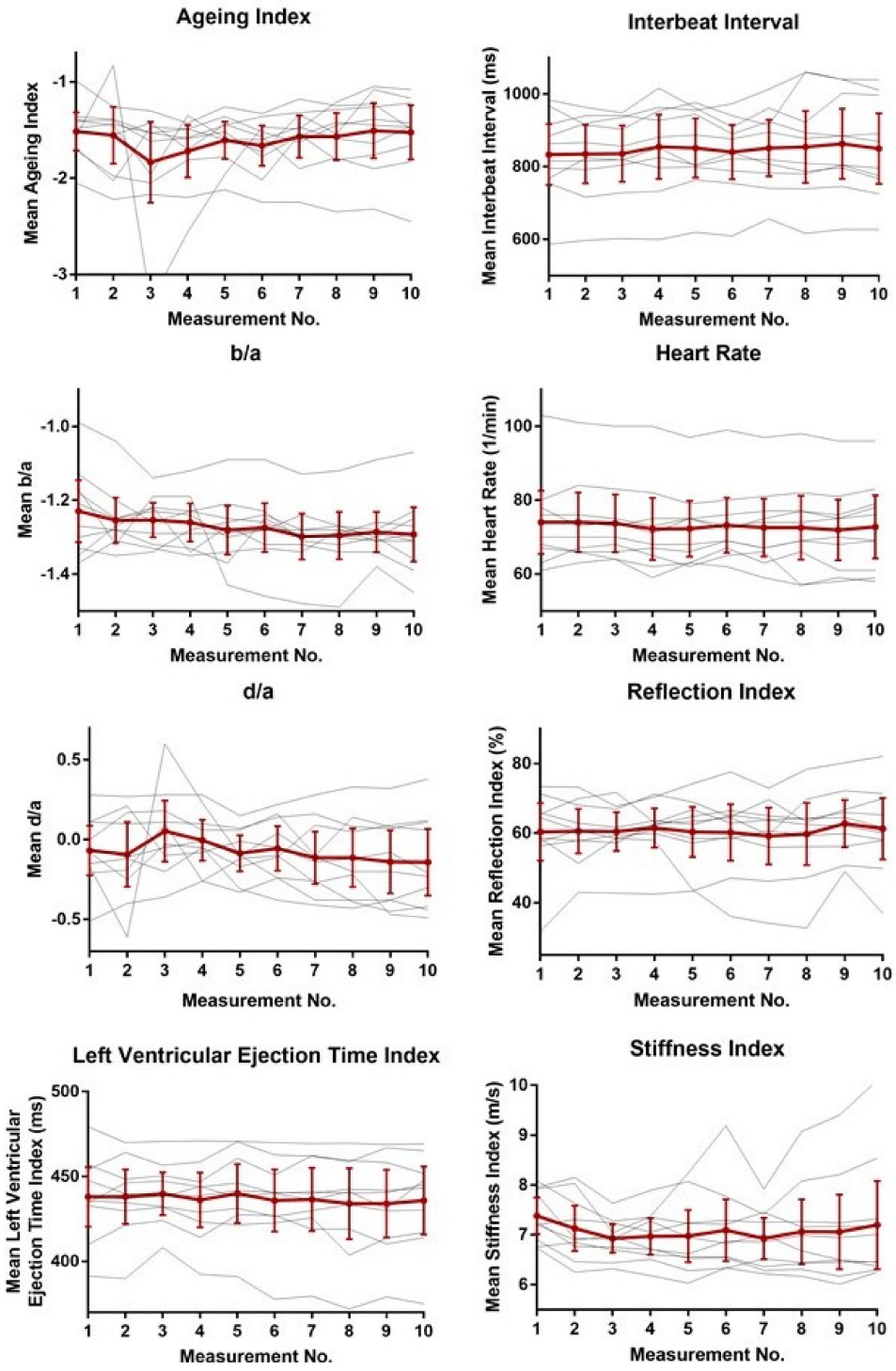


**Figure 4.** Graphs demonstrating the relationship between interpersonal variability and intrapersonal variations of the computed pulse contour parameters. Measurements were performed on 10 healthy volunteers 10 times repeatedly under standardized conditions. Means (±confidence intervals) are presented (red solid line) for each consecutive measurement along with individual measurement data (black lines). Individual lines are similar to each other and to the average line. The variability of the individual curves among measurements and the variability between the individual curves seem to fall in the same order of magnitude.

### 3.3. Parallel Measurements on Four Fingers

Concomitant measurements on four different fingers were also performed in 25 individuals to test how slightly different anatomic disposition of the fingers affects the detected pulse wave parameters. The results are summarized in Table 3. The mean measurements of the four fingers are presented, showing no relevant difference between the fingers. Moreover, the intraclass correlation coefficients were over 99% for mean interbeat interval, mean heart rate, and left ventricular ejection time index, indicating that the effect of using different fingers for measurement is negligible. The intraclass correlation coefficients (ICCs) for stiffness index and c–d point detection ratio were about 90%, and they were over 80% for reflection index, b/a, d/a, and aging index. These confirm that the effect of using different fingers on variability is much less than that of the interindividual differences for these parameters (see Table 3 for exact values for the different parameters).

**Table 3.** Results of measurements performed in parallel on 4 separate fingers on 25 healthy individuals. For each individual, 2 consecutive 4-finger measurements were taken, and the average of the 2 was used for further calculations. The results of the 25 subjects were averaged for each finger separately and are presented in the table with bracketed confidence intervals (CIs). Intraclass coefficients (ICC) were calculated to assess the correlation of results within the same individuals.

| | **Left Index Finger** | **Left Ring Finger** | **Right Index Finger** | **Right Ring Finger** | **ICC** |
|---|---|---|---|---|---|
| **Pulse contour variables** | *n = 25* *Mean [CI]* | *n = 25* *Mean [CI]* | *n = 25* *Mean [CI]* | *n = 25* *Mean [CI]* | |
| Aging index | −1.29 [−1.46; −1.13] | −1.30 [−1.47; −1.13] | −1.34 [−1.15; −1.12] | −1.47 [−1.17; −1.25] | 0.81 |
| b/a | −1.21 [−1.26; −1.152] | −1.22 [−1.29; −1.16] | −1.25 [−1.312; −1.20] | −1.24 [−1.30; −1.17] | 0.83 |
| c–d point detection ratio (%) | 33.8 [25.3; 42.4] | 31.3 [23.1; 39.5] | 31.9 [22.9; 40.8] | 32.3 [23.9; 40.78] | 0.90 |
| d/a | −0.15 [−0.24; −0.06] | −0.16 [−0.26; −0.07] | −0.17 [−0.29; −0.06] | −0.10 [−0.21; −0.01] | 0.82 |
| Left ventricular ejection time index (ms) | 148 [56; 240] | 148 [57; 240] | 147 [56; 238] | 147 [56; 237] | >0.99 |
| Heart rate (1/min) | 70.6 [67.1; 74.2] | 71.0 [67.5; 74.2] | 70.9 [67.4; 74.4] | 71.0 [67.4; 74.5] | >0.99 |
| Interbeat interval (ms) | 862 [817; 906] | 862 [818; 908] | 862 [816; 907] | 861 [817; 907] | >0.99 |
| Reflection index (%) | 62.2 [59.2; 65.1] | 60.8 [57; 64.6] | 61.5 [58.4; 64.5] | 61.3 [57.6; 65.0] | 0.81 |
| Stiffness index (ms) | 7.74 [7.37; 8.10] | 7.71 [7.32; 8.10] | 7.58 [7.20; 7.97] | 7.59 [7.13; 8.05] | 0.90 |

## 4. Discussion

Home monitoring of cardiovascular patients is a promising approach in patient care which is expected to gain ground in the upcoming decades and may constitute a relevant breakthrough in primary and secondary prevention of cardiovascular diseases. Implementation of noninvasive simple measurements, which give a deep insight into the momentary cardiovascular condition of the patient and thus allow extensive evaluation, and reliable fast data analysis are basic requirements for such telemedical systems. Incorporation of photoplethysmography-based analysis of the digital pulse wave in telemedical systems may be an optimal solution for cardiovascular telecare; however, its reliability is debated [21,33,34]. Our main purpose was to address the controversies related to the reliability of PPG-based cardiovascular evaluation. We showed that measurement and evaluation of most pulse contour parameters are reliable when analyzed with the SCN4ALL automated system, which is able to track stable signals with high repeatability. This was confirmed by low test–retest variability of repeated measurements performed under apparently constant cardiovascular conditions. Our study also showed that otherwise valuable pulse contour parameters derived from the second derivative of the DVP curve can only be evaluated with limitations. The detection of c and d deflections on this curve is prone to errors, which interferes with the reliable interpretation of the aging index and d/a parameter, which are indices of arterial stiffening and aging [14,24–28]. These limitations are related to typical alterations of pulse wave morphology rather than inaccuracies in analysis, as the automated algorithm used in this study was proven to detect c and d points reliably on normal stable

curves. In conclusion, our study showed that PPG-based pulse wave analysis performed in this study operates reliably with acceptable measurement errors and is capable of monitoring subtle alterations in cardiovascular functioning.

Although the reliability of PPG-based pulse contour analysis is debated, no data are available on the repeatability of the systems which are used for analysis in research studies. However, as these systems are complex and comprise several sources of measurement errors, it is impossible to validly interpret biological data obtained by PPG-based systems if information concerning repeatability is not available. Therefore, we firstly checked the repeatability of the pulse contour measurements of our telemonitoring system. This was assessed by calculating the variability of the DVP parameters obtained from successive measurements of stable artificial pulse signals, which simulated healthy pulse waves and were generated by a pulse oximeter simulator device. Such variability can be caused by measurement errors of the pulse oximeter instrument and also by the automated algorithm analyzing the detected pulse wave. The combined effect of these two factors on measurement variability was investigated by testing the agreement among the results of five successive measurements performed by the same randomly chosen pulse oximeter device. The variation was smaller than the predefined 2% criterion of acceptance for each parameter (Table 1; Normal condition). Afterward, we extended the investigation to four additional instruments with which we performed the same measurements. We pooled the $5 \times 5$ measurements and calculated the overall CVs, which then reflected the combined variation caused by measurement error of a single pulse oximeter, analysis by the algorithm, and also the "interinstrumental" variability of several pulse oximeters of the same product. The CVs calculated in this way were also below the limit of acceptance (Table 1; Normal condition), showing that measurements are highly repeatable even if different pulse oximeters are used. Testing of pulse oximeter reliability was relevant in this setting because the applied devices had only been tested for the reliability of oxygen saturation and heart rate calculations by the manufacturers, but it was unknown whether they accurately track a continuous pulse wave for minutes.

After proving that our system reliably tracks stable signals, we addressed our main question of determining whether PPG-based monitoring and analysis of the DVP are reliable. We aimed to resolve the controversy in which it is often doubted that PPG-based methods can be used as diagnostic tools [21,33,34] because they are highly sensitive to errors, causing pulse contour parameters to fluctuate even if there is no alteration in cardiovascular functioning. However, we postulate that these alterations reflect real changes in cardiovascular condition. To show this, we measured test–retest variability under standardized measurement conditions. Measurements were performed in a quiet room at room temperature; in the morning hours, preferably at least two hours after the last meal and coffee; in a sitting, resting position, with hands held calm on a table. Speaking, moving, and mental activity were avoided during data collection [24,26,35,36]. Naturally, this standardization does not remove variability completely. However, the output contour parameters of our telemedical system showed minimal test–retest variability for most of the parameters, namely for b/a, left ventricular ejection time index, mean interbeat interval, stiffness index, and mean heart rate (CVs lower than 10%; Table 2). This indicates that these parameters are suitable for patient follow-up and may well support clinical decision, as the deviation of a measurement from the standard individual value most probably indicates real, physiological, or pathological alterations in cardiovascular function. Anyway, to enhance the precision of pulse contour analysis, we need to advise the users of PPG-based telemedical systems to perform their daily measurements preferably under standard conditions. This standardization does not require any particular cooperation from users; the recommendations are as simple as those for blood pressure measurement and are confined to those conditions which have been reported to influence pulse contour parameters [24,26,35,36].

In our study, we also provided preliminary data on the interpersonal variability of the studied contour parameters (Figure 4). Based on our observations, we can conclude that interpersonal and intrapersonal variabilities of the studied parameters are in the same range for healthy individuals when measurements are performed under standard conditions. This indicates that normal ranges

can be identified for these parameters and that deviations from these ranges may reflect DVP—and hence cardiovascular—abnormalities both at individual (when compared to other results of the same patient) and at population levels (when data are compared to values of healthy individuals). However, larger studies should be conducted to define the normal reference ranges for the contour parameters computed by telemedicine systems and to determine which alterations can be considered clinically relevant. Indeed, reference ranges for these parameters are scant in the literature, and they have only limited validity for larger populations [6,14,25,27,28,37–40].

As a satellite question, we also tested in this study how different anatomical disposition of the fingers affects the results of pulse contour analysis. Without question, we recommend the use of the same finger for each measurement. However, for some reason, the occasional use of another finger may occur, which may limit the valid remote interpretation of the recordings. Therefore, we need to be aware of whether this error causes significant alterations in the output results. In healthy individuals, we could observe that there was no relevant difference in pulse contour parameters when measured in parallel on the index and ring fingers of the two hands (Table 3). The calculated ICCs showed that the effect of using different fingers on the variability of the outcomes is much less than the effect of interpersonal differences. Therefore, changing to different fingers does not constitute a relevant measurement error. However, we need to keep in mind that pathological alterations and diseases of the supplying arterial tree may have an impact on the blood flow of the digital arteries. For this reason, at the first patient visit, it is recommended to record pulse signals on several fingers on both sides and analyze whether there are differences in the output parameters.

Finally, we evaluated the reliability of our proprietary analysis engine to detect and analyze distinguished deflections of the second derivative PPG curve. Pulse wave analysis was originally extended to the second derivative of the DVP by Takazawa et al. [14]. They defined notable points of the curve which facilitate understanding of the pressure wave. Since then, several research groups have related the height of the b, c, and d waves to the a-wave to create measures that can index vascular pathologies (vascular aging, hypertension, arterial stiffness) and predict cardiovascular endpoints [14,28,41,42]. Among these points, c and d points are particularly valuable, as they are supposed to hold information about wave reflection [14], and the parameters derived from them provide information about arterial stiffening [14,35]. However, detection of c and d inflections has reportedly become a challenge for automated algorithms as their position and amplitude change along with pathophysiological alterations of the PPG [8,22,43]. In this study, we analyzed the success of c and d point identification by our algorithm and variability of parameters (namely d/a and aging index) derived from these points. When we tracked the stable, normal artificial signal of the pulse oximeter stimulator, the ratio of those cycles in which we could detect c and d points was 100% and the variability of the aging index and d/a was minimal (CVs below 1%) (Table 1; Normal condition). This shows that our engine reliably analyzes the second derivative curve. However, when we analyzed the abnormal signals offered by the pulse oximeter simulator, the success of c and d point detection became less reliable. We tested two different abnormal signal settings: Abnormal 1 setting generates a pulse signal of high heart rate and almost totally absent second derivative c–d points, whereas Abnormal 2 is a signal that simulates a weak pulse wave (e.g., similar to that observed in case of vasoconstriction due to cold). Second derivative c–d points are absent in this setting as well. With these settings, the calculation of other pulse contour parameters was still highly repeatable (CVs below 2%). However, c–d point detection ratio, the parameter which expresses the percent of those pulse cycles in which c and d points are recognized by the algorithm, fell below 5% for each setting (Table 1; Abnormal 1 and Abnormal 2 conditions). This increased the variability of all the parameters that are derived from c and d values, namely aging index and d/a.

When performing repeated human measurements, we also observed diminished reliability of c and d point analysis. Parameters derived from c and d points of the second derivative of the DVP became more variable (aging index, d/a) (Table 2). This concurs with the relatively high variations in c–d point detection ratio of consecutive measurements.

The optimum solution for this problem is to improve the automated algorithm in order to make the identification of second derivative c and d points more reliable. However, literature data suggest that this may have limitations (reviewed by M. Elgendi [22]). Although we recognize that attempts to make c–d point detection more precise are inevitable, we also propose the use of the c–d point detection ratio as a tool that aids clinical assessment of parameters derived from the second derivative. If the c–d point detection ratio reaches a certain value, we can reliably use parameters derived from the second derivative to support patient evaluation; however, when it is low, these parameters should be neglected. Determination of the minimum c–d point detection ratio that allows valid second derivative parameter interpretation requires further studies; however, based on our preliminary observations, it is around 30% (data not shown). Moreover, in the follow-up of a patient, a sudden or progressive change in c–d point detection may be evaluated as a warning for pulse wave abnormalities.

## 5. Conclusions

In this study, we characterized the reliability of using PPG-based pulse contour analysis to support clinical decision. For this purpose, we applied our self-developed SCN4ALL telemedical system and used a multidirectional approach to explore and characterize the possible measurement errors in depth in order to establish the reliability of this diagnostic tool. We showed that if we use a PPG-based telemedicine system, which is proven to track artificial signals with high repeatability, it can analyze most pulse contour parameters (e.g., stiffness index, reflection index, left ventricular ejection time index) with high precision in human measurements. This allows high-fidelity evaluation of these parameters and the detection of small cardiovascular alterations. However, correct evaluation of some parameters derived from the second derivative of the pulse wave (i.e., aging index, d/a) can be hindered by pathophysiological alterations or normal variants of the pulse wave which make c and d point identification difficult. To handle this limitation, we recommend the introduction of the c–d point detection ratio in pulse wave analysis and the consideration of second derivative parameters only if its value is acceptable. In summary, we can claim that PPG-based pulse wave analysis is a reliable measurement tool and meets the requirements set for cardiovascular telemonitoring devices. Clearly, further, large-population studies are warranted to establish the guidelines for its application in patient follow-up.

**Author Contributions:** Conceptualization, D.K., S.K., and Z.M.; methodology, F.A., D.K., and Z.M.; validation, S.K., and Z.M.; investigation, F.A., Z.M., D.K., and D.W.; resources, S.K.; data curation, D.S.V. and K.I.L.; writing—Original draft preparation, F.A., D.K., and Z.M.; writing—Review and editing, Z.M. and D.S.V.; visualization, F.A., K.I.L., and D.W.; supervision, Z.M.; project administration, F.A. and D.W.; funding acquisition, D.K. and S.K. All authors have read and agreed to the published version of the manuscript.

**Funding:** This research was funded by E-Med4All Europe Ltd.; Z.M. receives financial support from the Higher Education Institutional Excellence Program of the Ministry of Human Capacities in Hungary, within the framework of the Molecular Biology thematic program of the Semmelweis University, and D.S.V. receives financial support from the Thematic Excellence Programme (TKP) of the Ministry of Innovation and Technology of Hungary, within the framework of the BIOImaging Excellence programme at Semmelweis University.

**Acknowledgments:** The authors acknowledge the skilled contribution of László Szűcs, who provided and prepared the datasets for analysis. Authors express their special thanks for the great work of Balázs Szabó, who wrote the automated algorithm and leads the development of the software that is the core of the given telemedicine system.

**Conflicts of Interest:** D.K., F.A., K.I.L., S.K., and Z.M. are in financial terms with E-Med4All Europe Ltd. (D.K. and S.K. as co-owners, F.A. as employee, and K.I.L. and Z.M. as subcontractors). D.S.V. and D.W. did not receive compensation for their contribution by financial or any other means.

## References


1. GBD Causes of Death Collaborators. Global, regional, and national age-sex-specific mortality for 282 causes of death in 195 countries and territories, 1980–2017: A systematic analysis for the Global Burden of Disease Study 2017. *Lancet* **2018**, *392*, 1736–1788. [CrossRef]
2. Yusuf, S.; Joseph, P.; Rangarajan, S.; Islam, S.; Mente, A.; Hystad, P.; Brauer, M.; Kutty, V.R.; Gupta, R.; Wielgosz, A.; et al. Modifiable risk factors, cardiovascular disease, and mortality in 155 722 individuals from 21 high-income, middle-income, and low-income countries (PURE): a prospective cohort study. *Lancet* **2020**, *395*, 795–808. [CrossRef]
3. Ghamari, M. A review on wearable photoplethysmography sensors and their potential future applications in health care. *Int. J. Biosens. Bioelectron.* **2018**, *4*, 195–202. [CrossRef] [PubMed]
4. Elgendi, M. On the Analysis of Fingertip Photoplethysmogram Signals. *Curr. Cardiol. Rev.* **2012**, *8*, 14–25. [CrossRef] [PubMed]
5. O'Rourke, M.F.; Pauca, A.; Jiang, X.-J. Pulse wave analysis. *Br. J. Clin. Pharmacol.* **2001**, *51*, 507–522. [CrossRef]
6. Millasseau, S.; Kelly, R.; Ritter, J.; Chowienczyk, P. Determination of age-related increases in large artery stiffness by digital pulse contour analysis. *Clin. Sci.* **2002**, *103*, 371–377. [CrossRef]
7. Wesselink, R. Blood Pressure Waveform Analysis in Cardiogenic Shock & Acute Myocardial Infarction. Master's Thesis, University of Twente, Enschede, The Netherlands, 2016. Available online: https://essay.utwente.nl/69815/2/Wesselink_MA_TNW.pdf (accessed on 10 November 2020).
8. Pilt, K.; Meigas, K.; Ferenets, R.; Temitski, K.; Viigimaa, M. Photoplethysmographic signal waveform index for detection of increased arterial stiffness. *PubMed. Physiol. Meas.* **2014**, *35*, 2027–2036. [CrossRef]
9. Smulyan, H.; Safar, M.E. Systolic Blood Pressure Revisited. *J. Am. Coll. Cardiol.* **1997**, *29*, 1407–1413. [CrossRef]
10. Steppan, J.; Barodka, V.; Berkowitz, D.E.; Nyhan, D. Vascular Stiffness and Increased Pulse Pressure in the Aging Cardiovascular System. *Cardiol. Res. Pr.* **2011**, *2011*, 1–8. [CrossRef]
11. Avolio, A.; Butlin, M.; Walsh, A. Arterial blood pressure measurement and pulse wave analysis—their role in enhancing cardiovascular assessment. *PubMed. Physiol. Meas.* **2010**, *31*. [CrossRef]
12. Inoue, N.; Kawakami, H.; Yamamoto, H.; Ito, C.; Fujiwara, S.; Sasaki, H.; Kihara, Y. Second derivative of the finger photoplethysmogram and cardiovascular mortality in middle-aged and elderly Japanese women. *Hypertens. Res.* **2016**, *40*, 207–211. [CrossRef] [PubMed]
13. Haiden, A.; Eber, B.; Weber, T. U-Shaped Relationship of Left Ventricular Ejection Time Index and All-Cause Mortality. *Am. J. Hypertens.* **2014**, *27*, 702–709. [CrossRef] [PubMed]
14. Millasseau, S.C.; Guigui, F.G.; Kelly, R.P.; Prasad, K.; Cockcroft, J.R.; Ritter, J.M.; Chowienczyk, P.J. Noninvasive Assessment of the Digital Volume Pulse. *Hypertension* **2000**, *36*, 952–956. [CrossRef] [PubMed]
15. Takazawa, K.; Tanaka, N.; Fujita, M.; Matsuoka, O.; Saiki, T.; Aikawa, M.; Tamura, S.; Ibukiyama, C. Assessment of Vasoactive Agents and Vascular Aging by the Second Derivative of Photoplethysmogram Waveform. *Hypertension* **1998**, *32*, 365–370. [CrossRef] [PubMed]
16. Nirala, N.; Periyasamy, R.; Singh, B.K.; Kumar, A. Detection of type-2 diabetes using characteristics of toe photoplethysmogram by applying support vector machine. *Biocybern. Biomed. Eng.* **2019**, *39*, 38–51. [CrossRef]
17. Paradkar, N.; Chowdhury, S.R. Coronary artery disease detection using photoplethysmography. In Proceedings of the 2017 39th Annual International Conference of the IEEE Engineering in Medicine and Biology Society (EMBC), Seogwipo, Korea, 11–15 July 2017; Volume 2017, pp. 100–103. [CrossRef]
18. Huotari, M.; Vehkaoja, A.; Määttä, K.; Kostamovaara, J. Photoplethysmography and its detailed pulse waveform analysis for arterial stiffness. *J. Struct. Mech.* **2011**, *44*, 345–362.
19. Weber, T.; Auer, J.; O'Rourke, M.F.; Kvas, E.; Laßnig, E.; Berent, R.; Eber, B. Arterial Stiffness, Wave Reflections, and the Risk of Coronary Artery Disease. *Circulation* **2004**, *109*, 184–189. [CrossRef]
20. Korhonen, I.; Yli-Hankala, A. Photoplethysmography and nociception. *Acta Anaesthesiol. Scand.* **2009**, *53*, 975–985. [CrossRef]
21. Von Wowern, E.; Östling, G.; Nilsson, P.M.; Olofsson, P. Digital Photoplethysmography for Assessment of Arterial Stiffness: Repeatability and Comparison with Applanation Tonometry. *PLoS ONE* **2015**, *10*, e0135659. [CrossRef]

22. Elgendi, M. Detection of c, d, and e waves in the acceleration photoplethysmogram. *Comput. Methods Programs Biomed.* **2014**, *117*, 125–136. [CrossRef]
23. Jago, J.R.; Murray, A. Repeatability of peripheral pulse measurements on ears, fingers and toes using photoelectric plethysmography. *Clin. Phys. Physiol. Meas.* **1988**, *9*, 319–329. [CrossRef] [PubMed]
24. Bortolotto, L.A.; Blacher, J.; Kondo, T.; Takazawa, K.; Safar, M.E. Assessment of vascular aging and atherosclerosis in hypertensive subjects: second derivative of photoplethysmogram versus pulse wave velocity. *Am. J. Hypertens.* **2000**, *13*, 165–171. [CrossRef]
25. Imanaga, I.; Hara, H.; Koyanagi, S.; Tanaka, K. Correlation between Wave Components of the Second Derivative of Plethysmogram and Arterial Distensibility. *Jpn. Hear. J.* **1998**, *39*, 775–784. [CrossRef] [PubMed]
26. Hashimoto, J.; Chonan, K.; Aoki, Y.; Nishimura, T.; Ohkubo, T.; Hozawa, A.; Suzuki, M.; Matsubara, M.; Michimata, M.; Araki, T.; et al. Pulse wave velocity and the second derivative of the finger photoplethysmogram in treated hypertensive patients. *J. Hypertens.* **2002**, *20*, 2415–2422. [CrossRef] [PubMed]
27. Otsuka, T.; Kawada, T.; Katsumata, M.; Ibuki, C. Utility of Second Derivative of the Finger Photoplethysmogram for the Estimation of the Risk of Coronary Heart Disease in the General Population. *Circ. J.* **2006**, *70*, 304–310. [CrossRef] [PubMed]
28. Baek, H.J.; Kim, J.S.; Kim, Y.S.; Lee, H.B.; Park, K.S. Second Derivative of Photoplethysmography for Estimating Vascular Aging. In Proceedings of the 2007 6th International Special Topic Conference on Information Technology Applications in Biomedicine, Tokyo, Japan, 8–11 November 2007; Institute of Electrical and Electronics Engineers (IEEE): New York, NY, USA, 2007; pp. 70–72. [CrossRef]
29. Pilt, K.; Ferenets, R.; Meigas, K.; Lindberg, L.-G.; Temitski, K.; Viigimaa, M. New Photoplethysmographic Signal Analysis Algorithm for Arterial Stiffness Estimation. *Sci. World J.* **2013**, *2013*, 1–9. [CrossRef] [PubMed]
30. Segers, P.; Kips, J.; Trachet, B.; Swillens, A.; Vermeersch, S.; Mahieu, D.; Rietzschel, E.; De Buyzere, M.; Van Bortel, L. Limitations and pitfalls of non-invasive measurement of arterial pressure wave reflections and pulse wave velocity. *Artery Res.* **2009**, *3*, 79–88. [CrossRef]
31. Takazawa, K. Second derivative of photoplethysmogram—Comment on Tanaka et al., page 43-48. *Vasa* **2015**, *44*, 3–4. [CrossRef]
32. Sokal, R.R.; Rohlf, F.J. *Biometry: The Principles and Practice of Statistics in Biological Research*; Sokal, R.R., Rohlf, F.J., Eds.; W.H. Freeman: New York, NY, USA, 2012; Volume 937, ISBN 9780716786047.
33. Lee, J.; Yang, S.; Lee, S.; Kim, H.C. Analysis of Pulse Arrival Time as an Indicator of Blood Pressure in a Large Surgical Biosignal Database: Recommendations for Developing Ubiquitous Blood Pressure Monitoring Methods. *J. Clin. Med.* **2019**, *8*, 1773. [CrossRef]
34. Allen, J. Photoplethysmography and its application in clinical physiological measurement. *PubMed. Physiol. Meas* **2007**, *28*, R1–R39. [CrossRef]
35. Otsuka, T.; Kawada, T.; Katsumata, M.; Ibuki, C.; Kusama, Y. Independent Determinants of Second Derivative of the Finger Photoplethysmogram among Various Cardiovascular Risk Factors in Middle-Aged Men. *Hypertens. Res.* **2007**, *30*, 1211–1218. [CrossRef] [PubMed]
36. Inuma, J.; Murakoshi, M.; Kobayashi, T.; Io, H.; Kaneko, K.; Takahashi, T.; Hamada, C.; Horikoshi, S.; Tomino, Y. Relationship between acceleration plethysmography and aortic calcification index in chronic kidney disease patients. *Hong Kong J. Nephrol.* **2012**, *14*, 48–53. [CrossRef]
37. Padilla, J.M.; Berjano, E.; Sáiz, J.; Rodriguez, R.; Fácila, L. Pulse Wave Velocity and Digital Volume Pulse as Indirect Estimators of Blood Pressure: Pilot Study on Healthy Volunteers. *Cardiovasc. Eng.* **2009**, *9*, 104–112. [CrossRef]
38. Padilla, J.M.; Berjano, E.J.; Saiz, J.; Facila, L.; Diaz, P.; Merce, S. Assessment of relationships between blood pressure, pulse wave velocity and digital volume pulse. In Proceedings of the 2006 Computers in Cardiology, Valencia, Spain, 17–20 September 2006; IEEE Conference Publication: New York, NY, USA, 2006; pp. 893–896.
39. Alty, S.R.; Angarita-Jaimes, N.; Millasseau, S.C.; Chowienczyk, P.J. Predicting Arterial Stiffness from the Digital Volume Pulse Waveform. *IEEE Trans. Biomed. Eng.* **2007**, *54*, 2268–2275. [CrossRef] [PubMed]
40. Aiba, Y.; Ohshiba, S.; Horiguchi, S.; Morioka, I.; Miyashita, K.; Kiyota, I.; Endo, G.; Takada, H.; Iwata, H. Peripheral Hemodynamics Evaluated by Acceleration Plethysmography in Workers Exposed to Lead. *Ind. Health* **1999**, *37*, 3–8. [CrossRef] [PubMed]

41. Kohjitani, A.; Miyata, M.; Iwase, Y.; Sugiyama, K. Responses of the second derivative of the finger photoplethysmogram indices and hemodynamic parameters to anesthesia induction. *Hypertens. Res.* **2011**, *35*, 166–172. [CrossRef]
42. Millasseau, S.C.; Ritter, J.M.; Takazawa, K.; Chowienczyk, P.J. Contour analysis of the photoplethysmographic pulse measured at the finger. *J. Hypertens.* **2006**, *24*, 1449–1456. [CrossRef]
43. Elgendi, M.; Norton, I.; Brearley, M.; Abbott, D.; Schuurmans, D. Detection of a and b waves in the acceleration photoplethysmogram. *Biomed. Eng. Online* **2014**, *13*, 139. [CrossRef]

sensors

MDPI

*Article*

# Multimodal Assessment of the Pulse Rate Variability Analysis Module of a Photoplethysmography-Based Telemedicine System

**Flóra Antali [1,2,*], Dániel Kulin [1,2], Konrád István Lucz [2], Balázs Szabó [2], László Szűcs [2,3], Sándor Kulin [2,†] and Zsuzsanna Miklós [1,*,†]**

1 Institute of Translational Medicine, Semmelweis University, 1094 Budapest, Hungary; kulin.daniel@med.semmelweis-univ.hu
2 E-Med4All Europe Ltd., 1036 Budapest, Hungary; luczkonrad@gmail.com (K.I.L.); medessence@gmail.com (B.S.); szucs.laszlo@scn4all.com (L.S.); dr.kulin.sandor@pregnascan.eu (S.K.)
3 Antal Bejczy Center for Intelligent Robotics, Óbuda University, 1034 Budapest, Hungary
* Correspondence: antali.flora@gmail.com (F.A.); miklos.zsuzsanna@med.semmelweis-univ.hu (Z.M.); Tel.: +36-70-323-7431 (F.A.); +36-20-585-8099 (Z.M.)
† These authors contributed equally to the work.

**Abstract:** Alterations of heart rate variability (HRV) are associated with various (patho)physiological conditions; therefore, HRV analysis has the potential to become a useful diagnostic module of wearable/telemedical devices to support remote cardiovascular/autonomic monitoring. Continuous pulse recordings obtained by photoplethysmography (PPG) can yield pulse rate variability (PRV) indices similar to HRV parameters; however, it is debated whether PRV/HRV parameters are interchangeable. In this study, we assessed the PRV analysis module of a digital arterial PPG-based telemedical system (SCN4ALL). We used Bland–Altman analysis to validate the SCN4ALL PRV algorithm to Kubios Premium software and to determine the agreements between PRV/HRV results calculated from 2-min long PPG and ECG captures recorded simultaneously in healthy individuals (n = 33) at rest and during the cold pressor test, and in diabetic patients (n = 12) at rest. We found an ideal agreement between SCN4ALL and Kubios outputs (bias < 2%). PRV and HRV parameters showed good agreements for interbeat intervals, SDNN, and RMSSD time-domain variables, for total spectral and low-frequency power (LF) frequency-domain variables, and for non-linear parameters in healthy subjects at rest and during cold pressor challenge. In diabetics, good agreements were observed for SDNN, LF, and SD2; and moderate agreement was observed for total power. In conclusion, the SCN4ALL PRV analysis module is a good alternative for HRV analysis for numerous conventional HRV parameters.

**Keywords:** pulse rate variability; pulse wave analysis; photoplethysmography; telemedicine



**Citation:** Antali, F.; Kulin, D.; Lucz, K.I.; Szabó, B.; Szűcs, L.; Kulin, S.; Miklós, Z. Multimodal Assessment of the Pulse Rate Variability Analysis Module of a Photoplethysmography-Based Telemedicine System. *Sensors* **2021**, *21*, 5544. https://doi.org/10.3390/s21165544

Academic Editors: Mimma Nardelli and Raquel Bailón

Received: 30 June 2021
Accepted: 14 August 2021
Published: 18 August 2021



## 1. Introduction

The time duration between heart beats (interbeat intervals, IBIs) continuously changes, even at rest. These alterations are referred to as heart rate variability (HRV) and are brought about by various oscillating regulatory mechanisms that directly or indirectly affect heart rate (HR). These processes dominantly act by modifying the balance of sympathetic and parasympathetic effects on the heart; however, HR fluctuations due to other regulatory mechanisms (chemical, hormonal, and hemodynamic factors) also participate [1–4]. Control mechanisms contributing to HRV are diverse (e.g., respiratory rhythm, oscillations of baroreceptor activity, thermoregulation, etc.) and operate at different timescales [2,3,5,6]. In general, fluctuations of parasympathetic activity occur at higher frequencies, whereas those of sympathetic activity and hormonal effects at lower frequencies [6].

HRV analysis provides indices that characterize the variability of the IBIs (time-domain parameters) [2] and also that reflect the contribution of control mechanisms oscillating at

different frequencies to this variability (frequency-domain parameters). In addition, so-called non-linear parameters that characterize the unpredictability of HR are also derived. HRV analysis is performed by analyzing normal-to-normal (i.e., non-arrhythmic) IBIs of sequential heartbeats acquired from continuous ECG recordings of various lengths (from 2 min to 24 h) [1,5,7]. In general, healthy people tend to have higher HRV values, which reflect the flexibility of regulatory systems to respond to different cardiovascular and homeostatic challenges [8–13], whereas depressed HRV has been associated with a wide variety of diseases and pathophysiological disorders. Moreover, alterations of certain HRV indices have been proposed to be applicable for assessment of prognosis in post-infarction patients and in patients with congestive heart failure [14–26].

These observations indicate that HRV analysis has a promising potential to evolve to a useful medical tool to monitor cardiovascular status. Since physiological fluctuations of autonomic functions make HRV parameters highly variable even within the same individual, HRV evaluation offers the most benefit if regular measurements are available. This can be easily accomplished by using telemedical and wearable monitoring systems equipped with HRV analysis modules. Nowadays, photoplethysmography (PPG)-based devices to monitor heart rate and oxygen saturation are very common both in clinical practice and everyday activities. PPG is a technique that detects blood volume changes in the tissues with an optical method. The PPG signal is an invaluable source of information of cardiovascular and autonomic functions. Among others, continuous PPG recordings obviously offer the opportunity to determine IBIs from which pulse rate variability (PRV) indices similar to HRV indices can be derived. However, it is debated whether PPG-based PRV indices can be interpreted similarly to HRV parameters, since IBIs are defined as RR intervals from ECG, and as pulse durations from PPG are not obviously identical. RR intervals signify the duration of the electrical cardiac cycle, which may slightly differ from PPG pulse durations (most often defined as peak-to-peak intervals of PPG pulse waves), since the timing of peripheral pulse peaks is influenced by several additional factors including the dynamics of ventricular ejection, elasticity of large arteries, peripheral resistance, and the propagation velocity of the pulse wave [27–29]. Moreover, this implies that PRV parameters may bear additional information about cardiovascular functioning, which is not available in HRV indices. Disparities between HRV and PRV have already been studied by several researchers, and various HRV and PRV indices have been reported to highly correlate in healthy individuals [30–39]. However, most of these studies are restricted to selected HRV parameters and resting healthy conditions. Comprehensive investigations covering numerous HRV indices [27,31,34] (including time-domain, frequency-domain, and non-linear parameters in the same study) and studies focusing on agreements between HRV and PRV parameters under autonomic challenge [39] and in diseased conditions are scarce in the literature.

Our research group has recently introduced a telemedical system (SCN4ALL) that is designed for the remote monitoring of cardiovascular patients and is based on the photoplethysmographic (PPG) detection and analysis of the digital arterial pulse wave [40]. The system analyzes continuous 2-min long PPG recordings, which are used to evaluate morphological pulse characteristics [40]. In order to offer the most benefit for our users, we have also elaborated an automated algorithm for PRV computation and equipped the telemedical system with a PRV analysis module. The ultimate aim of this study is the comprehensive assessment of the performance of the SCN4ALL pulse rate variability analysis module.

First, we aimed to assess the agreements between the most widespread conventional HRV and PRV indices computed from ECG and PPG captures, respectively. For this purpose, we simultaneously recorded ECG and PPG on healthy individuals at rest and also under cold pressor challenge, when the autonomic balance was disrupted. We calculated IBIs and 17 HRV parameters from both captures using a clinically validated and widely accepted algorithm (Kubios HRV Premium) [41] and then compared the results with Bland–Altman analysis. The agreements of HRV and PRV parameters were also investigated in

diabetic patients in order to assess if the interchangeability observed in healthy individuals also holds for diseased conditions.

Automated algorithms used for HRV analysis use slightly different mathematical approaches for the power spectral and non-linear analysis of HRV. In this study, we also aimed to validate our proprietary SCN4ALL algorithm to a clinically accepted algorithm in order to show its reliability before introduction to clinical research and practice. For this purpose, we performed PRV analysis on 2-min long PPG recordings both with the Kubios HRV Premium [41] and the SCN4ALL algorithms and compared the results with Bland–Altman analysis.

## 2. Materials and Methods

### 2.1. Subjects

A total of 33 informed and consenting healthy (M/F: 14/19, age between 19 and 55, mean ± SD: 32.1 ± 9.7 years) and 12 type 2 diabetic (M/F:5/7, age between 43–79, mean ± SD: 61.1 ± 12.8 years) subjects participated in this study. None of the healthy volunteers had a history of cardiovascular disease, or cardiovascular medication, and none of them reported any symptoms that may affect autonomic balance (sleep deprivation, stress, headache, etc.). The participating diabetic patients had been treated for type 2 diabetes for more than one year. The study was approved by the Regional and Institutional Committee of Science and Research Ethics at Semmelweis University (approval number: 120/2018).

### 2.2. Measurements of HRV

#### 2.2.1. Signal Recording

**ECG.** Einthoven II lead ECG was recorded with the Biopac BSL MP45 data acquisition system (Biopac Systems Incl., Goleta, CA, USA). For ECG recording, disposable ECG electrodes were attached to the right shoulder, left lower abdomen, and right lower abdomen, and then connected to the negative, positive, and ground wires of a Biopac SS2LB electrode lead set, respectively. The signal was amplified by a Biopac MP45 data acquisition unit, which was directly connected to a desktop computer. BSL 3.7.7 software was used to capture ECG for 2 min at a sample rate of 1000 Hz. ECG recordings were saved as *.acq* files and were used to identify RR intervals by the Kubios HRV Premium analysis software (Kubios Ltd., Kuopio, Finland) [41]. RR intervals were used as IBIs (IBI-ECG) to calculate HRV parameters (for details, see data analysis).

**PPG.** For recording the PPG signal, a finger-clip transmission pulse oximeter (Berry Pulse Oximeter, Shanghai Berry Electronic Tech Co., Ltd., Shanghai, China) was attached to the left index finger. Pulse wave detection and analysis were performed by the SCN4ALL telemedicine system (E-Med4All Europe Ltd., Budapest, Hungary). In the system, the pulse oximeter communicates via Bluetooth connection with a mobile application, which initiates and terminates data acquisition and transmits the recording to a cloud-based automated algorithm, which has been developed by our research group. First, the signals sampled at a frequency of 200 Hz are upsampled to 1000 Hz; then, the algorithm identifies the pulse cycles and peak-to-peak intervals as IBIs (IBI-PPG). Time series of IBI-PPG were used to calculate PRV parameters (for details, see data analysis). Data captured by the SCN4ALL system is stored on a cloud-based server equipped with safe data protection, which conforms to the applicable regulations ((EU)2016/679) [40].

#### 2.2.2. Protocol

We performed the measurements on 33 healthy and 12 diabetic participants under the following conditions: measurement took place in a quiet room at room temperature, in a sitting, resting position, with hands held quietly on a table. The pulse oximeter was placed on the left index finger, and the ECG electrodes were attached as described above. After mounting the devices, participants were instructed to minimize movements. Measurements were initiated after 10 min of rest. First, we measured the blood pressure of the participants with an Omron M3 Intellisense arm-cuff blood pressure meter 3 times,

with 2-min intervals between the measurements (OMRON Corporation, Kyoto, Japan). Afterwards, ECG and PPG signals were simultaneously recorded for 2 min using Biopac 3.7.7 software and SCN4ALL application, respectively.

After completion of the resting examination, the healthy volunteers remained seated, and we repeated the measurements in these subjects also during a cold pressor cardiovascular challenge, which was applied to disturb the resting autonomic balance. First, we measured the participants' blood pressures. Then, the right hand was immersed in a bowl of cold water (+3–5 °C). ECG and PPG recordings were initiated simultaneously with the cold pressor challenge and lasted for 2 min. Blood pressure measurements were repeated immediately after the termination of the 2-min recording period.

### 2.3. Data Analysis

In the analysis, only those recordings were evaluated that consisted of normal-to-normal IBIs. For this reason, results of 3 healthy subjects were completely excluded from the study, because in 2 cases, previously unknown arrhythmia was seen on the ECG, and in 1 case, the PPG was contaminated with motion artefacts. Four additional healthy subjects were excluded from the 'cold pressor test' study either for not tolerating the challenge or for producing numerous PPG artefacts. Therefore, in the healthy group, results of control measurements are presented for 30 (M/F: 14/16, age range 19–55, mean ± SD: 33 ± 9.7 years), and those of the cold pressor study for 26 subjects (M/F: 11/15, age range 19–55, mean ± SD: 33 ± 9.9 years).

We calculated HRV/PRV parameters from the two detection modalities (ECG and PPG) by three methods:

1. ECG recordings (*.acq* files captured by the Biopac system) were opened in Kubios HRV Premium software (ver. 3.3.1), which identified RR intervals (IBI-ECG) and then computed HRV parameters. As only non-arrhythmic recordings were used, the calculations were made using no artefact correction and with unfiltered settings. As a result, HRV-ECG values were generated.
2. We saved peak-to-peak intervals calculated by the SCN4ALL algorithm from each PPG recording (IBI-PPG) as *.csv* files. The PRV analysis of the IBI-PPG datasets were executed with Kubios HRV Premium, with the same settings as in Point 1. As a result, PRV-Kubios values were created.
3. The automatic algorithm of the SCN4ALL system was also used to calculate PRV parameters from IBI-PPG data to produce PRV-SCN4ALL values. The functions of the algorithm were programmed in Matlab. The algorithm uses the statistical approaches recommended by the 'Task Force of the European Society of Cardiology and the North American Society of Pacing Electrophysiology' [5] to determine time-domain parameters. For frequency-domain analysis, a power spectrum density estimate was calculated by the algorithm using a Fast Fourier Transform (FFT)-based Welch's periodogram method. After obtaining the FFT spectrum, absolute power values for each frequency band were calculated by simply integrating the spectrum within the band limits. To compute non-linear PRV parameters, detrended fluctuation analysis was performed according to the work of C.G Peng et al. [42]. SCN4ALL also displays a Poincaré plot with SD1 and SD2 parameters. Poincaré plot is a graph of IBI(n) on the *x*-axis versus IBI(n + 1) on the *y*-axis [43,44]. SD1 is the standard deviation of the distance of the points from the "x = y" axis and reflects short-term changes, whereas SD2 is the standard deviation of the distance of the points from the "x = −y + 2xIBI(mean)" axis [44,45]. SD1 and SD2 determine the length and width of a fitted ellipsis, respectively, the center of which is at the coordinate of (IBI(mean);IBI(mean)). In fact, SD1 and SD2 can be mathematically derived from time-domain indices; therefore, we calculated SD1 and SD2 as follows [44,46–48]:

$$SD1 = rMSSD \times \frac{1}{\sqrt{2}}$$

$$SD2 = \sqrt{2 \times SDNN^2 - SD1^2}$$

Comparison of the HRV and PRV results derived according to points 1 and 2 describes the agreement between the ECG and PPG methodologies (performed for healthy individuals at rest and during cold pressor test and for diabetic subjects at rest). In contrast, comparison of the PRV results between points 2 and 3 provides information about the performance of the SCN4ALL PRV analysis engine compared to the widely used and clinically accepted Kubios HRV Premium analysis [41]. The analysis was performed for a wide range of HRV/PRV parameters, which are listed in Table 1.

**Table 1.** Heart rate variability parameters analyzed in the study.

| | |
|---|---|
| **Time-Domain Parameters** | |
| Mean IBI | The mean normal-to-normal interbeat interval (IBI) |
| SDNN | The standard deviation (SD) of IBIs (NN: normal-to-normal IBI) |
| MHR | Mean heart rate |
| RMSSD | The square root of the mean squared differences of successive IBIs |
| pNN50 | The proportion of differences of successive IBIs exceeding 50 ms (NN: normal-to-normal IBI) |
| MnHR | Minimum heart rate |
| MxHR | Maximum heart rate |
| **Frequency-Domain Parameters** | |
| LF power | Absolute power of the low-frequency (LF) band (0.04–0.15 Hz) |
| HF power | Absolute power of the high-frequency (HF) band (0.15–0.4 Hz) |
| LFnu | Relative power of the low-frequency (LF) band expressed in normalized units (nu) |
| HFnu | Relative power of the high-frequency (HF) band expressed in normalized units (nu) |
| Ptotal | Total spectral power (P) |
| LF/HF ratio | Ratio of low frequency (LF) to high frequency (HF) |
| **Non-Linear Parameters** | |
| SD1 | Standard deviation (SD) 1 of the Poincaré plot representing the length of the ellipse fitted to the plot |
| SD2 | Standard deviation (SD) 2 of the Poincaré plot representing the width of the ellipse fitted to the plot |
| SD1/SD2 | The ratio of SD1 and SD2 |
| DFA$\alpha$1 | Short term fluctuation slope ($\alpha$1) obtained by detrended fluctuation analysis (DFA) |

### *2.4. Bland–Altman Analysis*

The agreements between HRV/PRV parameter values (HRV-ECG vs. PRV-Kubios and PRV-Kubios vs. PRV-SCN4ALL) were assessed by Bland–Altman analysis [49,50]. The differences of measurements were plotted against the means of the measurements. Bias was defined as mean difference and is presented with 95% confidence intervals (C.I.). To calculate percentage bias, bias is expressed as the percentage of the mean of the measurements. Limits of agreement were calculated as bias $\pm$ 1.96 standard deviation. The analysis was performed with MedCalc Statistical Software v.19.6.4 (MedCalc Software, Ostend, Belgium).

## 3. Results

### *3.1. Agreements between ECG-Based HRV and PPG-Based PRV Parameters*

The Bland–Altman plots used for the analysis of agreement between PRV and HRV parameters derived from 2-min long PPG and ECG recordings, respectively, are shown in Figure 1. In this setting, conventional HRV indices were calculated by the algorithm of the Kubios HRV Premium software. The values of variables referring to IBI duration (IBI, mean HR, minimum HR, and maximum HR) are apparently identical in PPG and ECG based calculations (Figure 1A, and Supplementary Figure S1A). Among time-domain parameters, SDNN and RMSSD showed good agreement. The percentage biases were $-3.2\%$ (95% C.I.: $-5.2$; $-1.2$) and $-9.5\%$ (95% C.I.: $-14.3$; $-4.6$), respectively, indicating

that the values calculated from PPG recordings are slightly higher. However, in the case of pNN50, the bias was −27.3% (95% C.I.: −53.2; −1.4) (Figure 1A). Among frequency-domain parameters, good agreement was observed for total and low-frequency spectral power (percentage bias −8.2% (95% C.I.: −10.6; −5.8) for total power (Ptotal); and −2.7% (95% C.I.: −4.9; −0.5) for LF) (Figure 1B and Supplementary Figure S1B)). However, the agreement for high-frequency power was weaker (percentage bias −26.5% (95% C.I.: −35.6; −17.5) (Supplementary Figure S1B)), with significant overestimation of the parameter by the PPG based calculation. The calculated non-linear parameters (DFA$\alpha$1, SD1, SD2, and SD1/SD2) each showed good agreement (Figure 1C).

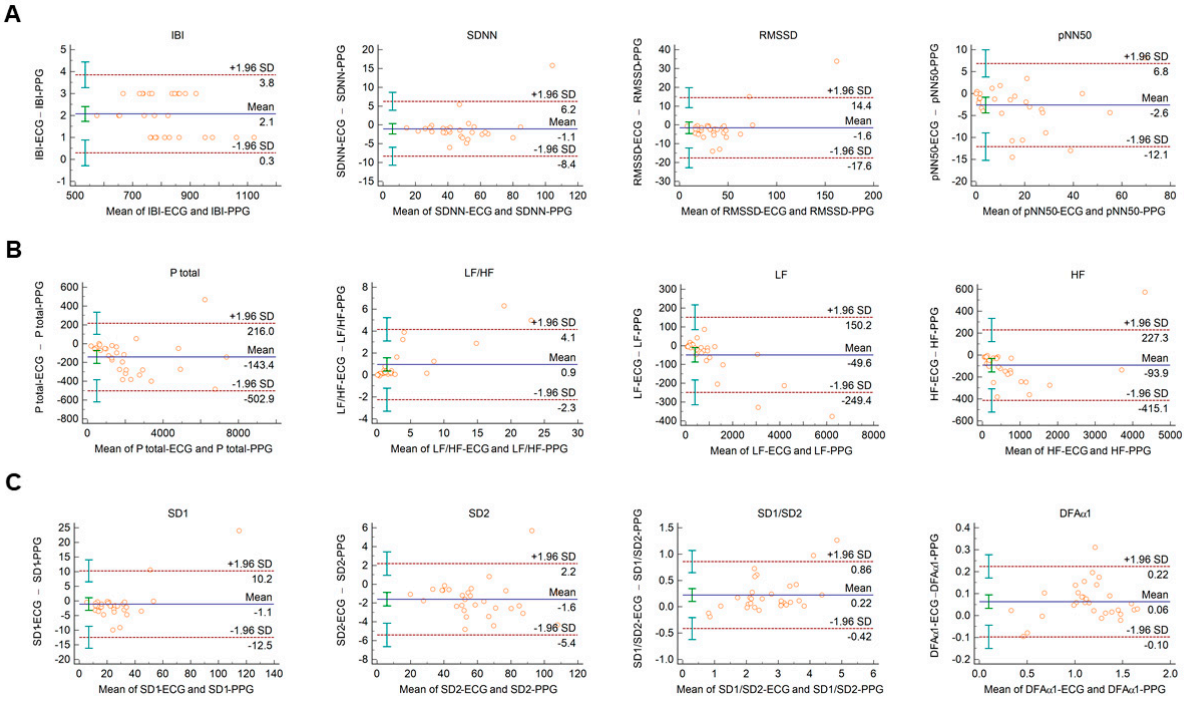


**Figure 1.** Bland–Altman plots of HRV/PRV parameters computed by the Kubios Premium algorithm from 2-min long ECG (indicated as 'parameter name-ECG') and PPG (indicated as 'parameter name-PPG') recordings captured under resting conditions. (**A**) Time-domain parameters: IBI (interbeat interval), SDNN (the standard deviation of IBIs), RMSSD (the square root of the mean squared differences of successive IBIs), pNN50 (the proportion of differences of successive IBIs exceeding 50 ms). (**B**) Frequency-domain parameters: Ptotal (total spectral power), LF/HF (ratio of low frequency to high frequency), LF (absolute power of the low-frequency band (0.04–0.15 Hz)), HF (absolute power of the high-frequency band (0.15–0.4 Hz)). (**C**) Non-linear parameters: SD1 (Poincaré plot standard deviation perpendicular to the line of identity), SD2 (Poincaré plot standard deviation along the line of identity), SD1/SD2 (ratio of SD1-to-SD2), DFA$\alpha$1 (short term fluctuation slope obtained by detrended fluctuation analysis). Bias is calculated as the mean of differences (indicated as 'Mean'—blue solid line) and is presented with 95% confidence intervals (green) and +/− 1.96 standard deviations (SD) and their confidence intervals.

When Bland–Altman analysis was performed on HRV vs. PRV parameters calculated from 2-min ECG and PPG recordings obtained from healthy individuals during cold pressor test, similar tendencies could be observed with similar IBI durations, and with good, clinically acceptable agreements for SDNN, RMSSD, total power, and LF; and also, for non-linear parameters (Figure 2 and Supplementary Figure S2.).

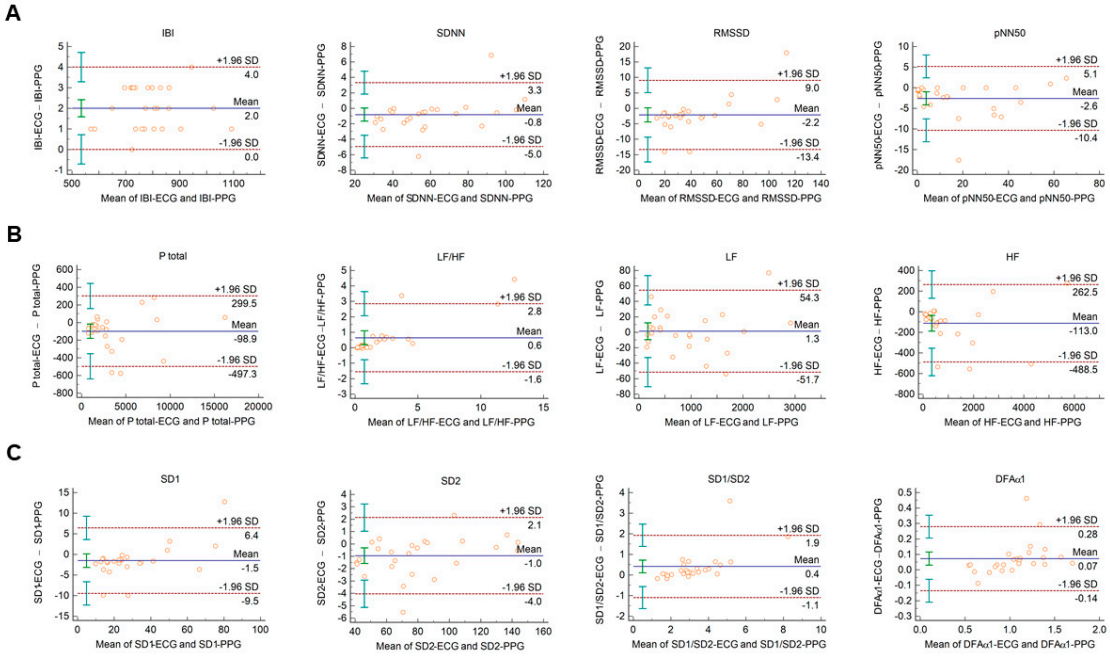


**Figure 2.** Bland–Altman plots of HRV/PRV parameters computed by the Kubios Premium algorithm from 2-min long ECG (indicated as 'parameter name-ECG') and PPG (indicated as 'parameter name-PPG') recordings obtained during cold pressor test. (**A**) Time-domain parameters: IBI (interbeat interval), SDNN (the standard deviation of IBIs), RMSSD (the square root of the mean squared differences of successive IBIs), pNN50 (the proportion of differences of successive IBIs exceeding 50 ms). (**B**) Frequency-domain parameters: Ptotal (total spectral power), LF/HF (ratio of low frequency to high frequency), LF (absolute power of the low-frequency band (0.04–0.15 Hz)), HF (absolute power of the high-frequency band (0.15–0.4 Hz)). (**C**) Non-linear parameters: SD1 (Poincaré plot standard deviation perpendicular to the line of identity), SD2 (Poincaré plot standard deviation along the line of identity), SD1/SD2 (ratio of SD1-to-SD2), DFA$\alpha$1 (short-term fluctuation slope obtained by detrended fluctuation analysis). Bias is calculated as the mean of differences (indicated as 'Mean'—blue solid line) and is presented with 95% confidence intervals (green) and +/− 1.96 standard deviations (SD) and their confidence intervals.

In diabetic individuals, the Bland–Altman analysis showed good agreements between HRV and PRV values for IBI durations (Figure 3A), SDNN (Figure 3A), LF power (Figure 3B), and SD2 variables (Figure 3C) (percentage bias < 10% for each parameter). Slightly weaker, moderate agreements were observed for total power (Figure 3B; percentage bias −14.2% (95% C.I.: −23.3; −5.1)); and for DFA$\alpha$1 non-linear parameter (Figure 3C; percentage bias 13.8% (95% C.I.: 0.0; 27.6)). However, in case of RMSSD and pNN50 time-domain variables (Figure 3A); HF and relative (HFnu, LFnu, LF/HF) frequency-domain indices (Figure 3B and Supplementary Figure S3); and SD1 and SD1/SD2 non-linear parameters (Figure 3C), the agreements were found to be insufficient (percentage bias > 20%).

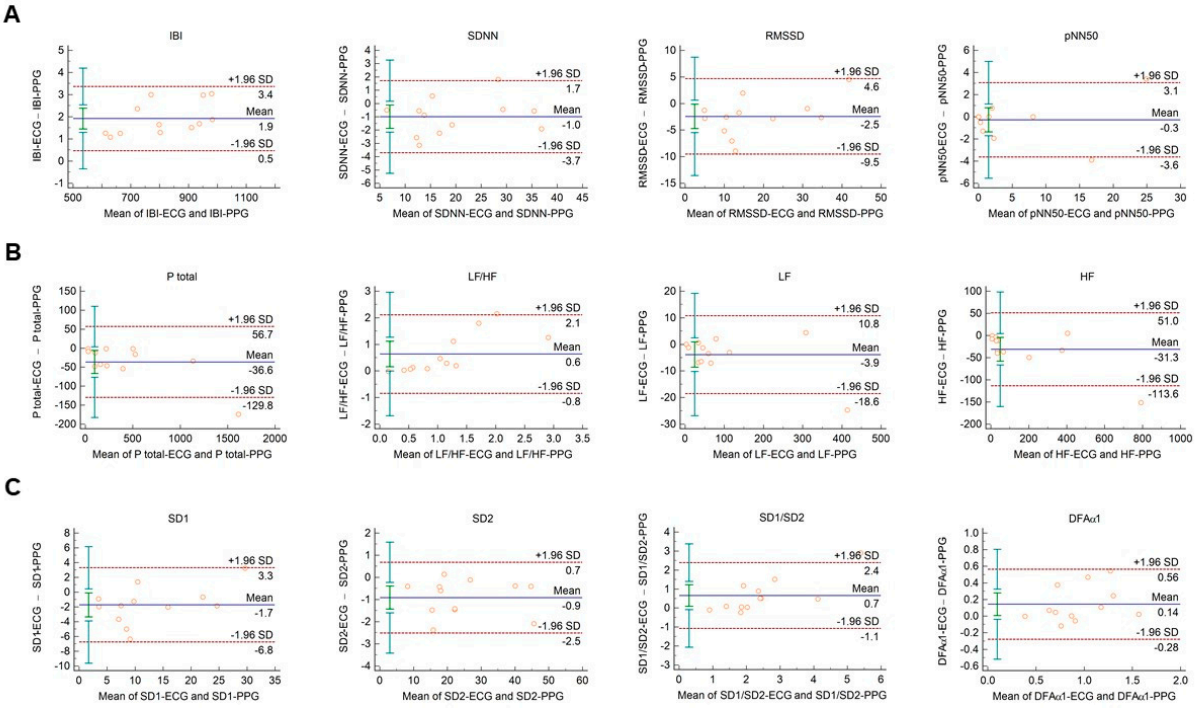


**Figure 3.** Bland–Altman plots of HRV/PRV parameters computed by the Kubios Premium algorithm from 2-min long ECG (indicated as 'parameter name-ECG') and PPG (indicated as 'parameter name-PPG') recordings obtained from diabetic patients under resting conditions. (**A**) Time-domain parameters: IBI (interbeat interval), SDNN (the standard deviation of IBIs), RMSSD (the square root of the mean squared differences of successive IBIs), pNN50 (the proportion of differences of successive IBIs exceeding 50 ms). (**B**) Frequency-domain parameters: Ptotal (total spectral power), LF/HF (ratio of low frequency to high frequency), LF (absolute power of the low-frequency band (0.04–0.15 Hz)), HF (absolute power of the high-frequency band (0.15–0.4 Hz)). (**C**) Non-linear parameters: SD1 (Poincaré plot standard deviation perpendicular to the line of identity), SD2 (Poincaré plot standard deviation along the line of identity), SD1/SD2 (ratio of SD1-to-SD2), DFA$\alpha$1 (short-term fluctuation slope obtained by detrended fluctuation analysis). Bias is calculated as the mean of differences (indicated as 'Mean'—blue solid line) and is presented with 95% confidence intervals (green) and +/− 1.96 standard deviations (SD) and their confidence intervals.

### *3.2. Agreements between PRV Calculations of the SCN4ALL and Kubios HRV Premium Algorithms*

Comparison of the PRV parameters calculated by the SCN4ALL and the Kubios HRV Premium algorithm from 2-min long PPG recordings showed perfect agreement in case of all PRV variables. For time-domain and non-linear variables (Supplementary Figure S3), the percentage biases were smaller than 0.5%. In case of frequency-domain variables, these values were below 2% and well within the clinically acceptable limits and with no significant difference between the outputs of the two algorithms (Figure 4).

The agreement between the outputs of the algorithms remained unaltered when 2-min long recordings acquired in healthy subjects during cold pressor test (Figure 5 and Supplementary Figure S5) and in diabetic patients at rest (Figure 6 and Supplementary Figure S6) were used for analysis.

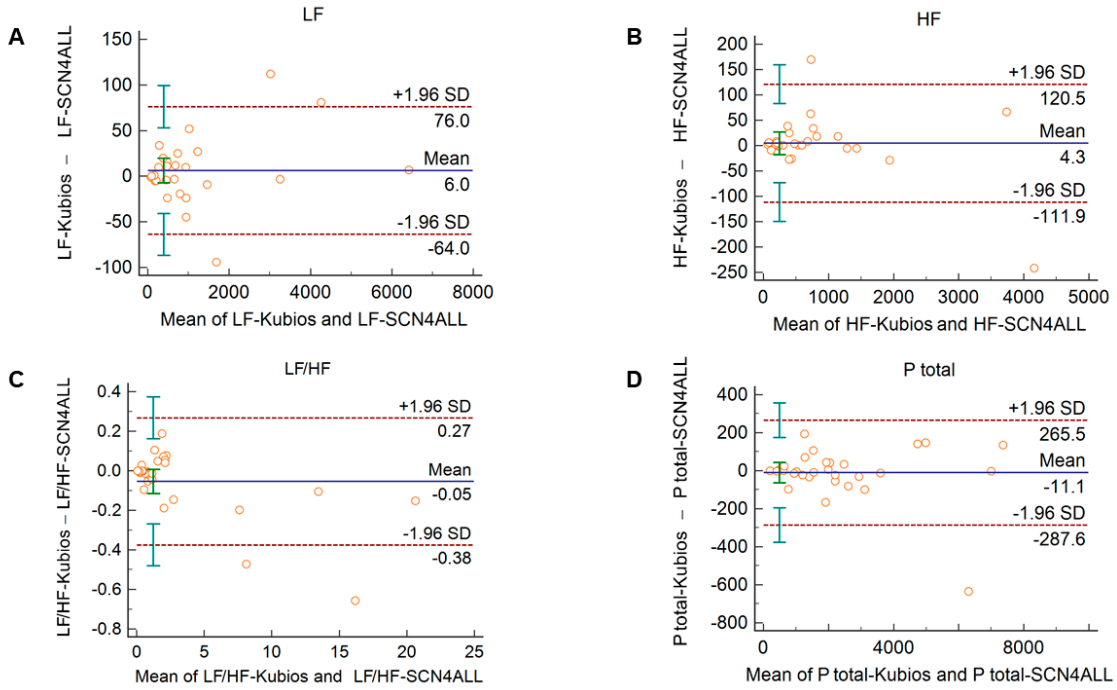


**Figure 4.** Bland–Altman plots of frequency-domain HRV/PRV parameters calculated by the SCN4ALL (indicated as 'parameter name-SCN4ALL') and the Kubios Premium HRV (indicated as 'parameter name-Kubios') algorithms from 2-min long PPG recordings captured under resting conditions. (**A**) Ptotal (total spectral power), (**B**) LF/HF (ratio of low frequency to high frequency), (**C**) LF (absolute power of the low-frequency band (0.04–0.15 Hz)), (**D**) HF (absolute power of the high-frequency band (0.15–0.4 Hz)). Bias is calculated as the mean of differences (indicated as 'Mean'—blue solid line) and is presented with 95% confidence intervals (green) and +/− 1.96 standard deviations (SD) and their confidence intervals.

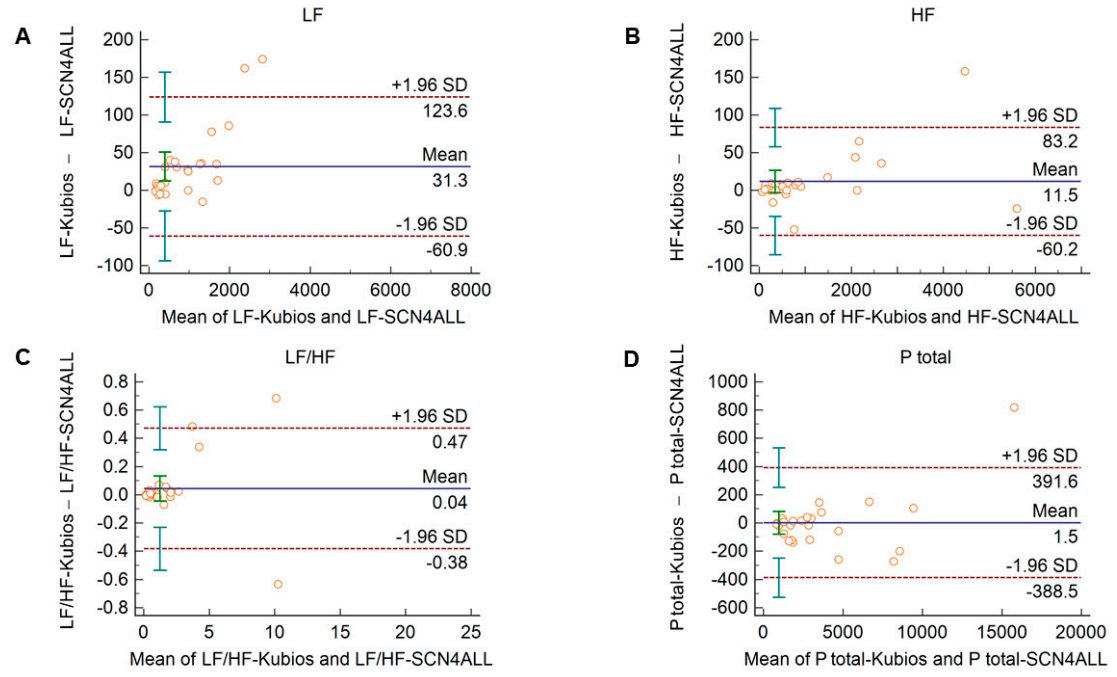


**Figure 5.** Bland–Altman plots of frequency-domain HRV/PRV parameters calculated by the SCN4ALL (indicated as 'parameter name-SCN4ALL') and the Kubios Premium HRV (indicated as 'parameter name-Kubios') algorithms from 2-min long PPG recordings obtained during cold pressor test. (**A**) Ptotal (total spectral power), (**B**) LF/HF (ratio of low frequency to high frequency), (**C**) LF (absolute power of the low-frequency band (0.04–0.15 Hz)), (**D**) HF (absolute power of the high-frequency band (0.15–0.4 Hz)) Bias is calculated as the mean of differences (indicated as 'Mean'—blue solid line) and is presented with 95% confidence intervals (green) and +/− 1.96 standard deviations (SD) and their confidence intervals.

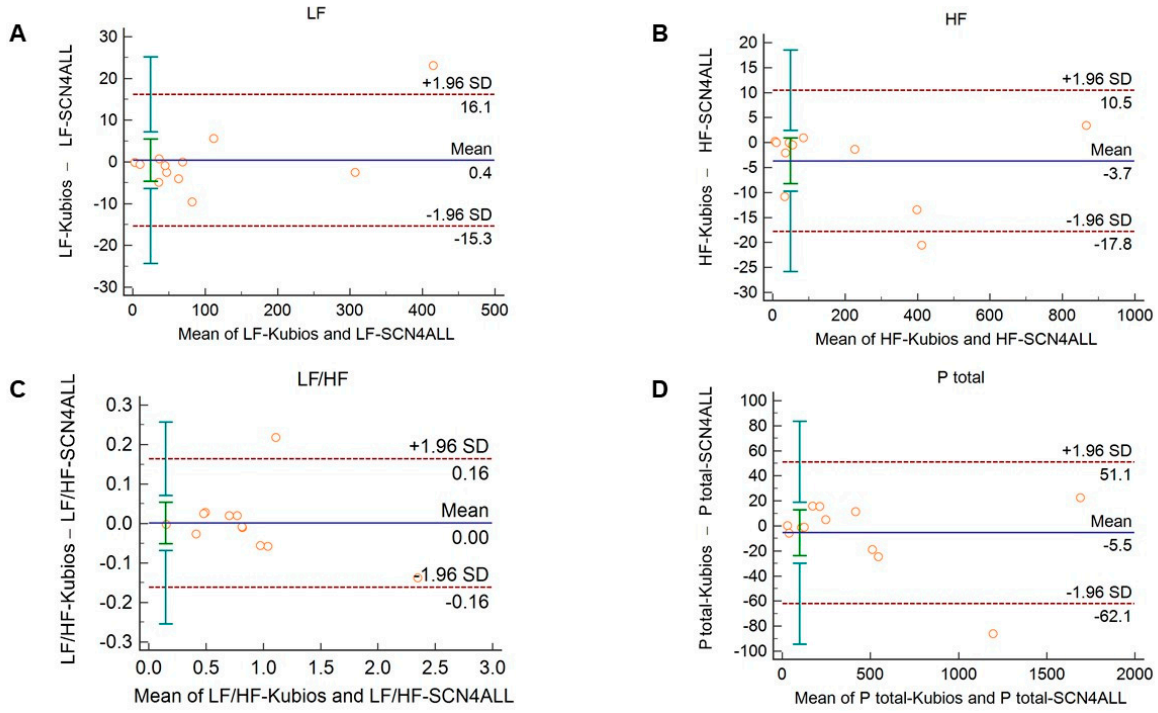


**Figure 6.** Bland–Altman plots of frequency-domain HRV/PRV parameters calculated by the SCN4ALL (indicated as 'parameter name-SCN4ALL') and the Kubios Premium HRV (indicated as 'parameter name-Kubios') algorithms from 2-min long PPG recordings obtained from diabetic patients under resting conditions. (**A**) Ptotal (total spectral power), (**B**) LF/HF (ratio of low frequency to high frequency), (**C**) LF (absolute power of the low-frequency band (0.04–0.15 Hz)), (**D**) HF (absolute power of the high-frequency band (0.15–0.4 Hz)). Bias is calculated as the mean of differences (indicated as 'Mean'—blue solid line) and is presented with 95% confidence intervals (green) and +/− 1.96 standard deviations (SD) and their confidence intervals.

## 4. Discussion

In our study, using Bland–Altman plots, we have shown that PRV and HRV calculations (obtained from PPG and ECG recordings, respectively) are in good agreement for several conventional HRV/PRV parameters when the analysis is performed using short (2-min long) recordings. Apparently, there is no significant difference in mean interbeat intervals defined from PPG and ECG captures, and for several HRV/PRV parameters computed by the Kubios software, the limits of agreement are within 10% (i.e., SDNN and RMSSD among time-domain variables, total power and LF frequency-domain indices, and non-linear parameters). The agreement of HRV parameters obtained by the two methods prevailed even if the resting autonomic balance had been disrupted by a cardiovascular challenge (cold pressor test). In diabetic individuals, the good agreements between HRV and PRV indices were also valid for SDNN, LF, and SD2 indices, and moderate agreements could be detected between total spectral power and DFA$\alpha$1 values. However, for parameters that are considered to be conventional markers of short-term HRV, weaker agreements were found. We have also shown that the outputs of the PRV algorithm of the SCN4ALL telemonitoring system are in perfect agreement with the values computed by Kubios HRV Premium when the analysis is performed on data derived from short (2-min long) PPG captures. Our study extends our scientific knowledge about the interchangeability of HRV and PRV analysis with relevant new pieces, as it is a comprehensive investigation covering a large number of HRV/PRV parameters and assessing their agreements not only in healthy individuals at rest but also under autonomic challenge and in diabetes.

Autonomic function has been in the focus of research for decades, and several non-invasive techniques have been proposed for its evaluation (ECG, PPG, electroencephalography, sudomotor function, etc.) [51–53]. Many of these may also be incorporated in remote

monitoring systems, and experiences acquired in signal analysis of one method have often facilitated progression in the procession of other signals. Using the HRV analysis approach for PPG signals is a good example of this. However, in the literature, it is controversial whether HRV parameters calculated from time series of RR intervals obtained from ECG recordings and from pulse durations obtained from PPG signals or continuous non-invasive blood pressure monitoring (e.g., Finapress) can be used alternatively [54]. Nowadays, the number of wearable and telemedical devices that are equipped with either ECG or PPG detectors dynamically increases [55,56]. This may open new prospects for scientists and physicians to exploit the opportunities offered by HRV/PRV analysis in patient evaluation. However, most of our scientific knowledge on HRV alterations in different (patho)physiological conditions relies on ECG-based studies, mostly following a task force statement of the European Society of Cardiology and the North American Society of Pacing Electrophysiology [5]. Therefore, it is important to assess the agreement between HRV and PRV under different (physiological and pathological) conditions in order to confidently accept the PPG-based PRV-analysis as a reliable alternative to monitor HRV changes. So far, several studies have compared PRV to the gold standard of ECG-derived HRV [30–39]. Some publications found good agreements between PRV and HRV, especially in younger subjects and at rest [31,57], or during sleep [58], and mostly in time-domain parameters. However, some studies have found weaker agreements between HRV and PRV values for HRV indices, which are generally influenced by short-term regulatory fluctuations (RMSSD, pNN50, HF, LF/HF, SD1) [32,34,36,54,59–61]. Their results indicate that PRV overestimates HF but underestimates LF/HF ratio and LF percentage. However, it is notable that this is observed more often in continuous blood pressure monitoring studies (Finapress) than in PPG studies. There is sparse evidence of whether frequency-domain PRV variables behave similarly to HRV variables and have some value in diagnosing autonomic function [38,62]. In our study, we have shown that among time-domain variables, PPG-based and ECG-based SDNN and RMSSD values have good agreements (Figure 1A). Similar to previous studies, pNN50 was overestimated when PPG-based IBIs were used [27,32,34,36,54,59]. On the other hand, total spectral power and low-frequency power computed from PPG and ECG had similar values (Figure 1B). Interestingly, high-frequency power was significantly overestimated by the PPG-based analysis (Figure 1B). This is in agreement with some studies, in which similar observations were made for certain frequency-domain variables [32,34,36,39,54,60,61,63]. It has been speculated that the reason for this disparity in HF power and other indices reflecting short-term variability is that spontaneous breathing rate lying within the HF frequency band has a greater impact on PRV than on ECG-based HRV [54,59,62,64].

We also observed good agreements for non-linear parameters. The relevance of these parameters in HRV analysis is not completely established, and there is no consensus on the measurement duration which can yield clinically informative non-linear variables [65–67]. Moreover, some of these parameters are in a direct mathematical relationship with other parameters and bear the same information (e.g., SD1 and RMSSD). Anyway, our results show that PPG-based PRV analysis is a good alternative for HRV analysis in case of non-linear parameters, too.

Although several studies have shown correlations between PRV and HRV variables, these were observed at rest or during sleep. However, exercise, stress, or changing position were observed to diminish these agreements. The authors speculated that in physically active states, the disagreement is most probably due to motion artefacts [34,39]. On the other hand, the disparity between PRV and HRV variables can also be the consequence of the altered autonomic balance, which may affect pulse rate and heart rate differentially. In our study, we used the cold pressor cardiovascular challenge to disrupt the resting autonomic balance. This allowed examination of the effects of altered autonomic function without producing motion artefacts. Although not every subject had the same usual and expected cardiovascular response during the test, there was some disruption of the autonomic balance in every case (average increase in systolic pressure: $5.4 \pm 7.7$ mmHg,

average increase in diastolic pressure: 3.7 ± 6.6 mmHg). The agreements in the PPG- and ECG-based analysis described at rest could also be observed during the cold pressor test (Figure 2, and Supplementary Figure S2), implying that PPG-based PRV analysis can be applicable also in conditions in which altered autonomic function has been described by HRV analysis. In our study, we chose a cold pressor test to modify autonomic balance, because this allowed us to avoid undesirable motion artefacts. However, this may have limitations, as in another study it has been shown that whole-body cold exposure has differential effects on HRV and PRV parameters, thereby modifying the agreements between them [27]. It was speculated that this can be most probably due to the unbalanced influence of cold exposure on central and peripheral sympathetic activity. In our study, cold exposure on one hand did not abolish the agreements of HRV and PRV parameters, presumably because its effects differ from those of whole-body cold exposure.

We have also conducted a pilot study to assess the agreements between HRV and PRV indices in type 2 diabetic patients in order to find out whether the agreements observed in healthy individuals are also valid in a diseased condition. Diabetes is characterized by reduced total and LF power, and also by the decrease of HRV parameters that signify mainly short-term variability (SDNN, RMSSD, pNN50, HF) [68–71]. These alterations are caused by the deleterious effects of the impaired glucose metabolism on autonomic nerves [70]. We found that for several relevant HRV parameters, such as SDNN, LF power, and SD2 parameters, good agreements can be detected between HRV and PRV derived values. Moreover, we observed moderate agreements (bias < 15%) in case of DFA$\alpha$1 and total power. However, in case of those parameters that describe short-term variability (RMSSD, pNN50, SD1) though both HRV and PRV values tended to be lower in the diabetic group, the HRV-PRV agreements were weaker than those observed in healthy individuals. Our results suggest that several conventional HRV/PRV parameters can be used interchangeably not only in healthy but also in diabetic individuals; however, there are other parameters with non-negligible disparities. It does not necessarily imply that those parameters that show weaker agreements in our study are not worth evaluating. However, our findings highlight the relevance of larger-scale comparative HRV vs. PRV studies to verify whether diabetes or various other disease conditions are associated with typical alterations of these PRV variables. Data mining techniques to identify correlations between PRV patterns and different diseases could effectively improve our scientific knowledge in this field. As a result, we may identify the differences even in localized autonomic responses accounting for HRV and PRV disparities in order to establish sound diagnostic indications for HRV and PRV analyses.

HRV algorithms used for calculation of HRV variables may apply different mathematical approaches. This may limit the comparison of studies and the valid interpretation of the HRV variables and their alterations in different conditions. Therefore, we considered it to be relevant to validate our algorithm to a clinically widely accepted and frequently used HRV algorithm, the Kubios HRV Premium. In case of time-domain variables, we should expect perfect agreement between algorithms, since these parameters are calculated as statistical parameters describing IBI variability using formulae recommended by a task force statement [5]. However, for spectral analysis, two main different approaches can be used to separate HRV into frequency components, namely Fast Fourier Transformation (FFT) and autoregressive modeling [5]. For each approach, several slightly different functions can be applied. The SCN4ALL algorithm uses an FFT-based Welch's periodogram method, which is similar to the one applied by the Kubios algorithm. For calculation of non-linear parameters, the SCN4ALL algorithm uses detrended fluctuation analysis according to the work of Peng et al. [42] and a Poincaré plot, which are characterized by SD1 and SD2 parameters defined in the "Methods" section above. Comparison of the SCN4ALL algorithm outputs to the Kubios outputs by Bland–Altman analysis showed perfect agreement between the methods when we analyzed 2-min long PPG-based IBI time series obtained from either healthy individuals at rest and during cold pressor cardiovascular challenge or from diabetic patients at rest. In case of those parameters where a simple mathematical for-

mula is applied (time-domain variables, SD1 and SD2 non-linear variables), the negligible differences between the SCN4ALL and Kubios results are attributable to slightly different rounding schemes used by the algorithms.

Signal processing of telemedical systems may be prone to signal loss and uncertainty due to multistep signal transformation [72,73]. This can be interpreted as the uncertainty of the data used for classification. Effective classification of evidence requires the use of fuzzy classifiers [74,75]. Based on multiple studies [76–78], the fuzzy data application allows to increase the accuracy of the classification of uncertain data [79]. In the case of the PPG-based system used in our study, there are two possible steps where signal loss may occur. The first is the analog-to-digital conversion of the signal. In the case of heart rate variability, only the quantization error can play a role. The SCN4ALL telemedicine system operates at a sampling rate of 200 Hz, meaning that at a heart rate of 60 beats/minutes, it only creates a 0.5% error. This is clinically acceptable and does not affect the diagnostic value of the given system. The second step where some information loss can be expected is at the filtering of the digitized signal. However, it only affects the morphology of the PPG signal but not the timely relations of the fiducial timepoints. Therefore, filtering the signal does not affect the peak-to-peak distances of the pulse wave from which IBIs for PRV calculation are derived. Furthermore, in our previous article [40], we examined how artificial non-variable PPG signals generated by a simulator (both normal and simulated pathological signals) were processed by the system, and the repeatability was found to be perfect in case of most studied parameters [40]. Although this study focused on morphological parameters, we also investigated the reliability of IBI determination, and the error (expressed as coefficient of variation) was virtually zero. Our PRV analysis module uses only IBIs as detected signals for further computation, so we think that signal loss and uncertainty have a negligible effect on our analysis.

## 5. Conclusions

Our study showed that the HRV algorithm of the SCN4ALL system is as accurate as the widely used Kubios HRV Premium algorithm for PRV analysis of short (2-min long) time series of interbeat intervals obtained by PPG recordings. PRV analysis performed on PPG pulse signals is in good agreement with ECG-based analysis for numerous clinically relevant HRV parameters, including SDNN and RMSSD time-domain parameters, total and low-frequency spectral power frequency-domain variables, and non-linear parameters in healthy individuals at rest, and also under an autonomic challenge. Moreover, we identified several parameters (SDNN, total power, LF, SD2, and DFA$\alpha$1) that showed moderate to good HRV-PRV agreements in diabetic patients. This indicates that these parameters can be reliably used for HRV-based evaluation of autonomic function in healthy and diabetic individuals regardless of whether ECG or PPG provides the time series of interbeat intervals. Other conventional PRV parameters computed from PPG recordings should be interpreted cautiously, keeping in mind that clinical evidence obtained on ECG-based HRV alterations in different disease conditions can be applied with limitations. Despite these limitations, we can claim that PPG-based PRV analysis of the SCN4ALL system is suitable for evaluation of PRV alterations, and to pursue research to establish the clinical relevance of PRV analysis in the follow-up of autonomic dysregulation in various diseases.

**Supplementary Materials:** The following are available online at https://www.mdpi.com/article/10.3390/s21165544/s1, Supplementary Figure S1: Bland–Altman plots of HRV/PRV parameters computed by the Kubios Premium algorithm from 2-min long ECG (indicated as 'parameter name-ECG') and PPG (indicated as 'parameter name-PPG') recordings captured in healthy individuals under resting conditions; Supplementary Figure S2: Bland–Altman plots of HRV/PRV parameters computed by the Kubios Premium algorithm from 2-min long ECG (indicated as 'parameter name-ECG') and PPG (indicated as 'parameter name-PPG') recordings obtained from healthy individuals during cold pressor test; Supplementary Figure S3: Bland–Altman plots of HRV/PRV parameters computed by the Kubios Premium algorithm from 2-min long ECG (indicated as 'parameter name-

ECG') and PPG (indicated as 'parameter name-PPG') recordings obtained from diabetic patients under resting conditions; Supplementary Figure S4. Bland–Altman plots of HRV/PRV parameters calculated by the SCN4ALL (indicated as 'parameter name-SCN4ALL') and the Kubios Premium HRV (indicated as 'parameter name-Kubios') algorithms from 2-min long PPG recordings captured in healthy individuals under resting conditions; Supplementary Figure S5: Bland–Altman plots of HRV/PRV parameters calculated by the SCN4ALL (indicated as 'parameter name-SCN4ALL') and the Kubios Premium HRV (indicated as 'parameter name-Kubios') algorithms from 2-min long PPG recordings obtained from healthy individuals during cold pressor test; Supplementary Figure S6: Bland–Altman plots of HRV/PRV parameters calculated by the SCN4ALL (indicated as 'parameter name-SCN4ALL') and the Kubios Premium HRV (indicated as 'parameter name-Kubios') algorithms from 2-min long PPG recordings obtained from diabetic patients under resting conditions.

**Author Contributions:** Conceptualization, D.K., F.A., S.K. and Z.M.; methodology, F.A., D.K. and Z.M.; validation, S.K. and Z.M.; software, B.S.; investigation, F.A., Z.M. and D.K.; resources, S.K., B.S.; data curation, K.I.L., L.S., F.A.; writing—original draft preparation, F.A., D.K. and Z.M.; writing—review and editing, Z.M.; visualization, F.A., K.I.L.; supervision, Z.M.; project administration, F.A.; funding acquisition, D.K. and S.K. All authors have read and agreed to the published version of the manuscript.

**Funding:** This study was funded by E-Med4All Europe Ltd. In addition, F.A. and D.K. received support from the EFOP-3.6.3-VEKOP-16-2017-00009 project during their current semester within their PhD studies. Z.M. receives financial support from the Higher Education Institutional Excellence Program (FIKP) of the Ministry for Innovation and Technology in Hungary, within the framework of the Molecular Biology thematic program of the Semmelweis University.

**Institutional Review Board Statement:** The study was conducted according to the guidelines of the Declaration of Helsinki, and Semmelweis University Regional and Institutional Committee of Science and Research Ethics approved the ethics license and issued the statement (SE-RKEB: 120/2018).

**Informed Consent Statement:** We have the statements of consent to participate from the subjects, if requested, we can provide the copies of these in Hungarian. Written informed consents were obtained from the subjects for publication. The copies of the written consents are available, if requested, we can provide the copies in Hungarian.

**Data Availability Statement:** The data that support the findings of this study are available from E-Med4All Europe Ltd., but restrictions apply to the availability of these data, which were used under license for the current study, and so are not publicly available. Data are however available from the authors upon reasonable request and with permission of E-Med4All Europe Ltd.

**Acknowledgments:** The authors express their special thanks to Dániel Sándor Veres, for his guidance in data analysis, and also to all volunteers who participated in the study.

**Conflicts of Interest:** F.A., D.K., K.I.L., B.S., L.S., Z.M. and S.K. are in financial terms with E-Med4All Europe Ltd. (D.K., B.S. and S.K. as co-owners, F.A. as employee, K.I.L., L.S. and Z.M. as subcontractors).

## References

1. Shaffer, F.; Ginsberg, J.P. An Overview of Heart Rate Variability Metrics and Norms. *Front. Public Health* **2017**, *5*, 258. [CrossRef]
2. Mccraty, R.; Shaffer, F. Heart Rate Variability: New Perspectives on Physiological Mechanisms, Assessment of Self-regulatory Capacity, and Health Risk. *Glob. Adv. Health Med.* **2015**, *4*, 46–61. [CrossRef]
3. Gevirtz, R.; Lehrer, P.; Schwarz, M. *Cardiorespiratory Biofeedback a Pract. Guid*, 4th ed; Schwartz, M., Andrasik, F., Eds.; The Guilford Press: New York, NY, USA, 2016; pp. 196–213.
4. Beckers, F.; Verheyden, B.; Aubert, A.E. Aging and nonlinear heart rate control in a healthy population. *Am. J. Physiol. Circ. Physiol.* **2006**, *290*, H2560–H2570. [CrossRef] [PubMed]
5. Task Force of the European Society of Cardiology and the North American Society of Pacing and Electrophysiology. Heart rate variability: Standards of measurement, physiological interpretation and clinical use. *Circulation* **1996**, *93*, 1043–1065. [CrossRef]
6. Shaffer, F.; McCraty, R.; Zerr, C.L. A healthy heart is not a metronome: An integrative review of the heart's anatomy and heart rate variability. *Front. Psychol.* **2014**, *5*, 1040. [CrossRef] [PubMed]
7. McNames, J.; Aboy, M. Reliability and accuracy of heart rate variability metrics versus ECG segment duration. *Med. Biol. Eng. Comput.* **2006**, *44*, 747–756. [CrossRef] [PubMed]
8. Zulfiqar, U.; Jurivich, D.A.; Gao, W.; Singer, D.H. Relation of High Heart Rate Variability to Healthy Longevity. *Am. J. Cardiol.* **2010**, *105*, 1181–1185. [CrossRef] [PubMed]

9. Ernst, G. Heart-Rate Variability—More than Heart Beats? *Front. Public Health* **2017**, *5*, 240. [CrossRef] [PubMed]
10. Billman, G.E.; Huikuri, H.V.; Sacha, J.; Etrimmel, K. An introduction to heart rate variability: Methodological considerations and clinical applications. *Front. Physiol.* **2015**, *6*, 55. [CrossRef]
11. Jarczok, M.N.; Kleber, M.; Koenig, J.; Loerbroks, A.; Herr, R.M.; Hoffmann, K.; Fischer, J.E.; Benyamini, Y.; Thayer, J.F. Investigating the Associations of Self-Rated Health: Heart Rate Variability Is More Strongly Associated than Inflammatory and Other Frequently Used Biomarkers in a Cross Sectional Occupational Sample. *PLoS ONE* **2015**, *10*, e0117196. [CrossRef]
12. Lampert, R.; Bremner, J.D.; Su, S.; Miller, A.; Lee, F.; Cheema, F.; Goldberg, J.; Vaccarino, V. Decreased heart rate variability is associated with higher levels of inflammation in middle-aged men. *Am. Heart J.* **2008**, *156*, 759.e1–759.e7. [CrossRef]
13. Akselrod, S.; Gordon, D.; Ubel, A.F.; Shannon, D.C.; Berger, A.C.; Cohen, R.J. Power spectrum analysis of heart rate fluctuation: A quantitative probe of beat-to-beat cardiovascular control. *Science* **1981**, *213*, 220–222. [CrossRef]
14. Musialik-Łydka, A.; Sredniawa, B.; Pasyk, S. Heart rate variability in heart failure. *Kardiol. Pol.* **2003**, *58*, 14–16.
15. Coviello, I.; Pinnacchio, G.; Laurito, M.; Stazi, A.; Battipaglia, I.; Barone, L.; Mollo, R.; Russo, G.; Villano, A.; Sestito, A.; et al. Prognostic Role of Heart Rate Variability in Patients with ST-Segment Elevation Acute Myocardial Infarction Treated by Primary Angioplasty. *Cardiology* **2013**, *124*, 63–70. [CrossRef] [PubMed]
16. Mäkikallio, T.H.; Høiber, S.; Køber, L.; Torp-Pedersen, C.; Peng, C.-K.; Goldberger, A.L.; Huikuri, H.V. Fractal analysis of heart rate dynamics as a predictor of mortality in patients with depressed left ventricular function after acute myocardial infarction. *Am. J. Cardiol.* **1999**, *83*, 836–839. [CrossRef]
17. Girgis, I.; Chakko, S.; De Marchena, E.; Jara, C.; Diaz, P.; Castellanos, A.; Myerburg, R.J. Effect of clonidine on heart rate variability in congestive heart failure. *Am. J. Cardiol.* **1998**, *82*, 335–337. [CrossRef]
18. Pousset, F.; Copie, X.; Lechat, P.; Jaillon, P.; Boissel, J.-P.; Hetzel, M.; Fillette, F.; Remme, W.; Guize, L.; Le Heuzey, J.-Y. Effects of bisoprolol on heart rate variability in heart failure. *Am. J. Cardiol.* **1996**, *77*, 612–617. [CrossRef]
19. Kienzle, M.G.; Ferguson, D.W.; Birkett, C.L.; Myers, G.A.; Berg, W.J.; Mariano, D. Clinical, hemodynamic and sympathetic neural correlates of heart rate variability in congestive heart failure. *Am. J. Cardiol.* **1992**, *69*, 761–767. [CrossRef]
20. Malik, M.; Farrell, T.; Camm, A. Circadian rhythm of heart rate variability after acute myocardial infarction and its influence on the prognostic value of heart rate variability. *Am. J. Cardiol.* **1990**, *66*, 1049–1054. [CrossRef]
21. Lombardi, F.; Sandrone, G.; Spinnler, M.T.; Torzillo, D.; Lavezzaro, G.C.; Brusca, A.; Malliani, A. Heart rate variability in the early hours of an acute myocardial infarction. *Am. J. Cardiol.* **1996**, *77*, 1037–1044. [CrossRef]
22. Karp, E.; Shiyovich, A.; Zahger, D.; Gilutz, H.; Grosbard, A.; Katz, A. Ultra-Short-Term Heart Rate Variability for Early Risk Stratification following Acute ST-Elevation Myocardial Infarction. *Cardiology* **2009**, *114*, 275–283. [CrossRef]
23. Casolo, G.; Balli, E.; Taddei, T.; Amuhasi, J.; Gori, C. Decreased spontaneous heart rate variability in congestive heart failure. *Am. J. Cardiol.* **1989**, *64*, 1162–1167. [CrossRef]
24. Manno, G.; Novo, G.; Novo, S.; Corrado, E.; Coppola, G. Alteration of Heart Rate Variability as an Early Predictor of Cardiovascular Events: A Look at Current Evidence. *Am. J. Cardiol.* **2020**, *125*, 831–833. [CrossRef]
25. Stein, P.K.; Domitrovich, P.P.; Huikuri, H.V.; Kleiger, R.E. Traditional and Nonlinear Heart Rate Variability Are Each Independently Associated with Mortality after Myocardial Infarction. *J. Cardiovasc. Electrophysiol.* **2005**, *16*, 13–20. [CrossRef] [PubMed]
26. Stein, P.K.; Reddy, A. Non-Linear Heart Rate Variability and Risk Stratification in Cardiovascular Disease. *Indian Pacing Electrophysiol. J.* **2005**, *5*, 210–220. [PubMed]
27. Mejía-Mejía, E.; Budidha, K.; Abay, T.Y.; May, J.M.; Kyriacou, P.A. Heart Rate Variability (HRV) and Pulse Rate Variability (PRV) for the Assessment of Autonomic Responses. *Front. Physiol.* **2020**, *11*, 779. [CrossRef] [PubMed]
28. Mejía-Mejía, E.; May, J.M.; Torres, R.; Kyriacou, A.P. Pulse rate variability in cardiovascular health: A review on its applications and relationship with heart rate variability. *Physiol. Meas.* **2020**, *41*, 07TR01. [CrossRef]
29. Yuda, E.; Yamamoto, K.; Yoshida, Y.; Hayano, J. Differences in pulse rate variability with measurement site. *J. Physiol. Anthr.* **2020**, *39*, 1–6. [CrossRef] [PubMed]
30. Nardelli, M.; Vanello, N.; Galperti, G.; Greco, A.; Scilingo, E.P. Assessing the Quality of Heart Rate Variability Estimated from Wrist and Finger PPG: A Novel Approach Based on Cross-Mapping Method. *Sensors* **2020**, *20*, 3156. [CrossRef] [PubMed]
31. Selvaraj, N.; Jaryal, A.; Santhosh, J.; Deepak, K.K.; Anand, S. Assessment of heart rate variability derived from finger-tip photoplethysmography as compared to electrocardiography. *J. Med. Eng. Technol.* **2008**, *32*, 479–484. [CrossRef]
32. Carrasco, S.; Gonzàlez, R.; Jiménez, J.; Román, R.; Medina, V.; Azpiroz, J. Comparison of the heart rate variability parameters obtained from the electrocardiogram and the blood pressure wave. *J. Med. Eng. Technol.* **1998**, *22*, 195–205. [CrossRef]
33. Lu, S.; Zhao, H.; Ju, K.; Shin, K.; Lee, M.; Shelley, K.; Chon, K.H. Can Photoplethysmography Variability Serve as an Alternative Approach to Obtain Heart Rate Variability Information? *J. Clin. Monit.* **2008**, *22*, 23–29. [CrossRef] [PubMed]
34. Lu, G.; Yang, F.; Taylor, J.A.; Stein, J.F. A comparison of photoplethysmography and ECG recording to analyse heart rate variability in healthy subjects. *J. Med. Eng. Technol.* **2009**, *33*, 634–641. [CrossRef] [PubMed]
35. Srinivas, K.; Reddy, L.R.G.; Srinivas, R. Estimation of heart rate variability from peripheral pulse wave using PPG sensor. In *IFMBE Proceedings*; Springer: Berlin/Heidelberg, Germany, 2007; pp. 325–328. [CrossRef]
36. Giardino, N.D.; Lehrer, P.M.; Edelberg, R. Comparison of finger plethysmograph to ECG in the measurement of heart rate variability. *Psychophysiology* **2002**, *39*, 246–253. [CrossRef] [PubMed]
37. Khandoker, A.H.; Karmakar, C.K.; Palaniswami, M. Comparison of pulse rate variability with heart rate variability during obstructive sleep apnea. *Med. Eng. Phys.* **2011**, *33*, 204–209. [CrossRef]

38. Bolanos, M.; Nazeran, H.; Haltiwanger, E. Comparison of Heart Rate Variability Signal Features Derived from Electrocardiography and Photoplethysmography in Healthy Individuals. *Conf. Proc. IEEE Eng. Med. Biol. Soc.* **2006**, *2006*, 4289–4294. [CrossRef]
39. Gil, E.; Orini, M.; Bailón, R.; Vergara, J.M.; Mainardi, L.; Laguna, P. Photoplethysmography pulse rate variability as a surrogate measurement of heart rate variability during non-stationary conditions. *Physiol. Meas.* **2010**, *31*, 1271–1290. [CrossRef]
40. Kulin, D.; Antali, F.; Kulin, S.; Wafa, D.; Lucz, K.I.; Veres, D.S.; Miklós, Z. Preclinical Assessment of a Novel Cardiovascular Telemedicine System. *Appl. Sci.* **2020**, *10*, 7977. [CrossRef]
41. Tarvainen, M.P.; Niskanen, J.-P.; Lipponen, J.; Ranta-Aho, P.O.; Karjalainen, P. Kubios HRV—Heart rate variability analysis software. *Comput. Methods Programs Biomed.* **2014**, *113*, 210–220. [CrossRef]
42. Peng, C.; Havlin, S.; Stanley, H.E.; Goldberger, A.L. Quantification of scaling exponents and crossover phenomena in nonstationary heartbeat time series. *Chaos Interdiscip. J. Nonlinear Sci.* **1995**, *5*, 82–87. [CrossRef]
43. Huikuri, H.V.; Mäkikallio, T.H.; Peng, C.-K.; Goldberger, A.L.; Hintze, U.; Møller, M. Fractal Correlation Properties of R-R Interval Dynamics and Mortality in Patients with Depressed Left Ventricular Function After an Acute Myocardial Infarction. *Circulation* **2000**, *101*, 47–53. [CrossRef] [PubMed]
44. Ciccone, A.B.; Siedlik, J.A.; Wecht, J.M.; Deckert, J.A.; Nguyen, N.D.; Weir, J.P. Reminder: RMSSD and SD1 are identical heart rate variability metrics. *Muscle Nerve* **2017**, *56*, 674–678. [CrossRef]
45. Penzel, T.; Kantelhardt, J.; Grote, L.; Peter, J.; Bunde, A. Comparison of detrended fluctuation analysis and spectral analysis for heart rate variability in sleep and sleep apnea. *IEEE Trans. Biomed. Eng.* **2003**, *50*, 1143–1151. [CrossRef]
46. Piskorski, J.; Guzik, P. Geometry of the Poincaré plot of RRintervals and its asymmetry in healthy adults. *Physiol. Meas.* **2007**, *28*, 287–300. [CrossRef]
47. Piskorski, J.; Guzik, P. Asymmetric properties of long-term and total heart rate variability. *Med. Biol. Eng. Comput.* **2011**, *49*, 1289–1297. [CrossRef]
48. Brennan, M.; Palaniswami, M.; Kamen, P. Do existing measures of Poincare plot geometry reflect nonlinear features of heart rate variability? *IEEE Trans. Biomed. Eng.* **2001**, *48*, 1342–1347. [CrossRef]
49. Altman, D.G.; Bland, J.M. Measurement in Medicine: The Analysis of Method Comparison Studies. *J. R. Stat. Soc. Ser. D Stat.* **1983**, *32*, 307–317. [CrossRef]
50. Bland, J.M.; Altman, D.G. Statistical methods for assessing agreement between two methods of clinical measurement. *Lancet* **1986**, *1*, 307–310. [CrossRef]
51. Zygmunt, A.; Stanczyk, J. Methods of evaluation of autonomic nervous system function. *Arch. Med. Sci.* **2010**, *1*, 11–18. [CrossRef] [PubMed]
52. Subhani, A.R.; Likun, X.; Malik, A. Association of Autonomic Nervous System and EEG Scalp Potential During Playing 2D Grand Turismo 5. *Annu. Int. Conf. IEEE Eng. Med. Biol. Soc.* **2012**, *2012*, 3420–3423. [PubMed]
53. Stancin, I.; Cifrek, M.; Jovic, A. A Review of EEG Signal Features and Their Application in Driver Drowsiness Detection Systems. *Sensors* **2021**, *21*, 3786. [CrossRef]
54. Schäfer, A.; Vagedes, J. How accurate is pulse rate variability as an estimate of heart rate variability? *Int. J. Cardiol.* **2013**, *166*, 15–29. [CrossRef]
55. Hernández-Vicente, A.; Hernando, D.; Marín-Puyalto, J.; Vicente-Rodríguez, G.; Garatachea, N.; Pueyo, E.; Bailón, R. Validity of the Polar H7 Heart Rate Sensor for Heart Rate Variability Analysis during Exercise in Different Age, Body Composition and Fitness Level Groups. *Sensors* **2021**, *21*, 902. [CrossRef] [PubMed]
56. Natarajan, A.; Pantelopoulos, A.; Emir-Farinas, H.; Natarajan, P. Heart rate variability with photoplethysmography in 8 million individuals: A cross-sectional study. *Lancet Digit. Health* **2020**, *2*, e650–e657. [CrossRef]
57. Shi, P.; Hu, S.; Zhu, Y. A Preliminary Attempt to Understand Compatibility of Photoplethysmographic Pulse Rate Variability with Electrocardiogramic Heart Rate Variability. *J. Med. Biol. Eng.* **2008**, *28*, 173–180.
58. Hayano, J.; Barros, A.K.; Kamiya, A.; Ohte, N.; Yasuma, F. Assessment of pulse rate variability by the method of pulse frequency demodulation. *Biomed. Eng. Online* **2005**, *4*, 62. [CrossRef]
59. Rauh, R.; Limley, R.; Bauer, R.-D.; Radespiel-Tröger, M.; Mueck-Weymann, M. Comparison of heart rate variability and pulse rate variability detected with photoplethysmography. *SPIE Proc.* **2004**, 115–126. [CrossRef]
60. Dawson, C.; Panerai, R.; Potter, J. Potter Should one use electrocardiographic or Finapres-derived pulse intervals for calculation of cardiac baroreceptor sensitivity? *Blood Press. Monit.* **1998**, *3*, 315–320.
61. Suhrbier, A.; Heringer, R.; Walther, T.; Malberg, H.; Wessel, N. Comparison of three methods for beat-to-beat-interval extraction from continuous blood pressure and electrocardiogram with respect to heart rate variability analysis. *Biomed. Tech. Eng.* **2006**, *51*, 70–76. [CrossRef]
62. Selvaraj, N.; Santhosh, J.; Anand, S. Feasibility of Photoplethymographic Signal for Assessment of Autonomic Response using Heart Rate Variability Analysis. In *IFMBE Proceedings*; Springer: Berlin/Heidelberg, Germany, 2007; Volume 15, pp. 391–395. [CrossRef]
63. Constant, I.; Laude, D.; Murat, I.; Elghozi, J.-L. Pulse rate variability is not a surrogate for heart rate variability. *Clin. Sci.* **1999**, *97*, 391. [CrossRef]
64. Nilsson, L.; Goscinski, T.; Kalman, S.; Lindberg, L.-G.; Johansson, A. Combined photoplethysmographic monitoring of respiration rate and pulse: A comparison between different measurement sites in spontaneously breathing subjects. *Acta Anaesthesiol. Scand.* **2007**, *51*, 1250–1257. [CrossRef]

65. Nardelli, M.; Greco, A.; Bolea, J.; Valenza, G.; Scilingo, E.P.; Bailon, R. Reliability of Lagged Poincaré Plot Parameters in Ultrashort Heart Rate Variability Series: Application on Affective Sounds. *IEEE J. Biomed. Health Inform.* **2017**, *22*, 741–749. [CrossRef] [PubMed]
66. Nussinovitch, U.; Elishkevitz, K.P.; Katz, K.; Nussinovitch, M.; Segev, S.; Volovitz, B.; Nussinovitch, N. Reliability of Ultra-Short ECG Indices for Heart Rate Variability. *Ann. Noninvasive Electrocardiol.* **2011**, *16*, 117–122. [CrossRef] [PubMed]
67. Pecchia, L.; Castaldo, R.; Montesinos, L.; Melillo, P. Are ultra-short heart rate variability features good surrogates of short-term ones? State-of-the-art review and recommendations. *Health Technol. Lett.* **2018**, *5*, 94–100. [CrossRef] [PubMed]
68. Benichou, T.; Pereira, B.; Mermillod, M.; Tauveron, I.; Pfabigan, D.; Maqdasy, S.; Dutheil, F. Heart rate variability in type 2 diabetes mellitus: A systematic review and meta–analysis. *PLoS ONE* **2018**, *13*, e0195166. [CrossRef] [PubMed]
69. Cha, S.-A.; Park, Y.-M.; Yun, J.-S.; Lee, S.-H.; Ahn, Y.-B.; Kim, S.-R.; Ko, S.-H. Time-and frequency-domain measures of heart rate variability predict cardiovascular outcome in patients with type 2 diabetes. *Diabetes Res. Clin. Pr.* **2018**, *143*, 159–169. [CrossRef] [PubMed]
70. Vinik, A.I.; Ziegler, D. Diabetic Cardiovascular Autonomic Neuropathy. *Circulation* **2007**, *115*, 387–397. [CrossRef]
71. Tarvainen, M.P.; Laitinen, T.P.; Lipponen, J.; Cornforth, D.J.; Jelinek, H.F. Cardiac Autonomic Dysfunction in Type 2 Diabetes â€“ Effect of Hyperglycemia and Disease Duration. *Front. Endocrinol.* **2014**, *5*, 130. [CrossRef]
72. Geiger, B.C.; Kubin, G. *Information Loss in Deterministic Signal Processing Systems*; Springer: Singapore, 2018.
73. Potapov, P. On the loss of information in PCA of spectrum-images. *Ultramicroscopy* **2017**, *182*, 191–194. [CrossRef]
74. Rabcan, J.; Levashenko, V.; Zaitseva, E.; Kvassay, M.; Subbotin, S. Application of Fuzzy Decision Tree for Signal Classification. *IEEE Trans. Ind. Inform.* **2019**, *15*, 5425–5434. [CrossRef]
75. Biswal, M.; Dash, P.K. Measurement and Classification of Simultaneous Power Signal Patterns With an S-Transform Variant and Fuzzy Decision Tree. *IEEE Trans. Ind. Inform.* **2013**, *9*, 1819–1827. [CrossRef]
76. Ley, D. Approximating process knowledge and process thinking: Acquiring workflow data by domain experts. In Proceedings of the 2011 IEEE International Conference on Systems, Man, and Cybernetics, Anchorage, AK, USA, 9–12 October 2011; Volume 2011, pp. 3274–3279.
77. Gueorguieva, N.; Valova, I.; Georgiev, G. Fuzzyfication of principle component analysis for data dimensionalty reduction. In Proceedings of the 2016 IEEE International Conference on Fuzzy Systems (FUZZ-IEEE), Vancouver, BC, Canada, 24–29 July 2016; Volume 2016, pp. 1818–1825.
78. Tsipouras, M.G.; Exarchos, T.P.; Fotiadis, D.I. A methodology for automated fuzzy model generation. *Fuzzy Sets Syst.* **2008**, *159*, 3201–3220. [CrossRef]
79. Rabcan, J.; Levashenko, V.; Zaitseva, E.; Kvassay, M. Review of Methods for EEG Signal Classification and Development of New Fuzzy Classification-Based Approach. *IEEE Access* **2020**, *8*, 189720–189734. [CrossRef]

# Supplementary Material

**Supplementary Figure S1**: *Bland-Altman plots of HRV/PRV parameters computed by the Kubios Premium algorithm from 2-min long ECG (indicated as 'parameter name-ECG') and PPG (indicated as 'parameter name-PPG') recordings captured in healthy individuals under resting conditions.*

**A**

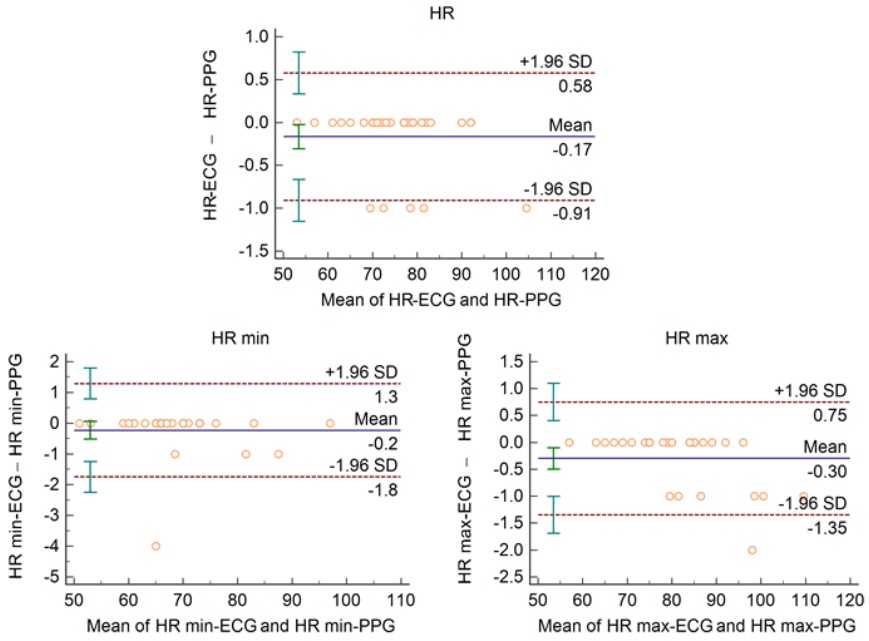


**B**

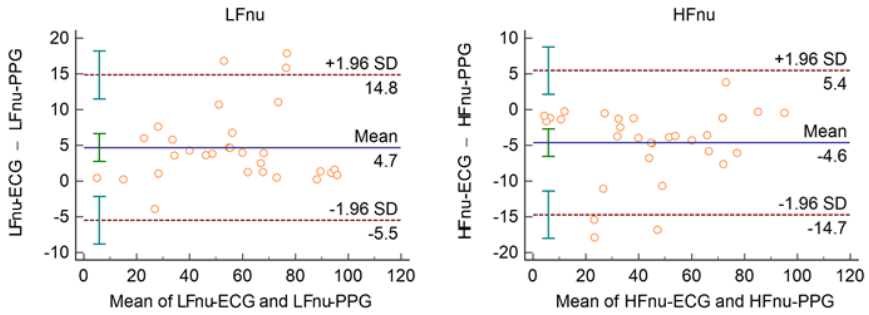


***A:*** *Time-domain parameters: HR (mean heart rate), HR min (minimum heart rate), HR max (maximum heart rate)* ***B:*** *Frequency-domain parameters: LFnu (relative power of the low-frequency band), HFnu (relative power of the high-frequency band). Bias is calculated as the mean of differences (indicated as 'Mean' - blue solid line) and is presented with 95% confidence intervals (green) and +/- 1.96 standard deviations (SD) and their confidence intervals.*

**Supplementary Figure S2**: *Bland-Altman plots of HRV/PRV parameters computed by the Kubios Premium algorithm from 2-min long ECG (indicated as 'parameter name-ECG') and PPG (indicated as 'parameter name-PPG') recordings obtained from healthy individuals during cold pressor test.*

**A**

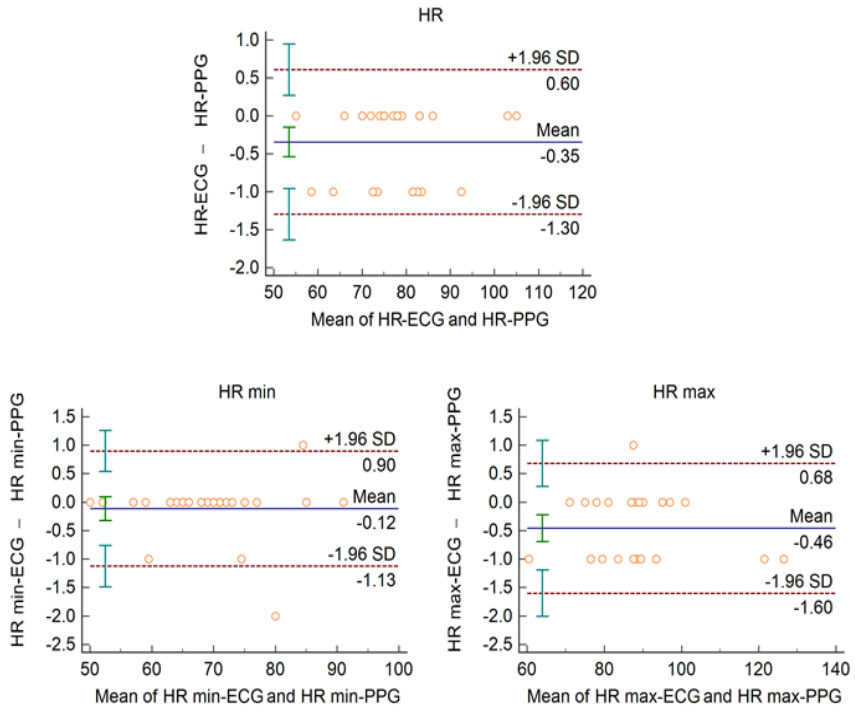


**B**

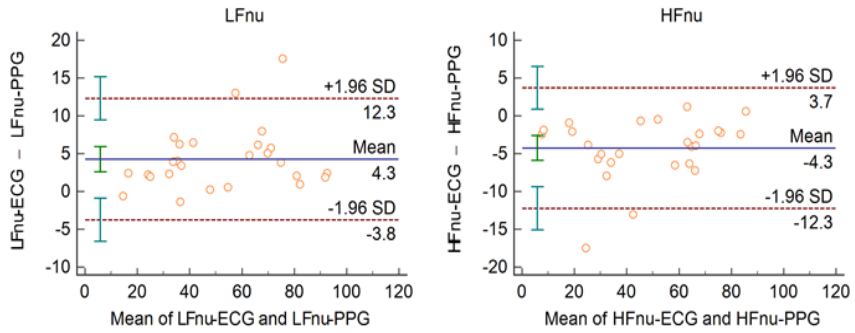


***A**: Time-domain parameters: HR (mean heart rate), HR min (minimum heart rate), HR max (maximum heart rate) **B**: Frequency-domain parameters: LFnu (relative power of the low-frequency band), HFnu (relative power of the high-frequency band). Bias is calculated as the mean of differences (indicated as 'Mean' - blue solid line) and is presented with 95% confidence intervals (green) and +/- 1.96 standard deviations (SD) and their confidence intervals.*

.

**Supplementary Figure S3:** *Bland-Altman plots of HRV/PRV parameters computed by the Kubios Premium algorithm from 2-min long ECG (indicated as 'parameter name-ECG') and PPG (indicated s 'parameter name-PPG') recordings obtained from diabetic patients under resting conditions.*

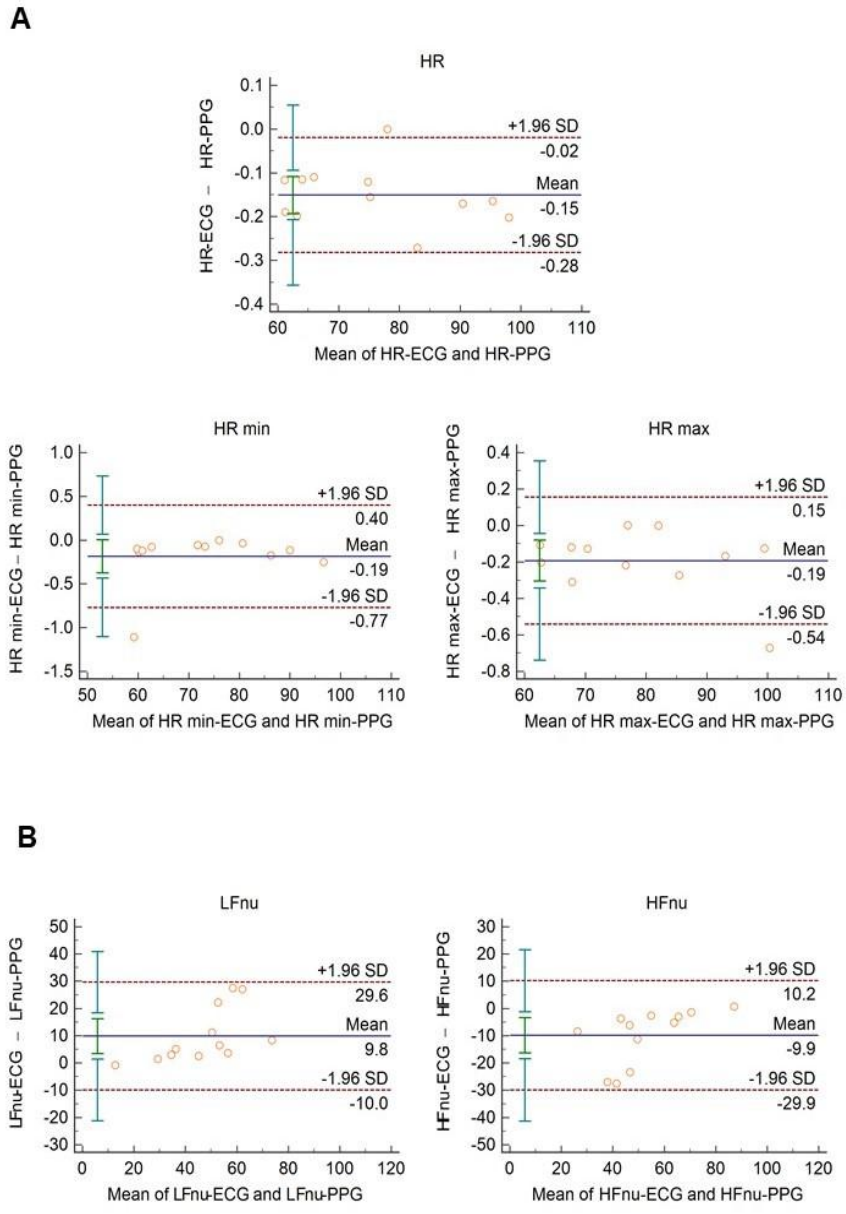


***A****: Time-domain parameters: HR (mean heart rate), HR min (minimum heart rate), HR max (maximum heart rate)* ***B****: Frequency-domain parameters: LFnu (relative power of the low-frequency band), HFnu (relative power of the high-frequency band). Bias is calculated as the mean of differences (indicated as 'Mean' - blue solid line) and is presented with 95% confidence intervals (green) and +/- 1.96 standard deviations (SD) and their confidence intervals.*

**Supplementary Figure S4**: *Bland-Altman plots of HRV/PRV parameters calculated by the SCN4ALL (indicated as 'parameter name-SCN4ALL') and the Kubios Premium HRV (indicated as 'parameter name-Kubios') algorithms from 2-min long PPG recordings captured in healthy individuals under resting conditions.*

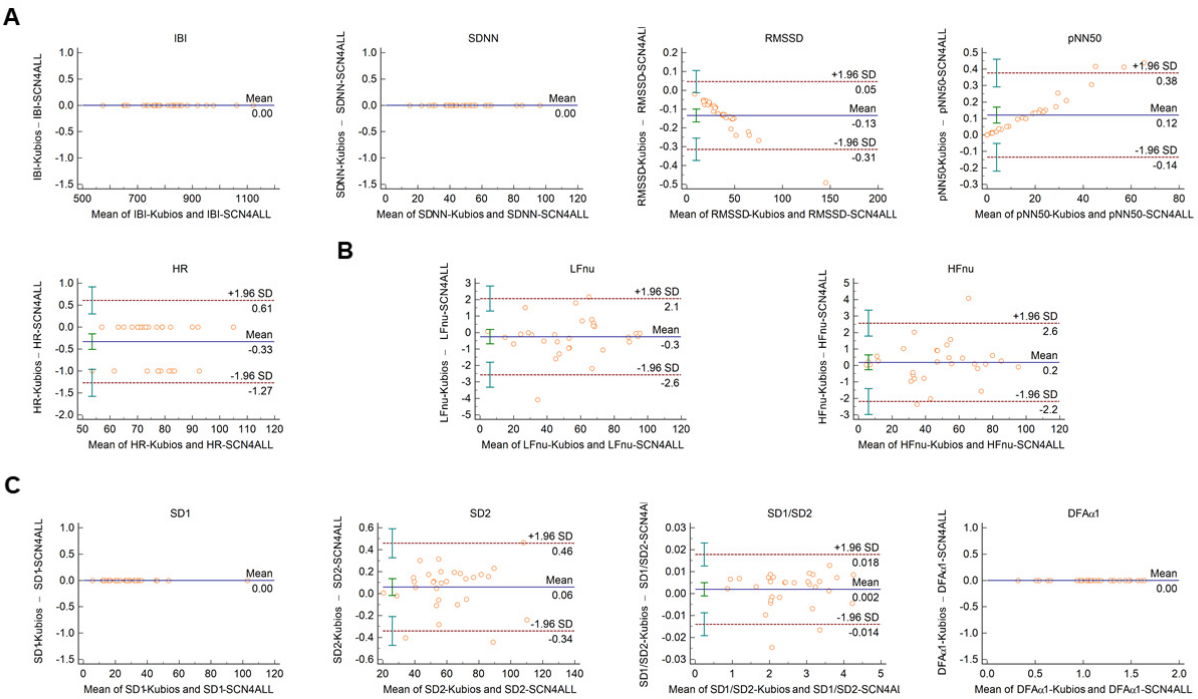


***A**: Time-domain parameters: IBI (interbeat interval), SDNN (the standard deviation of IBIs), RMSSD (the square root of the mean squared differences of successive IBIs), pNN50 (the proportion of differences of successive IBIs exceeding 50 ms), HR (mean heart rate). **B**. Frequency-domain parameters: LFnu (relative power of the low-frequency band), HFnu (relative power of the high-frequency band). **C:** Non-linear parameters: SD1 (Poincaré plot standard deviation perpendicular the line of identity), SD2 (Poincaré plot standard deviation along the line of identity), SD1/SD2 (ratio of SD1-to-SD2), DFAα1 (short term fluctuation slope obtained by detrended fluctuation analysis)*
*Bias is calculated as the mean of differences (indicated as 'Mean' - blue solid line) and is presented with 95% confidence intervals (green) and +/- 1.96 standard deviations (SD) and their confidence intervals.*

**Supplementary Figure S5**: *Bland-Altman plots of HRV/PRV parameters calculated by the SCN4ALL (indicated as 'parameter name-SCN4ALL') and the Kubios Premium HRV (indicated as 'parameter name-Kubios') algorithms from 2-min long PPG recordings obtained from healthy individuals during cold pressor test.*

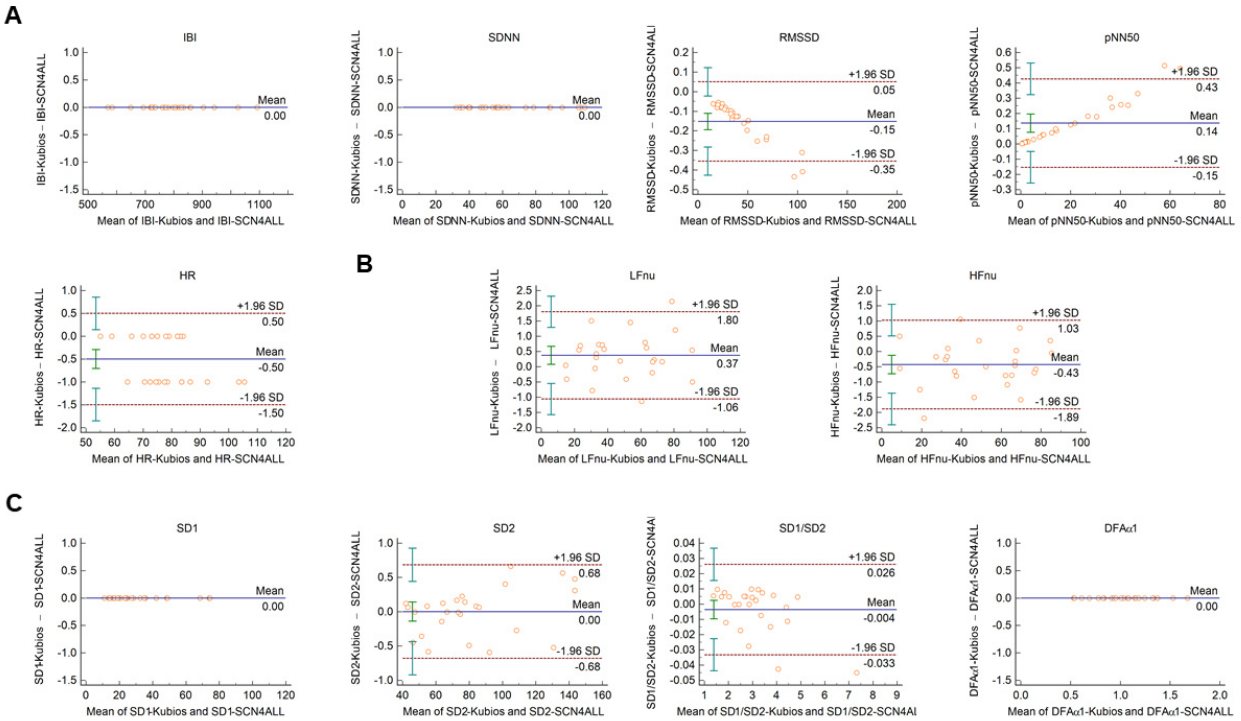


***A**: Time-domain parameters: IBI (interbeat interval), SDNN (the standard deviation of IBIs), RMSSD (the square root of the mean squared differences of successive IBIs), pNN50 (the proportion of differences of successive IBIs exceeding 50 ms), HR (mean heart rate). **B**. Frequency-domain parameters: LFnu (relative power of the low-frequency band), HFnu (relative power of the high-frequency band). **C:** Non-linear parameters: SD1 (Poincaré plot standard deviation perpendicular the line of identity), SD2 (Poincaré plot standard deviation along the line of identity), SD1/SD2 (ratio of SD1-to-SD2), DFAα1 (short term fluctuation slope obtained by detrended fluctuation analysis)*
*Bias is calculated as the mean of differences (indicated as 'Mean' - blue solid line) and is presented with 95% confidence intervals (green) and +/- 1.96 standard deviations (SD) and their confidence intervals.*

**Supplementary Figure S6:** *Bland-Altman plots of HRV/PRV parameters calculated by the SCN4ALL (indicated as 'parameter name-SCN4ALL') and the Kubios Premium HRV (indicated as 'parameter name-Kubios') algorithms from 2-min long PPG recordings obtained from diabetic patients under resting conditions.*

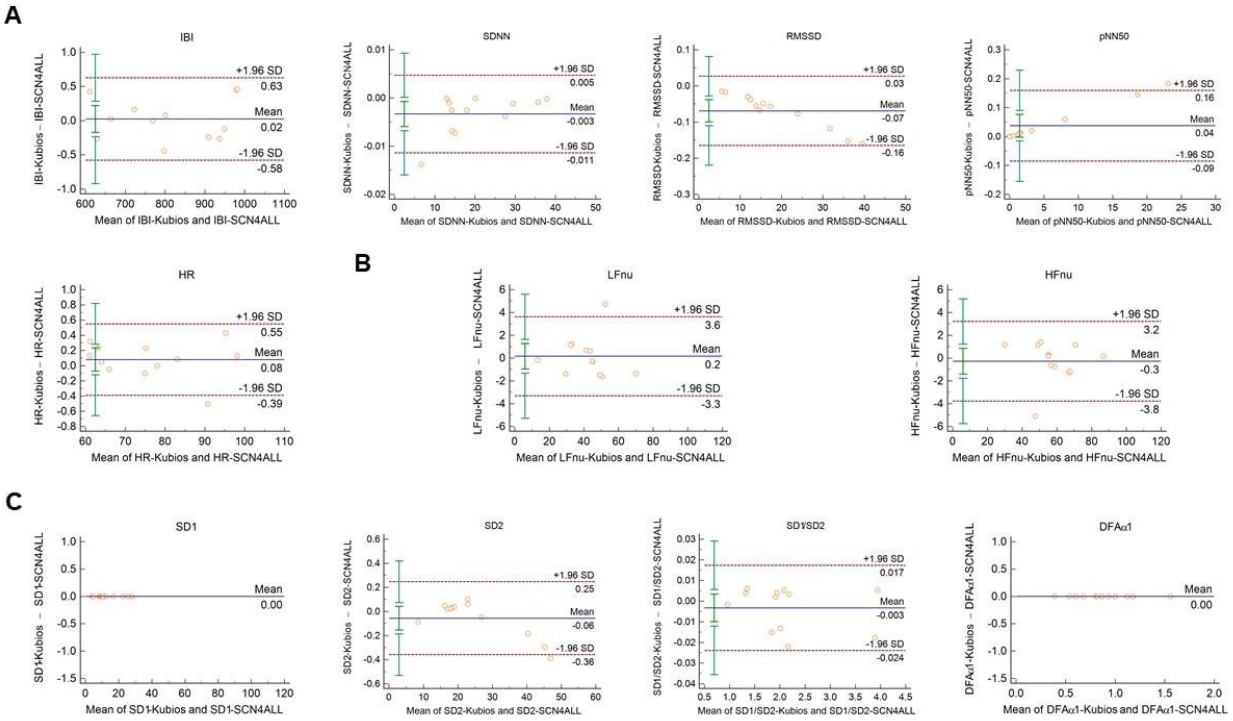


***A**: Time-domain parameters: IBI (interbeat interval), SDNN (the standard deviation of IBIs), RMSSD (the square root of the mean squared differences of successive IBIs), pNN50 (the proportion of differences of successive IBIs exceeding 50 ms), HR (mean heart rate). **B**. Frequency-domain parameters: LFnu (relative power of the low-frequency band), HFnu (relative power of the high-frequency band). **C:** Non-linear parameters: SD1 (Poincaré plot standard deviation perpendicular the line of identity), SD2 (Poincaré plot standard deviation along the line of identity), SD1/SD2 (ratio of SD1-to-SD2), DFAα1 (short term fluctuation slope obtained by detrended fluctuation analysis)*
*Bias is calculated as the mean of differences (indicated as 'Mean' - blue solid line) and is presented with 95% confidence intervals (green) and +/- 1.96 standard deviations (SD) and their confidence intervals.*

Antali *et al. Artery Research* (2025) 31:5
https://doi.org/10.1007/s44200-025-00068-w

Artery Research

RESEARCH ARTICLE Open Access

# Evaluation of the Age Dependence of Conventional and Novel Photoplethysmography Parameters

Flóra Antali[1*], Dániel Kulin[1,2], Sándor Kulin[2] and Zsuzsanna Miklós[1,3]

## Abstract

**Background** Cardiovascular (CV) mortality increases with age partly due to physiological ageing of the CV system. Early vascular ageing raises CV risks. Personalizing CV risk assessment by defining CV age could reduce CV events. Photoplethysmography (PPG), which analyses the peripheral arterial pulse wave, may be an effective method for estimating CV age. Ageing index (AGEi) and some other PPG parameters were proven to have age correlation; however, the age dependence of many other pulse wave parameters remains unclear. We aimed to identify age correlations of PPG indices and pulse rate variability (PRV) parameters including a few novel parameters which were calculated to further investigate the various aspects of ageing.

Our study included 118 healthy (M/F: 53/65, mean age: 31.8 ± 11.8 SD) volunteers for PPG parameter calculation and 106 (M/F: 44/62, mean age: 32.6 ± 12.2 SD) for PRV parameters (age: 19–74). 2-min pulse wave recording was obtained using a pulse oximeter. An automated, proprietary software evaluated PPG and PRV parameter values, which were compared with chronological age (Pearson correlation and non-linear analysis).

**Results** PPG parameters describing various time-dependent aspects of cardiac ejection positively correlated with age, while those indicating arterial elasticity showed negative correlation. Composite PPG parameters proposed as indicators of CV health and fitness had negative, non-linear correlation. Most PRV parameters exhibited negative correlation, indicating reduced adaptive capacity due to ageing ($p < 0.05$, $|r| > 0.3$).

**Conclusions** PPG-based pulse waveform analysis provides a wide range of age-related parameters which display different patterns of age correlation, making it a promising method for estimating cardiovascular age. Future studies will include subjects with vascular ageing conditions beyond physiological values (e.g., hypertension, heart failure, coronary artery disease).

**Keywords** Photoplethysmography, Vascular ageing, Pulse wave analysis, Pulse rate variability

## 1 Introduction

Cardiovascular (CV) diseases, including atherosclerosis and stroke are major public health challenges, consistently ranking among the leading causes of death worldwide in recent decades, especially in the elderly population [1, 2]. Age-related phenotypic alterations in the CV system, and more importantly their accelerated development brought about by CV risk factors, are among the most relevant (patho)physiological changes that drive these diseases [3, 4]. Therefore, identifying

*Correspondence:
Flóra Antali
antali.flora@gmail.com
[1] Institute of Translational Medicine, Semmelweis University, Tűzoltó Utca 37-49, Budapest 1094, Hungary
[2] E-Med4All Europe Ltd., Bécsi Út 85, Budapest 1036, Hungary
[3] National Korányi Institute for Pulmonology, Korányi Frigyes Út 1, Budapest 1122, Hungary

new, affordable biomarkers that reflect (CV) aging is critical for improving treatments and preventive strategies.

Peripheral pulse wave analysis may offer a valuable method for monitoring CV health and predicting disease progression [5, 6]. Calculating heart rate from continuous pulse wave recordings may have relevance in diagnostics, as pulse rate variability (PRV) is an important indicator of various diseases [7–9]. Beyond PRV, the morphological characteristics of pulse waves have yielded considerable attention, with numerous studies suggesting that these parameters may be associated with CV disease states such as atherosclerosis and heart failure [5, 10, 11].

Photoplethysmography (PPG) is a simple, easily accessible, and highly repeatable method for real-time monitoring of pulse waves [12]. This non-invasive technique involves illuminating the skin and tissues below, typically the finger, with an LED and measuring the intensity of the reflected or transmitted light, which corresponds to pressure changes in the vascular system. Importantly, PPG has no known adverse effects [13].

The promising results from previous studies suggest that PPG-based pulse wave analysis could gain traction in CV diagnostics and home monitoring in the near future [14]. While it holds potential as a tool for assessing CV aging, its broader use is constrained by the limited investigation of age-related correlations in most PPG-derived parameters. Although some parameters have been linked to age-related changes, most studies have focused on the age dependence of individual or a few selected parameters, leaving the majority unexplored [6, 15–17].

However, a combination of parameters or composite measures derived from multiple parameters might better capture age-related changes than single parameters alone. PPG-based monitoring devices, equipped with advanced algorithms, enable the simultaneous assessment and complex analysis of numerous parameters [5, 18]. Consequently, research aimed at identifying a set of simultaneously recorded PPG features with the strongest correlation to CV age could significantly enhance the potential of PPG-based pulse wave analysis. Additionally, most published studies have assumed linear age dependence of parameters [15–17], which may not accurately reflect reality. Many parameters could exhibit non-linear relationships with age, particularly in women, where CV changes accelerate after menopause.

The primary goal of our research was to identify age-dependent changes in a large set of simultaneously recorded pulse wave parameters, including PRV parameters, pulse morphology parameters and newly developed composite score parameters, aiming to establish the utility of PPG-based pulse wave analysis as a tool to assess CV aging. For this purpose, we utilized an efficient, automated software that enables accurate, rapid, and reproducible evaluation of large datasets; and a comprehensive database of pulse wave data from a healthy adult population was established. To better characterize age-dependent parameter changes, we used both linear and non-linear analyses to describe age-related trends.

## 2 Methods

Participants were required to meet specific inclusion criteria, including self-reported good physical and mental health, absence of CV disease, no use of CV medications, non-pregnancy, a BMI between 18 and 26 kg/m$^2$, non-smoker status, negligible alcohol consumption, and no reported history of chronic or cancerous diseases.

Subjects were primarily recruited from among the healthy employees, relatives of employees, and students of Semmelweis University. Recruitment was facilitated by the University's Occupational Health Service and social networking platforms. All tests were conducted in the laboratory facilities of Semmelweis University. The study protocol was designed in accordance with the Declaration of Helsinki and approved by the Semmelweis University Regional and Institutional Committee of Science and Research Ethics (approval number: 120/2018).

Participants provided informed consent and completed a health questionnaire, which collected personal and health-related data, including medical history, lifestyle, and medication use. Blood pressure (BP) was measured three times using an automatic sphygmomanometer. Subjects with systolic BP higher than 140, and/or diastolic BP exceeding 90 mmHg were excluded from the study. All data was recorded anonymously.

Pulse wave recordings were obtained using a Berry BM 1000B pulse oximeter placed on the right index finger. This non-invasive device, certified by the manufacturer, recorded pulse waves for 140 s while the participant remained seated and still. The pulse oximeter transmitted data via Bluetooth to a mobile application (SCN4ALL/HeartReader), developed by E-Med4All Europe Ltd. (Budapest, Hungary), which uploaded the recordings to a secure online database. The studies for the repeatability and reliability of the measurements, along with the detailed description of signal processing methods of the system have already been published [19, 20]. Briefly, the measurement takes 140 s to be completed. Due to filtering and preprocessing reasons discussed in detail by Kulin et al. [19], 120 s of the recording is used for further analysis. Parameters were defined for each individual cycle that met certain predefined signal quality criteria, and the average of these values was reported.

The proprietary software used for analysis identified fiducial points on the pulse wave, allowing for the calculation of both classical and novel pulse wave parameters (PPG parameters), including pulse rate variability (PRV

parameters) metrics. The primary criterion for selecting parameters was to choose those that, according to the literature, describe various aspects of CV function—such as temporal relationships, arterial elasticity, and autonomic function—and have previously been reported to correlate with CV age, mortality, and (severity) of various CV diseases. Table 1. shows the parameters and their descriptions.

The parameter values obtained from the pulse waveform analysis were compared with the age (in years) of the volunteers (JASP 0.19.1 software, JASP Team (2024)) using Pearson correlation and Generalised Additive Models (GAM) analysis (Google Colaboratory. Retrieved December 14, 2024, from https://colab.research.google.com/). GAM is an advanced statistical modelling method designed to capture both linear and non-linear relationships between variables. (see the 'Additional file1.docx' for a more detailed description of the model). A $p$ value of $<=0.05$ was accepted as significant throughout.

During the preparation of this work the author(s) used ChatGPT and Grammarly to improve the readability and find shorter expressions to fit word limit. After using these tools/services, the authors reviewed and edited the content as needed and took full responsibility for the content of the publication.

## 3 Results

Our study included 118 healthy (M/F: 53/65, mean age: 31.8 ± 11.8 SD) volunteers for PPG parameter calculation and 106 (M/F: 44/62, mean age: 32.6 ± 12.2 SD) for PRV parameters. Participants were aged between 19 and 74 years.

The relationship between age and CV function may encompass both linear and non-linear factors. To comprehensively evaluate this, we performed two distinct analyses: a Pearson correlation to assess linear associations and a GAM analysis to capture potential non-linear trends.

Tables 2. and 3. summarize the results of Pearson correlation and GAM analysis between PPG and PRV parameters and age.

### 3.1 Pearson Correlation Analysis

Among the conventional PPG morphology parameters that significantly correlated with age, AGEi (r = 0.485), SysAlpha (r = − 0.418), and d/a (r = − 0.376) (Fig. 1A) demonstrated the strongest age dependence. Additionally, time-related parameters of the PPG curve that characterize ejection-related ventricular activity, such as ET(PPG) (r = 0.589), Crest Time (r = 0.570), LVETi (r = 0.539), and the proprietary parameters eLVET1* (r = 0.548) and eLVET2* (r = 0.450), also exhibited strong correlations with age (Table 2., Fig. 2.).

Furthermore, age correlation was observed in other novel parameters, including DNi* (r = -0.517) and c-d incidence* (r = 0.419) (Fig. 1B). Finally, all proprietary score parameters demonstrated significant correlations with age: Heart Fitness Score (r = − 0.493), CV Health Score (r = − 0.450), and Total Score (r = − 0.301) ($p < 0.001$ for all cases).

Several of the PRV parameters exhibited a moderate, but significant negative correlation with age (Table 3. and Fig. 3.). The cTotalPower (r = − 0.325) (Fig. 3A) and cSDRR (r = − 0.401) parameters (Fig. 3B) exhibited the strongest age dependence ($p < 0.001$) among frequency-domain and time-domain measures, respectively. The age correlation of non-linear PRV parameters proved to be weaker, except for cSD2 (r = − 0.428).

### 3.2 GAM Analysis

The GAM analysis allowed the identification of non-linear trends. Similar to the Pearson correlation analysis, this analysis also found significant correlations ($p < 0.05$) between age and PPG parameters, except for Si and b/a parameters. Among the PRV parameters, cSDRR, cTotalPower, cHFpow and cSD2 were significantly correlated with age based on GAM analysis. The GAM analysis confirmed linear (for AGEi, LVETi, eLVET2*, DNi*, SysAlpha) or near-linear (for b/a, d/a, Ri, Si) relationship between most PPG parameters and age. However, for some parameters, a non-linear trend with age was observed.

All Score parameters demonstrated a clear non-linear decline, especially after the age of 40. (Fig. 4A and B). The eLVET1* and c-d incidence* parameters showed a moderate non-linear upward trend followed by a plateau.

Crest Time exhibited extreme non-linearity with multiple inflection points (Fig. 4C).

For PRV parameters, cTotalPower and cSDRR showed a clear linear decrease with age. The cMHR did not have a significant correlation with age (nor did it when Pearson correlation analysis was performed) (Fig. 4D).

## 4 Discussion

From a public health perspective, addressing the assessment and monitoring of CV ageing is crucial, as CV diseases continue to be the leading cause of mortality, particularly in older populations. As the global population ages, the demand for reliable, non-invasive methods to meet this need is increasing. Photoplethysmography (PPG) appears to be a promising tool in this regard, as it offers a simple but effective way to monitor CV function by pulse wave analysis. Although the age correlation of some PPG parameters has been investigated, the full scope of age-related changes in pulse wave characteristics is not yet fully evaluated. [21–23] This study, by

**Table 1** PPG and PRV parameter names and descriptions

| PPG/PRV parameters | Abbreviations/ parameter names | Descriptions |
|---|---|---|
| Stiffness index | Si | Si = h/ PTT (m/s); h is the height of the person in meters. PTT is the pulse transit time in seconds [6]. |
| b/a | b/a | The ratio of the first two inflection points of the second derivative of the pulse wave. Correlates with the elasticity of the large arteries and the contractility of the left ventricle [6]. |
| d/a | d/a | The ratio of the first and fourth inflection points of the second derivative of the pulse wave. Independent cardiovascular risk factor [6]. |
| Ageing-index | AGEi | The value derived from the second derivative of the pulse wave. AGEi = b-c-d-e/a [6]. |
| Reflection index | Ri | The ratio of the amplitude of the diastolic peak to the amplitude of the systolic peak [6]. |
| Systolic slope inclination | SysAlpha | The angle between the maximal inclination of systolic upstroke and the horizontal axis [37]. |
| c-d point detection ratio * | c-d incidence * | c-d point detection ratio specifies the percentage of those pulse cycles in the recording in which c and d points of the second derivative of the pulse wave curve are successfully identified by the algorithm over all identified heart cycles |
| Left ventricular ejection time index | LVETi | Left ventricular ejection time indexed for heart rate (LVETi) was calculated from sex-specific resting regression equations LVETi(male) = 1,7 × heart rate + ET, LVETi(female) = 1,6 × heart rate + ET [26]. |
| Dicrotic notch index * | DNi * | Describes the relative position of the diastolic peak to the dicrotic notch (the valley induced by the aortic valve closure before the diastolic peak) |
| Early left ventricular ejection time 1 and Early left ventricular ejection time 2 | eLVET1 *<br>eLVET2 * | The early left ventricular ejection time 1 and 2 are the two-time components of "Crest Time". eLVET1 is measured from the start of the period to the first peak of the first derivative of the pulse, whereas eLVET2 is defined as the time duration from the first peak of the first derivative PTG to the peak of the systolic wave |
| Crest Time | Crest Time | The time elapsed between the beginning of the period (foot) and the maximum systolic amplitude (peak) [6]. |
| Left ventricular ejection time | ET(PPG) | The ejection time is the time elapsed between the beginning of the pulse period and the aortic valve closure (dicrotic notch/e-point) [38]. |
| Score parameters: Scores were calculated based on the 30 + parameters derived from the proprietary analysis of the 2 min pulse-wave recording. The max. value is 100. Values below 70 might indicate that there is reason to evaluate details and to consult professionals for a more thorough health check | | |
| Scores * | Total Score * | Calculated on the basis of the all 30 + cardiovascular and pulse rate variability parameters derived from the proprietary analysis of the 2 min pulse-wave recording. The Total Score is the master of all the other sub-scores, which can help to identify stronger and weaker aspects of the subject's CV status/health |
| | CV Health Score * | Obtained from the parameters that correspond with the function of the heart and the condition and aging of the arteries |
| | Heart Fitness Score * | Certain pulse wave parameters are influenced by the athletic lifestyle and athletic capabilities of the subject, so these aspects are marked by this score. This score provides information mostly about the health level of the HEART |
| PRV Time-domain parameters | | |
| correctedMHR | cMHR | PRV Time-domain parameter. The mean heart rate. Corrected: see comment at "cTotal-Power" |

**Table 1** (continued)

| PPG/PRV parameters | Abbreviations/ parameter names | Descriptions |
|---|---|---|
| correctedMNN | cMRR | PRV Time-domain parameter. The mean normal-to-normal interbeat interval [39]. Corrected: see comment at "cTotalPower" |
| corrected SDNN | cSDRR | PRV Time-domain parameter. The standard deviation of the interbeat intervals (ms). Its value is influenced by all cyclic components affecting heart rate variability and can be considered a quasi-summative autonomic nervous system index. Corrected: see comment at "cTotalPower" [39]. |
| correctedrMSSD | crMSSD | PRV Time-domain parameter. The square root of the mean squared differences of successive interbeat intervals. Its value provides information primarily about the parasympathetic regulation of the heart and used to estimate the vagally mediated changes. The value of rMSSD could refer to the quality of electrical stability of the heart [39]. Corrected: see comment at "cTotalPower" |
| corrected pNN50 | cpNN50 | PRV Time-domain parameter. The proportion of differences of successive IBIs exceeding 50 ms. It characterizes parasympathetic activity.[39] Corrected: see comment at "cTotalPower" |
| PRV Frequency-domain parameters | | |
| corrected Total Power (ms2) | cTotalPower | PRV Frequency-domain parameter. It specifies the area under the complete frequency-domain analysis curve. This reflects the activity of the entire autonomic nervous system. Corrected: automatic detection of irregular cycle lengths and application of cubic spline interpolation applied [39]. |
| corrected HF Power | cHFpow | PRV Frequency-domain parameter. Absolute power of the high-frequency band (0.15–0.4 Hz). HF power is the marker of parasympathetic activity [39]. Corrected: see comment at "cTotalPower" |
| corrected LF Power | cLFpow | PRV Frequency-domain parameter. Absolute power of the low-frequency band (0.04–0.15 Hz). LF power is a marker of both sympathetic and parasympathetic activity. The LF band mainly reflects fluctuations in baroreceptor activity during resting conditions. LF power value correlates with the progression of atherosclerosis [40]. Corrected: see comment at "cTotalPower" |
| PRV Non-linear-domain parameters | | |
| corrected SD1 | cSD1 | PRV Non-linear parameter. Standard deviation 1 of the Poincaré plot representing the length of the ellipse fitted to the plot [39].Corrected: see comment at "cTotalPower" |
| corrected SD2 | cSD2 | PRV Non-linear parameter. Standard deviation 2 of the Poincaré plot representing the width of the ellipse fitted to the plot [39]. Corrected: see comment at "cTotalPower" |

*These parameters are developed by our research group. Most of them are not yet validated in clinical studies

**Table 2** Results of correlation analysis of PPG parameters and age

| PPG parameters | Correlation values of PPG parameters with age | | Results of GAM analysis of the relationship between age and PPG parameters | | |
|---|---|---|---|---|---|
| | Pearson's r | *p* | Deviance explained | EDOF | *p* |
| Conventional PPG parameters | | | | | |
| ET(PPG) | 0.589 | < .001 | 0.4000 | 5.6458 | < .001 |
| Crest Time | 0.570 | < .001 | 0.5092 | 12.4659 | < .001 |
| LVETi | 0.539 | < .001 | 0.2944 | 2.5483 | < .001 |
| AGEi | 0.485 | < .001 | 0.2385 | 2.5483 | < .001 |
| SysAlpha | -0.418 | < .001 | 0.1834 | 2.5483 | < .001 |
| d/a | -0.376 | < .001 | 0.1540 | 2.5483 | < .001 |
| b/a | 0.207 | 0.025 | 0.0487 | 2.5483 | 0.052 |
| Si | 0.181 | 0.050 | 0.0708 | 2.7463 | 0.099 |
| Ri | -0.159 | 0.085 | 0.0635 | 2.8567 | 0.010 |
| Novel PPG parameters | | | | | |
| eLVET1* | 0.548 | < .001 | 0.3574 | 5.6458 | < .001 |
| DNi* | -0.517 | < .001 | 0.2693 | 2.5483 | < .001 |
| eLVET2* | 0.450 | < .001 | 0.2063 | 2.5483 | < .001 |
| c-d incidence* | 0.419 | < .001 | 0.2459 | 5.6458 | < .001 |
| PPG Score parameters | | | | | |
| Heart Fitness Score* | -0.493 | < .001 | 0.3310 | 3.3728 | < .001 |
| CV Health Score* | -0.450 | < .001 | 0.2253 | 2.7463 | < .001 |
| Total Score* | -0.301 | < .001 | 0.1815 | 3.3728 | < .001 |

*EDOF* effective degrees of freedom, *ET(PPG)* left ventricular ejection time measured by PPG, *LVETi* left ventricular ejection time index, *AGEi* ageing-index, *SysAlpha* systolic slope inclination, *d/a and b/a* ratios of the different inflection points of the second derivative of the pulse wave, *Si* stiffness index, *Ri* reflection index, *eLVET1* and eLVET2** the early left ventricular ejection time 1 and 2 are the two-time components of "Crest Time", *DNi** dicrotic notch index, *c-d incidence** c-d point detection ratio, *Score parameters* scores were calculated based on the 30 + parameters derived from the proprietary analysis of the 2 min pulse-wave recording

* These parameters are developed by our research group. Most of them are not yet validated in clinical studies

For more information on GAM and an explanation of its measured values, see the Additional file1.docx

For a more detailed description of the PPG parameters, see Table 1

examining both conventional and novel PPG parameters, as well as PRV characteristics, provides a more comprehensive understanding of the effects of chronological ageing on the pulse waveform morphology. The importance of our research is emphasized by the fact that age is arguably the most significant risk factor for CV morbidity and mortality. This is supported by the results of Pencina et al. who found that age, sex, and race capture 63% to 80% of the prognostic performance of CV risk models [24]. This is further emphasized in the Framingham risk score, where age contributes more to the total risk score than any other variable. [25] Our study identified a diverse set of simultaneously recorded PPG parameters including ones that are related to cardiac ejection time, arterial elasticity and loss of PRV. These findings highlight the correlation of PPG parameters with chronological age, suggesting their potential use for monitoring age-related CV changes and evaluating CV health across different age groups. In addition, a major strength of this study lies in the use of a proprietary, automated software system capable of analyzing large datasets with high efficiency that enhance reliability, ensures the reproducibility of study's results [19].

Among the 16 PPG morphology parameters, ET, including its subcomponent eLVET1, as described by our research group, and LVETi, as described by Weber et al., demonstrated the strongest correlations with age, indicating a gradual decline in CV efficiency as individuals age [21, 26, 27]. Using GAM analysis, an extreme nonlinear relationship with multiple inflection points was observed between crest time and age. This is probably due to sparse sampling in older age groups. This highlights the sensitivity of nonlinear models to small sample sizes and outliers.

Arterial stiffening due to loss of arterial elasticity and structural changes in the vascular wall, such as increased collagen deposition and reduced elastin, is a hallmark of CV aging and contributes to elevated CV risk [28]. Therefore, reliable characterization of arterial distensibility by easily accessible biomarkers is an important step toward early detection and prevention of CV diseases, as well as the assessment of vascular aging [5, 29].

Our results also confirmed the findings of previous studies describing age-dependent changes in the AGEI. AGEi is a parameter derived from the second derivative of the pulse contour wave, and its correlation with age and arterial stiffness is widely recognized (as noted by Takazawa and colleagues) [15].

While pulse wave velocity (PWV) is often considered a better measure for assessing CV aging because of its broader predictive power at the population level, AGEi shows considerable potential as a complementary tool, particularly in individual risk assessment. The strong correlation between the second-derivative PPG signal parameters, particularly AGEi and PWV, has been published in several publications [16, 30]. These results highlight the potential of AGEi as a practical, non-invasive measure of individual risk stratification, especially when measurement of PWV is less accessible. The sensitivity of AGEi to age-related vascular changes is a valuable addition to CV diagnostics, complementing PWV's population-level insights. Our study has also shown that DNi has stronger age dependence than AGEi suggesting that it may have relevant potential in monitoring a progressive decline in arterial distensibility (DNi, a proposed

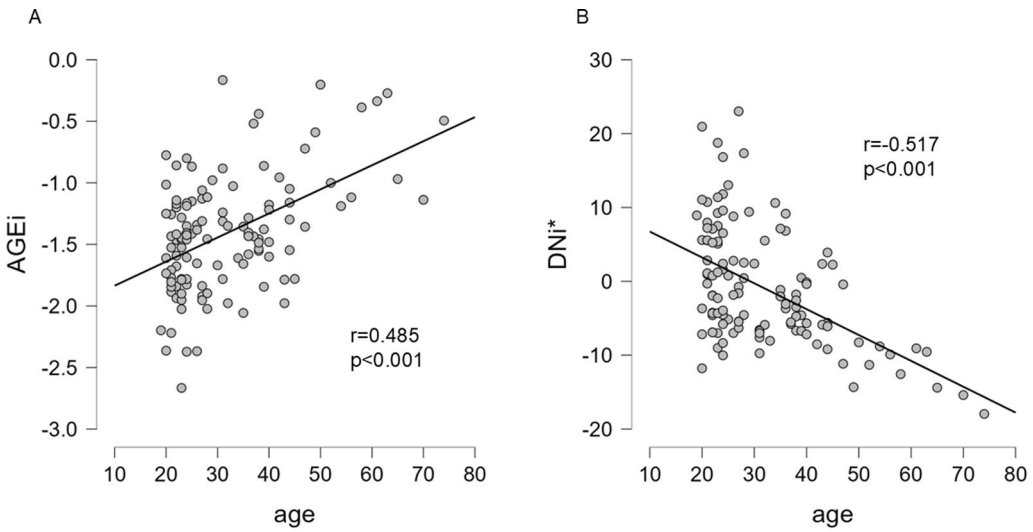


**Fig. 1** Scatter plots of correlation results between age and PPG parameters (AGEi and DNi*). **A** The scatter plot of the correlation analysis between age and AGEi, and **B** the scatter plot of the correlation analysis between age and DNi* parameters

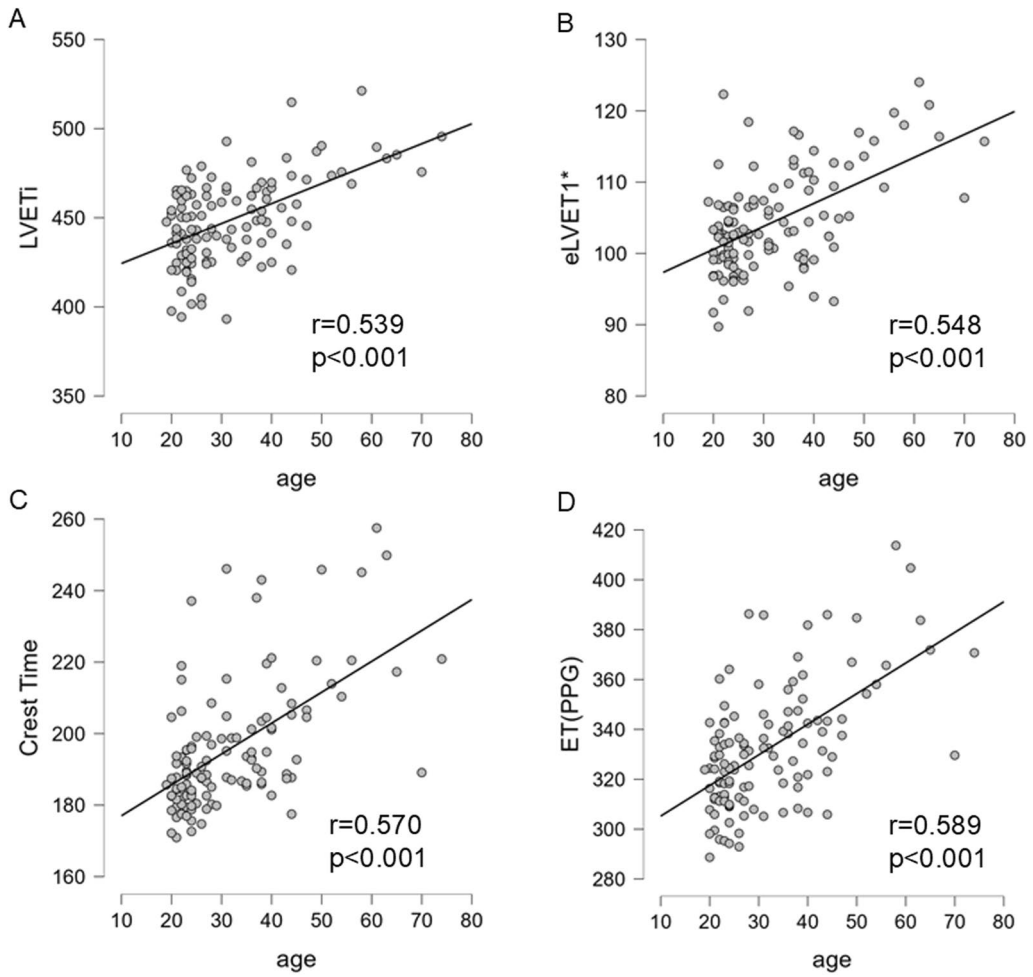


**Fig. 2** Scatter plots of correlation results between age and the ejection-related PPG parameters. **A** The scatter plots of the correlation analysis between LVETi, **B** eLVET1, **C** Crest Time and **D** ET(PPG) and age

**Table 3** Results of correlation analysis of PRV parameters and age

| | Correlation values of PRV parameters with age | | Results of GAM analysis of the relationship between age and PRV parameters | | |
|---|---|---|---|---|---|
| | Pearson's r | p | Deviance Explained | EDOF | *p* |
| Time domain parameters | | | | | |
| cSDRR | – 0.401 | < .001 | 0.1627 | 2.5413 | < .001 |
| crMSSD | – 0.266 | 0.006 | 0.0807 | 2.5413 | 0.058 |
| cpNN50 | – 0.225 | 0.021 | 0.0940 | 2.9638 | 0.080 |
| cMRR | 0.082 | 0.404 | 0.0628 | 3.7356 | 0.413 |
| cMHR | – 0.109 | 0.264 | 0.0711 | 3.7356 | 0.472 |
| Frequency domain parameters | | | | | |
| cTotalPower | – 0.325 | < .001 | 0.1065 | 2.5413 | 0.028 |
| cHFpow | – 0.299 | 0.002 | 0.0902 | 2.5413 | 0.035 |
| cLFpow | – 0.277 | 0.004 | 0.0768 | 2.5413 | 0.270 |
| Non-linear parameter | | | | | |
| cSD2 | – 0.428 | < .001 | 0.1887 | 2.5413 | < .001 |
| cSD1 | – 0.266 | 0.006 | 0.0807 | 2.5413 | 0.058 |

*EDOF* Effective degrees of Freedom, *cSDRR* The standard deviation of the interbeat intervals (ms), *crMSSD* The square root of the mean squared differences of successive interbeat intervals, *cpNN50* the proportion of differences of successive IBIs exceeding 50 ms, *cMRR* the mean normal-to-normal interbeat interval, *cMHR* the mean heart rate, *cTotalPower* It specifies the area under the complete frequency-domain analysis curve, *cHFpow* absolute Power of the high-frequency band, *cLFpow* absolute power of the low-frequency band; cSD1 and cSD2: standard deviation 1 and 2 of the Poincaré plot representing the length and width of the ellipse fitted to the plot. The c in front of the parameter name stands for: corrected: automatic detection of irregular cycle lengths and application of cubic spline interpolation applied

For more information on GAM and an explanation of its measured values, see the Additional file1.docx

For a more detailed description of the PRV parameters, see Table 1

marker of aortic distensibility and coronary flow pressure gradient). Si is another PPG parameter proposed by several authors to characterize arterial stiffening. Based on the previous publication of Millasseau (Determination of age-related increases in large artery stiffness by digital pulse contour analysis), PWV and Si are significantly correlated with each other, and both are correlated with age. Interestingly, the Si showed a weak correlation with age in our study [31]. One possible explanation for this may be the different age and sex distribution of the two studies. In the study of Millaseau et al., 29 of the 87 participants were women; the mean age was 47 years, with a range of 21–68 years. Whereas our study age distribution for females found to contain a higher proportion of women mostly in premenopausal age. These observations emphasize that precise characterization of age correlation may require accounting for sex-specific differences and other confounding factors in the analysis; however, this necessitates analysis performed on large datasets.

In addition to the individual parameters, "composite scores" of multiple PPG parameters, such as the Total Score, Heart Fitness Score and CV Health Score, also showed significant correlations with age, both using Pearson correlation and GAM analysis. This supports the unpublished observations of the manufacturer that suggested strong age dependence of these parameters in a large inhomogeneous patient population coming from real-world data of more than 98 000 processed measurements from more than 5 800 individuals in various age, sex and health status [32]. The composite scores were developed to simplify the interpretation of CV health indicators by aggregating multiple PPG-derived parameters into a single, more user-friendly metric. This

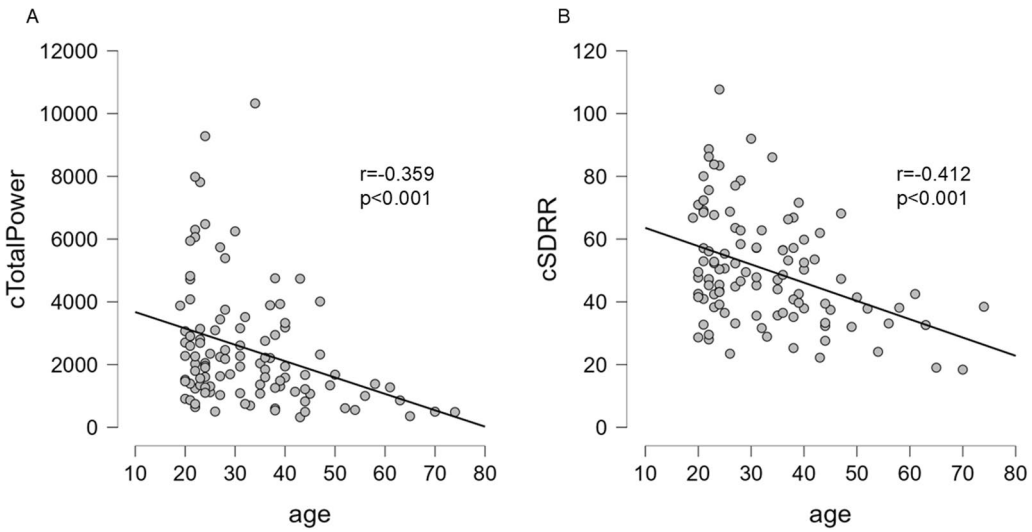


**Fig. 3** Scatter plots of correlation results between age and PRV parameters **A** The scatter plot of the correlation analysis between age and cTotalPower, and **B** the scatter plot of the correlation analysis between age and cSDRR parameters

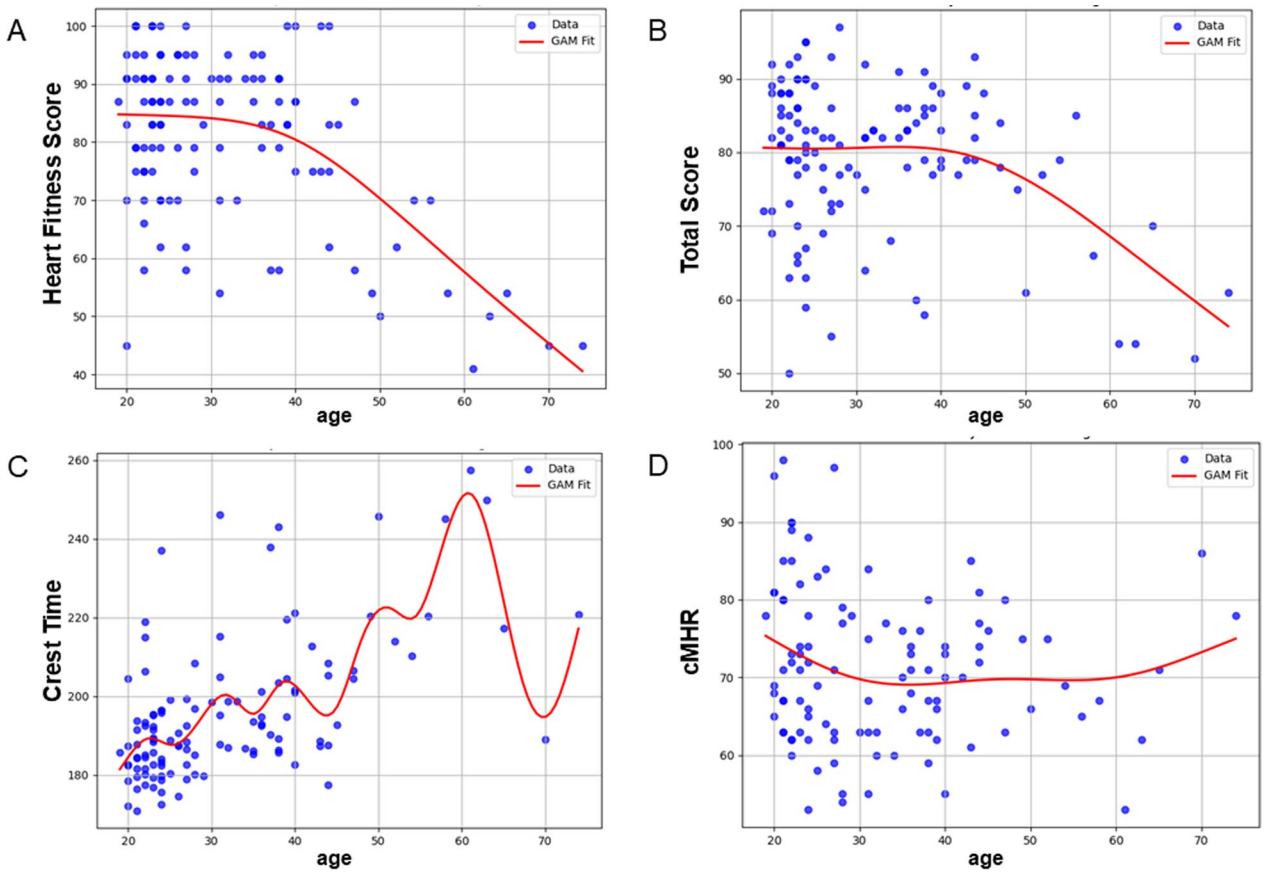


**Fig. 4** Plots of GAM analysis. **A, B** The plot of the GAM analysis between age and Heart Fitness and Total Score parameters, **C** the plot of the GAM analysis between age and Crest Time PPG parameter and **D** the plot of the GAM analysis between age and cpNN50 PRV parameter

approach can make it easier for end-users to track and understand their metrics, especially for non-specialists for whom interpretation of multiple individual parameters (e.g. 15–20) can be challenging. While the exact calculation methods for these scores are proprietary, they are based on established PPG signal features associated with vascular and cardiac health. These include parameters related to arterial stiffness, pulse wave characteristics, and temporal signal dynamics, all of which are linked to age-dependent CV changes. The validation of these composite scores as independent predictors of CV health. requires further studies. However, preliminary findings suggest that they could support CV risk evaluations. All score parameters in this study showed a clear non-linear, decreasing relationship with age, especially after age 40. This sharp decline is consistent with published data showing accelerated ageing during middle age [33].

Some PRV parameters, such as total power (cTotalPower) and SDNN (cSDRR), showed a significant correlation with age. Both parameters showed a decrease with increasing age; this could indicate a less sensitive autonomic nervous system, which may contribute to the reduced cardiovascular adaptive capacity observed in the elderly. This finding is consistent with the existing literature, which suggests that decreased heart rate variability reflects reduced autonomic control of the CV system, and highlights the importance of monitoring autonomic function through PRV parameters as part of a comprehensive CV health assessment. [7–9, 34].

In summary, our results reveal a set of PPG and PRV parameters associated with age-related changes with distinct differences between parameters in the aspect of linearity, emphasizing the potential of simultaneous recording and analysis of multiple PPG parameters in CV prevention, though further research is required. Additionally, combining different PPG parameters has yielded composite scores with unique age-dependent patterns which might reflect the non-linear trends of ageing, which may prove useful in identifying age-related CV events or conditions. We believe that our study may serve as a foundational step in developing personalized PPG-based CV age assessment tools. However, future research should explore whether individuals positioned above or

below the correlation trend line represent distinct CV aging phenotypes, such as early vascular aging or supernormal vascular aging. [35, 36].

## 5 Limitations of the study

A limitation of our study is that the age distribution of the sample population is not fully uniform and may not be fully representative of the general population. Future research should, therefore, be extended to a wider, more diverse cohort to further verify these results.

Clinical validation of the proprietary PPG parameters introduced could be a critical next step towards their wider use and clinical utility. Although the aim of this study was primarily to explore the age dependence of these parameters, it is important to outline possible avenues for future validation. Future studies are planned to focus on the correlation of the new PPG composite scores with widely accepted CV risk scores such as the Framingham Risk Score or the HeartScore (European Society of Cardiology), as well as with established measures such as lipid profiles, hs-CRP, plasma creatinine, carotid Doppler and echocardiography results, and pulse wave velocity (PWV). Further validation efforts include analysing how composite scores interact with clinical and lifestyle factors, including patient history and modifiable risk behaviours, to increase their predictive accuracy. In addition, to ensure wider applicability, we plan to evaluate the performance of these scores in different patient subgroups, including individuals with different CV risk profiles and comorbidities. These studies may be beneficial to further refine the interpretation of the identified age-related indicators, as different PPG parameters may be more relevant in certain pathological contexts, such as hypertension or heart failure.

## 6 Conclusion

This study has successfully identified age-related linear and non-linear correlations across both conventional and novel PPG parameters, highlighting their potential as valuable indicators of CV ageing. The findings demonstrate that parameters related to cardiac ejection time, arterial elasticity, and PRV, among others, consistently correlate with age, offering a comprehensive view of how the CV system evolves over time. The introduction of novel composite PPG score parameters, which showed notable age correlations, may complement traditional metrics, although further validation is needed to confirm their specific contributions. The clinical relevance of these findings is that they draw attention to the potential of pulse wave analysis to monitor CV ageing non-invasively and position PPG as a promising tool in both clinical and preventive cardiology. However, translation of this method to clinical settings requires further research in patients with various CV conditions and comorbidities.

## Supplementary Information

The online version contains supplementary material available at https://doi.org/10.1007/s44200-025-00068-w.

Below is the link to the electronic supplementary material.Supplementary file1 (DOCX 24 KB)

**Acknowledgements**

We would like to acknowledge all our participants for their time and assistance during the study. F.A and D.K. are PhD candidates at Semmelweis University. S.K. is the CEO and co-owner of E-Med4All Europe Ltd. F.A. is a former employee of E-Med4All Europe Ltd. Z.M. is the head of the Department of Translational Medicine at the National Korányi Institute for Pulmonology.

**Author Contributions**

F.A. and D.K. designed the study and conducted the data collection; furthermore, they drafted the first version of the manuscript. S.K. contributed to the analysis and interpretation of the results. Z.M. provided critical revisions to the manuscript. All authors read and approved the final manuscript.

**Funding**

No specific funding was received for this study.

**Data Availability**

The datasets generated and analysed during the current study are not publicly available, but are available from the corresponding author on reasonable request.

## Declarations

**Conflict of interest**

F.A., D.K. and S.K. had financial relationships with E-Med4All Europe Ltd. (D.K. and S.K. as co-owners; F.A. is a former employee who worked during the data collection period). Z.M. is the PhD supervisor of D.K. and F.A. Z.M. did not receive any compensation for their contributions.

**Ethical approval and consent to participate**

The study was conducted in accordance with the Declaration of Helsinki. All tests were conducted in the laboratory facilities of Semmelweis University. IRB approval number: 120/2018. Written informed consent was obtained from all participants involved in the study.

**Consent for publication**

Participants provided written consent for the publication of study results as part of their agreement to participate in the study.

Received: 31 October 2024 Accepted: 8 January 2025
Published online: 25 March 2025

**References**

1. Cardiovascular diseases (CVDs) [Internet]. [cited 2020 Nov 30]. https://www.who.int/news-room/fact-sheets/detail/cardiovascular-diseases-(cvds)
2. Van Camp G. Cardiovascular disease prevention. Acta Clin Belg [Internet]. 2014;69(6):407–11. https://doi.org/10.1179/2295333714Y.0000000069.
3. Kovacic JC, Moreno P, Hachinski V, Nabel EG, Fuster V. Cellular senescence, vascular disease, and aging: Part 1 of a 2-part review. Circulation. 2011. https://doi.org/10.1161/CIRCULATIONAHA.110.007021.
4. Kovacic JC, Moreno P, Nabel EG, Hachinski V, Fuster V. Cellular senescence, vascular disease, and aging: Part 2 of a 2-part review: Clinical vascular

disease in the elderly. Circulation. 2011. https://doi.org/10.1161/CIRCULATIONAHA.110.009118.
5. Charlton PH, Paliakaite B, Pilt K, Bachler M, Zanelli S, Kulin D, et al. Assessing hemodynamics from the photoplethysmogram to gain insights into vascular age: a review from VascAgeNet. Am J Physiol - Hear Circ Physiol. 2022. https://doi.org/10.1152/ajpheart.00392.2021.
6. Elgendi M. On the analysis of fingertip photoplethysmogram signals. Curr Cardiol Rev. 2012. https://doi.org/10.2174/157340312801215782.
7. Muhadi NSA, Putranto R, Harimurti K. The ability of detecting heart rate variability with the photoplethysmography to predict major adverse cardiac event in acute coronary syndrome. Acta Med Indones. 2016;48(1):48–53.
8. McManus DD, Chong JW, Soni A, Saczynski JS, Esa N, Napolitano C, et al. PULSE-SMART: pulse-based arrhythmia discrimination using a novel smartphone application. J Cardiovasc Electrophysiol. 2016. https://doi.org/10.1111/jce.12842.
9. Moreno EM, Lujan MJA, Rusinol MT, Fernandez PJ, Manrique PN, Trivino CA, et al. Type 2 diabetes screening test by means of a pulse oximeter. IEEE Trans Biomed Eng. 2017. https://doi.org/10.1109/TBME.2016.2554661.
10. O'Rourke MF, Jiang APXJ. Pulse wave analysis. Brit J Clin Pharmacol. 2001. https://doi.org/10.1046/j.0306-5251.2001.01400.x.
11. Hametner B, Weber T, Wassertheurer S. Heart failure: insights from the arterial waves. J Am Heart Assoc. 2023. https://doi.org/10.1161/JAHA.123.029116.
12. Allen J. Photoplethysmography and its application in clinical physiological measurement. Physiol Meas. 2007. https://doi.org/10.1088/0967-3334/28/3/R01.
13. Allen J, Kyriacou P. Photoplethysmography: Technology, Signal Analysis and Applications. Photoplethysmography Technol Signal Anal Appl. 2021 Jan 1;1–490. ISBN: 9780128233740
14. Charlton PH, Allen J, Bailon R, Baker S, Behar JA, Chen F, The, et al. Wearable photoplethysmography roadmap. Physiol Meas. 2023. https://doi.org/10.1088/1361-6579/acead2.
15. Takazawa K, Tanaka N, Fujita M, Matsuoka O, Saiki T, Aikawa M, et al. Assessment of vasoactive agents and vascular aging by the second derivative of photoplethysmogram waveform. Hypertension. 1998. https://doi.org/10.1161/01.HYP.32.2.365.
16. Bortolotto LA, Blacher J, Kondo T, Takazawa K, Safar ME. Assessment of vascular aging and atherosclerosis in hypertensive subjects: Second derivative of photoplethysmogram versus pulse wave velocity. Am J Hypertens. 2000;13(2):165–71. https://doi.org/10.1016/s0895-7061(99)00192-2.
17. Allen J, Murray A. Age-related changes in peripheral pulse timing characteristics at the ears, fingers and toes. J Hum Hypertens. 2002. https://doi.org/10.1038/sj.jhh.1001478.
18. Wu H. Multiscale entropy with electrocardiograph, electromyography, electroencephalography, and photoplethysmography signals in healthcare: a twelve-year systematic review. Biomed Signal Process Control. 2024;1(93): 106124. https://doi.org/10.1016/j.bspc.2024.106124.
19. Kulin D, Antali F, Kulin S, Wafa D, Lucz KI, Veres DS, et al. Preclinical, multi-aspect assessment of the reliability of a photoplethysmography-based telemonitoring system to track cardiovascular status. Appl Sci. 2020;10(22):1–17. https://doi.org/10.3390/app10227977.
20. Antali F, Kulin D, Lucz KI, Szabó B, Szűcs L, Kulin S, et al. Multimodal assessment of the pulse rate variability analysis module of a photoplethysmography-based telemedicine system. Sensors. 2021. https://doi.org/10.3390/s21165544.
21. Allen J, O'Sullivan J, Stansby G, Murray A. Age-related changes in pulse risetime measured by multi-site photoplethysmography. Physiol Meas. 2020. https://doi.org/10.1088/1361-6579/ab9b67.
22. Lin WH, Zheng D, Li G. Age-related changes in blood volume pulse wave at fingers and ears. IEEE J Biomed Heal informatics. 2024. https://doi.org/10.1109/JBHI.2023.3282796.
23. Djurić B, Žikić K, Nestorović Z, Lepojević-Stefanović D, Milošević N, Žikić D. Using the photoplethysmography method to monitor age-related changes in the cardiovascular system. Front Physiol. 2023;19(14):1191272. https://doi.org/10.3389/fphys.2023.1191272.
24. Pencina MJ, Navar AM, Wojdyla D, Sanchez RJ, Khan I, Elassal J, et al. Quantifying importance of major risk factors for coronary heart disease. Circulation. 2019. https://doi.org/10.1161/CIRCULATIONAHA.117.031855.
25. Wilson PWF, D'Agostino RB, Levy D, Belanger AM, Silbershatz H, Kannel WB. Prediction of coronary heart disease using risk factor categories. Circulation. 1998. https://doi.org/10.1161/01.cir.97.18.1837.
26. Haiden A, Eber B, Weber T. U-shaped relationship of left ventricular ejection time index and all-cause mortality. Am J Hypertens. 2014. https://doi.org/10.1093/ajh/hpt185.
27. Biering-Sørensen T, Querejeta Roca G, Hegde SM, Shah AM, Claggett B, Mosley TH, et al. Left ventricular ejection time is an independent predictor of incident heart failure in a community based cohort. Eur J Heart Fail. 2017. https://doi.org/10.1002/ejhf.928.
28. Ungvari Z, Tarantini S, Donato AJ, Galvan V, Csiszar A. Mechanisms of vascular aging. Circ Res. 2018. https://doi.org/10.1161/CIRCRESAHA.118.311378.
29. Laurent S. Defining vascular aging and cardiovascular risk. J Hypertens. 2012. https://doi.org/10.1097/HJH.0b013e328353e501.
30. Hashimoto J, Chonan K, Aoki Y, Nishimura T, Ohkubo T, Hozawa A, et al. Pulse wave velocity and the second derivative of the finger photoplethysmogram in treated hypertensive patients: their relationship and associating factors. J Hypertens J Hypertens. 2002. https://doi.org/10.1097/00004872-200212000-00021.
31. Millasseau S, Kelly R, Ritter J, Chowienczyk P. Determination of age-related increases in large artery stiffness by digital pulse contour analysis. Clin Sci. 2002. https://doi.org/10.1042/cs1030371.
32. Correlation of HeartReader parameters and scores with age – HeartReader . https://readingtheheart.com/heartreader/correlation_with_age/ Accessed 2024 Nov. 20.
33. Shen X, Wang C, Zhou X, Zhou W, Hornburg D, Wu S, et al. Nonlinear dynamics of multi-omics profiles during human aging. Nat Aging. 2024. https://doi.org/10.1038/s43587-024-00692-2.
34. Siepmann M, Weidner K, Petrowski K, Siepmann T. Heart rate variability: a measure of cardiovascular health and possible therapeutic target in dysautonomic mental and neurological disorders. Appl Psychophysiol Biofeedback. 2022. https://doi.org/10.1007/s10484-022-09572-0.
35. Cunha PG, Boutouyrie P, Nilsson PM, Laurent S. Early vascular ageing (EVA): definitions and clinical applicability. Curr Hypertens Rev. 2017. https://doi.org/10.2174/1573402113666170413094319.
36. Bruno RM, Nilsson PM, Engström G, Wadström BN, Empana JP, Boutouyrie P, et al. Early and supernormal vascular aging: clinical characteristics and association with incident cardiovascular events. Hypertens. 2020. https://doi.org/10.1161/HYPERTENSIONAHA.120.14971.
37. Besleaga T. Photoplethysmography use for Assessment of Mechanical Alternans in Human Cardiovascular Disease . University College London; 2020. https://discovery.ucl.ac.uk/id/eprint/10100901/
38. Chan GSH, Middleton PM, Celler BG, Wang L, Lovell NH. Automatic detection of left ventricular ejection time from a finger photoplethysmographic pulse oximetry waveform: comparison with Doppler aortic measurement. Physiol Meas. 2007. https://doi.org/10.1088/0967-3334/28/4/009.
39. Task Force of the European Society of Cardiology and the North American Society of Pacing and Electrophysiology. Heart rate variability: standards of measurement, physiological interpretation and clinical use. Circulation . 1996 Mar 1 [cited 2016 Nov 25];93(5):1043–65. http://www.ncbi.nlm.nih.gov/pubmed/8598068
40. Gottsäter A, Ahlgren ÅR, Taimour S, Sundkvist G. Decreased heart rate variability may predict the progression of carotid atherosclerosis in type 2 diabetes. Clin Auton Res. 2006;16(3):228–34. https://doi.org/10.1007/s10286-006-0345-4.

## Publisher's Note

# Supplementary material for Generalized Additive Models (GAM)

Generalized Additive Models (GAM) are an advanced statistical modeling method designed to flexibly capture linear and non-linear relationships between predictor and response variables. Unlike traditional linear regression, GAMs allow for smooth, data-driven fits using spline-based smoothing functions, enabling the analysis to identify complex trends in datasets without imposing a rigid functional form. In this study, GAM was employed to assess the relationship between age (predictor variable) and various PPG (Photoplethysmography) and PRV (Pulse Rate Variability) parameters (response variables). This method proved particularly useful in identifying both linear trends and non-linear patterns, offering insights that traditional linear approaches like Pearson correlation might overlook.

**Main parameters calculated by the GAM analysis**

**Deviance Explained**: Measures the proportion of variability in the response variable that is explained by the predictor variable. Higher values indicate a better fit of the model to the data, similar to the R-squared in linear regression.

**Effective Degrees of Freedom (EDOF)**: Reflects the model's complexity and the smoothness of the curve. A higher EDOF indicates a more flexible, non-linear fit, while lower EDOF corresponds to simpler (near-linear) relationships.

**Generalized Cross-Validation (GCV) Score**: A measure of model performance that balances fit and complexity. Lower GCV values indicate better model performance and smoother curves without overfitting.

**Scale**: The residual variance (error term) of the model, indicating how well the model predicts the data.

**p-Value**: Represents the statistical significance of the smoothing term (relationship between predictor and response). $p < 0.05$ indicates a significant relationship.

**Determination of Optimal Lambda (λ) Values**

In GAM analysis, the smoothing parameter λ plays a critical role in determining the trade-off between curve smoothness and model fit. Small λ produces a highly flexible curve, which can overfit the data. Large λ results in a very smooth (near-linear) curve, potentially underfitting the data. To ensure that the models were optimized, a grid search approach was used to identify the best lambda values for each parameter. The lambda grid covered a broad range of values, from highly flexible to very smooth:

- Logarithmic Scaling (0.01 to 10): Captures smaller, more flexible fits.
- Fine Grid (90 to 110): Focuses on tuning lambda around commonly observed optimal values.
- Extended Range (100 to 1000): Allows for extremely smooth curves when necessary.

For each response variable, GAM was applied iteratively, and the Generalized Cross-Validation (GCV) score was used to identify the optimal λ: The model with the lowest GCV score was selected as the optimal solution. This ensured that each parameter had the most appropriate balance between smoothness and fit.

Summary

The GAM method successfully identified optimal λ values for every PPG and PRV parameter by minimizing the GCV score. This allowed for precise modeling of age-related trends while accommodating both linear and non-linear relationships. This approach ensures that GAM results provide robust insights into the complex interactions between age and cardiovascular parameters, emphasizing the importance of non-linear analyses for understanding biological aging.

***Suppl. Table: Results of GAM analysis of the relationship between Age and PPG parameters***

| PPG and PRV parameters | GCV Score | Scale | Optimal "lambda" | Deviance Explained | EDOF | p |
|---|---|---|---|---|---|---|
| Conventional PPG parameters | | | | | | |
| ET(PPG) | 414.757 | 379.197 | 10 | 0.4000 | 5.6458 | < .001 |
| Crest Time | 214.855 | 174.428 | 0.1 | 0.5092 | 12.4659 | < .001 |
| LVETi | 447.489 | 430.128 | 1000 | 0.2944 | 2.5483 | < .001 |
| AGEi | 0.183 | 0.176 | 1000 | 0.2385 | 2.5483 | <.001 |
| SysAlpha | 5.397 | 5.188 | 1000 | 0.1834 | 2.5483 | <.001 |
| d/a | 0.041 | 0.040 | 1000 | 0.1540 | 2.5483 | <.001 |
| b/a | 0.024 | 0.023 | 1000 | 0.0487 | 2.5483 | 0.052 |
| Si | 0.776 | 0.743 | 599.484 | 0.0708 | 2.7463 | 0.099 |
| Ri | 116.139 | 111.089 | 464.159 | 0.0635 | 2.8567 | 0,01 |
| Novel PPG parameters | | | | | | |
| eLVET1* | 35.413 | 32.377 | 10 | 0.3574 | 5.6458 | <.001 |
| DNi* | 49.289 | 47.376 | 1000 | 0.2693 | 2.5483 | <.001 |
| eLVET2* | 169.317 | 162.748 | 1000 | 0.2063 | 2.5483 | <.001 |
| c-d incidence* | 410.381 | 375.196 | 10 | 0.2459 | 5.6458 | <.001 |
| PPG Score parameters | | | | | | |
| Heart Fitness Score* | 157.167 | 149.102 | 166.810 | 0.3310 | 3.3728 | <.001 |
| CV Health Score* | 132.846 | 127.292 | 599.484 | 0.2253 | 2.7463 | <.001 |
| Total Score* | 91.313 | 86.627 | 166.810 | 0.1815 | 3.3728 | <.001 |
| Time domain PRV parameters | | | | | | |

| | | | | | | |
|---|---|---|---|---|---|---|
| cSDRR | 276.899 | 264.976 | 1000 | 0.1627 | 2.5413 | < .001 |
| crMSSD | 372.614 | 356.570 | 1000 | 0.0807 | 2.5413 | 0.058 |
| cpNN50 | 352.120 | 334.444 | 359.381 | 0.0940 | 2.9638 | 0.080 |
| cMRR | 13943.825 | 13062.171 | 90 | 0.0628 | 3.7356 | 0.413 |
| cMHR | 97.989 | 91.793 | 90 | 0.0711 | 3.7356 | 0,472 |
| Frequency domain PRV parameters | | | | | | |
| cTotalPower | 3618748.208 | 3462928.12 | 1000 | 0.1065 | 2.5413 | 0,028 |
| cHFpow | 684814.250 | 655326.756 | 1000 | 0.0902 | 2.5413 | 0.035 |
| cLFpow | 854121.978 | 817344.243 | 1000 | 0.0768 | 2.5413 | 0.270 |
| Non-linear PRV parameters | | | | | | |
| cSD2 | 435.314 | 416.570 | 1000 | 0.1887 | 2.5413 | < .001 |
| cSD1 | 186.307 | 178.285 | 1000 | 0.0807 | 2.5413 | 0,058 |

**Physiology International**
DOI: 10.1556/2060.2025.00675

# Evaluating photoplethysmography-based pulsewave parameters and composite scores for assessment of cardiac function: A comparison with echocardiography

DÁNIEL KULIN[1,2†*], FLÓRA ANTALI[1†], MÁRTON HORVÁTH[3], SÁNDOR KULIN[2], SÁNDOR KULIN JR.[2], ZSUZSANNA MIKLÓS[1,4†] and ANDREA SZŰCS[3†]

[1] Institute of Translational Medicine – Semmelweis University, Budapest, Hungary

[2] E-Med4All Europe Kft, Budapest, Hungary

[3] Heart and Vascular Centre – Semmelweis University, Budapest, Hungary

[4] National Korányi Institute for Pulmonology, Budapest, Hungary

Received: May 20, 2025 • Revised manuscript received: July 16, 2025 • Accepted: August 1, 2025



## ABSTRACT

*Introduction:* This study assesses the utility of photoplethysmography (PPG) as a non-invasive method to evaluate cardiac function, addressing the critical need for accessible biomarkers in various cardiovascular conditions, including heart failure management. *Methods:* By conducting simultaneous echocardiography and PPG measurements on 37 healthy volunteers, we analyzed both traditional and novel composite pulse wave scores to correlate peripheral PPG data with central echocardiographic outcomes. *Results:* Our results show a good correlation between PPG-based and echocardiography-derived ejection times ($r = 0.648$, $P < 0.001$), though Bland-Altmann analysis results reveal that PPG consistently overestimated ejection times by a mean difference of +95 ms. Moreover, eleven PPG parameters significantly correlated with key echocardiographic indicators of systolic and diastolic function, such as left ventricular dimensions, global longitudinal strain, aortic functionality, atrial contraction (MV-A), and ventricular filling pressure (E/e' lat) with clinical relevance indicated by correlations ($r$) above 0.4 ($P < 0.05$). *Conclusion:* The findings pave the

* Corresponding author. 1036 Budapest, Bécsi út. 85, Hungary. Tel.: +36 30 9226206. E-mail: kulin.daniel@phd.semmelweis.hu; kulindaniel@gmail.com

† Equal contributors of the study.

way for further studies in various patient groups to explore the potential of PPG in enhancing home monitoring and regular cardiovascular assessments. This work not only broadens our understanding of the physiological relationships between peripheral and central cardiovascular measures but also introduces innovative metrics that might bring some added value to the current standards of patient care by facilitating early detection and personalized management of heart conditions.

**KEYWORDS**

photoplethysmography (PPG), echocardiography, cardiac function, pulse wave analysis, central hemodynamics, peripheral hemodynamics

## INTRODUCTION

The rising prevalence of cardiovascular (CV) diseases, including heart failure — projected to increase from 6.7 million to 8.5 million Americans by 2030 — underscores the urgent need for advanced diagnostic and home monitoring solutions to manage better and mitigate their growing impact on public health [1, 2].

Managing heart failure requires pharmacotherapy, routine cardiology visits, and patient adherence to prescribed regimens. Echocardiography provides detailed insights into heart morphology and function [3]. Given the challenge of screening and monitoring the growing affected population, there is a pressing need for new biophysical, remote-monitoring biomarkers to improve personalized treatment and continuous monitoring of heart failure [4].

The peripheral arterial pulse wave (PPW) holds promise as a potential biomarker. PPW, influenced by cardiac dynamics, arterial elasticity, and resistance vessel tone, reflects changes in CV status [5, 6].

Mathematical analysis of PPW parameters has shown potential in identifying CV pathologies associated with HF [7]. The term PPW is most commonly used when referring to pressure waveforms measured by tonometry. In contrast, photoplethysmography (PPG) records related but distinct signals: it optically measures pulsatile changes in blood volume within the illuminated tissue, including contributions from small arteries, arterioles, and the microvascular bed, rather than directly capturing arterial pressure. This is particularly relevant for transmissive PPG recordings, such as fingertip measurements, where the entire cross-section of perfused tissue contributes to the composite signal. Despite this difference, the resulting PPG waveform retains morphological features analogous to the pressure pulse wave. Because PPG is non-invasive, widely accessible, and simple to use, it has become increasingly common in devices such as pulse oximeters and smartwatches [5]. In the remainder of this manuscript, for simplicity, we will refer to the PPG-derived signal as the pulse wave and to its evaluation as pulse wave analysis (PWA), while acknowledging this refers specifically to volume-based measurements.

Regardless of the many potential benefits, integration of PPG-based PWA into patient monitoring faces a challenge, mainly because the relationship between routinely used cardiac ultrasound measures and PPG-derived parameters is not established. The limited number of studies addressing this gap focused on exploring relationships between selected parameters [8–10].

The goal is to identify those characteristics of the pulse wave that offer the greatest potential for monitoring cardiovascular status, especially when echocardiography is not available.

Our study aims to comprehensively analyze the association between echocardiographic and PPW parameters in healthy subjects, thereby advancing our understanding of PPG's possible role in the future of heart failure monitoring.

## MATERIALS AND METHODS

### Subjects

Subjects were recruited through multiple channels, including internal invitations distributed among university staff members and outreach via our professional and personal networks, in order to obtain a diverse volunteer population. The study involved healthy adult volunteers ($n = 37$), who claimed themselves healthy by filling out a detailed questionnaire, had a normal body mass index (BMI: 18–25 kg/m$^2$), had no history of smoking, and denied drinking alcohol regularly. Those who had been diagnosed with or had received treatment for diabetes or any CV disease were excluded from the study. Further exclusion criteria involved: pregnancy, previous cancerous disease, wearing false nails, and SARS-CoV-2 infection in the last 6 months before the exam. The measurements were conducted at Semmelweis University's Városmajor Heart and Vascular Centre.

### Ethical Compliance

The study protocols were rigorously designed to align with the highest ethical standards, conforming to the principles outlined in the 2013 Declaration of Helsinki. Informed consent was obtained from all participants, documented in writing. The study received approval from the Regional and Institutional Committee of Science and Research Ethics at Semmelweis University, Budapest (Approval No. 120/2018-3).

### Protocol

After arriving for the exam, patients were allowed to rest for 20 min before starting the study protocol. The protocol consisted of a simultaneous echocardiographic examination and recording of PPG signals from a peripheral artery using a pulse oximeter placed on the right index finger.

### Echocardiography

The echocardiographic protocol followed the methodology described by Horváth et al. (2023) [11]. Blood pressure (BP) was measured three times using an automatic sphygmomanometer before conducting a cardiac ultrasound scan. During the scan, the participant lay on the examination bed with the upper body undressed, positioned on the left side. 2D echocardiography examinations were performed with a GE Vivid E95 system with a 4Vc-D phased-array transducer (GE Vingmed Ultrasound, Horten, Norway). LV-focused, ECG-gated datasets were obtained from parasternal long and short axis, apical four-chamber, apical three-chamber, and apical two-chamber views at a minimum rate of 50 frames per second. Offline analyses of these

datasets were performed after selecting the optimal heart cycles using commercially available software (Autostrain LV, TOMTEC Imaging Systems GmbH, Unterschleissheim, Germany); echocardiographic parameter data were derived by averaging the data from 1 to 3 heartbeats. The algorithm automatically generated the endocardial contours of the cavities, which were manually corrected throughout the entire cardiac cycle. The speckle tracking technique was used for the deformation analysis. The assessed parameters can be found in Table 1.

## PPG measurements

During the cardiac ultrasound, a pulse waveform was recorded for 140 s using a special pulse oximeter on the patient's right index finger, with a 200 Hz sampling frequency (Shanghai Berry Electronic Tech Co., Ltd., Shanghai, China). The patients lay on their side, staying still. The oximeter, wirelessly connected to the SCN4ALL mobile app (E-Med4All Europe Ltd, Budapest, Hungary), sent the anonymized data in real time to a secure online database as described previously [19].

The SCN4ALL software analyzed the signals, its proprietary algorithm identifies points of interest on the pulse wave from which it calculates over 30 morphological and pulse rate variability parameters online. PPG parameters were calculated by averaging measurements from each heartbeat of the continuous recordings. The system's reliability, repeatability, and detailed descriptions of its architecture and signal processing have been published previously [19, 20] (The SCN4ALL parameters assessed in this study are found in – List of echocardiographic and PPG parameters, with abbreviations and definitions Table 1). Besides "conventional" PPG parameters, already known from the literature, composite parameters, called "Scores" were also analyzed. The different "Scores" are constructed using different combinations of parameters, each of which is assigned a value based on specific cutoff values along a monotonous or U-shaped Likert scale. The scores, with a maximum of 100, indicate health levels for evaluated aspects. Their actual reliability and validity in clinical practice are evaluated based on the current and upcoming studies. The exact constituents of the Scores are a proprietary secret, kept confidential at the manufacturer's discretion.

## Statistics, data analysis

To evaluate the agreement between ejection time measurements derived from photoplethysmography (PPG) and echocardiography (Echo), Bland–Altman analysis was performed. For each paired observation, the mean of the two methods and the absolute difference (PPG − Echo) were calculated. The bias (mean difference) and 95% limits of agreement (mean ± 1.96 standard deviations) were determined to quantify systematic and random error. In addition, ratios between PPG- and Echo-derived ejection times were computed to assess proportional differences. The mean ratio and the mean percent difference were reported to describe relative agreement. Bland–Altman calculations were performed in Google Colab using a custom Python script.

Parameter values obtained by echocardiography were compared with corresponding PPG-derived parameter values using correlation analysis performed in JASP software (JASP Version 0.19.3; JASP Team, 2025). Normality of each variable was assessed with the Shapiro–Wilk test. For variable pairs where both distributions did not significantly deviate from

*Table1.* List of echocardiographic and PPG parameters, with abbreviations and definitions

| Echocardiography parameter abbreviations | Echocardiography parameter definition | PPG parameter abbreviations | PPG parameter definition [5] |
|---|---|---|---|
| ET (ECHO) (ms) | Left ventricular ejection time | $Si^{(s)}$ ($m\ s^{-1}$) | **Stiffness index** $Si = h/\Delta T$ ($m\ s^{-1}$); h is the height of the person in meters. ΔT is the time between the systolic peak and diastolic peak on the pulse curve [12]. |
| LV-EDD (mm) | Left ventricular end-diastolic diameter | b/a | The ratio of the first two inflection points of the second derivative of the pulse wave [13]. |
| LV-ESD (mm) | Left ventricular end-systolic diameter | d/a | The ratio of the fourth to the first inflection points of the second derivative of the pulse wave [14]. |
| LV-EDV (mL) | Left ventricular end-diastolic volume | AGEi | **Ageing-index** Value calculated from the fiducial points of the second derivative of the pulse wave. AGEi = b-c-d-e/a |
| LV-ESV (mL) | Left ventricular end-systolic volume | $Ri^{(s)}$ | **Reflection index** The ratio of the amplitude of the diastolic peak to the amplitude of the systolic peak. |
| LV-SV (mL) | Left ventricular stroke volume | $SysAlpha^{(s)}$ (°) | **Systolic slope inclination** The angle between the maximal inclination of systolic upstroke and the horizontal axis [15]. |
| LV-GLS (%) | Global longitudinal strain | LVETi (ms) | Left ventricular ejection time indexed for heart rate (LVETi) was calculated from sex-specific resting regression equations LVETi(male) = 1,7 × heart rate + ET, LVETi(female) = 1,6 × heart rate + ET [16]. |
| LVOT-VTI (cm) | Left ventricular outflow tract velocity time integral | DNi * | **Dicrotic notch index** * Describes the relative position of the diastolic peak to the dicrotic notch (the valley induced by the aortic valve closure before the diastolic peak). |
| MV-grad (av) (Hgmm) | Mean pressure difference between the left atrium and left ventricle measured at the mitral valve during diastole | eLVET1 * (ms) | **Early left ventricular ejection time 1 and Early left ventricular ejection time 2** ELVET1 is measured from the start of the period to the first peak of the first derivative of the pulse, whereas ELVET2 is defined as |

*(continued)*

*Table1.* Continued

| Echocardiography parameter abbreviations | Echocardiography parameter definition | PPG parameter abbreviations | PPG parameter definition [5] |
|---|---|---|---|
| MV-E (cm $s^{-1}$) | Mitral E-wave velocity | eLVET2 *(ms) | the time duration from the first peak of the first derivative PTG to the peak of the systolic wave. |
| MV-A (cm $s^{-1}$) | Mitral A-wave velocity | eLVET1 @75 *(s) (ms) | |
| MV-E/A | The ratio between E-wave and A-wave | eLVET2 @75 * (ms) | |
| DT (ms) | Left ventricular deceleration time | Crest Time (ms) | **Crest Time** - The time elapsed between the beginning of the period (foot) and the maximum systolic amplitude (peak) |
| e'-lat (cm $s^{-1}$) | Mitral lateral annulus velocity | Crest Time @75 (ms) | |
| E/e' - lat | Ratio of early diastolic mitral inflow velocity to early diastolic mitral annulus velocity | ET(PPG) (ms) | **PPG based Left ventricular ejection time.** It is the time elapsed between the lowest point between consecutive systolic peaks and the marker of aortic valve closure (dicrotic notch/e-point on the second derivative of the PPG) [17]. |
| e'-med (cm $s^{-1}$) | Mitral medial annulus velocity | ET(PPG) @75(s) (ms) | |
| Ao, root diam (mm) | Aortic root diameter | Sys/Dias Time(s) | **Systolic/diastolic time ratio** Systolic/diastolic time ratio relates the duration of cardiac systole to diastole. |
| Ao-vmax (m $s^{-1}$) | Aortic maximum flow velocity | HR (1/min) | **Mean Heart Rate** The mean value of the heart beats per minute (1/min). The algorithm calculates a heart rate from the length of each period of the 120-s recording and averages them. |
| Ao-gr (peak) (Hgmm) | Peak aortic pressure gradient | CV Health Score * | Obtained from the parameters that correspond with the function of the heart and the condition and aging of the arteries. |
| Ao-gr (av) (Hgmm) | Average aortic pressure gradient | Heart Fitness Score * | Certain pulse wave parameters are influenced by the athletic lifestyle and athletic capabilities of the subject, so these aspects are marked by this score. |
| Ao-VTI (cm) | Aortic maximum flow velocity time integral | | |
| Ao-accT (ms) | Aortic acceleration time | | |

*These parameters are developed by the scientific team behind the SCN4ALL system. Most of them are not yet validated in clinical studies, their definition and meaning are hypotheses based on the current understanding of pulsewave physiology. (s)The findings for these parameters are presented in the supplementary materials, due to their correlation being lower than 0.4 (Supplementary Tables 1 and 2). Meaning of "@75" after some PPG indices: the original time value is corrected to 75/min heart rate [18].

normality, Pearson correlation coefficients were calculated; for pairs in which at least one variable showed non-normal distribution, Spearman correlation was used.

Significant correlations ($P < 0.05$) with correlation coefficients above $r = 0.4$ are presented in the main manuscript; additional correlations, including those weaker or influenced by heart rate as determined by partial correlation analyses, are provided in Supplementary Table 1.

## RESULTS AND DISCUSSION

### Results

The results of a total of 37 healthy volunteers aged 20–57 years were used in the data analysis (M/F: 16/21; mean age: 36.9 ± 11.4 SD years, BMI mean: 22.4 ± 2.3 SD, Systolic brachial BP: 115 ± 12 SD Hgmm, Diastolic brachial BP: 64 ± 9 SD).

The results of the correlation tests are shown in Table 2 and Supplementary Tables 1 and 2.

### Results related to left ventricular ejection time (LVET)

***Agreement between PPG and echocardiographic ejection times.*** Bland–Altman analysis demonstrated a mean difference (bias) of 95 ms between PPG- and Echo-derived ejection times (SD = 21 ms), with 95% limits of agreement ranging from 53.98 to 136.02 ms. The mean ratio of PPG to Echo measurements was 1.353, corresponding to an average relative overestimation of 29.74% by PPG. The Bland–Altman plots showed a consistent positive bias across the measurement range, with no substantial evidence of proportional error in the log-transformed ratios (Fig. 1).

ET (ECHO) (ms) measured by cardiac ultrasound showed a good correlation with ejection time measured by PPG (ET(PPG)) ($r = 0.648$; $P < 0.001$) (Fig. 2).

We also found correlations with other parameters related to systolic time, such as Crest Time ($r = 0.567$; $P < 0.001$); and the early left ventricular ejection time 1 (eLVET1 *) ($r = 0.478$; $P = 0.003$ – result in Supplementary Table 1) and 2 (eLVET2 *) ($r = 0.472$; $P = 0.003$).

ET (ECHO) inversely correlated with the Dicrotic notch index (DNi*), too ($r = -0.496$; $P = 0.002$).

Given the significant, inverse correlation between heart rate measured by PPG and echocardiographic LVET ($r = -0.538$; $P < 0.001$), we conducted partial correlation tests conditioned on heart rate. The correlation persisted for the parameters ET(PPG), Crest Time, eLVET2*, DNi*, suggesting an independent relationship with heart rate. However, the correlation disappeared for the parameters eLVET1*, indicating that the association was driven by the relationship with heart rate in this case.

### Results related to cardiac systolic function

Several PPG parameters were significantly correlated with echocardiographic parameters which are routinely used in monitoring of systolic function and have known prognostic values. The parameters with the strongest correlation are shown in Table 2 and Fig. 3.

*Table 2.* Results of Pearson's and Spearman's correlations: comparisons of echocardiographic parameters and PPG parameters

| **Correlation of echocardiography parameters with PPG (Pearson)** | | | | | |
|---|---|---|---|---|---|
| **Echocardiography: ejection time** | **PPG parameters** | **Pearson's correlations** | | **Pearson's partial correlations conditioned on HR** | |
| | | ***r*** | ***P*** | ***r*** | ***P*** |
| ET (ECHO) (ms) | ET(PPG) | 0.648 | <0.001 | 0.555 | <0.001 |
| | Crest Time | 0.567 | <0.001 | 0.371 | 0.026 |
| | DNi * | −0.496 | 0.002 | −0.479 | 0.003 |
| | HR | −0.538 | <0.001 | N/A | N/A |
| **Echocardiography: systolic function** | **PPG parameters** | **Pearson's correlations** | | **Pearson's partial correlations conditioned on HR** | |
| | | ***r*** | ***P*** | ***r*** | ***P*** |
| LV-EDD (mm) | AGEi | −0.51 | 0.001 | N/A | N/A |
| | d/a | 0.47 | 0.003 | N/A | N/A |
| | b/a | −0.41 | 0.013 | N/A | N/A |
| LV-ESD (mm) | AGEi | −0.52 | 0.001 | N/A | N/A |
| | d/a | 0.45 | 0.005 | N/A | N/A |
| | b/a | −0.42 | 0.01 | N/A | N/A |
| LV-GLS (%) | DNi * | 0.5 | 0.001 | N/A | N/A |
| LVOT-VTI (cm) | DNi * | −0.4 | 0.015 | N/A | N/A |
| Ao-VTI (cm) | DNi * | −0.44 | 0.007 | N/A | N/A |
| **Echocardiography: diastolic function** | **PPG parameters** | **Pearson's correlations** | | **Pearson's partial correlations conditioned on HR** | |
| | | ***r*** | ***P*** | ***r*** | ***P*** |
| MV-A (cm $s^{-1}$) | b/a | 0.52 | <0.001 | 0.51 | 0.001 |
| | HR | 0.5 | 0.005 | N/A | N/A |
| MV-E (cm $s^{-1}$) | AGEi | 0.4 | 0.014 | N/A | N/A |
| e'-med (cm $s^{-1}$) | Crest Time | −0.41 | 0.012 | N/A | N/A |
| **Correlation of echocardiography parameters with PPG (Spearman)** | | | | | |
| **Echocardiography: ejection time** | **PPG parameter** | **Spearman's correlations** | | **Spearman's partial correlations conditioned on HR** | |
| | | ***ρ*** | ***P*** | ***ρ*** | ***P*** |
| LVET (ms) | eLVET2 * | 0.496 | 0.002 | 0.404 | 0.015 |

*(continued)*

*Table 2.* Continued

| **Echocardiography: systolic function** | **PPG parameters** | **Spearman's correlations** | | **Spearman's partial correlations conditioned on HR** | |
|---|---|---|---|---|---|
| | | ***ρ*** | ***P*** | ***ρ*** | ***P*** |
| LV-EDD (mm) | Heart Fitness Score * | 0.492 | 0.002 | N/A | N/A |
| | CV Health Score * | 0.459 | 0.004 | N/A | N/A |
| | Crest Time @75 | −0.472 | 0.003 | N/A | N/A |
| | eLVET2 @75 * | −0.436 | 0.007 | N/A | N/A |
| LV-ESD (mm) | Heart Fitness Score * | 0.479 | 0.003 | N/A | N/A |
| | eLVET2 @75 * | −0.409 | 0.012 | N/A | N/A |
| Ao, root diam (mm) | DNi * | 0.482 | 0.003 | N/A | N/A |
| **Echocardiography: diastolic function** | **PPG parameters** | **Spearman's correlations** | | **Spearman's partial correlations conditioned on HR** | |
| | | ***ρ*** | ***P*** | ***ρ*** | ***P*** |
| MV-A (cm $s^{-1}$) | eLVET2 @75 * | 0.572 | <0.001 | NA | NA |
| | Heart Fitness Score * | −0.516 | 0.001 | −0.375 | 0.024 |
| | Crest Time @75 | 0.517 | 0.001 | NA | NA |
| | HR | 0.5 | 0.005 | N/A | N/A |
| MV-E/A | HR | −0.451 | 0.005 | N/A | N/A |
| E/e' - lat | LVETi | 0.423 | 0.009 | N/A | N/A |

*r*: Pearson's correlation coefficient; **ρ**(rho): Spearman's correlation coefficient, *P* = *P*-value (significance value <0.05) Given the correlation between heart rate measured by PPG and some echocardiographic parameters, where applicable, partial correlation tests were performed as a function of heart rate.
*: Proprietary SCN4ALL parameters. List of abbreviations found in Table 1.

### Results related to cardiac diastolic function

PPG parameters like eLVET2@75, b/a, HeartFitnessScore, or LVETi showed the strongest (but still moderate) correlations with indicators of atrial contraction (MV-A) and left ventricular filling pressure (E/e' lat). Given that some parameter pairs exhibited correlations with heart rate, we further analyzed these relationships using partial correlation to account for heart rate variability. Table 2 and Fig. 4 showcase these significant correlations.

## DISCUSSION

The ongoing quest for effective, accessible methods to assess heart function is a key focus in cardiovascular research, particularly in the field of echocardiography.

Although other authors have presented some aspects of the correlation between cardiac function and PWA, to our knowledge, our publication is the first to offer comprehensive insights into how echocardiography relates to pulse wave measurements at the periphery. In addition, in

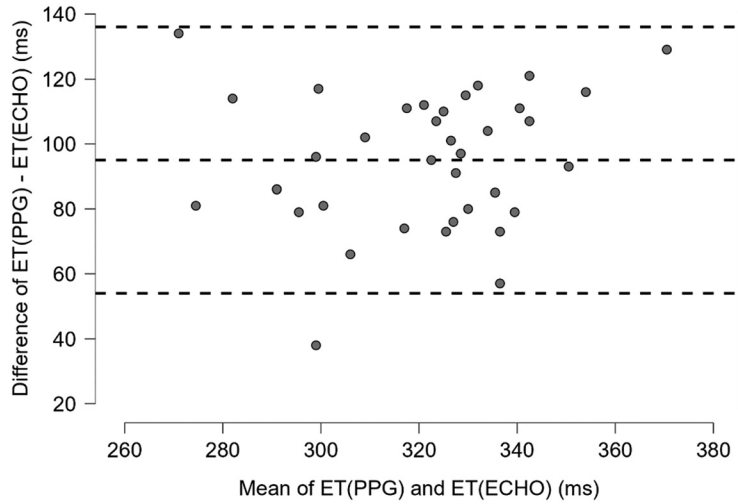


*Fig. 1.* Agreement between photoplethysmography (PPG) and echocardiography (ECHO) in measuring ejection time (ET) in milliseconds (ms) using Bland-Altman analysis.
Middle dashed line: mean difference (95.0), upper and lower dashed line are mean difference ± 1.96 SD (standard deviation) (136.0 and 54.0), respectively

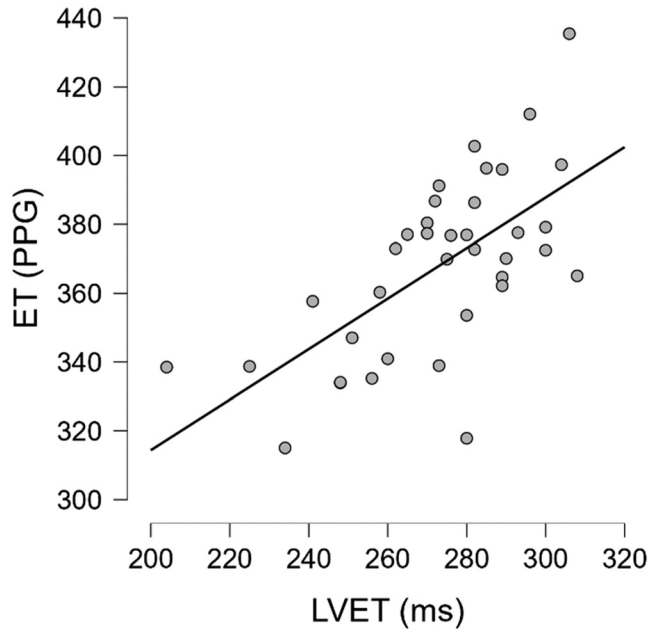


*Fig. 2.* Correlation between ejection times with the two methods.
Pearson's correlation of LVET (ECHO) (ms) and ejection time (ms) measured by PPG (ET(PPG)) (r= 0.648; $P < 0.001$)

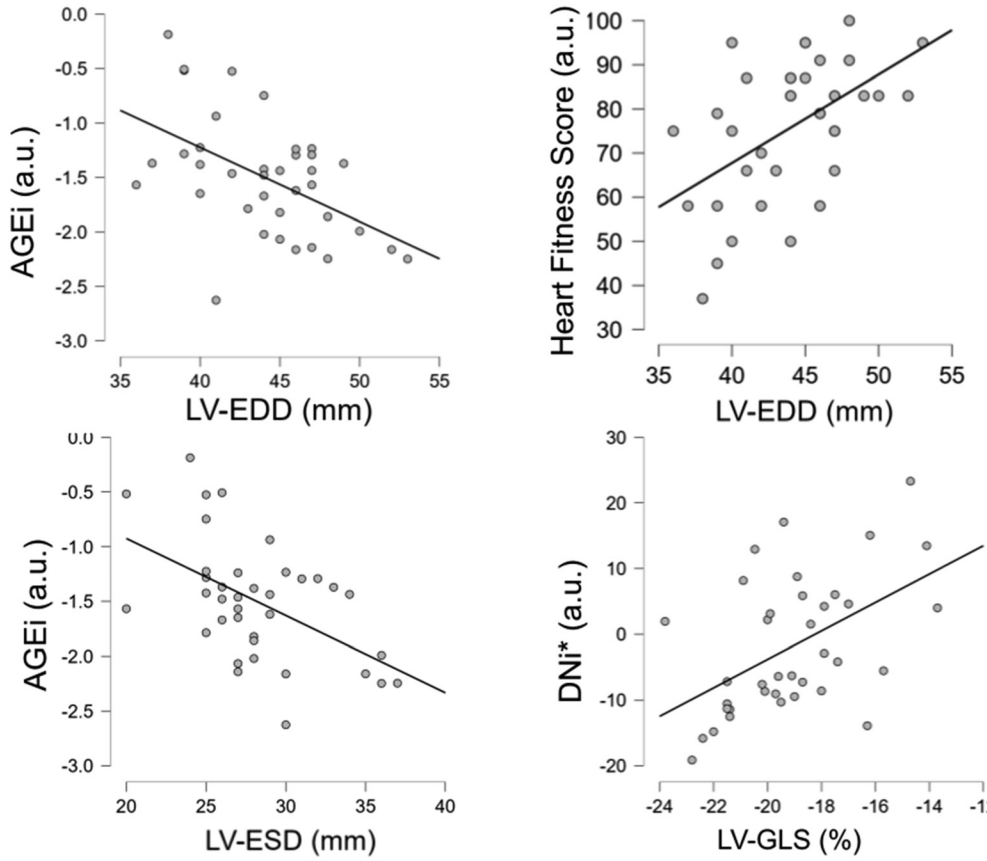


*Fig. 3.* Correlation plots between parameters describing systolic function
**LV-EDD** – left ventricular(LV) end diastolic diameter, **LV-ESD** – LV end systolic diameter, **LV-GLS** – LV global longitudinal strain, **Heart Fitness Score** - Certain pulse wave parameters are influenced by the athletic lifestyle and athletic capabilities of the subject, so these aspects are marked by this score. **AGEi** - Value calculated from the fiducial points of the second derivative of the pulse wave. AGEi = b-c-d-e/a**, DNi** - Describes the relative position of the diastolic peak to the dicrotic notch. $P < 0.05$ for all parameters

this paper, we have presented the performance of a novel pulse wave analysis system with both established and novel composite parameters and scores in healthy individuals. We identified several PPG parameters that can be good candidates to support home monitoring of the alterations of several aspects of cardiac function, such as ejection time, systolic, and diastolic performance. Our findings offer a basis for future research to establish the utility of PPG analysis in regular cardiology care and self-management for HF patients.

Despite extensive research, PPG-based PWA has not become common in clinical practice due to issues like sensitivity to artifacts, varying algorithms, scientific debates over physiological interpretations, and the complexity of pulsewave changes in the arterial tree [21]. However, the growing interest in PPG technology, especially given its inclusion in over 1.1 billion wearables

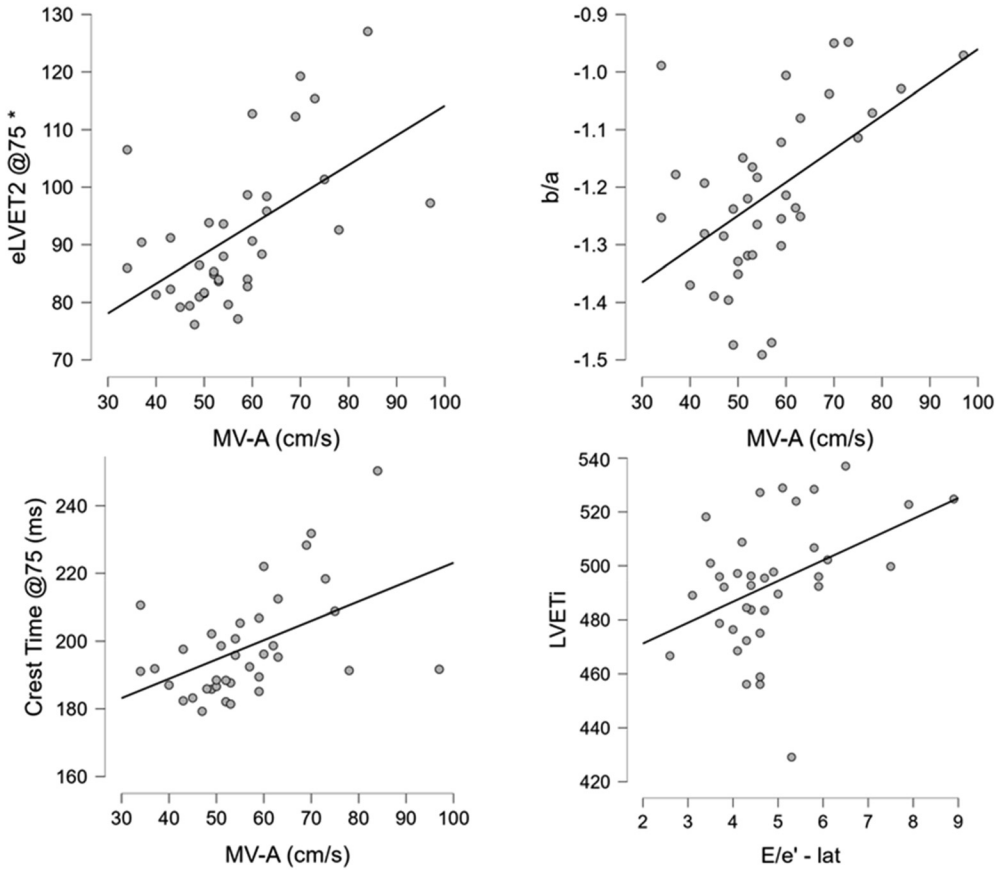


*Fig. 4.* Correlation plots between parameters describing diastolic function
PPG parameters with some of the strongest correlations with echocardiographic parameters indicative of diastolic function. **MV-A** – Mitral A-wave velocity, **E/e'-lat** - Ratio of early diastolic mitral inflow velocity to early diastolic mitral annulus velocity**, eLVET2@75*** - ELVET2 is defined as the time duration from the first peak of the first derivative PTG to the peak of the systolic wave, **b/a** - The ratio of the first two inflection points of the second derivative of the pulse wave, **Crest Time**@75 - The time elapsed between the beginning of the period (foot) and the maximum systolic amplitude (peak), **@75** - the original time value is corrected to 75/min heart rate, **LVETi** - Left ventricular ejection time indexed for heart rate (LVETi) was calculated from sex-specific resting regression equations. $P < 0.05$ for all parameters

[22], suggests its potential in health and disease monitoring might outweigh these limitations [21], aided by advances in machine learning and big data analysis [23].

Furthermore, our results support that peripheral cardiovascular parameters may be valuable in the assessment of central hemodynamics, which is consistent with previous studies investigating this concept, even with different methods [7, 24, 25].

## Ejection time

The left ventricular ejection time (ET), a crucial parameter for evaluating left ventricular function, holds increasing clinical significance. It can independently predict all-cause mortality in heart failure (HF) with reduced ejection fraction. Additionally, it proves useful as an indicator for assessing the impact of various drugs in HF [26].

Despite echocardiography being the prevalent method for ET assessment, the easily accessible PPG method offers broader availability and emerges as a potential alternative for estimating ET [18]. Nevertheless, the performance of PPG in ejection time calculation is not firmly established, partly due to the use of different algorithms across various devices. In our study, we evaluated the performance of the SCN4ALL algorithm in ejection time calculation.

Our study showed that ET(ECHO) significantly correlated with several PPG parameters: ET(PPG), Crest Time, eLVET1*, eLVET2*, DNi, in healthy subjects, which indicates that these PPG parameters or a combination of them may be appropriate indices to estimate ET. Though most probably the ET(PPG) has the highest clinical value among these, it is important to highlight that it is not identical to ET(ECHO). We observed a significant, but moderate correlation between them, but the absolute values were different. This is consistent with the results of Obata and colleagues, who showed that peripherally recorded ejection time was significantly increased compared to centrally measured values [27]. These results suggest that, although the peripheral parameters alone do not allow an accurate clinical evaluation of central left ventricular ET, they support the applicability of PPG in the assessment of ejection time.

The correlation of ET(ECHO) with DNI* - a novel parameter hypothesized to describe ventriculo-arterial coupling and aortic distensibility - reveals a wider interconnectedness of the hemodynamic elements beyond time-domain parameters.

## Systolic function

Monitoring systolic function, especially in HF patients, is crucial in secondary and tertiary prevention, therapy monitoring, and timely clinical decision making. Echocardiography is considered the first-choice tool to assess systolic performance by evaluating global and segmental myocardial contractility [28].

***Left ventricular diameters and volumes.*** The anatomical measures of the left ventricle, including end-diastolic and end-systolic diameters and volumes, are key indicators of cardiac health [3].

In this study, LV-EDD showed the strongest correlation with AGEi and the proprietary Heart Fitness Score, which may indicate that these PPG parameters can be peripheral candidates to reflect changes in LV-EDD. A large study by Li et al. ($N = 33{,}147$) has confirmed the predictive value of LV-EDD in the outcome of patients with coronary artery disease [29]. Moreover, the findings of this study might have further clinical relevance as there are significant associations between LV-EDD and mortality from hypertrophic-, dilatative cardiomyopathy, and heart failure [29].

Concerning LV-ESD, a remarkable association with AGEi was found. In a recent study by Takada et al., it was found that LV-ESD is the strongest predictor in heart failure with reduced ejection fraction (HFrEF) patients for non-improvement one year after hospital discharge. Moreover, persistent HFrEF patients had significantly worse prognosis and outcomes [30].

LV-ESD plays an important role in the determination of the severity of mitral and aortic regurgitation and the necessity of surgery in those conditions [31]. Therefore, it is conceivable that PPG monitoring of AGEi might have relevance in these conditions.

Volume parameters showed significant, but weaker (r/rho<0,4) correlations with composite PPG parameters, especially the CardioVascular Health Score and Heart Fitness Score (Results found in Supplementary Tables 1 and 2). However, Ageing-index, d/a, and CrestTime@75 might also be useful in the future in the differentiation of patients with altered LV anatomy and function, as they also exhibited significant but weak correlations.

To our knowledge, no other publication has described a correlation between PPG-derived features and ventricular volumes. However, a recent article by Kavas et al. demonstrated the potential of using machine learning to classify PPG signals in differentiating HFpEF and HFrEF from healthy measurements [23].

***Stroke volume, ejection fraction and global longitudinal strain (GLS).*** Similar to LV-ESV and LV-EDV, stroke volume (LV-SV) showed significant, but weaker correlation with several PPG parameters, like Heart Fitness Score, followed by Cardiovascular Health Score and d/a (Supplementary Tables 1 and 2). In clinical practice, LV-SV is often considered inferior to ejection fraction (EF). However, it is mostly relevant in the assessment of valvular diseases and HFpEF, independent of EF [32]. Interestingly, we observed an absence of significant correlation between ejection fraction (EF) and parameters derived from the PPG. This reflects that a peripheral signal like PPG is less likely to convey precise data about the volume ratio of blood ejected from the left ventricle compared to the residual blood volume in the chamber. Instead, PPG parameters are more indicative of the general efficiency of heart contractions and vascular elasticity, which collectively contribute to either adequate or inadequate blood perfusion.

The importance of GLS is emerging, and in most cases, it is added to the assessment of EF to get more comprehensive information on the ventricular function [32]. It has undergone extensive evaluation and has been proven to offer additional prognostic insights into mortality rates among patients with an LVEF greater than 35% [33]. It's worth noting that early signs of left myocardial dysfunction are observable in heart failure cases with HFpEF [34]. In such cases, cardiac malfunction starts with compromised longitudinal strains, even if the EF remains standard for extended periods.

To our knowledge, this is the first study that compares ventricular strain with PPG-related indices.

Our study's findings highlight a significant correlation between the Dicrotic Notch Index and GLS. This connection is particularly important given its attributes in the management of HFpEF patients [34]. This discovery might open the door for using PPG-based PWA in monitoring and preventing issues in HFpEF patients, pending further research validation.

***Aortic root diameter, aortic-, and left ventricular outflow tract velocity time integral (Ao-VTI, LVOT-VTI).*** Aortic root diameter is crucial for diagnosing and managing aortic diseases, and guiding follow-up and surgery decisions [35]. The left ventricular outflow tract velocity time integral (LVOT-VTI) is essential for assessing cardiac systolic function and output, predicting survival and hospitalization in heart failure and coronary artery disease, and is reliable even in severe heart failure [36]. The Aortic Velocity Time Integral (Ao VTI) estimates stroke volume and cardiac output, key in evaluating heart function, especially in aortic valve disease and heart failure [37].

DNi is a proprietary pulsewave parameter that was created when evaluating pulsewave recordings of elderly subjects with severe atherosclerosis and found that the Stiffness index, originally created to inform about aortic stiffness [5], was not sensitive enough. However, the height ratio of the dicrotic notch to the diastolic peak might serve as a sensitive tool in the differentiation between elderly individuals and younger subjects (unpublished data). We hypothesize the DNi to be a surrogate marker of ventriculo-arterial coupling; however, further studies are needed to confirm this hypothesis. Nonetheless, interestingly, DNi demonstrated a significant correlation with static and dynamic parameters related to aortic functions, such as aortic root diameter, Ao-VTI, LVOT-VTI, ejection time (besides GLS%) with a correlation coefficient higher than 0.4, the second-highest correlation with Ao-root diameter (rho = 0.482) (the strongest correlation of DNi was found with ET(ECHO)). Further research is required to confirm these initial findings and fully establish DNi as a reliable marker of ejection function, aortic distensibility, and ventriculo-arterial coupling.

## Diastolic function

Our study reveals significant correlations between PPG parameters, such as the eLVET2@75, b/a, CrestTime@75, or Heart Fitness Score, and echocardiographic indicators of diastolic function. Additionally, LVETi (which in this study showed the strongest correlation with E/e'-lat.) has been independently linked to diastolic dysfunction in prior research using other techniques [16]. This comprehensive analysis of a wide range of PPG-derived parameters is unprecedented, highlighting its possible utility in evaluating diastolic function.

This study found significant correlations between PPG parameters and MV-A, a parameter that measures late mitral velocity characterizing atrial contraction and its contribution to ventricular filling. MV-A's increase, which can be influenced by aging and impaired ventricular relaxation, is linked to diastolic function and post-surgical recovery insights [38, 39].

The E/e'-lat ratio, an echocardiography parameter, that estimates left ventricular filling pressure and has diagnostic and prognostic value in heart failure (HF) and diastolic dysfunction. Higher values suggest increased filling pressure and are linked to worse HF outcomes, influencing treatment decisions [40]. In this study, LVETi (formerly published to possibly correlate with diastolic function) presented significant and moderate correlation with E/e'-lat, whereas Cardiovascular Health Score and d/a showed weaker, but still significant correlations indicating PPG's future potential in assessing cardiac diastolic function.

In heart failure (HF), diastolic dysfunction significantly affects symptoms, functionality, and prognosis, making its assessment crucial, especially in systolic LV impairment [41]. Our study suggests that photoplethysmography data could offer a non-invasive, accessible, and cost-effective way to be added to the existing tools to screen and follow-up patients with diastolic dysfunction, aiding in identifying or monitoring asymptomatic HFpEF patients. Future research aims to extend these findings across diverse HF patient groups, examining how diastolic dysfunction parameters correlate with clinical outcomes and respond to treatments like SGLT2 inhibitors. This could help pinpoint high-risk individuals or those in early HF stages, potentially benefiting from more intensive monitoring or treatment strategies.

## CONCLUSIONS

PPG-recorded pulse waves hold potential as an insightful source of information on cardiovascular function and have been shown to exhibit altered characteristics in different CV diseases, including heart failure. Its utility in cardiovascular monitoring of HF patients largely depends on the extent to which PPG-derived parameters correspond with established measures of cardiovascular function, such as echocardiographic measurements. However, medical literature still lacks sufficient studies on estimating cardiac function using peripheral signals. In this study, we observed **moderate correlations in the majority of cases** between echocardiographic parameters and PPG indices in healthy individuals that may have clinical relevance. These preliminary findings support that PPG-based monitoring could be considered a complementary tool for CV assessment. However, further research in HF patients is necessary to verify the observed relationships between PPG and echocardiography parameters, in order to assess the potential clinical relevance of PPG analysis in supporting patient care in HF.

*Author contributions:* Dániel Kulin: Conceptualization, Methodology, Formal analysis, Investigation, Project administration, Visualization, Writing – Original draft preparation. Flóra Antali: Conceptualization, Formal analysis, Investigation, Data curation, Project administration, Visualization, Writing – Original draft preparation. Sándor Kulin: Methodology, Writing – Review and editing. Sándor Kulin Jr.: Methodology, Software. Márton Horváth: Investigation, Data curation. Zsuzsanna Miklós: Conceptualization, Resources, Supervision, Writing – Review and editing. Andrea Szűcs: Conceptualization, Resources, Supervision, Writing – Review and editing. All authors read and approved the final manuscript.

*Competing interests:* The authors declare no competing interests beyond those disclosed in the Conflicts of Interest statement.

*Data availability statement:* Data collected in the study relevant to this article can be found in a shared database. Kulin (2025). Data analyzed for the article of Evaluating photoplethysmography-based pulsewave parameters and composite scores for assessment of cardiac function: A comparison with echocardiography figshare. Dataset. https://doi.org/10.6084/m9.figshare.28632488.

*Declaration on the use of Artificial Intelligence:* During the preparation of this work, the authors used ChatGPT and Grammarly to improve readability and to identify more concise expressions where needed. After using these tools, the authors reviewed and edited the content as required and take full responsibility for the final content of the publication.

*Consent to publish:* All authors have reviewed the final version of the manuscript and consent to its publication.

*Conflicts of Interest:* D.K., F.A., and S.K., S.K. Jr. have or had financial relationships with E-Med4All Europe Ltd. (D.K. and S.K. as co-owners; F.A. as a former employee during the data collection period; S.K. Jr. as a current employee of the company at the date of the submission). S.K. also serves as the CEO of E-Med4All Europe Kft., Budapest, Hungary. Z.M. is the

PhD supervisor of D.K. and F.A. M.H., Z.M., and A.S. did not receive any compensation for their contributions.

*Funding/financial support:* The study did not receive any external funding. All authors contributed their time and expertise without further financial support, as detailed in the "Conflict of Interest" section.

## SUPPLEMENTARY DATA

Supplementary data to this article can be found online at https://doi.org/10.1556/2060.2025.00675.

## REFERENCES

1. World Health Organization. Cardiovascular diseases; n.d. https://www.who.int/health-topics/cardiovascular-diseases#tab=tab_1 [accessed 14 August 2023].
2. Bozkurt B, Ahmad T, Alexander KM, Baker WL, Bosak K, Breathett K, et al. Heart failure epidemiology and outcomes statistics: a report of the heart failure society of America. J Card Fail 2023; 29: 1412–51. https://doi.org/10.1016/j.cardfail.2023.07.006
3. Voigt J-U. Left ventricular function, heart failure, and resynchronization therapy. In: The ESC textbook of cardiovascular medicine. Oxford University Press. p. 450–4. https://doi.org/10.1093/med/9780198784906.003.0092
4. Kobe EA, McVeigh T, Hameed I, Fudim M. Heart failure remote monitoring: a review and implementation How-To. J Clin Med 2023; 12. https://doi.org/10.3390/jcm12196200
5. Charlton PH, Paliakaitė B, Pilt K, Bachler M, Zanelli S, Kulin D, et al. Assessing hemodynamics from the photoplethysmogram to gain insights into vascular age: a review from VascAgeNet. Am J Physiol Circ Physiol 2022; 322: H493–522. https://doi.org/10.1152/ajpheart.00392.2021
6. O'Rourke MF, Pauca A, Jiang XJ. Pulse wave analysis. Br J Clin Pharmacol 2001; 51: 507–22. https://doi.org/10.1046/j.0306-5251.2001.01400.x
7. Hametner B, Weber T, Wassertheurer S. Heart failure: insights from the arterial waves. J Am Heart Assoc 2023; 12: 12–5. https://doi.org/10.1161/JAHA.123.029116
8. Duan W, Zheng D, Eggett C, Langley P, Murray A. Development of techniques for measurement of left ventricular ejection time. Comput Cardiol 2010) 2014; 41: 241–4.
9. Meah VL, Backx K, Shave RE, Stöhr EJ, Cooper SM. Comparison between Modelflow® and echocardiography in the determination of cardiac output during and following pregnancy at rest and during exercise. J Hum Sport Exerc 2022; 17: 116–35. https://doi.org/10.14198/JHSE.2022.171.12
10. Blanié A, Soued M, Benhamou D, Mazoit JX, Duranteau J. A comparison of photoplethysmography versus esophageal doppler for the assessment of cardiac index during major noncardiac surgery. Anesth Analg 2016; 122: 430–6. https://doi.org/10.1213/ANE.0000000000001113
11. Horváth M, Farkas-Sütő K, Fábián A, Lakatos B, Kiss AR, Grebur K, et al. Highlights of right ventricular characteristics of left ventricular noncompaction using 3D echocardiography. Int J Cardiol Heart Vasc 2023; 49: 101289. https://doi.org/10.1016/j.ijcha.2023.101289. 38035261.

12. Millasseau S, Kelly R, Ritter J, Chowienczyk P. Determination of age-related increases in large artery stiffness by digital pulse contour analysis. Clin Sci 2002; 103: 371–7.
13. Takazawa K, Tanaka N, Fujita M, Matsuoka O, Saiki T, Aikawa M, et al. Assessment of vasoactive agents and vascular aging by the second derivative of photoplethysmogram waveform. Hypertens (Dallas, Tex 1979) 1998; 32: 365–70.
14. Inoue N, Kawakami H, Yamamoto H, Ito C, Fujiwara S, Sasaki H, et al. Second derivative of the finger photoplethysmogram and cardiovascular mortality in middle-aged and elderly Japanese women. Hypertens Res 2017; 40: 207–11. https://doi.org/10.1038/hr.2016.123
15. Besleaga T. Photoplethysmography use for assessment of mechanical alternans in human cardiovascular disease. University College London; 2020.
16. Weber T, Auer J, O'Rourke MF, Punzengruber C, Kvas E, Eber B. Prolonged mechanical systole and increased arterial wave reflections in diastolic dysfunction. Heart 2006; 92: 1616–22. https://doi.org/10.1136/hrt.2005.084145
17. Elgendi M. On the analysis of fingertip photoplethysmogram signals. Curr Cardiol Rev 2012; 8: 14–25. https://doi.org/10.2174/157340312801215782
18. von Wowern E, Östling G, Nilsson PM, Olofsson P. Digital photoplethysmography for assessment of arterial stiffness: repeatability and comparison with applanation tonometry. PLoS One 2015; 10: 1–19. https://doi.org/10.1371/journal.pone.0135659
19. Kulin D, Antali F, Kulin S, Wafa D, Lucz KI, Veres DS, et al. Preclinical, multi-aspect assessment of the reliability of a photoplethysmography-based telemonitoring system to track cardiovascular status. Appl Sci 2020; 10: 1–17. https://doi.org/10.3390/app10227977
20. Antali F, Kulin D, Lucz KI, Szabó B, Szűcs L, Kulin S, et al. Multimodal assessment of the pulse rate variability analysis module of a photoplethysmography-based telemedicine system. Sensors 2021; 21: 5544. https://doi.org/10.3390/s21165544
21. Fine J, Branan KL, Rodriguez AJ, Boonya-ananta T, Ajmal, Ramella-Roman JC, et al. Sources of inaccuracy in photoplethysmography for continuous cardiovascular monitoring. Biosensors 2021; 11: 126. https://doi.org/10.3390/bios11040126
22. Statista.com. Global connected wearable devices 2019-2022; n.d. https://www.statista.com/statistics/487291/global-connected-wearable-devices/ [accessed 2 May 2024].
23. Özen Kavas P, Recep Bozkurt M, Kocayiğit İ, Bilgin C. Machine learning-based medical decision support system for diagnosing HFpEF and HFrEF using PPG. Biomed Signal Process Control 2023; 79. https://doi.org/10.1016/j.bspc.2022.104164
24. Green EM, van Mourik R, Wolfus C, Heitner SB, Dur O, Semigran MJ. Machine learning detection of obstructive hypertrophic cardiomyopathy using a wearable biosensor. npj Digit Med 2019; 2: 1–4. https://doi.org/10.1038/s41746-019-0130-0
25. Miyashita H. The time is ripe to reevaluate the second derivative of the digital photoplethysmogram (SDPTG), originating in Japan, as an important tool for cardiovascular risk and central hemodynamic assessment. Hypertens Res 2017; 40: 429–31. https://doi.org/10.1038/hr.2016.175
26. Alhakak AS, Teerlink JR, Lindenfeld J, Böhm M, Rosano GMC, Biering-Sørensen T. The significance of left ventricular ejection time in heart failure with reduced ejection fraction. Eur J Heart Fail 2021; 23: 541–51. https://doi.org/10.1002/ejhf.2125
27. Obata Y, Mizogami M, Singh S, Nyhan D, Berkowitz DE, Steppan J, et al. Ejection time: influence of hemodynamics and site of measurement in the arterial tree. Hypertens Res 2017; 40: 811–8. https://doi.org/10.1038/hr.2017.43

28. Zerbib Y, Maizel J, Slama M. Echocardiographic assessment of left ventricular function. J Emerg Crit Care Med 2019; 3: 33–33. https://doi.org/10.21037/JECCM.2019.07.05
29. Li Q, Huang H, Lu X, Yang Y, Zhang Y, Chen W, et al. The association between left ventricular end-diastolic diameter and long-term mortality in patients with coronary artery disease. Rev Cardiovasc Med 2023; 24: 84. https://doi.org/10.31083/j.rcm2403084
30. Takada T, Nakata Y, Matsuura K, Minami Y, Kishihara M, Watanabe S, et al. Left ventricular end-systolic diameter may predict persistent heart failure with reduced ejection fraction. Int Heart J 2023; 64: 23–293. https://doi.org/10.1536/ihj.23-293
31. Vahanian A, Beyersdorf F, Praz F, Milojevic M, Baldus S, Bauersachs J, et al. 2021 ESC/EACTS guidelines for the management of valvular heart disease: developed by the task Force for the management of valvular heart disease of the European Society of Cardiology (ESC) and the European Association for Cardio-Thoracic Surgery (EACTS). Eur Heart J 2022; 43: 561–632. https://doi.org/10.1093/eurheartj/ehab395
32. Marwick TH. Ejection fraction pros and cons: JACC state-of-the-art review. J Am Coll Cardiol 2018; 72: 2360–79. https://doi.org/10.1016/j.jacc.2018.08.2162
33. Stanton T, Leano R, Marwick TH. Prediction of all-cause mortality from global longitudinal speckle strain: Comparison with ejection fraction and wall motion scoring. Circ Cardiovasc Imaging 2009; 2: 356–64. https://doi.org/10.1161/CIRCIMAGING.109.862334
34. Brann A, Miller J, Eshraghian E, Park JJ, Greenberg B. Global longitudinal strain predicts clinical outcomes in patients with heart failure with preserved ejection fraction. Eur J Heart Fail 2023; 25: 1755–65. https://doi.org/10.1002/EJHF.2947
35. Goldstein SA, Evangelista A, Abbara S, Arai A, Asch FM, Badano LP, et al. Multimodality imaging of diseases of the thoracic aorta in adults: from the American society of echocardiography and the european association of cardiovascular imaging: endorsed by the society of cardiovascular computed tomography and society for cardiova. J Am Soc Echocardiogr 2015; 28: 119–82. https://doi.org/10.1016/j.echo.2014.11.015
36. Tan C, Rubenson D, Srivastava A, Mohan R, Smith MR, Billick K, et al. Left ventricular outflow tract velocity time integral outperforms ejection fraction and Doppler-derived cardiac output for predicting outcomes in a select advanced heart failure cohort. Cardiovasc Ultrasound 2017; 15: 18. https://doi.org/10.1186/s12947-017-0109-4
37. Lang RM, Badano LP, Victor M-A, Afilalo J, Armstrong A, Ernande L, et al. Recommendations for cardiac chamber quantification by echocardiography in adults: an update from the American Society of Echocardiography and the European Association of Cardiovascular Imaging. J Am Soc Echocardiogr 2015; 28: 1. https://doi.org/10.1016/j.echo.2014.10.003
38. Nishimura RA, Tajik AJ. Evaluation of diastolic filling of left ventricle in health and disease: Doppler echocardiography is the clinician's Rosetta Stone. J Am Coll Cardiol 1997; 30: 8–18. https://doi.org/10.1016/S0735-1097(97)00144-7
39. Alsaddique AA. Recognition of diastolic heart failure in the postoperative heart. Eur J Cardio-Thoracic Surg 2008; 34: 1141–8. https://doi.org/10.1016/J.EJCTS.2008.05.030
40. Park J-H, Marwick TH. Use and limitations of E/e' to assess left ventricular filling pressure by echocardiography. J Cardiovasc Ultrasound 2011; 19: 169. https://doi.org/10.4250/jcu.2011.19.4.169
41. Mottram PM, Marwick TH. Assessment of diastolic function: what the general cardiologist needs to know. Heart 2005; 91: 681–95. https://doi.org/10.1136/HRT.2003.029413

## Supplementary Material

# Evaluating photoplethysmography-based pulsewave parameters and composite scores for assessment of cardiac function: A comparison with echocardiography

Daniel Kulin[1, 2, †], Flora Antali[1, †], Marton Horvath[3], Sandor Kulin[2], Sandor Kulin Jr.[2], Zsuzsanna Miklos[1, 4, ††], Andrea Szűcs[3, ††]

**Doi:** https://doi.org/10.1556/2060.2025.00675

| Correlation of echocardiography parameters with PPG | | | | | |
|---|---|---|---|---|---|
| **Echocardiography: Ejection time** | **PPG parameters** | **Pearson's correlations** | | **Pearsosn's Partial correlations condition on HR** | |
| | | **r** | **p** | **r** | **p** |
| LVET (ms) | Ri | 0.346 | 0.036 | -0.086 | 0.618 |
| | eLVET1 * | 0.478 | 0.003 | 0.155 | 0.367 |
| | HR | -0.538 | < .001 | N/A | N/A |
| **Echocardiography parameters indicating systolic function** | **PPG parameters** | **Pearson's correlations** | | | |
| | | **r** | **p** | | |
| LV-EDD (mm) | SysAlpha | 0.328 | 0.048 | | |
| | DNi * | 0.348 | 0.035 | | |
| | eLVET2 * | -0.331 | 0.045 | | |
| LV-ESD (mm) | SysAlpha | 0.363 | 0.027 | | |
| | DNi * | 0.341 | 0.039 | | |
| | eLVET2 * | -0.366 | 0.026 | | |
| | Crest Time @75 | -0.37 | 0.024 | | |
| LV-EDV (ml) | CV Health Score * | 0.383 | 0.021 | | |
| | d/a | 0.334 | 0.046 | | |
| | AGEi | -0.338 | 0.044 | | |
| | Crest Time @75 | -0.333 | 0.047 | | |
| LV-ESV (ml) | CV Health Score * | 0.358 | 0.032 | | |

| | | | | | |
|---|---|---|---|---|---|
| | Heart Fitness Score * | 0.369 | 0.027 | | |
| LV-SV (ml) | CV Health Score * | 0.387 | 0.020 | | |
| | d/a | 0.356 | 0.033 | | |
| | AGEi | -0.343 | 0.040 | | |
| | Crest Time @75 | -0.341 | 0.042 | | |
| Ao, root diam (mm) | Si | -0.36 | 0.029 | | |
| | AGEi | -0.356 | 0.030 | | |
| | eLVET1 @75 * | -0.375 | 0.022 | | |
| | Crest Time @75 | -0.389 | 0.017 | | |
| | Crest Time | -0.356 | 0.030 | | |
| Ao-vmax (m/s) | AGEi | -0.332 | 0.045 | | |
| | DNi * | -0.389 | 0.017 | | |
| | eLVET2 @75 * | 0.352 | 0.033 | | |
| Ao-gr (av) (Hgmm) | DNi * | -0.326 | 0.049 | | |
| Ao-gr (peak) (Hgmm) | DNi * | -0.378 | 0.021 | | |
| | eLVET2 @75 * | 0.332 | 0.044 | | |
| Ao-VTI (cm) | eLVET2 | 0.335 | 0.046 | | |
| | Crest Time | 0.334 | 0.047 | | |
| **Echocardiography parameters indicating diastolic function** | **PPG parameters** | **Pearson's correlations** | | **Pearsosn's Partial correlations condition on HR** | |
| | | **r** | **p** | **r** | **p** |
| MV-A (cm/s) | ET(PPG) @75 | 0.464 | 0.004 | 0.272 | 0.109 |
| | AGEi | 0.337 | 0.042 | 0.434 | 0.008 |
| | LVETi | 0.362 | 0.028 | 0.279 | 0.100 |
| | Sys/Dias Time | 0.545 | <.001 | 0.258 | 0.129 |
| | HR | 0.5 | 0.005 | N/A | N/A |
| MV-grad (av) (Hgmm) | Heart Fitness Score * | -0.359 | 0.031 | -0.248 | 0.151 |
| | b/a | 0.366 | 0.028 | 0.332 | 0.051 |
| | Crest Time @75 | 0.369 | 0.027 | 0.344 | 0.043 |
| | ET(PPG) @75 | 0.374 | 0.024 | 0.203 | 0.242 |
| | Sys/Dias Time | 0.485 | 0.003 | 0.273 | 0.113 |
| | HR | 0.42 | 0.011 | N/A | N/A |
| MV-E/A | Sys/Dias Time | -0.37 | 0.024 | 0.055 | 0.751 |
| | HR | -0.46 | 0.004 | | |
| MV-E (cm/s) | SysAlpha | -0.329 | 0.047 | | |
| | DNi * | -0.375 | 0.022 | | |
| | eLVET2 @75 * | 0.37 | 0.024 | | |
| | Crest Time @75 | 0.368 | 0.025 | | |
| e'-med (cm/s) | eLVET1 * | -0.365 | 0.026 | | |

| | | | | | |
|---|---|---|---|---|---|
| | ET(PPG) | -0.345 | 0.036 | | |
| E/e' - lat | CV Health Score * | -0.398 | 0.015 | | |
| | d/a | -0.382 | 0.020 | | |
| | SysAlpha | -0.377 | 0.022 | | |
| | ET(PPG) @75 | 0.373 | 0.023 | | |
| DT (ms) | CV Health Score * | 0.392 | 0.016 | | |
| | b/a | -0.365 | 0.026 | | |
| | LVETi | -0.347 | 0.035 | | |
| | eLVET2 @75 * | -0.394 | 0.016 | | |
| | eLVET2 * | -0.347 | 0.035 | | |
| | Crest Time @75 | -0.36 | 0.029 | | |
| | ET(PPG) @75 | -0.34 | 0.040 | | |

*Supplementary Table 1. - Results of Pearson's correlation: comparisons of echocardiographic parameters and PPG parameters not included in Table 2. r: correlation coefficient; p= p value (significance value <0.05) Given the correlation between heart rate measured by PPG and some echocardiographic parameters, where applicable, partial correlation tests were performed as a function of heart rate. *:proprietary SCN4ALL parameters*